THE UNIVERSITY OF MICHIGAN
7692-1-F

AFAL-TR-68-132

Electromagnetic Coupling Reduction Techniques

J.A.M. Lyon, C.J. Digenis,
W.W. Parker and M.A.H. Ibrahim

June 1968

FOREWORD

This report, AFAL-TR-68-132, was prepared by the University of Michigan, Ann Arbor, Michigan, under the direction of Professor Ralph E. Hiatt and Professor John A. M. Lyon and on Air Force Contract AF 33(615)-3371 under Task No. 435709 of Project 4357 (U) "Electromagnetic Coupling Reduction Techniques." The work was administered under the direction of the Air Force Avionics Laboratory, Electronic Warfare Division, Wright-Patterson Air Force Base, Ohio. The Task Engineer was Mr. Olin E. Horton, the Project Engineer Mr. Herbert Bartman.

This report covers the period 15 November 1965 through 14 March 1968.

This technical report has been reviewed and is approved.

Ronald G. Stimmel

JOSEPH A. DOMBROWSKI
Lt Colonel, USAF
Chief, Electronic Warfare Division

ABSTRACT

This report describes studies of various methods of decoupling one antenna from another. The decoupling of slot antennas has been analyzed over a range of frequencies including X-band as well as S-band. Decoupling between such antennas has been achieved through the use of intervening fences or parasitic elements. Another method of decoupling has used absorbing material placed between the antennas. Still another method of decoupling which has been examined in detail has been the use of circumferential corrugations. Such circumferential corrugations can be considered as surface reactive loading on one of the antennas. This particular method of decoupling has also been applied to Archimedean spirals and horns as well as quarter wave monopoles; the latter have been erected perpendicular to the ground plane. A considerable amount of effort has also been placed upon the use of a compensating circuit whereby an unwanted signal in the receiving antenna has been canceled out by means of an auxiliary link. This last method has the great advantage of being applicable for almost any frequency band.

TABLE OF CONTENTS

LIST OF FIGURES

List of Figures (Cont'd)

List of Figures (Cont'd)

List of Figures (Cont'd)

List of Figures (Cont'd)

List of Figures (Cont'd)

I

INTRODUCTION

This final report reviews the various techniques which have been found useful in reducing the electromagnetic coupling between antennas. In many instances the antennas studied have been flush mounted antennas. On this basis the results would be immediately useful for intrasystem interference problems encountered on aerospace vehicles. The problem of reducing coupling is a relatively simple one if only a narrow range of frequency is involved. However the studies encountered in this report give emphasis to methods and techniques which are applicable on a broadband basis. Additional emphasis has been placed upon the effects of different coupling reduction methods on the far field radiation patterns of the antennas involved.

Power interference between antennas can be mitigated in two different ways. First considerable isolation can be obtained by means deduced from the coupling prediction analysis. Such analysis involving the influence of spacing, orientation, and polarization has been discussed in length in the final report of the preceding contract (Lyon et al, April 1966). Certainly a considerable increase in isolation is possible if design choices are based upon this analysis.

The second general approach to the problem of reduction of interference is the one described most fully in this report. This second approach involves corrections, modifications, and possibly supplements that can be made to previously planned or installed systems. In some cases the modifications would require extensive changes including additional equipment. This second class of methods involves the reduction of coupling by absorbing, phasing out, or reflecting the flow of energy between two antennas mounted on a common metal surface. In the succeeding section details are given concerning the analysis and techniques useful for the decoupling methods associated with this second category.

Although the methods described in this report are obviously immediately applicable in many cases of power interference between two systems which are located on a common vehicle, the methods are not necessarily restricted to such cases of intrasystem interference. For instance, the method utilizing the compensating link or bridge can be readily applied to a situation involving two or more systems where the systems are located at some distance. Actually, the compensating link may be composed only in simple cases of waveguide or coaxial cable as described in the experimental procedures in this report. It is possible to consider an extension of this method where the auxiliary circuit is not such a simple case. The auxiliary circuit may involve an additional propagation path through the air and possibly for this auxiliary link a new carrier frequency would be used; necessary terminal equipment would complete such a link. The fundamental requirements of matching dispersion characteristics as described in this report would of necessity hold.

With the exception of certain preliminary investigations, the experiments reported here were conducted in an anechoic chamber with dimensions 50 ft. x 30 ft. x 15 ft. with a 12 ft. square aluminum ground plane mounted in the center of one end wall. This plane has a removable 2 ft. x 3 ft. center section for mounting antennas of various sizes. An electric continuation to the square aluminum ground plane is provided by means of interlocking aluminum foil sheets which provide a known uniform termination for the absorbing material and also shield the room from external signals.

For all coupling measurements the antennas were mounted near the center of the 12 ft. square ground plane. Of prime interest in this work was the frequency range over which a method would be applicable; therefore a swept frequency technique was used with fixed antenna positions to show the dependence of coupling upon frequency. With frequency sweeping it is true that

the two systems may not be optimally matched for each frequency. However, for the antenna types considered it was found that the absence of matching devices did not affect coupling data by more than 1 db.

The term "coupling" as used here means the ratio of the power received by one antenna to the power transmitted by another antenna. To establish a reference, the flanges connecting the two transmission lines with the two antennas were mated together while a certain amount of attenuation was introduced in the system through a precision attenuator. The level so obtained has been marked as "direct coupling" or "calibration" in the various coupling charts in this report. Leveled Sweep Oscillators were used as sources except for some of the preliminary experiments where a mechanically tuned Reflex Klystron was used. When the power available from the Sweep Oscillators was not adequate for recording weak coupling, a TWT amplifier was used with external feedback for leveling. A crystal detector was used for the swept frequency measurements.

Two arrangements have been used for radiation pattern measurements. In the first, the test antenna was mounted at the center of the large ground plane and used as a transmitter while a receiving antenna was mounted on a wooden boom, covered with hairflex absorber, and rotated in front of the ground plane at a radius of 6 ft. A special fixture allowing the pick-up antenna to come as close as 0.5^{o} from the ground plane at X-band (or 4^{o} at S-band) was used for some patterns. In this case the pick-up antenna travel in the other direction near the ground plane is limited to about 75^{o}, so these patterns may appear at first as being asymmetrical for this reason. At X-band frequencies, a small E-sectoral horn with a flare angle of 32^{o} and aperture 2.8 cm x 2.3 cm was used as a pick-up antenna. This horn has a gain of 8 to 10 db at X-band frequencies. At S-band frequencies, a log periodic antenna with a gain of 6 to 8 db replaced the horn.

In the second arrangement, the test antenna was used as a receiver and was mounted on a small ground plane, supported by a rotating pedestal which was located 28 ft from the large ground plane. In this case the large ground plane was covered with hairflex absorber except for the aperture of a standard gain horn used to illuminate the test antenna.

It should be pointed out that the term "gain" is used with the meaning "directivity times efficiency". This clarification becomes necessary because some authors use the term gain with the meaning of directivity. When absorbing materials are used in the vicinity of the aperture of a microwave antenna with the purpose of reducing the interference to a nearby antenna it has been observed (see Chapter II) that in some cases although the antenna directivity is not seriously affected, the antenna efficiency is reduced resulting in considerable loss of gain. Since any decoupling method resulting in gain reduction is not considered an acceptable solution, the variation of gain must always be studied. Since as the frequency is swept, both the gain of the pick-up antenna and the isolation due to separation between the test antenna and the pick-up antenna vary, the gain patterns indicate only the change in level due to a particular decoupling method and not the absolute antenna gain.

II

ABSORBING MATERIALS

2.1 General

The purpose of this study was to examine the possibilities of increasing the isolation between two flush mounted microwave antennas by using absorbing materials. The experiments were conducted in the frequency range 8.2 - 12.4 GHz (X-band). Two types of antennas were used; broadband slots (2.3 cm by 1.0 cm) and E-sectoral horns, both fed by waveguide. In every experiment two identical antennas were used, mounted flush in a metal ground plane. The absorbing materials were used in three different configurations; (a) a slab of absorbing material was placed on the ground plane between the two antennas, (b) a piece of absorbing material was placed in a cavity in the ground plane, being flush with the metal surface, either at some position between the two antennas, or surrounding the antenna aperture, (c) wedges made of absorber were used to line the flared side of a sectoral horn or replace part of the waveguide feeding a slot. The relative merits and drawbacks of each arrangement and the effectiveness of the method in reducing coupling are presented in the following sections.

The absorbing materials used and their characteristics, as specified by the manufacturer, are as follows:

1. Eccosorb - CR (Emerson and Cuming Co.)

   Type: Casting resin absorber

Frequency:	8.6 GHz	10 GHz
Attenuation:	23 db/cm	34 db/cm
Dielectric constant:	21	21
Dielectric dissipation factor:	0.08	0.08
Permeability:	2.2	1.6
Magnetic dissipation factor:	0.6	0.75

2. RF-X (B. F. Goodrich Co.)

   Type: Resonant absorber

   Attenuation: 25 db

3. Eccosorb MF 124 (Emerson and Cuming Inc.)
   Properties at 10 GHz: attenuation 69 db/cm,
   dielectric constant 26, dielectric dissipation factor 0.12,
   permeability 2.1, magnetic dissipation factor 1.2.

2.2 Absorber Obstacle on the Ground Plane.

2.2.1 Broadband Slots

In this case the two slot antennas were oriented for E-plane coupling at a fixed distance of the order of 2 to 3 wavelengths at the middle of the X-band. Slabs of different dimensions of Eccosorb-CR were placed on the ground plane between the two slots (Fig. 2-1). The maximum height of the absorber pieces was 2.0 cm. It was generally observed that placing the absorber near either of the two antennas instead of in a midposition decreased coupling by about 2 db. The coupling of two slots spaced 6.5 cm center-to-center was reduced from a maximum of -24 db to -49 db over the entire X-band, using a piece with dimensions a = b = 5 cm, c = 2 cm symmetrically located between the two slots (see also Lyon et al, March 1966). The presence of the absorber obstacle near the slot aperture modifies the radiation pattern of the slot as indicated in Fig. 2-2. In this figure the E-plane radiation pattern of the slot is shown for the following three cases; (a) no obstacle on the ground plane, (b) absorber obstacle as described, (c) metal obstacle of identical dimensions and position with the absorber obstacle. The left side of Fig. 2-2 corresponds to the side of the slot nearest the obstacle. The absorber acts similarly with the metal obstacle, being better in two ways: (a) it creates a lower sidelobe in its direction by the surface attenuation of the waves diffracted at the leading thick edge, and (b) it avoids the 8 db depression created by the metal obstacle in the other direction (at $\theta = 50^{\circ}$) which is due to reflection and phase cancellation.

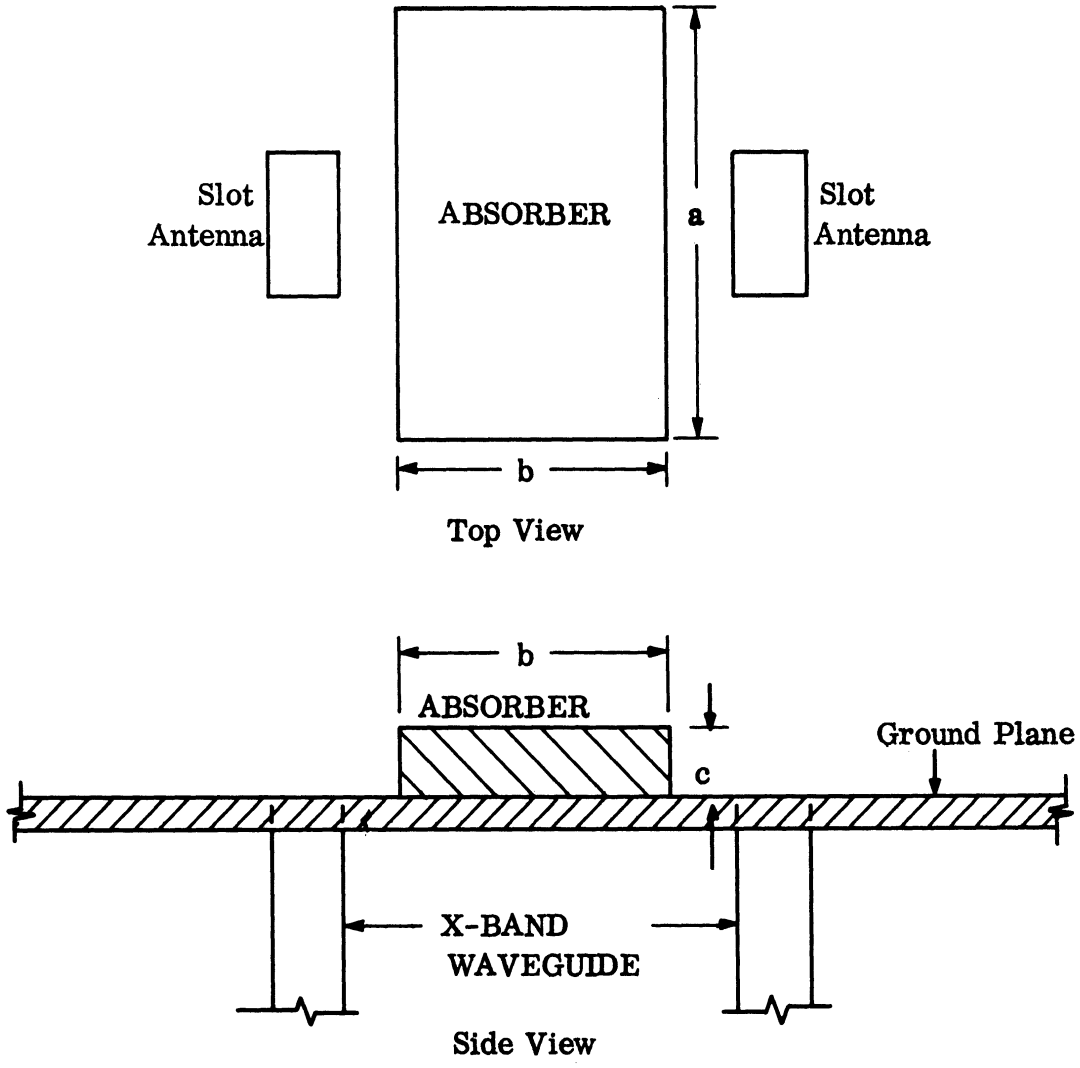

FIG. 2-1: GENERAL GEOMETRY: E-PLANE COUPLING

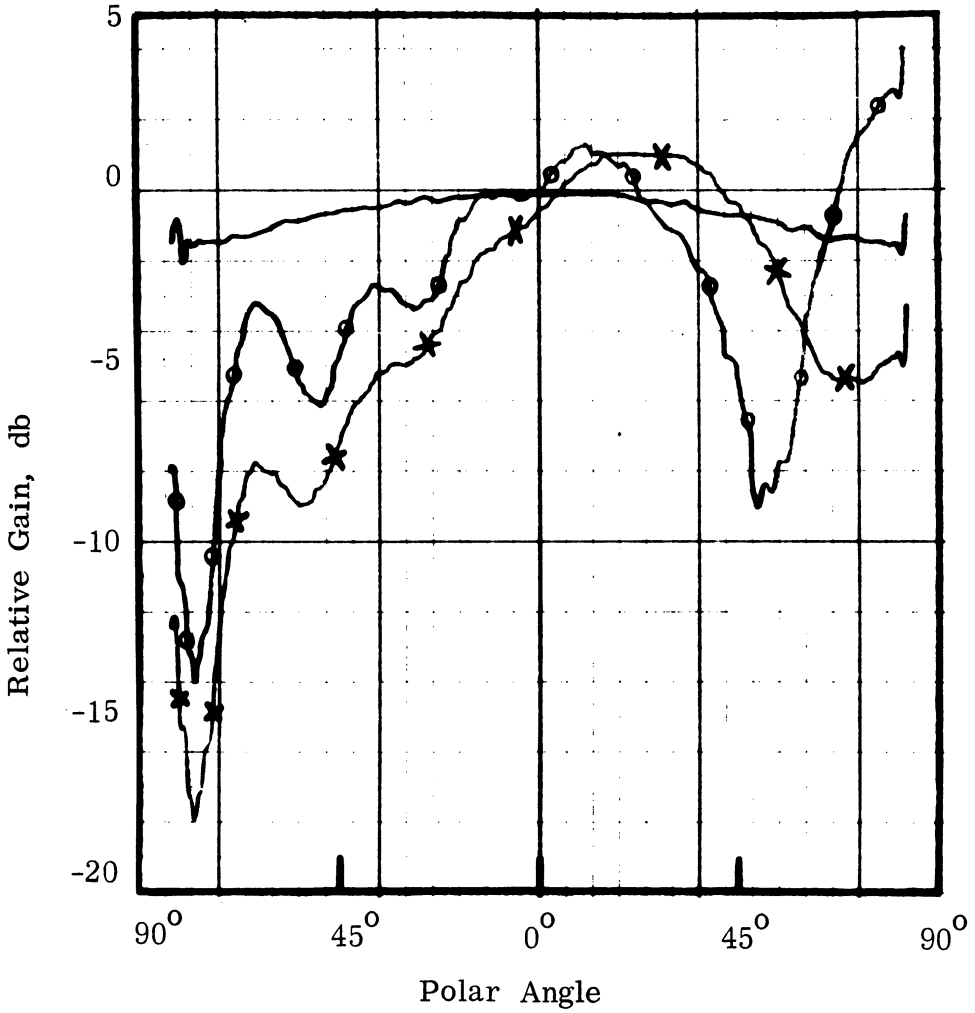

FIG. 2-2: E-PLANE RADIATION PATTERN AT 10 GHz OF A SLOT IN A 12 FT SQUARE GROUND PLANE.

—— Plain Slot
—x— With Absorber Obstacle
—o— With Metal Obstacle

Similar experiments were performed using layers of RFX absorber. This type of absorber is limited to narrow band applications because of its resonant character. Use of repeated layers backed by aluminum foil produced a coupling reduction of 15 db over the entire X-band, with the absorber being resonant at about 10 GHz (See Lyon et al, March 1966).

The presence of an obstacle on the ground plane near the slot aperture can be expected to change the antenna standing wave ratio. When a wave is propagating through a waveguide terminated at a slot, reflections occur at the point of discontinuity giving rise to a standing wave in the transmission line. Let E_i be the incident wave component and $E_{r,1}$ the reflected wave component. Then the reflection coefficient is:

$$\rho_1 = \frac{E_{r,1}}{E_i}$$

The presence of an obstacle on the ground plane in the near field of the slot creates additional reflections, the amplitude of which depend upon the size and conductivity of the obstacle as well as the distance R_λ from the slot (distance expressed in wavelengths). Let this be denoted by $E_{r,2}(R_\lambda)$. The phase of $E_{r,2}$ will vary with respect to $E_{r,1}$ with a period of 0.5λ. Therefore it can be expressed as:

$$E_{r,2}(R_\lambda)\cos(2\pi\frac{R}{0.5\lambda}+\phi) = E_{r,2}(R_\lambda)\cos(4\pi R_\lambda+\phi) \quad ,$$

where ϕ is a reference phase angle. Thus the reflection coefficient becomes:

$$\rho_t = \frac{E_{r,1} + E_{r,2}(R_\lambda)\cos(4\pi R_\lambda + \phi)}{E_i} \quad . \tag{2.1}$$

The corresponding standing wave ratio is:

$$S_t = \frac{1+|\rho_t|}{1-|\rho_t|} \quad .$$

If an impedance matching device is used between the transmission line and the slot, when no obstacle is present, $E_{r,1}$ can be made practically zero and then one can obtain ρ_2 and $E_{r,2}(R_\lambda)$ according to Eq. (2.1).

The reflection coefficient has been determined experimentally. Since in applications the standing wave ratio is used more often, this is the quantity that has been measured and which is presented in Fig. 2-3. The size and location of the obstacle is shown in the same figure. The slot was in a 2 ft. by 3 ft. copper ground plane facing a cubic anechoic chamger 2 ft. on each side. In Fig. 2-3 curve A simply shows the value of the slot SWR at 9.0 GHz when no obstacle is present. In the presence of the absorber obstacle the slot SWR was found to vary as shown in curve B. By using a slide-screw tuner, a nearly perfect match between the slot and the transmission line was obtained with no obstacle (SWR = 1.01). Then without changing the setting of the slide-screw tuner, the obstacle was placed on the ground plane and the SWR measured again, resulting in curve C. For comparison this was repeated with the obstacle covered by aluminum foil, which gave curve D. Now, the slot SWR in the presence of the absorber slab (curve B) can be checked against the information of curve C, the plain slot SWR and Eq. (2.1); e.g. the reflection coefficient of the slot only is:

$$\rho_1 = \frac{0.625}{2.625} = 0.238 \quad .$$

At the position of the first maximum, from curve C there is obtained

$$\rho_2 = \frac{0.13}{2.13} = 0.061 \quad ,$$

then

$$\rho_t = \rho_1 + \rho_2 \cos(4\pi R_\lambda + \phi) = 0.238 + 0.061 = 0.299 \quad . \qquad (2.2)$$

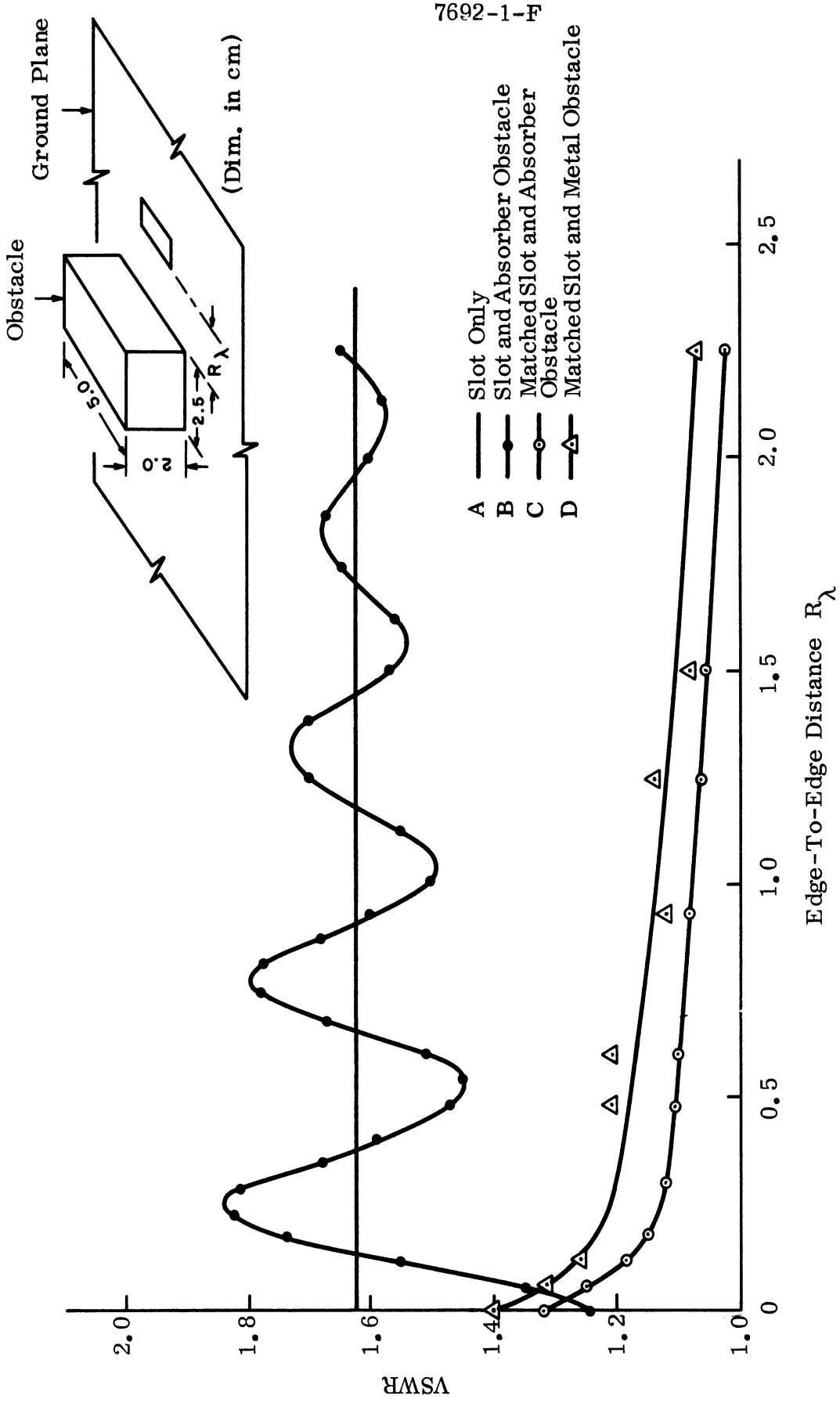

FIG. 2-3: VARIATION IN THE VSWR OF A SLOT ANTENNA IN THE PRESENCE OF AN OBSTACLE ON THE GROUND PLANE. EDGE-TO-EDGE DISTANCE MEASURED IN (FREE SPACE) WAVELENGTHS. f = 9.00 GHz

Besides, from curve B there is obtained:

$$\rho_t = \frac{0.85}{2.85} = 0.298$$

in agreement with (2.2). In general, the agreement is within 2 percent.

2.2.2 Sectoral Horns

The same technique has been used to reduce the coupling between two E-sectoral horns. The E-sectoral horns differ from the slots in that their E-plane radiation pattern presents low sidelobes along the ground plane, while that of slots shows near-maximum gain. The horns used in this case had a flare angle of 20°, aperture dimensions 3.9 cm by 2.3 cm and were located at a center-to-center spacing of 11.4 cm. With two pieces of Eccosorb-CR of dimensions 8 cm x 1.8 cm x 1.8 cm each placed adjacent to the apertures and between the two horns, the E-plane coupling at 10 GHz was reduced from -39 db to -63 db. At the same time, the E-plane radiation pattern showed a reduction in maximum gain of 0.5 db while the sidelobe in the direction of the absorber obstacle was reduced by 19 db. A metal object of the same dimensions as the absorber slab was then placed on the ground plane at the same position. The resulting radiation pattern was similar to that obtained with the absorber slab except that with the metal object the sidelobe was higher by 6 db from the level obtained with the absorber.

Due to the fact that in these experiments the absorber was not flush with the ground plane, which is a usual requirement in many applications, more detailed results and radiation patterns are not presented. The results of these experiments, however, besides showing what can be accomplished with certain configurations provided information which led to the design of a modified horn antenna as described later in Section 2.4.

Summarizing the results obtained with slots and E-sectoral horns it can be concluded that the coupling reduction obtained with absorbing materials placed on the ground plane is mostly due to reflection of the electromagnetic waves and to a lesser extent to absorption.

2.3 Absorber Embedded in the Ground Plane

2.3.1 Absorber in Cavity Between the Two Antennas

The absorbing material was placed in a cavity between the two antennas as shown in Fig. 2-4. The dimensions of the cavity were a = 7.2 cm, b = 2.3 cm, c = 2.2 cm. (See Fig. 2-1 for symbol identification). The two X-band slot antennas were at a spacing of 6.5 cm, center-to-center. Two types of absorbing materials were used to fill the cavity: Eccosorb -CR and RF-X. A coupling reduction of 2 db, throughout X-band was obtained with the Eccosorb-CR. A greater reduction was obtained with the RF-X material; however, it was limited to a smaller range of the X-band because of the resonant characteristics of this type of absorber. The maximum reduction was 6 db at 10 GHz. The presence of the cavity with the absorbing material affected the radiation patterns of the slots by creating peaks and troughs of the order of 2 db near the broadside direction (Lyon et al, May 1966).

2.3.2 Absorber in Cavity Surrounding the Antenna

In another series of experiments a cavity of circular cross-section was filled with absorbing material (Eccosorb MF-124) except for a rectangular opening the size of an X-band waveguide. (See Fig. 2-5). Two different cases were considered: (a) the waveguide extends all the way to the surface, being flush with the ground plane; (b) the waveguide stops at the cavity bottom being flush with it.

In case (a), with one slot only of a transmitter-receiver system being modified, a decoupling of 3.5 db was observed in the E-plane across the X-band, due to an equal amount of sidelobe reduction of the slot E-plane radiation pattern .

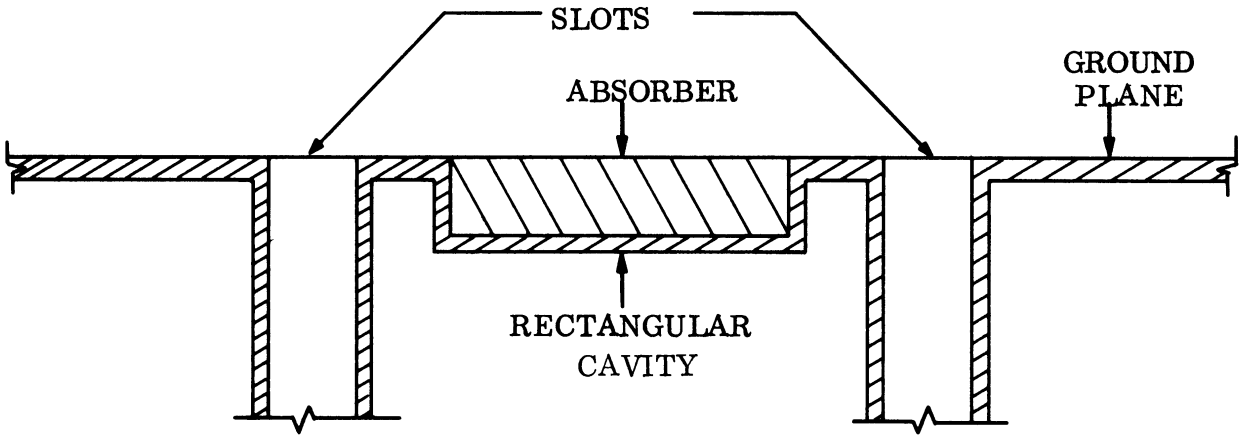

FIG. 2-4: ABSORBER PLACED IN SHALLOW CAVITY.

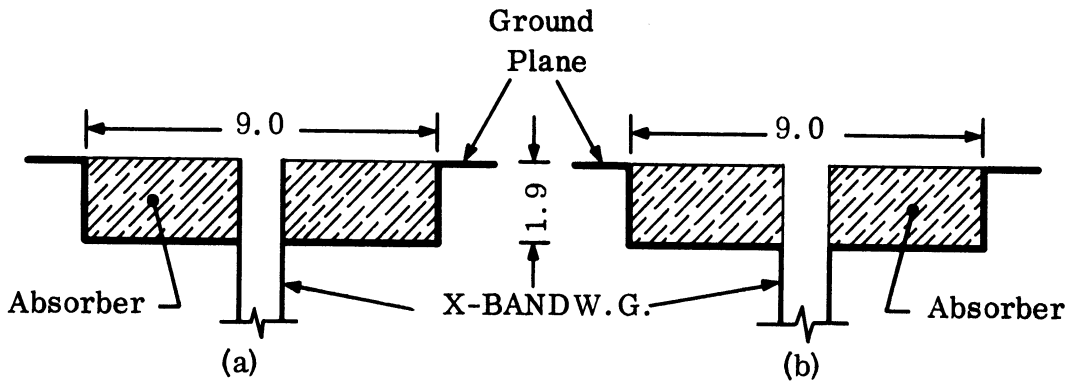

FIG. 2-5: GEOMETRY OF SLOT AND CAVITY (DIMENSIONS IN CM).

However, this results in a loss of maximum gain for the modified slot varying from 0.5 to 1.5 db depending upon the frequency. In case (b) a decoupling of 11 db across the X-band was measured, again with one slot only being modified (E-plane). The loss in maximum gain though was also significant varying from 8 db at 8 GHz to 4 db at 12 GHz.

The above information leads to the conclusion that absorbing materials alone used flush on a ground plane does not offer an acceptable means to achieve coupling reduction.

2.3.3 Absorber Wedges in E- and H-Sectoral Horns

The flared walls of an E-sectoral horn were lined with wedges of Eccosorb-CR absorber as shown in Fig. 2-6. Metal wedges of the same size were also available and were used in place of the absorber wedges to create a control horn. Both types of wedges were held in place by adhesion; silver paint was also used with the metal wedges to create the continuous, smooth metal surface.

The coupling between two identical E-sectoral horns, flush-mounted in a 12 ft square ground plane was greatly reduced when the flared walls of both horns were lined with the absorber wedges. In Fig. 2-7 the coupling between the absorber-lined horns is compared to the coupling of two sets of control horns, one pair with flare angles of 45^{o} and the other pair with a flare angle of 20^{o}.

Radiation patterns at three frequencies indicated that the absorber lined horn suffers a very substantial gain loss when compared with the control horn (flare angle 20^{o}). This loss is 16.5 db at 8.23 GHz, 11 db at 10.03 GHz and 9 db at 12.03 GHz. Typical radiation patterns at 10.03 GHz are shown in Fig. 2-8. This loss in gain is mainly due to antenna efficiency decrease since the radiation patterns indicate a small change in the antenna directivity. It should be noted that the decoupling obtained in this case, 31 db for the trans-

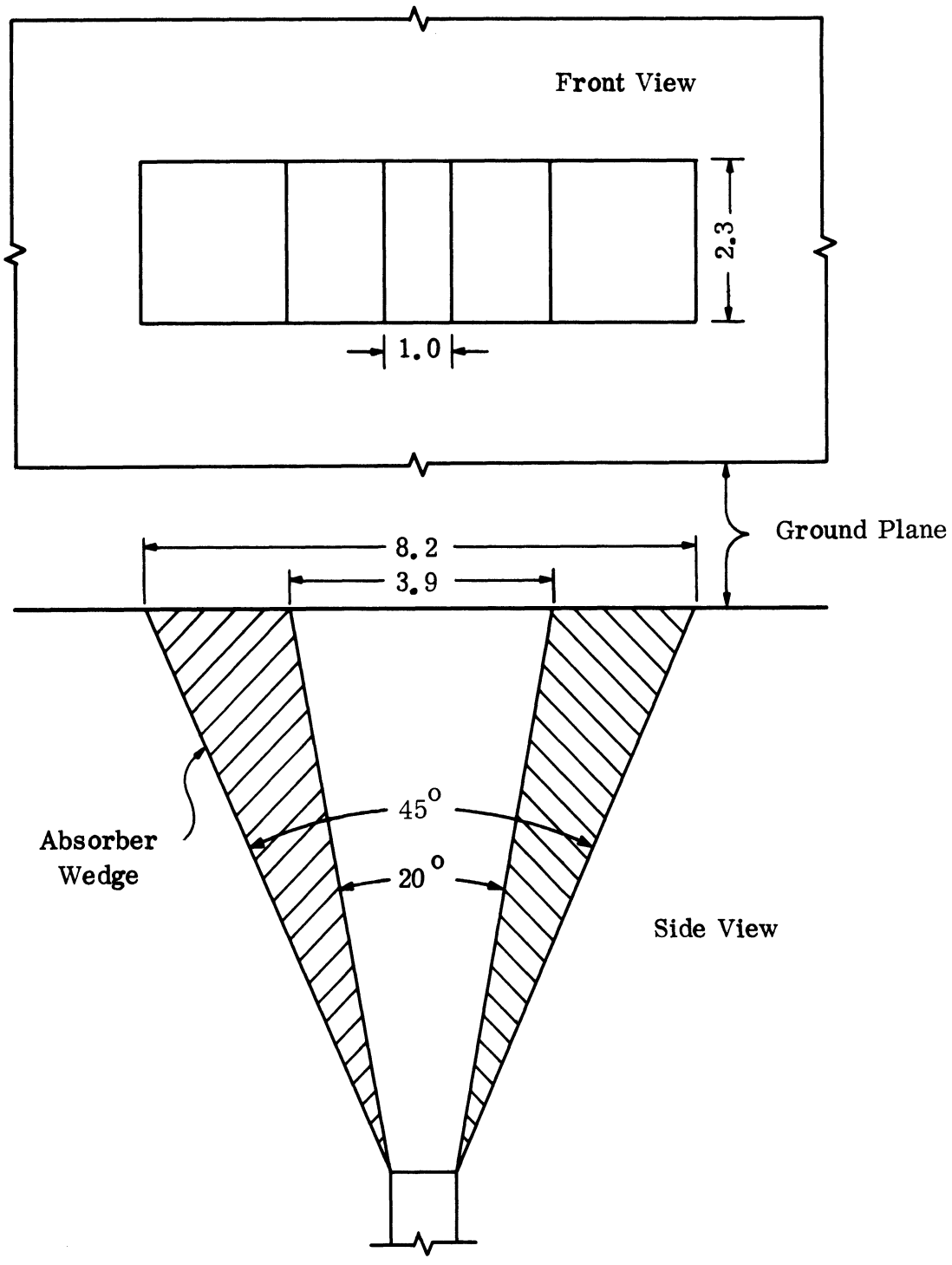

FIG. 2-6: FRONT AND SIDE VIEW OF E-SECTORAL HORN WITH ABSORBER WEDGES (DIMENSIONS IN cm)

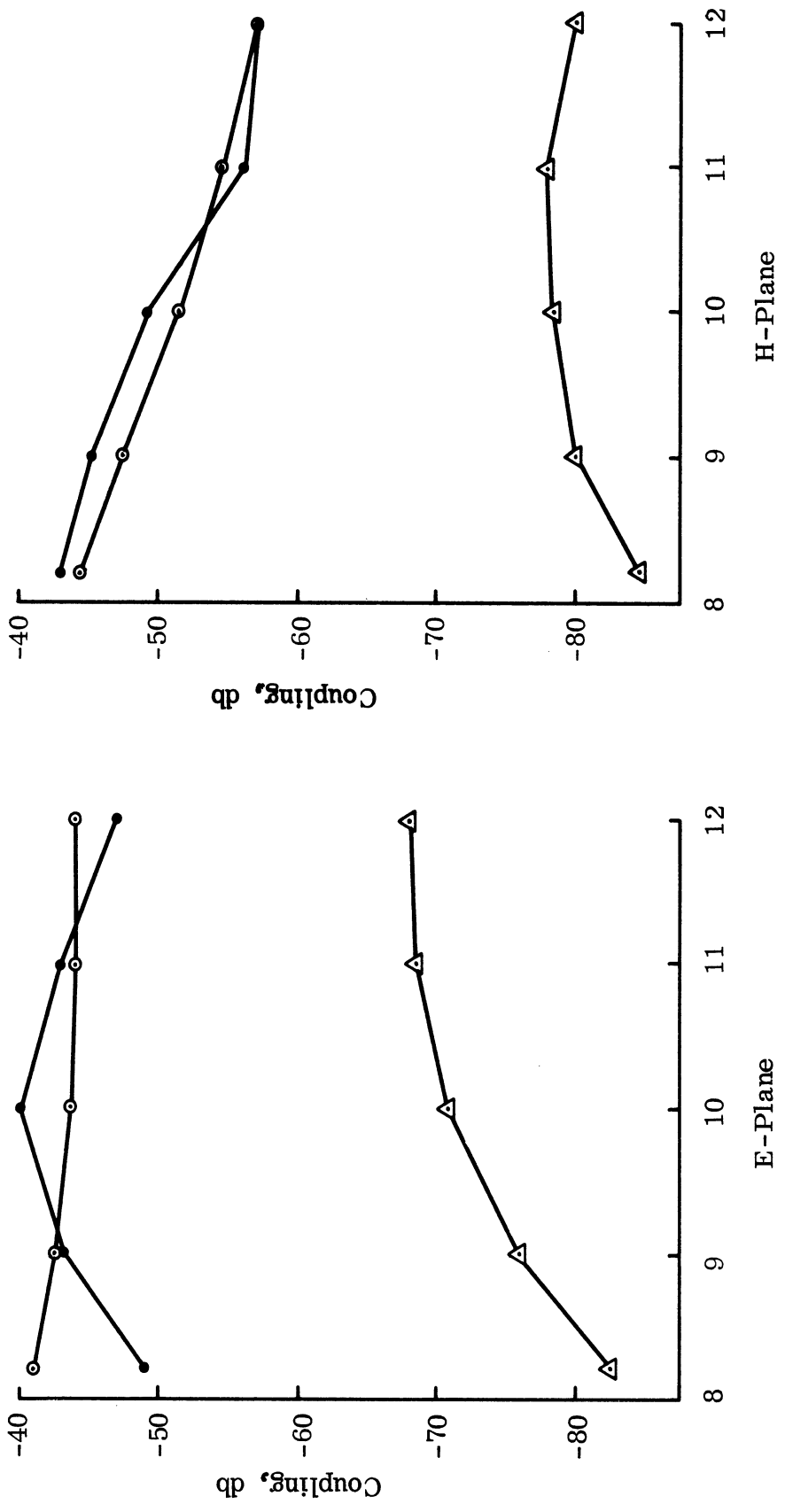

FIG. 2-7: E- AND H-PLANE COUPLING VERSUS FREQUENCY FOR TWO IDENTICAL E-SECTORAL HORNS FLUSH MOUNTED ON A COMMON GROUND PLANE. CENTER-TO-CENTER DISTANCE 11.43 cm. FLARE ANGLES: (—●—) 20°; (—⊙—) 45°; (—△—) 45° MODIFIED TO 20° BY THE USE OF ABSORBER WEDGES.

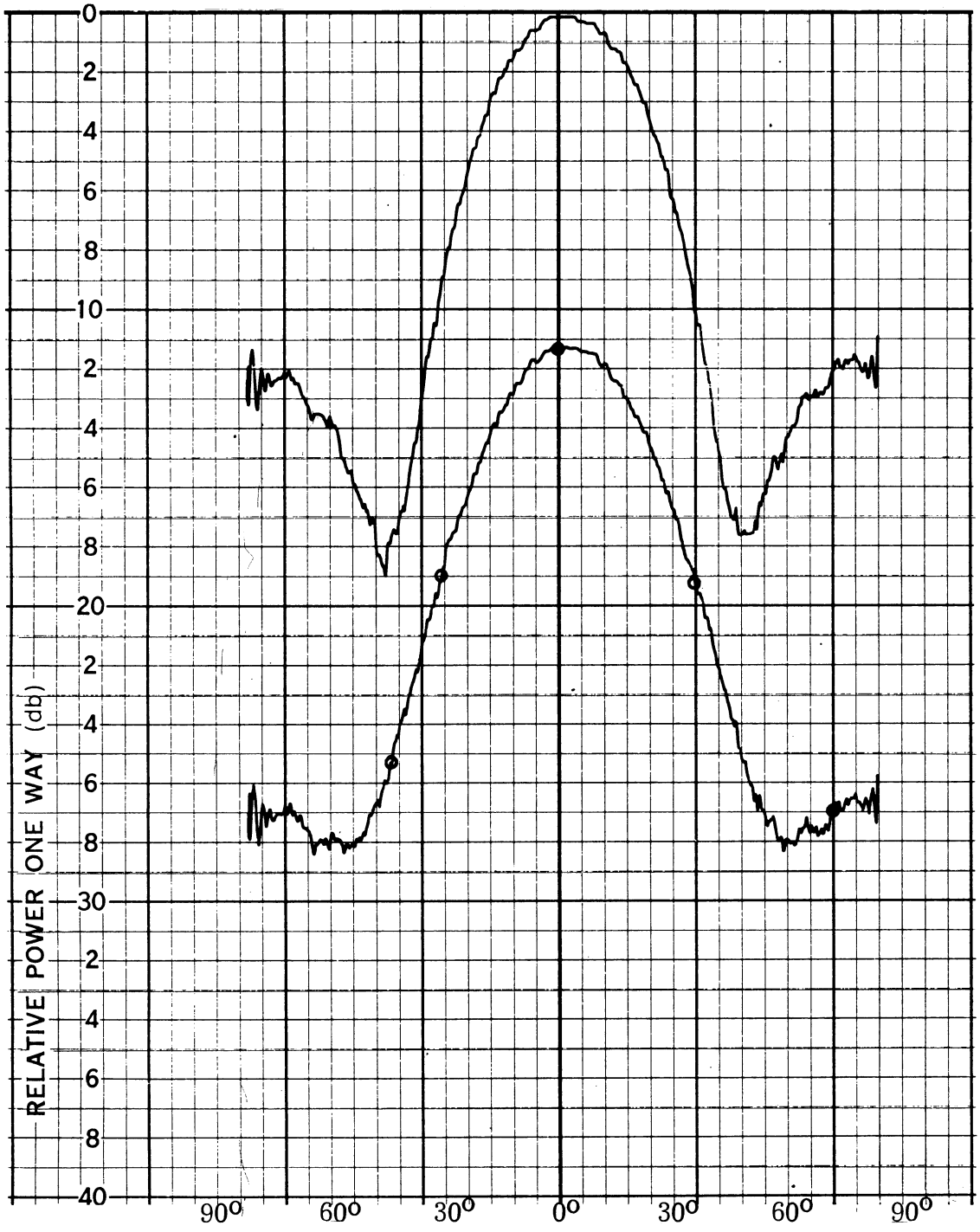

FIG 2-8a: E-PLANE RADIATION PATTERNS OF E-SECTORAL HORNS AT 10.03 GHz. (——) Flare angle 20°; (—o—) Flare angle 45° reduced to 20° by the use of absorber wedges.

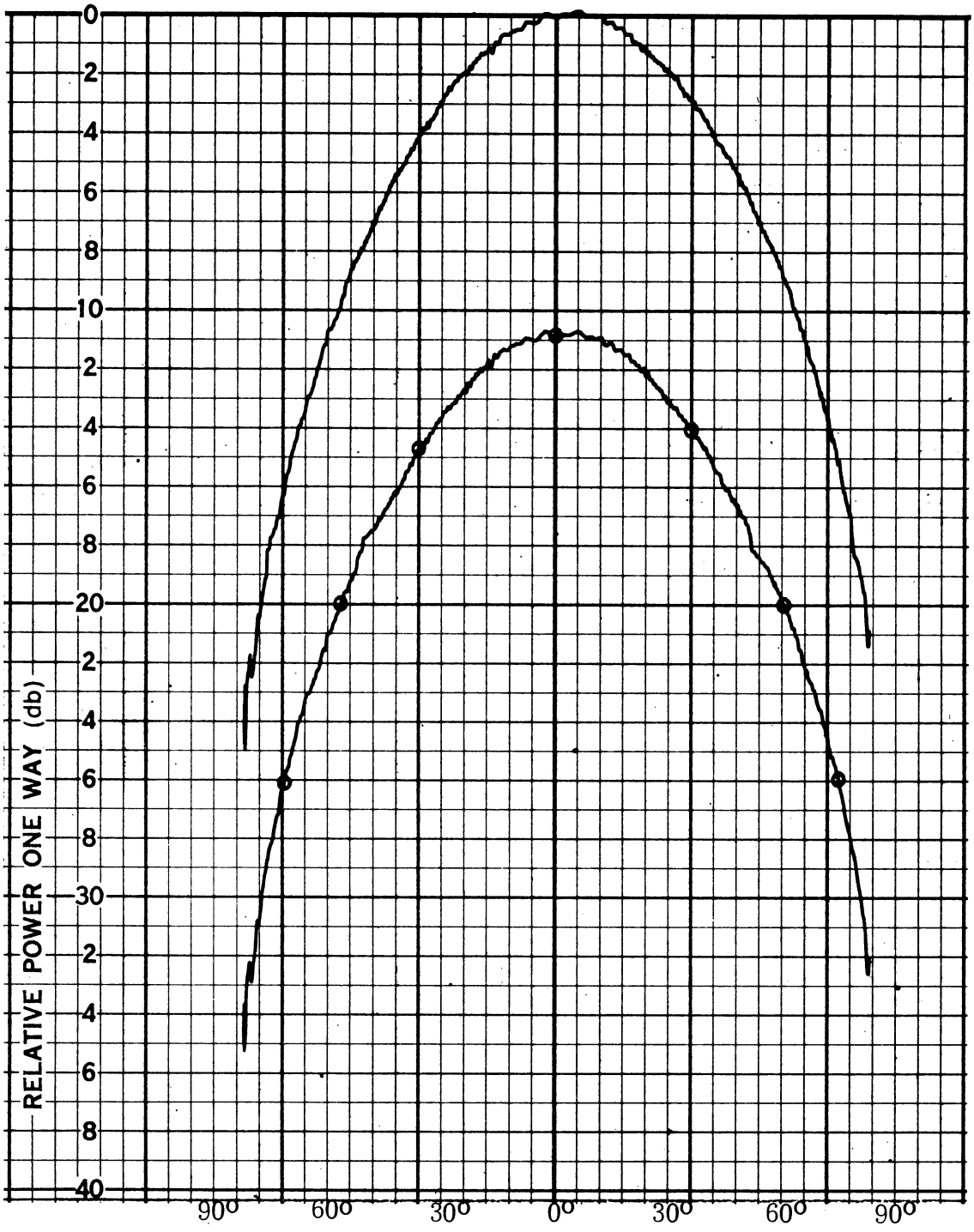

FIG. 2-8b: H-PLANE RADIATION PATTERNS OF E-SECTORAL HORNS AT 10.030 GHz. Flare angle (——) 20^{o}; (—o—) 45^{o} reduced to 20^{o} by the use of absorber wedges.

mitter-receiver system or 16.5 db per antenna, is still greater than the loss in maximum gain, i.e., the sidelobe reduction is greater than that of the mainlobe. Similar results were observed at 12.03 GHz; however, at 8.23 GHz the mainlobe was reduced more than the sidelobes (approximately 2 db).

The use of absorber wedges lining the flared walls of an H-sectoral horn affected coupling very little. The maximum coupling reduction observed was 3 db. This should be expected since the flared walls are in the H-plane and coupling is largely due to diffraction occurring at the aperture edges perpendicular to the antenna E-plane which were not affected by this modification.

In general, the loss in antenna gain observed in the E-sectoral horn and the relatively minor changes in the case of the H-sectoral horn make this method unsatisfactory for coupling reduction.

2.4 Antenna Recessed in Cavity with Absorber

2.4.1 E-Sectoral Horns

A new arrangement was designed and manufactured to permit the placing of absorbing material around the aperture of an E-sectoral horn in a way similar to that described earlier in section 2.2.2. In the new arrangement, however, the horn aperture was recessed in a shallow cavity which was partially filled with absorbing material, creating a structure resembling a compound horn, (see Fig. 2-9). The advantage of this structure is that it can be mounted flush with the ground plane surface. The absorber initially used in the cavity was Eccosorb MF-124.

A comparison of the maximum gain of the modified horn antenna with that of the original E-sectoral horn, used as a control antenna, is shown in Fig. 2-10. The comparison shows that the modified antenna suffers a loss in gain at parts of the X-band of the order of 0.5 db. Radiation patterns have been recorded at three frequencies: 8.23 GHz, 10.03 GHz and 12.03 GHz. A typical

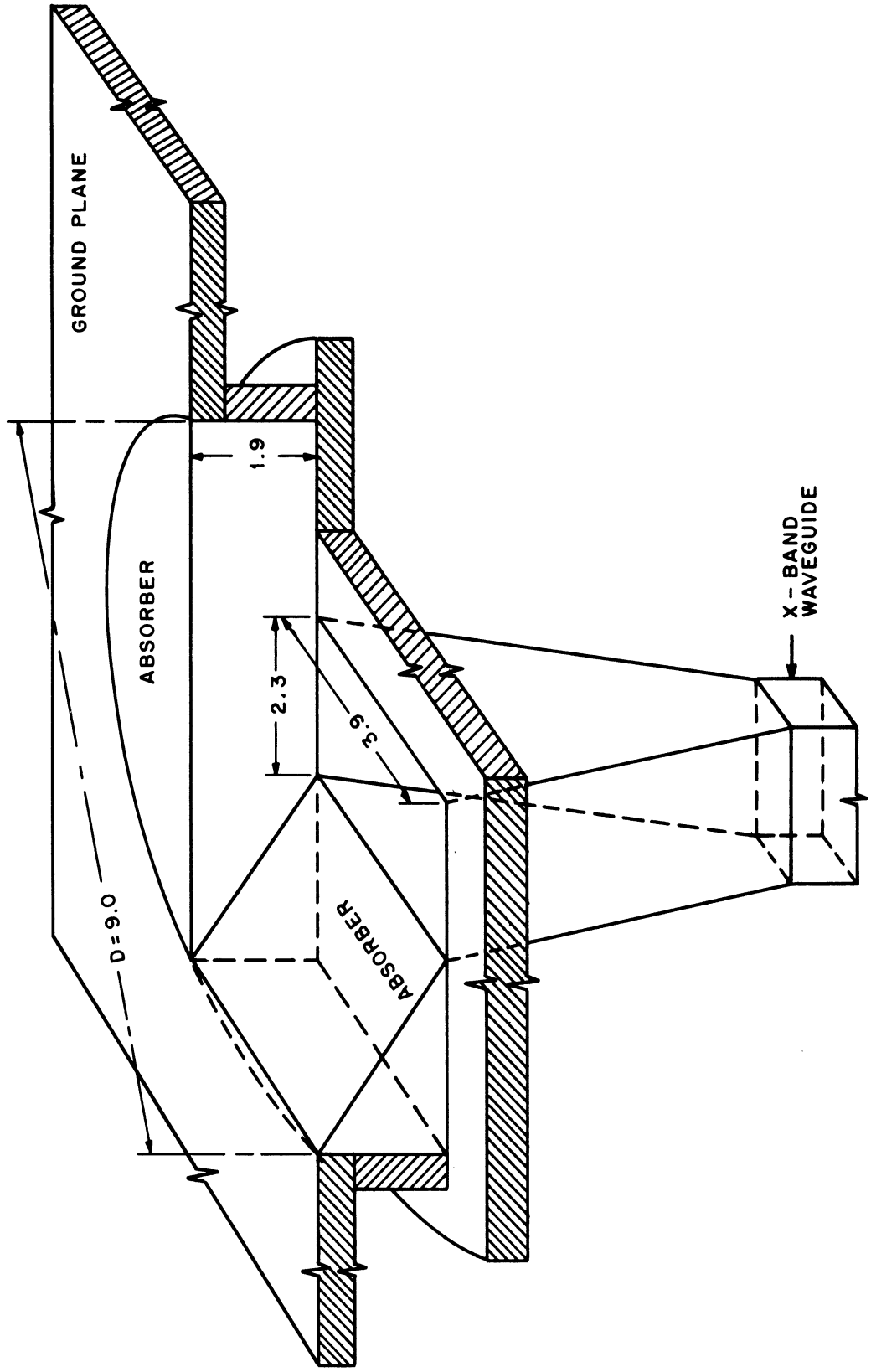

FIG. 2-9: RECESSED E-SECTORAL HORN AND ABSORBER GEOMETRY
(Dimensions in cm)

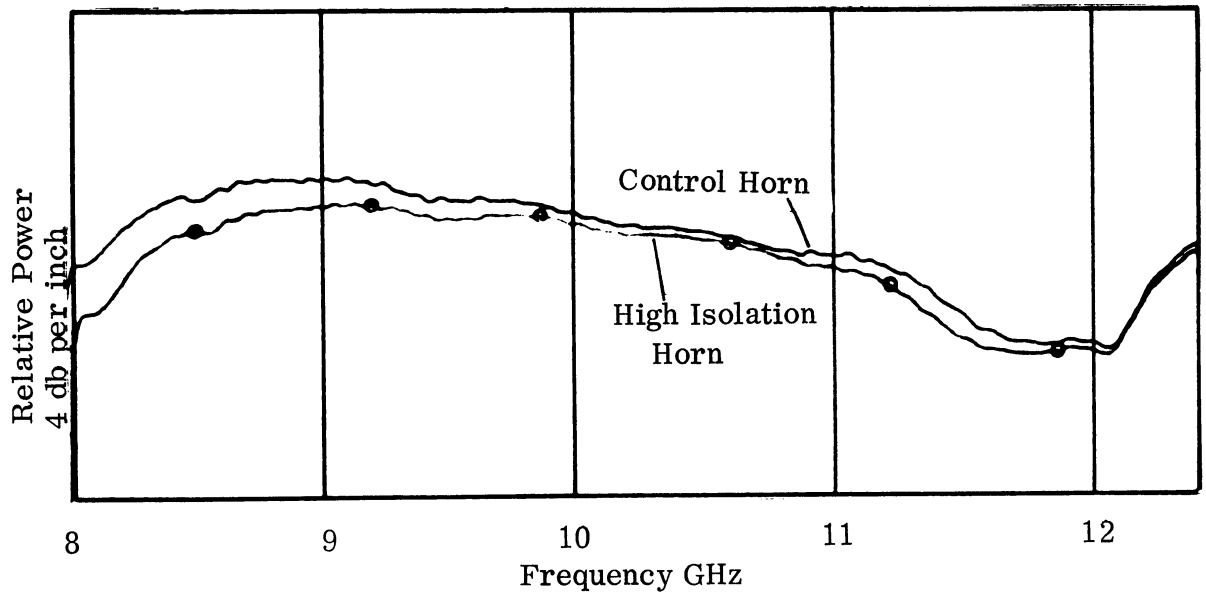

FIG. 2-10: MAXIMUM GAIN VERSUS FREQUENCY FOR E-SECTORAL HORNS

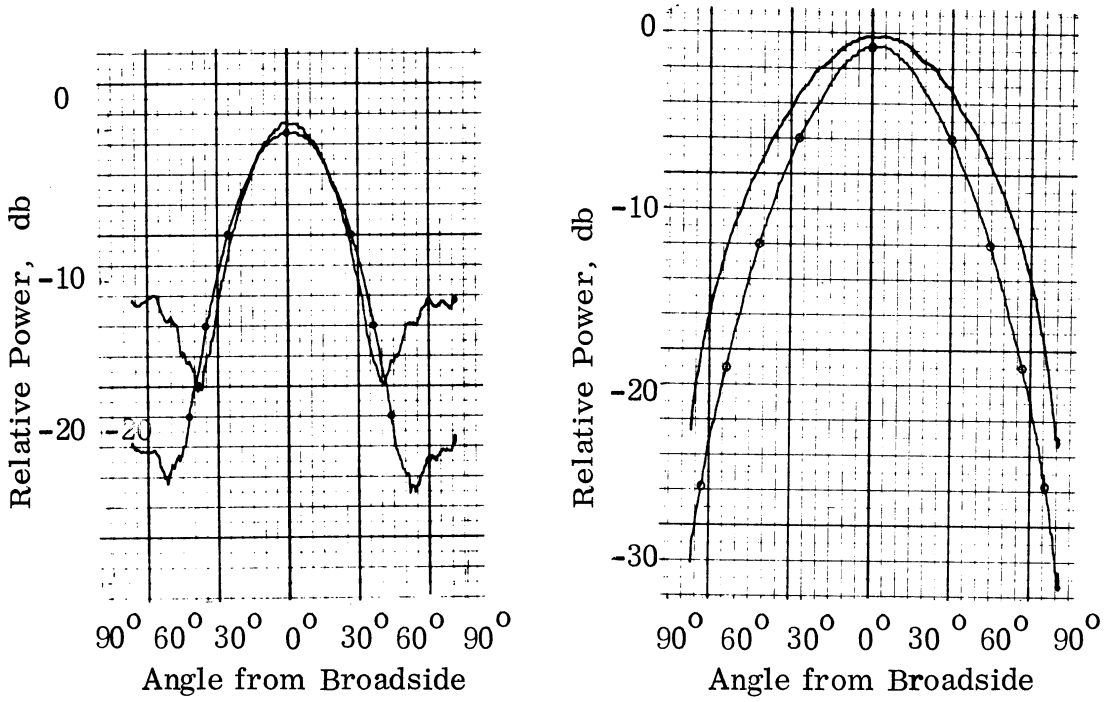

FIG. 2-11: E- AND H-PLANE RADIATION PATTERNS OF E-SECTORAL HORNS AT 10 GHz. (——) Control horn; (—o—) High isolation horn.

pattern at 10 GHz (Fig. 2-11), where the strongest coupling has been observed, shows that the presence of the absorber leaves the mainlobe practically unchanged, while it reduces the sidelobes by approximately 9 db (Lyon et al, August 1966).

Coupling patterns versus frequency for both the modified (high isolation) horn and the control horn are shown in Fig. 2-12. It should be noted that the high-isolation modification was applied only to the transmitting horn, i.e., the same receiver was used for all the coupling patterns of Fig. 2-12. Therefore, according to the symmetry argument, twice as much decoupling should be expected if both transmitter and receiver were similarly modified. Thus for E-plane coupling the increase in isolation would be 18 db while for H-plane, 15 db.

Since the swept-frequency generator output varied with frequency (by $\pm$ 0.75 db) constant coupling levels are no longer horizontal. A reference line corresponding to - 34 db below direct coupling is shown on top in Fig. 2-12. This reference level was obtained as described in the introduction.

Patterns of coupling versus receiver orientation were also measured but are not presented here since they do not contain any new information beyond that in previously published data (Lyon, et al, April 1966), except of course for the overall coupling level.

A different absorber (Eccosorb-CR) was also used in the cavity, in exactly the same arrangement. The decoupling obtained in the E-plane was of the same order of magnitude with that obtained previously by using Eccosorb MF-124 material; in the H-plane the Eccosorb-CR type material turned out to be less effective by as much as 3 db.

Next, the absorbing material sectors and wedges were covered completely with aluminum foil to test how much, if any at all, of the decoupling obtained by this modification was simply due to the different geometry. In this case the

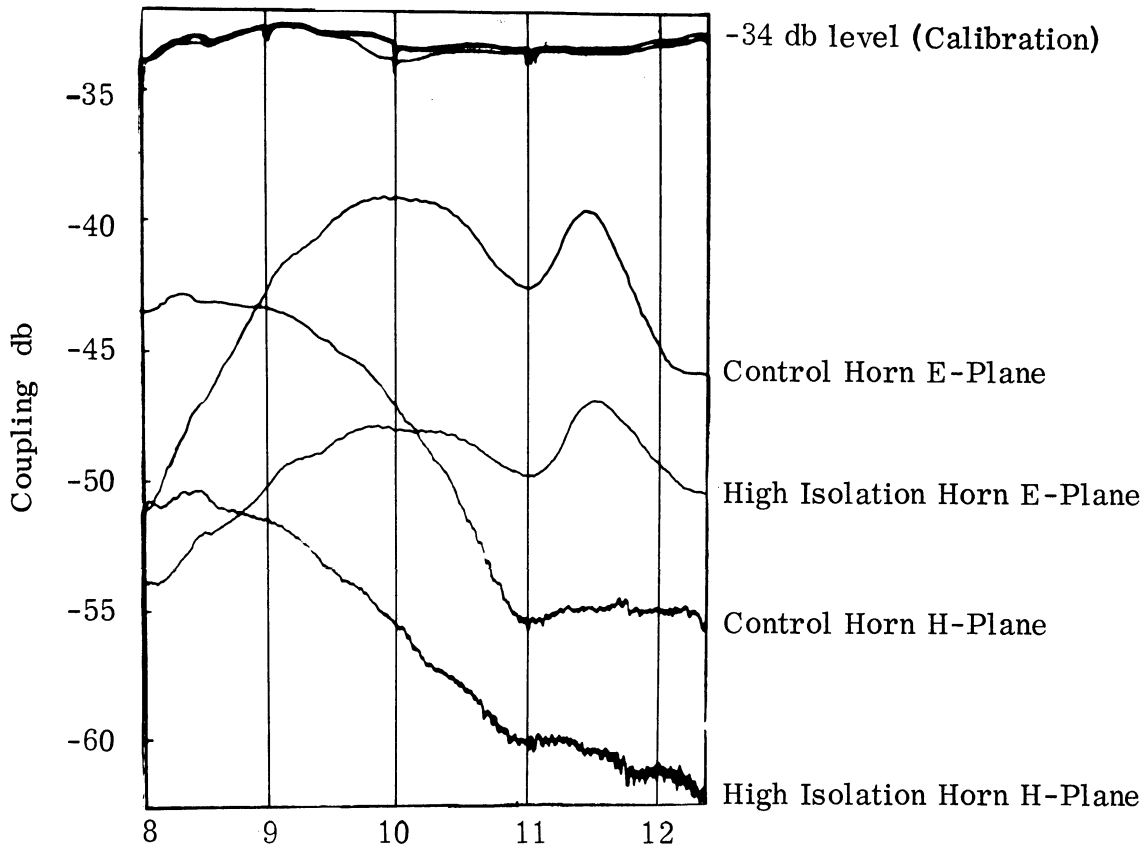

Fig. 2-12: E- AND H-PLANE COUPLING VERSUS FREQUENCY FOR TWO E-SECTORAL HORNS SPACED 11.43 cm. (Eccosorb MF-124 Absorber).

swept frequency E-plane coupling measurement revealed that with the metal wedges and sectors in the cavity the coupling was at ± 4.5 db, depending upon the frequency, from the coupling level of the control horn. Therefore, the absorbing material is actually responsible for the coupling reduction described in this section.

2.4.2 Broadband Slots

A slot was recessed in a shallow cavity which was partially filled with absorber. The cavity dimensions and absorber geometry and the type are the same as the ones used with the E-Sectoral Horn (Fig. 2-9). This modification was found to increase the maximum gain of the slot by approximately 0.5 to 1.0 db throughout the X-band while decreasing the radiation along the surface of the ground plane. Typical radiation patterns taken at a frequency of 10 GHz are presented in Fig. 2-13.

The E-plane coupling between a modified and a plain slot was compared to the coupling between two plain slots. A reduction of maximum coupling by 6.5 db was observed over the X-band of frequencies (Lyon et al, August 1966). If both antennas were similarly modified a 13 db coupling reduction would be expected.

In general, the method of recessing an antenna in a cavity partially filled with absorbing material, properly placed, was found to offer the most effective use of absorbing materials for coupling reduction purposes. The method produced significant decoupling without affecting adversely any of the antenna properties. The flush mounting requirement is satisfied, so that this modification can be used in aerospace antennas.

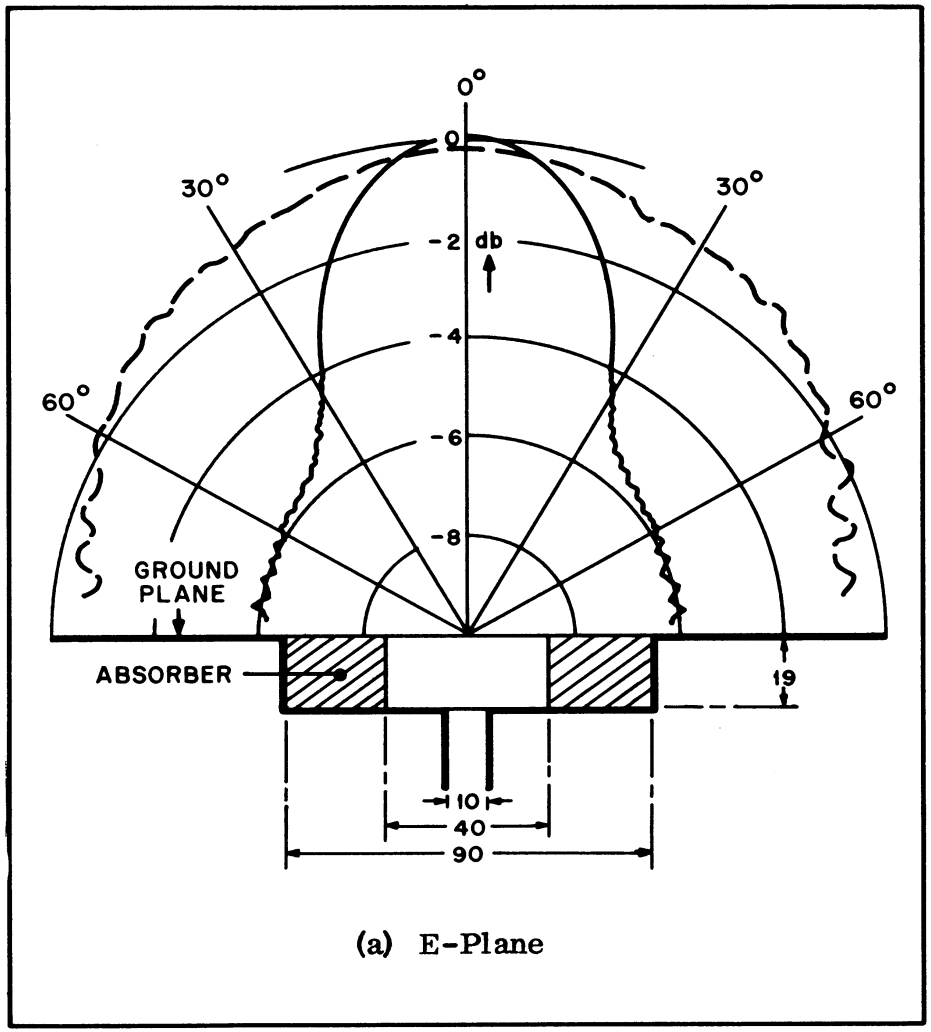

(a) E-Plane

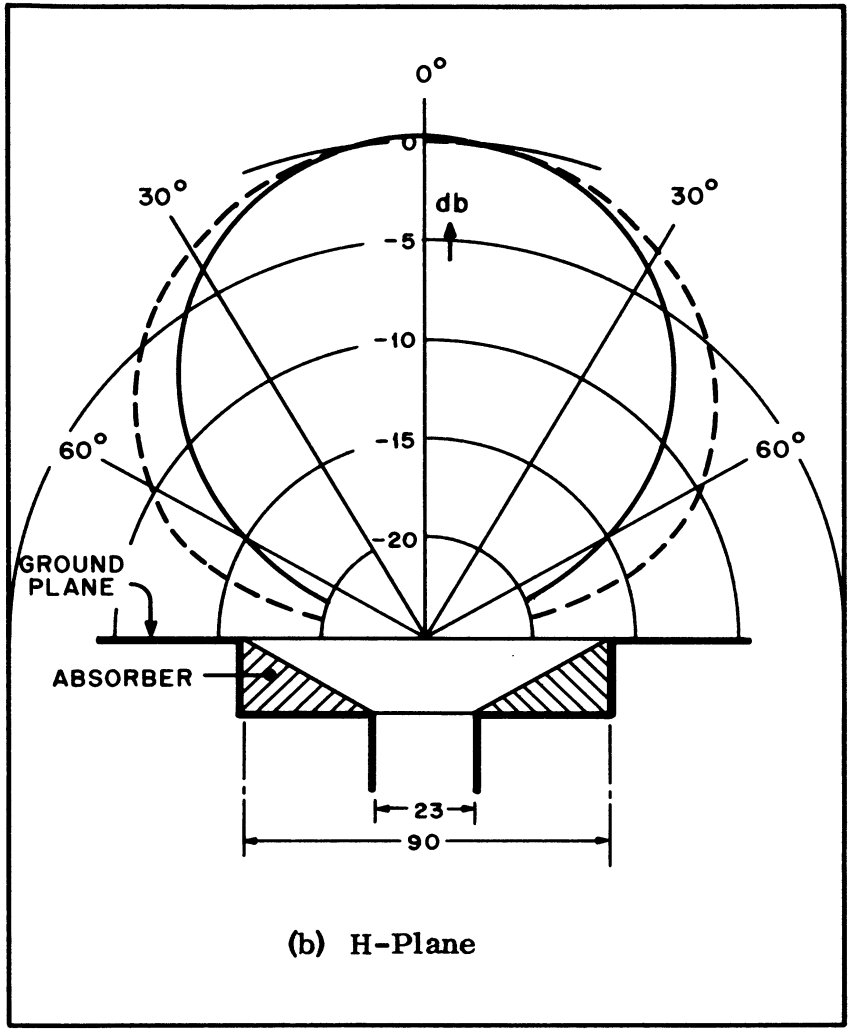

(b) H-Plane

FIG. 2-13: SLOT IN CAVITY WITH ABSORBER (Eccosorb MF-124) ANTENNA GEOMETRY AND FAR-FIELD RADIATION PATTERNS AT 10 GHz (Dashed Lines Show Corresponding Radiation Patterns of Plain Slot Dimensions in cm).

III

SURFACE REACTIVE LOADING *

3.1 Introduction

The technique of reactive loading consists of modifying a part or the whole of the surface of a perfectly conducting body to create a surface impedance different than zero. This modification has been found useful in controlling the scattering behavior of a diffracting object. At microwave frequencies this impedance may be created either by coating the surface with absorbing materials or by cutting in the metal surface one or more slots backed by a cavity. In the former case the impedance has both a resistive and a reactive part. In the latter, the resistive part is either zero (for a perfectly conducting body) or very small (for a metal of high but finite conductivity) and can be neglected compared to the much larger reactive part. In this case then, it is proper to speak of "reactive" rather than "impedance" loading. The term "isolated reactive loading" is used to include all cases where the loading is restricted along one dimension of the surface as opposed to the case where the loading extends over some area. The term "continuous reactive loading" will be used for the latter case.

The scattering problem with isolated reactive loading has been studied by theory and experiment for the case of the cylinder (Chen and Liepa, 1964) and the sphere (Senior, 1965). Experimental results have also been reported for continuous reactive loading of ogives (Lawrie and Peters, 1966).

Reactive loading of the ground plane near a microwave antenna has also been investigated as a means of creating end-fire antennas (Rotman, 1951; Fernando and Barlow, 1956). A non-perfect conductor has a generally small surface impedance given by

---

* The material of this chapter, except for section 3.3, is part of the PhD thesis of Mr. C.J. Digenis.

$$Z_s = (1 + j) \frac{\omega \mu \delta}{2} \tag{3.1}$$

where δ is the skin depth, μ the permeability and ω the angular frequency. An increased surface reactance was found to be desirable in order that high frequency energy could propagate along the interface between conductor and air without radiation. Corrugated surfaces have been used as an alternative to dielectric coating to produce an enhanced surface reactance. A corrugated metal surface has a surface reactance X_s, given to a first approximation by

$$X_s = \frac{w}{s} \eta \tan (kd) \tag{3.2}$$

where w is the slot width, s the slot center-to-center spacing, d the depth of the cavity under the slot, k the propagation coefficient for free space and η the free space characteristic impedance, provided that there are at least three corrugations per wavelength along the surface. For corrugations cut in metal the resistive component of the surface impedance is relatively small, compared to the reactive component, and can be neglected.

By appropriate choice of the parameters involved, corrugations can also be used to create a capacitive surface reactance which does not allow the existence of a surface wave. Thus the energy would be radiated rather than propagated along the surface. This suggests a method to reduce the antenna sidelobes along the ground plane and consequently decrease the coupling between antennas that are mounted on a common metal surface. The frequency dependence of X_s imposes a restriction on the bandwidth over which the method is effective. However this disadvantage is offset to some extent by the fact that coupling is also frequency dependent. In the case where the

antennas are so oriented that their respective E-planes coincide, the coupling is reduced at a rate of 6 db per octave of frequency while when the H-planes coincide the reduction is 12 db per octave provided that the distance between the two antennas is greater than one wavelength.

The action of continuous reactive loading as used in end-fire antennas has been explained in terms of the theory of surface waves. The use of capacitive reactive loading, proposed here, excludes the possibility of existence of a surface wave; therefore a new mathematical model has to be used to explain the antenna radiation in the presence of the capacitive loading. A number of applications are presented in this report showing the amount of coupling reduction that can be obtained for different antenna types and also the effect on other antenna characteristics. A theoretical treatment of a two-dimensional model with certain size limitations has already been presented (Lyon et al, May 1966, Chapter 2).

3.2 Isolated Reactive Loading

3.2.1 Loading with a Single Slot

The type of antenna that was examined is the open ended waveguide. Such slot antennas are often found flush mounted in close proximity. In such cases the low directivity which characterizes this type of antenna gives rise to a strong interference which is due to the mainlobe of the pattern and not just weak sidelobes.

A single, circumferential trench (choke) was used to create a capacitive impedance (Fig. 3-1). The width of this choke was very small compared to both the depth and the free-space wavelength so that higher order modes inside would be quickly attenuated. Two slot antennas of a transmitter-receiver system each surrounded by a single choke of depth equal to a quarter wavelength

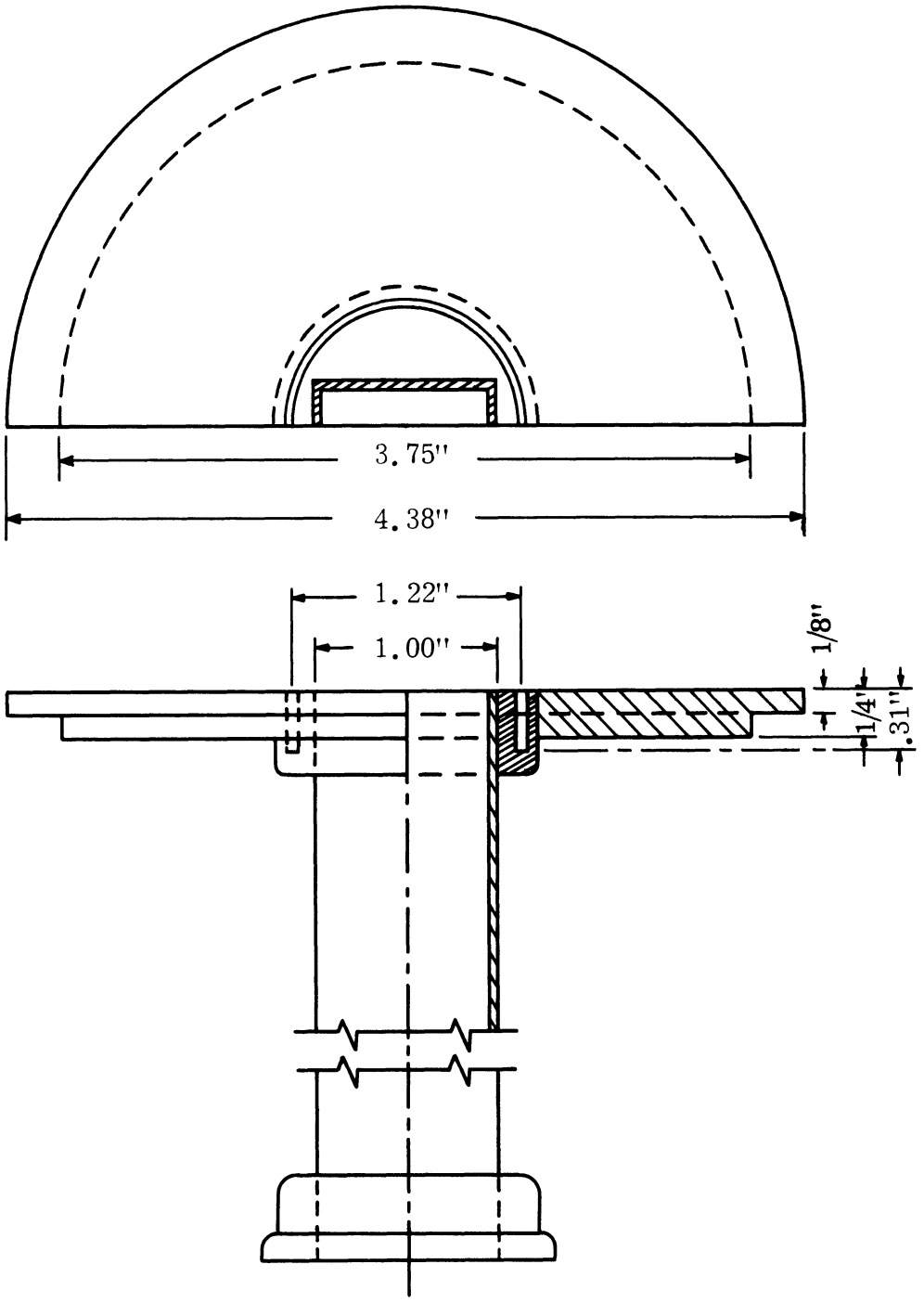

FIG. 3-1: SLOT ANTENNA WITH CHOKE.

at 8.0 GHz were manufactured and tested at X-band frequencies. The coupling measured was compared with the one in the case of two slots without chokes in the same geometry. It was found that maximum decoupling (approximately 9 db) occurred at 8.2 GHz, the lowest frequency used in the measurements. At 10 GHz, however, the decoupling was reduced to approximately 4 db.

In the case where only one of the two slots had a choke it was found that the decoupling was not dependent upon whether the choke was on the transmitter or the receiver. The decoupling observed was equal to 50 percent of that observed when both antennas were equipped with chokes.

In order to examine the behavior of the choke at lower frequencies, the trench depths of the transmitter and receiver were modified so that they would be equal to a quarter wavelength at 10.0 GHz and 9.2 GHz respectively. This was realized by the addition of two copper rings which were covered with silver paint. The dimensions of the trenches were then as follows:

Depth: $d_t = 0.75$ cm

$d_r = 0.82$ cm

Width: $w = 0.16$ cm (1/16") .

The E-plane coupling versus frequency for this case is shown in Fig. 3-2. In the same figure the coupling of two slots without a surrounding trench is given as a reference. Also the coupling reduction when only the transmitting slot is surrounded by a trench (depth 0.75 cm) is given. In this case the trench depth is equal to one-quarter of the free space wavelength at 10.0 GHz. The coupling reduction, however, is largest at 9.4 GHz. At this frequency $d = 0.235\lambda$.

Patterns of coupling variation, when one slot is fixed and the other rotated about the waveguide axis, were obtained for the cases of E- and H-plane coupling

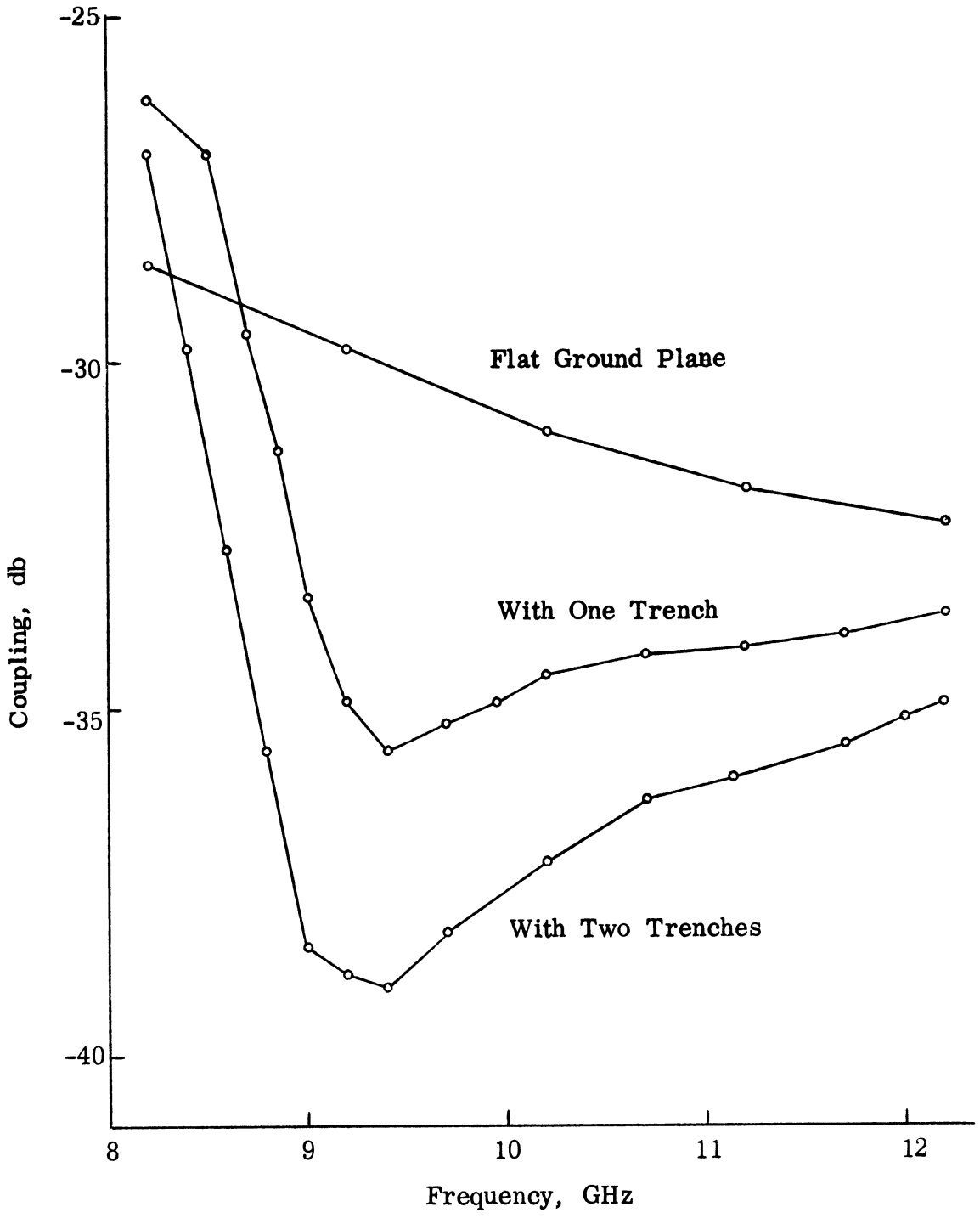

FIG. 3-2: E-PLANE COUPLING OF TWO SLOTS SPACED 11.4 CM.

(geometry shown in Fig. 3-3), and compared with similar patterns for two plain slots. Such patterns are shown in Figs. 3-4 and 3-5 for a frequency of 10.03 GHz. Figure 3-4 shows that, for E-plane coupling, the decoupling obtained with the choke is practically constant, i.e., independent of the relative orientation of one slot with respect to the other.

The coupling increase or decrease shown in Fig. 3-2 is due to corresponding changes in the antenna radiation patterns. Such patterns were measured at several frequencies and two representative patterns are shown in Figs. 3-6 and 3-7. The trench with d = 0.75 cm was used for these patterns. The two frequencies shown were selected so that one corresponds to $d < \lambda/4$ and the other to $d \geq \lambda/4$. The corresponding patterns for a slot in a flat ground plane are shown for gain comparison.

These figures show that although the shape of the H-plane radiation pattern is very little affected, the shape of the E-plane pattern is greatly affected and shows a substantial improvement in gain (at 10.03 GHz) and in directivity. At the frequency of 8.23 GHz, however, which is outside the cutoff frequency range, the antenna gain is reduced.

3.2.2. Loading with Four Slots

In order to obtain greater coupling reduction, another antenna was constructed with an X-band waveguide-fed slot (2.3 cm by 1 cm) surrounded by four circumferential trenches (Fig. 3-8). The trenches were spaced radially by 0.8 cm, with the one closest to the slot aperture having a radius of 1.9 cm. Each trench had a depth of 0.914 cm, corresponding to $\lambda/4$ at 8.2 GHz, and a width of 0.17 cm. This antenna was mounted flush in a 12 ft square aluminum ground plane.

The antenna gain was measured in the range 8 to 12.4 GHz by sweeping the frequency and compared to the gain of a similar slot without the reactive loading.

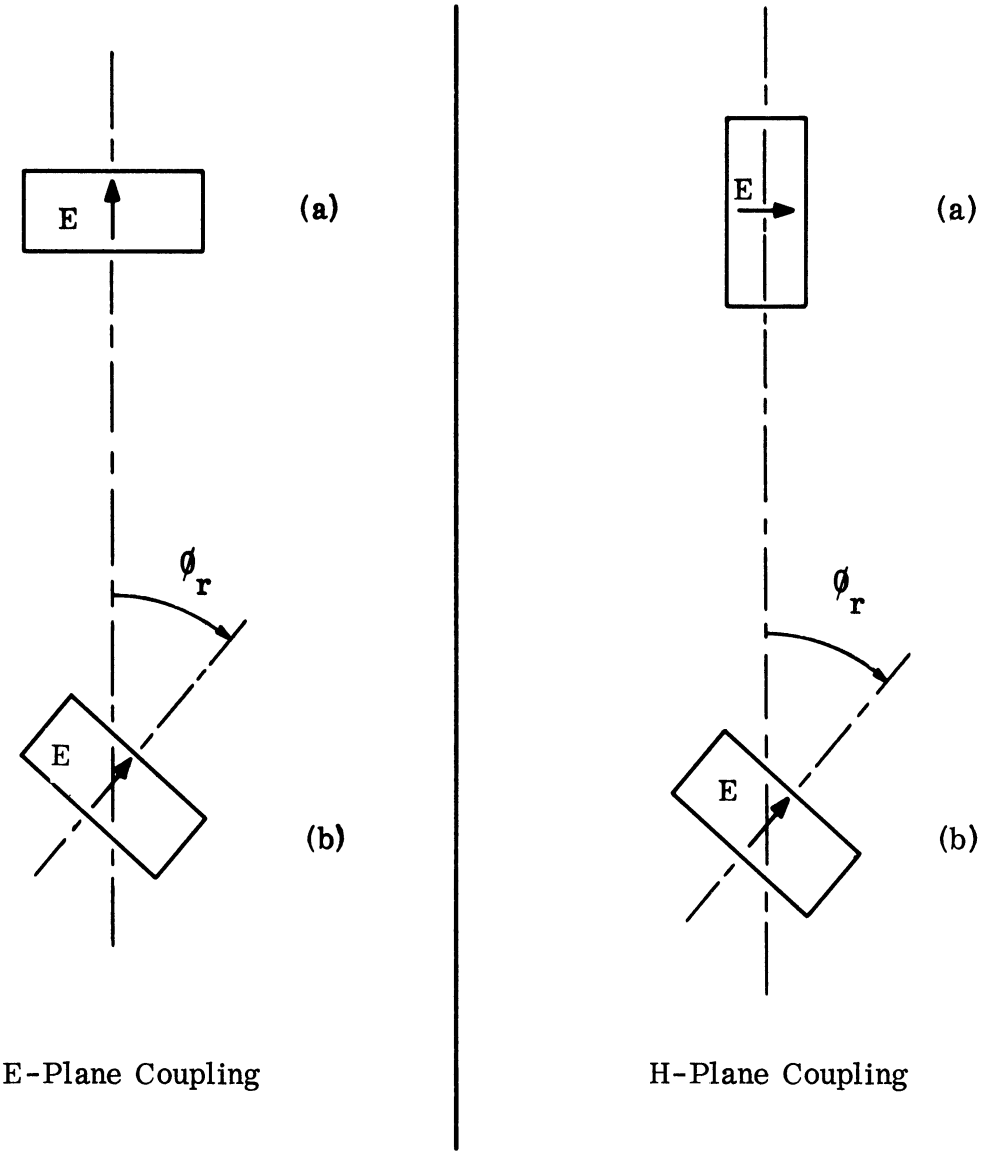

FIG. 3-3: GEOMETRY OF TWO SLOT ANTENNAS SHOWING E- AND H-PLANE COUPLING. (a) TRANSMITTER-FIXED POSITION (b) RECEIVER-ROTATABLE.

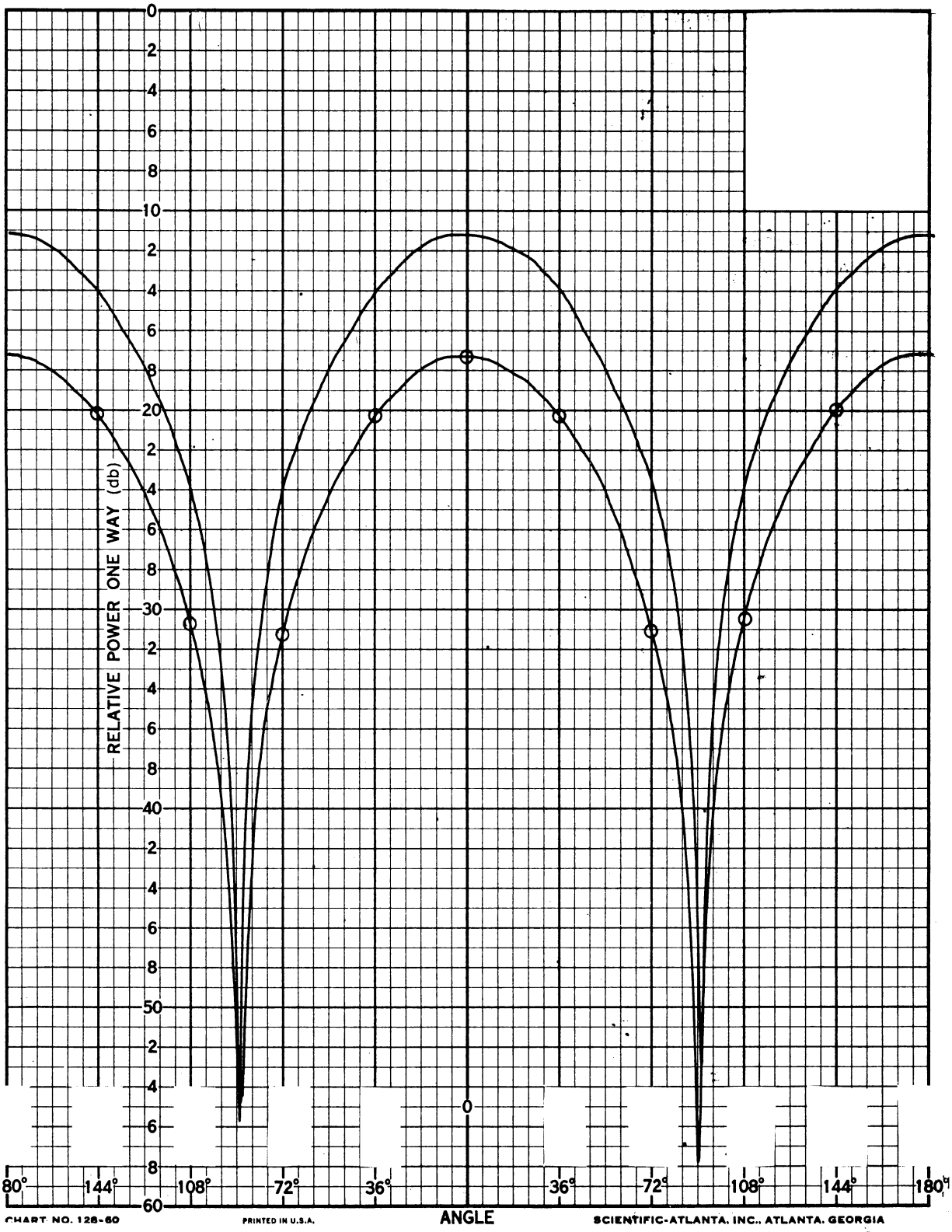

FIG. 3-4: E-PLANE COUPLING PATTERNS FOR TWO SLOTS ON A COMMON GROUND PLANE, (—) plain slots; (-o-) slots surrounded by chokes. f = 10.030 GHz, D = 11.43 cm, 0 = -20 db.

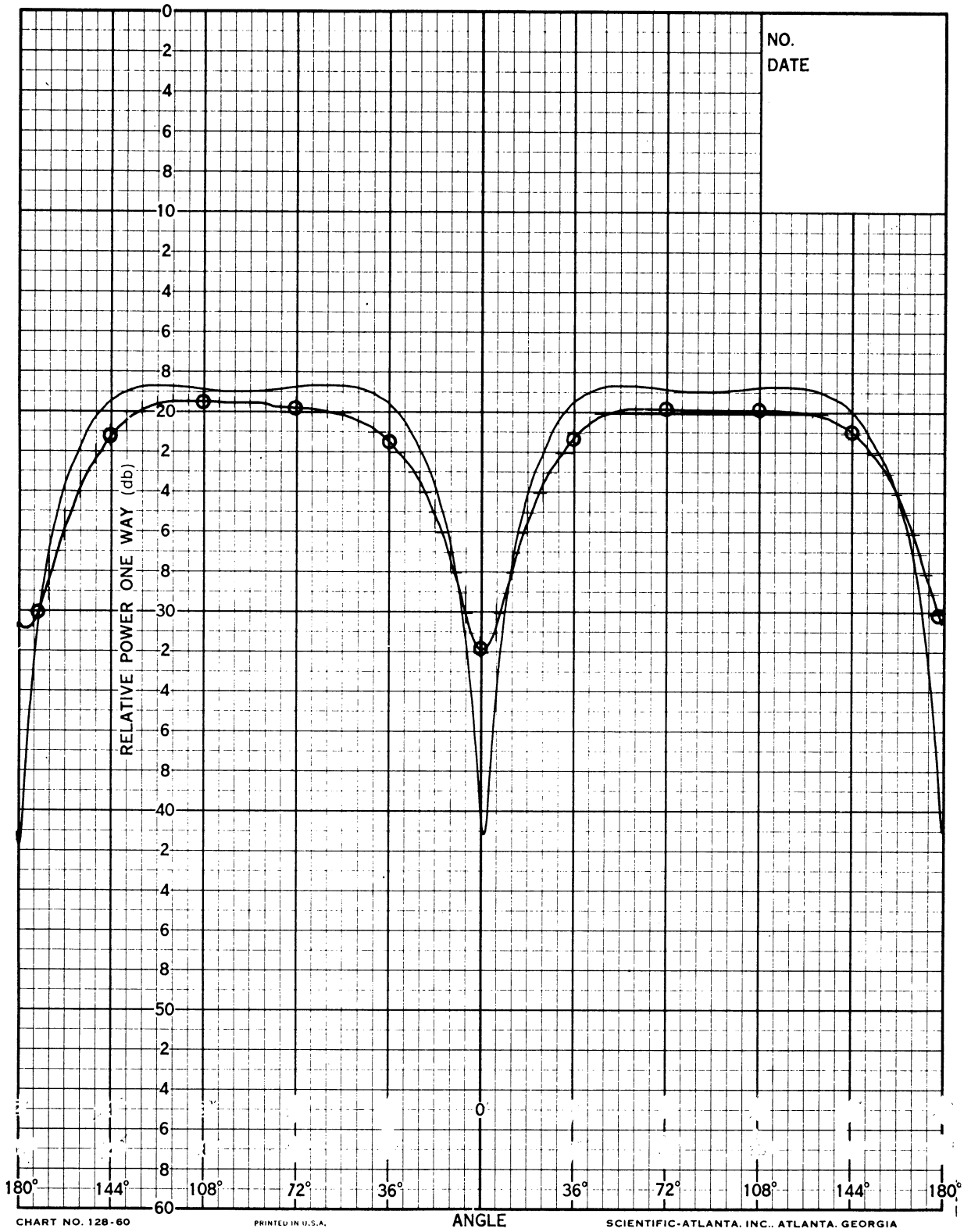

FIG. 3-5: H-PLANE COUPLING PATTERNS FOR TWO SLOTS ON A COMMON GROUND PLANE, (—) plain slots; (-o-) slots surrounded by chokes. f = 10.030 GHz, D = 11.43 cm, 0 = -40 db.

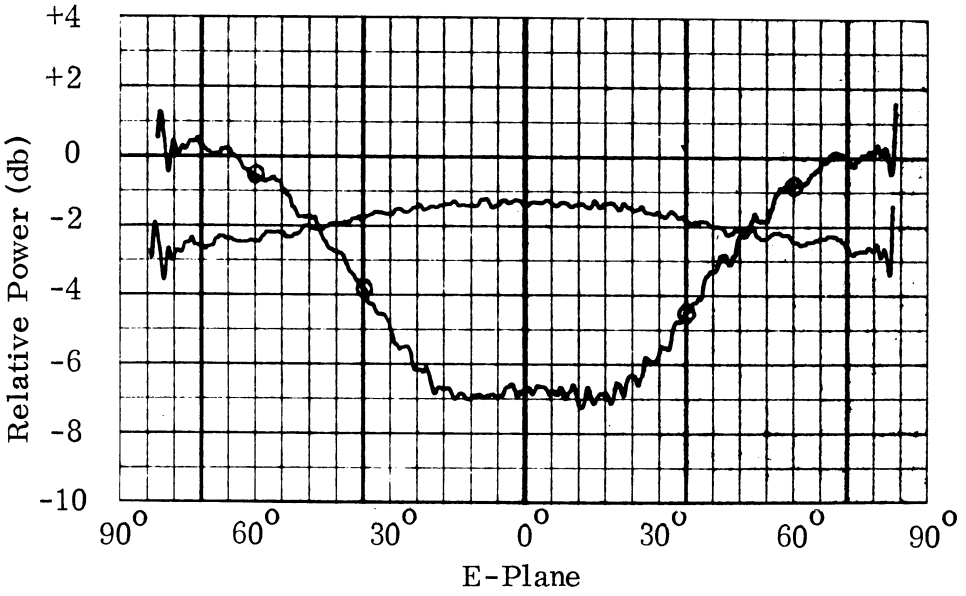

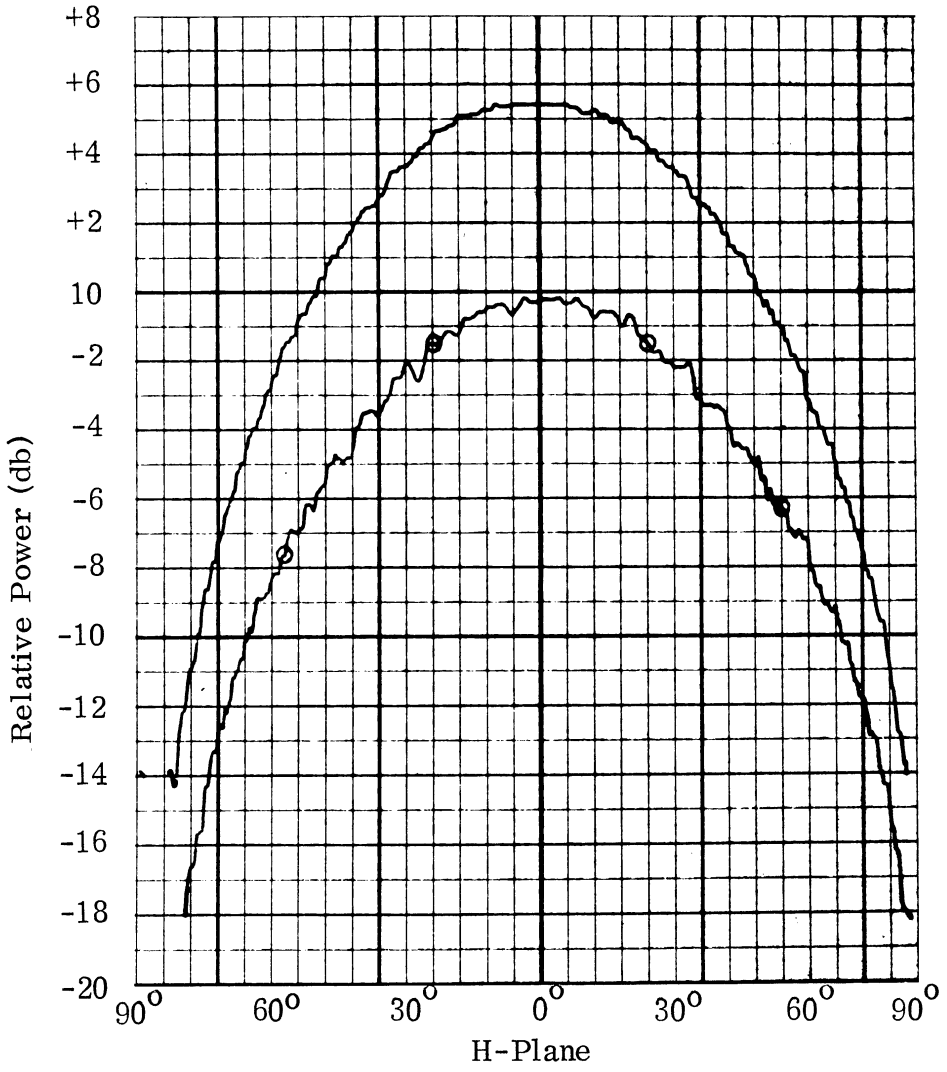

FIG. 3-6: E- AND H-PLANE RADIATION PATTERNS OF PLANE SLOT (——) AND THE SLOT SURROUNDED BY A CHOKE (—o—) AT 8.23 GHz.

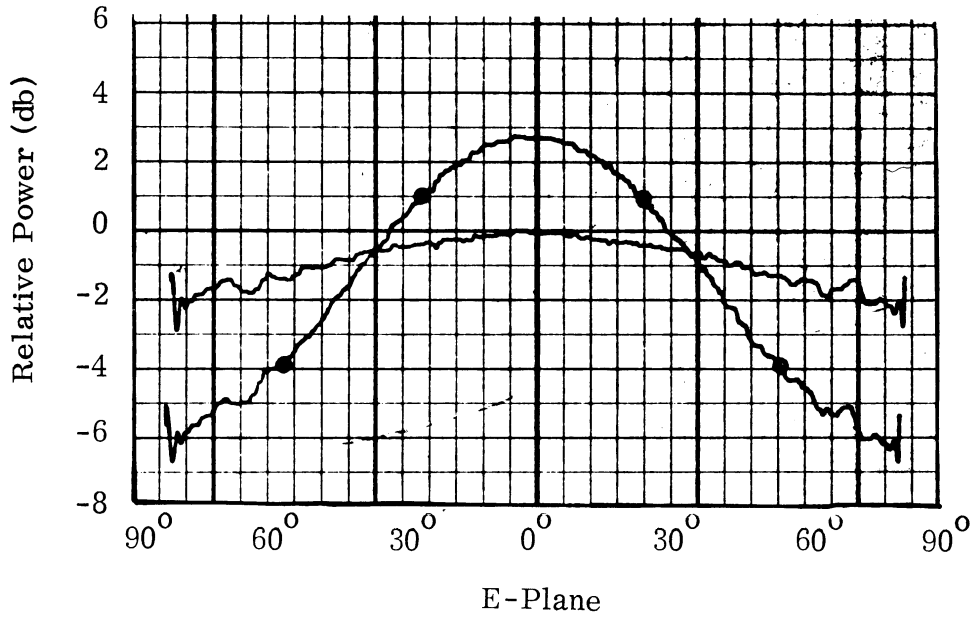

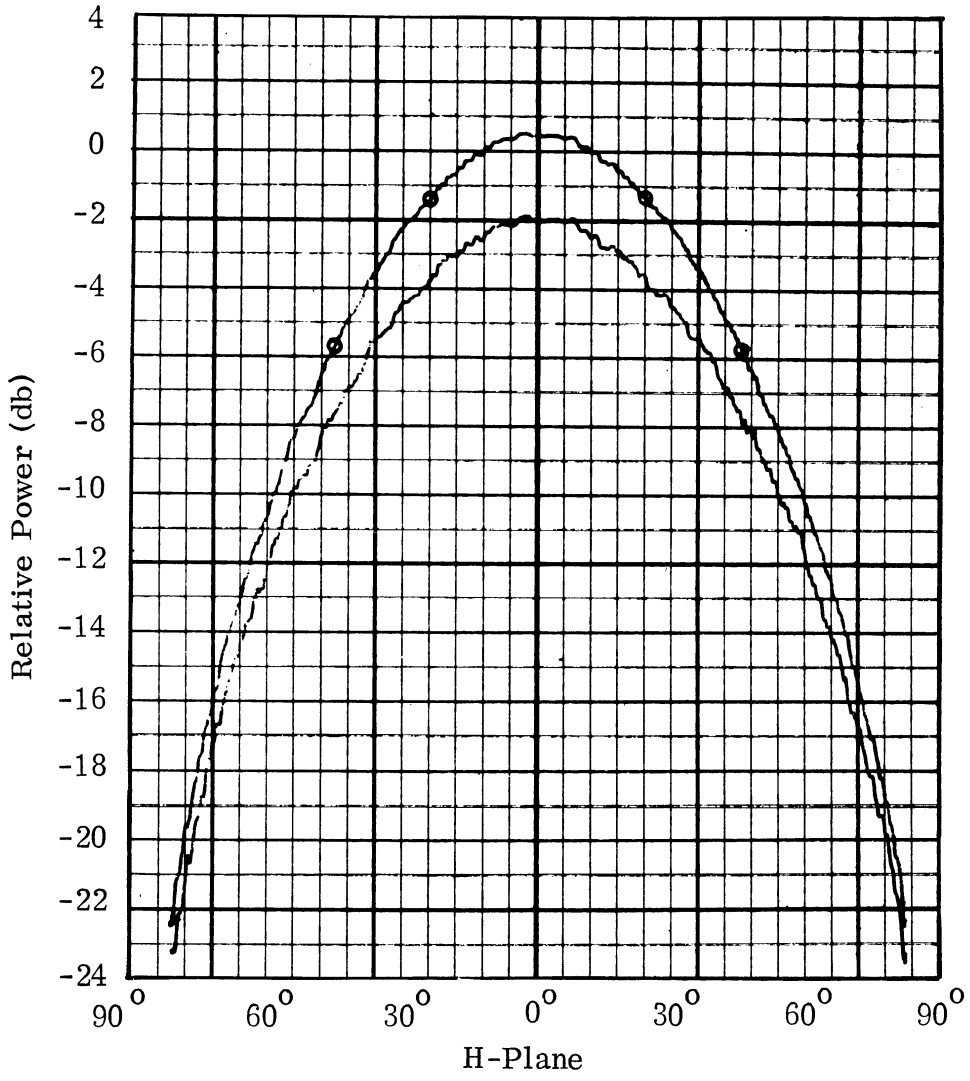

FIG. 3-7: E- AND H-PLANE RADIATION PATTERNS OF PLANE SLOT (——) AND THE SLOT SURROUNDED BY A CHOKE (-o-) AT 10.03 GHz.

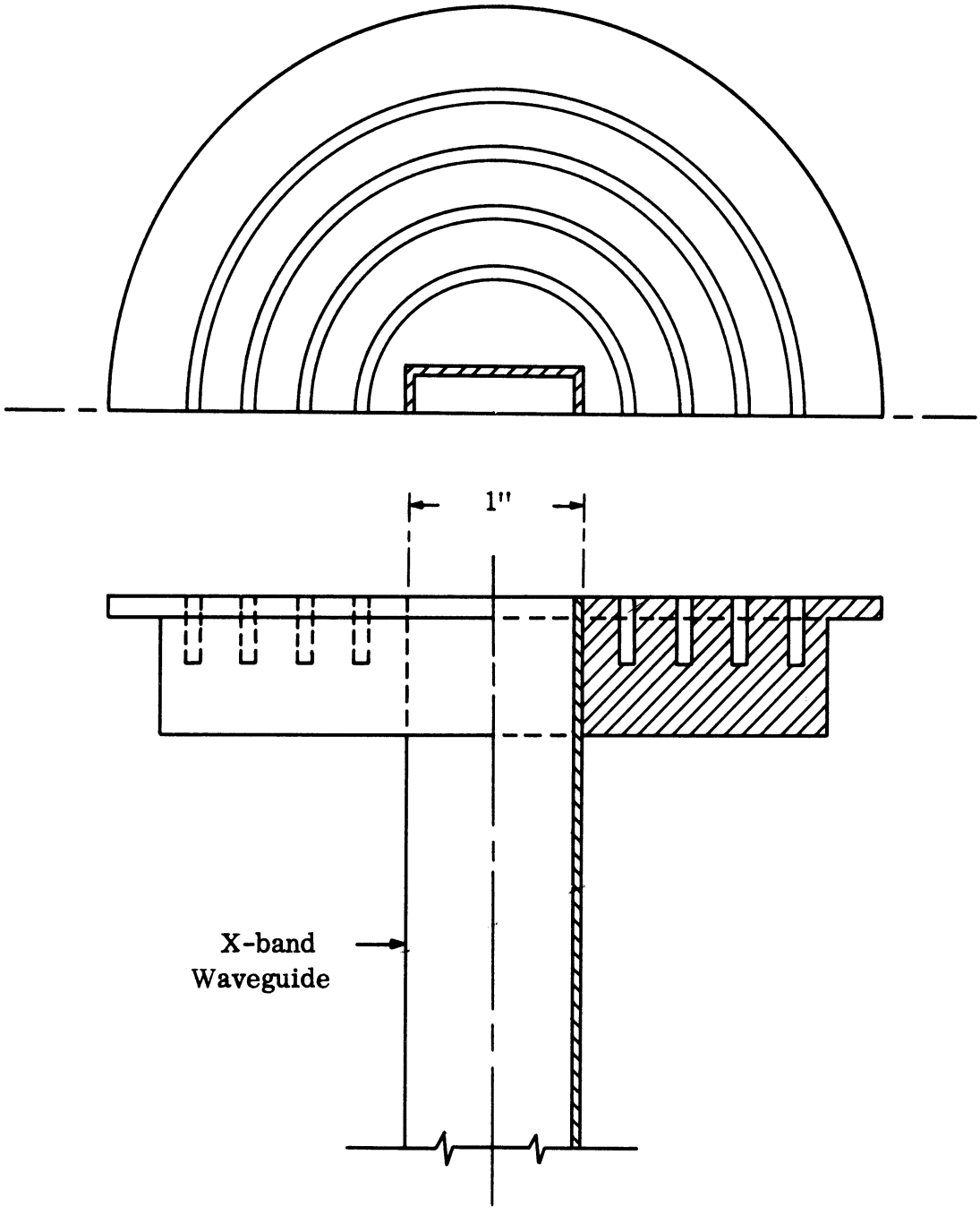

FIG. 3-8: SLOT ANTENNA WITH FOUR CHOKES.

It was found that the ground plane loading increased the slot gain throughout this frequency range, with the increase tapering gradually from a maximum of 3.5 db at 8.2 GHz to a minimum of 0.3 db at 12.4 GHz. (Lyon et al, August 1966).

The radiation patterns in Fig. 3-9 show a decrease of more than 10 db in the radiation along the ground plane. This is reflected in a reduction of the E-plane coupling between two slots mounted in the same ground plane at a center-to-center spacing of 11.4 cm (Fig. 3-10). The decoupling, however, was gradually reduced at the higher frequencies. Thus the decoupling over the entire X-band, would be approximately 13 db if both slots were surrounded by chokes. The H-plane coupling was very little affected by the presence of chokes. The decoupling observed was of the order of 1 to 2 db.

3.3 Continuous Reactive Loading - Parallel Wall Corrugations

Two slot antennas were arranged with a cavity in between. This is the same arrangement that was used to measure the effect of flush-mounted absorbing materials on coupling (see Fig. 2-4). The center-to-center spacing of the two slot antennas was 6.5 cm while the cavity dimensions were 7.2 cm x 2.3 cm x 2.2 cm. A set of corrugations with dimensions s = 0.21 cm (center-to-center spacing between two adjacent trenches) and d = 0.9 cm (depth) was placed in the cavity so that the tips of the corrugations would be flush with the ground plane (see Fig. 3-11).

The corrugations were found to reduce the coupling between the two slots by 1 to 5 db over the X-band, (see Fig. 3-12). Then another set of corrugations was placed in the cavity with s = 0.15 cm and d = 0.6 to 0.9 cm. In this set the depth of the trenches was varied in equal steps monotonically, so that in an E-plane cross-section the trench bottoms would be in a ladder form. The orientation of these corrugations was such that the shallowest

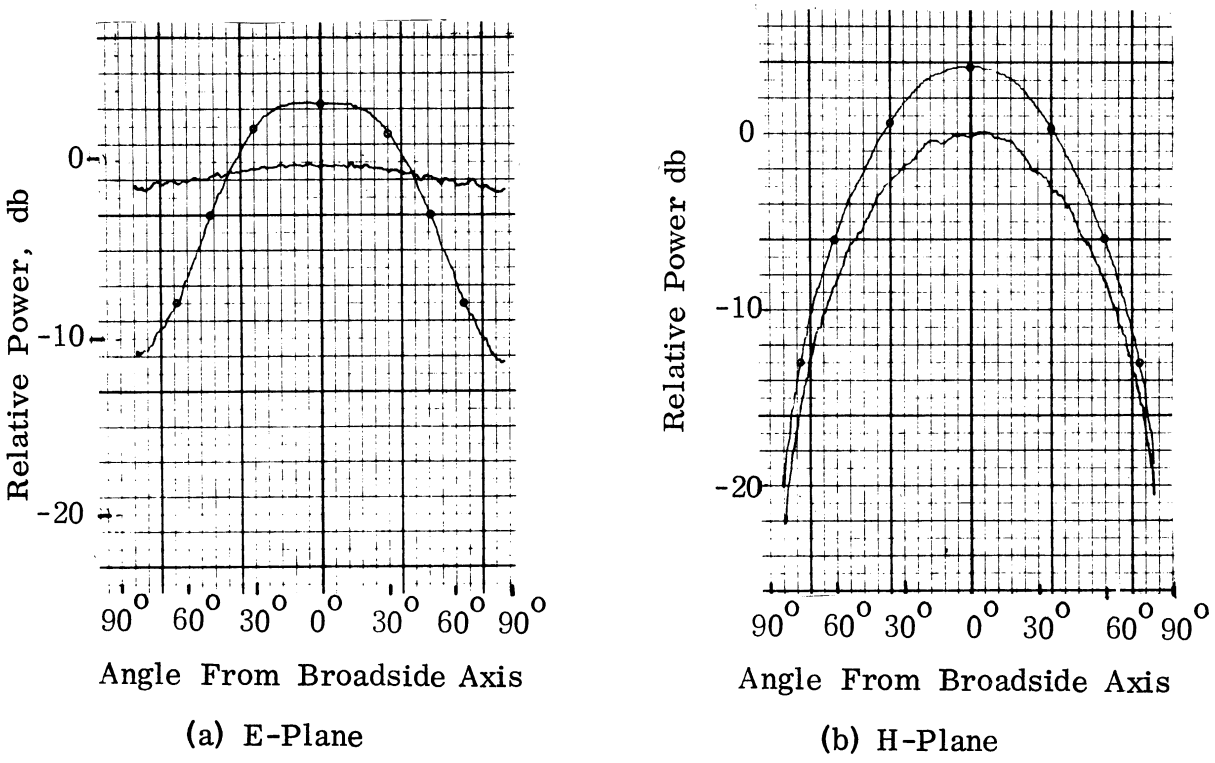

FIG. 3-9: E- AND H-PLANE RADIATION PATTERNS AT 8.23 GHz, (——) Flat Ground Plane; (-o—) With Four Chokes.

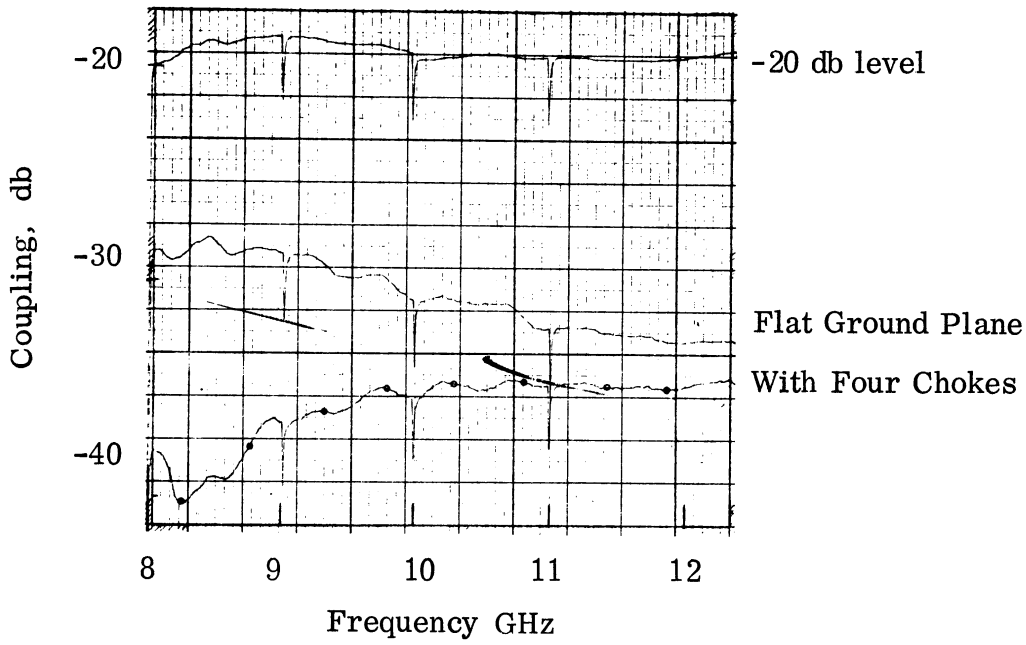

FIG. 3-10: E-PLANE COUPLING VERSUS FREQUENCY FOR TWO SLOTS SPACED 11.43 CM.

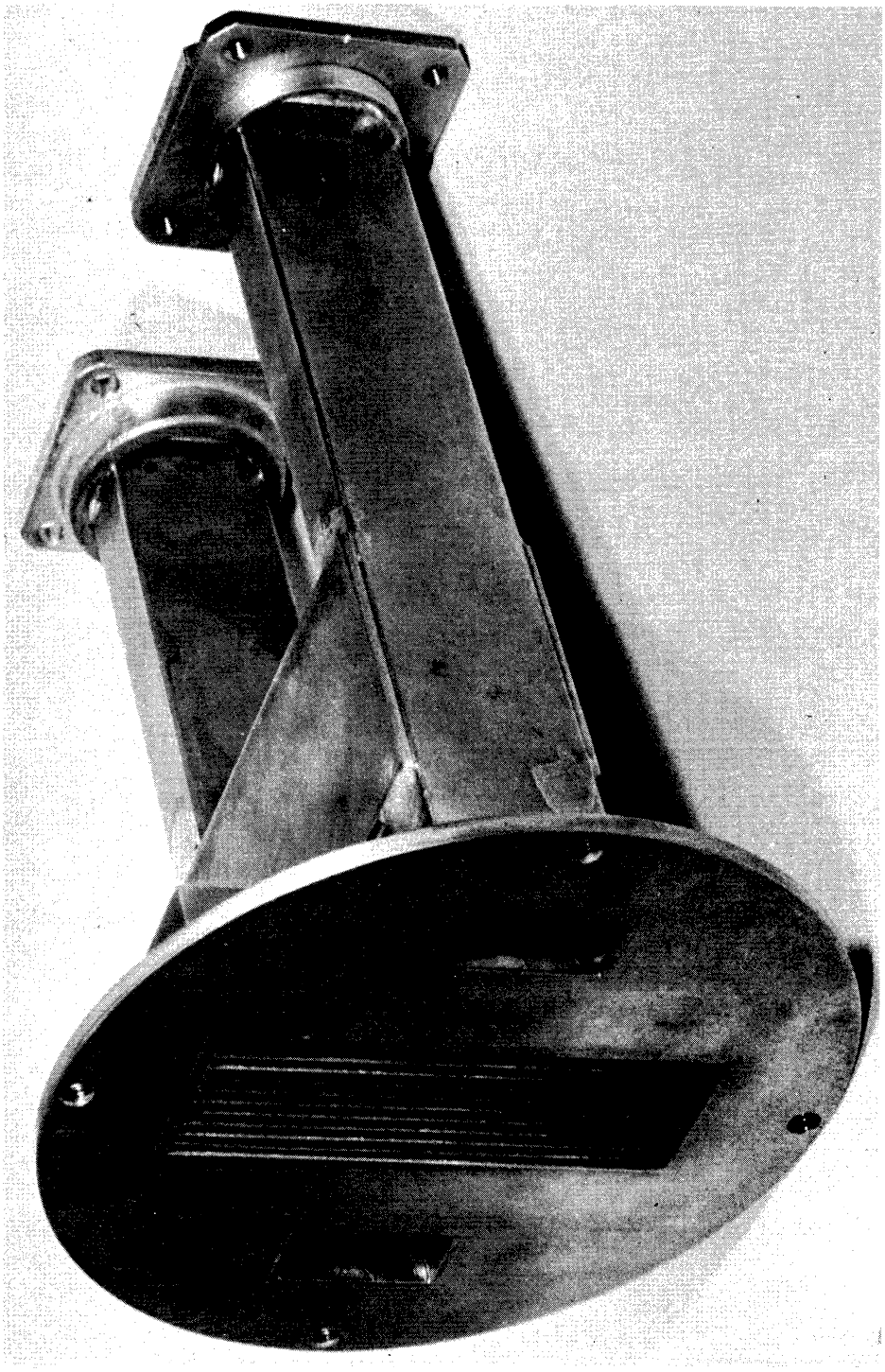

FIG. 3-11: PHOTOGRAPH OF THE FLUSH MOUNTED CORRUGATED STRUCTURE

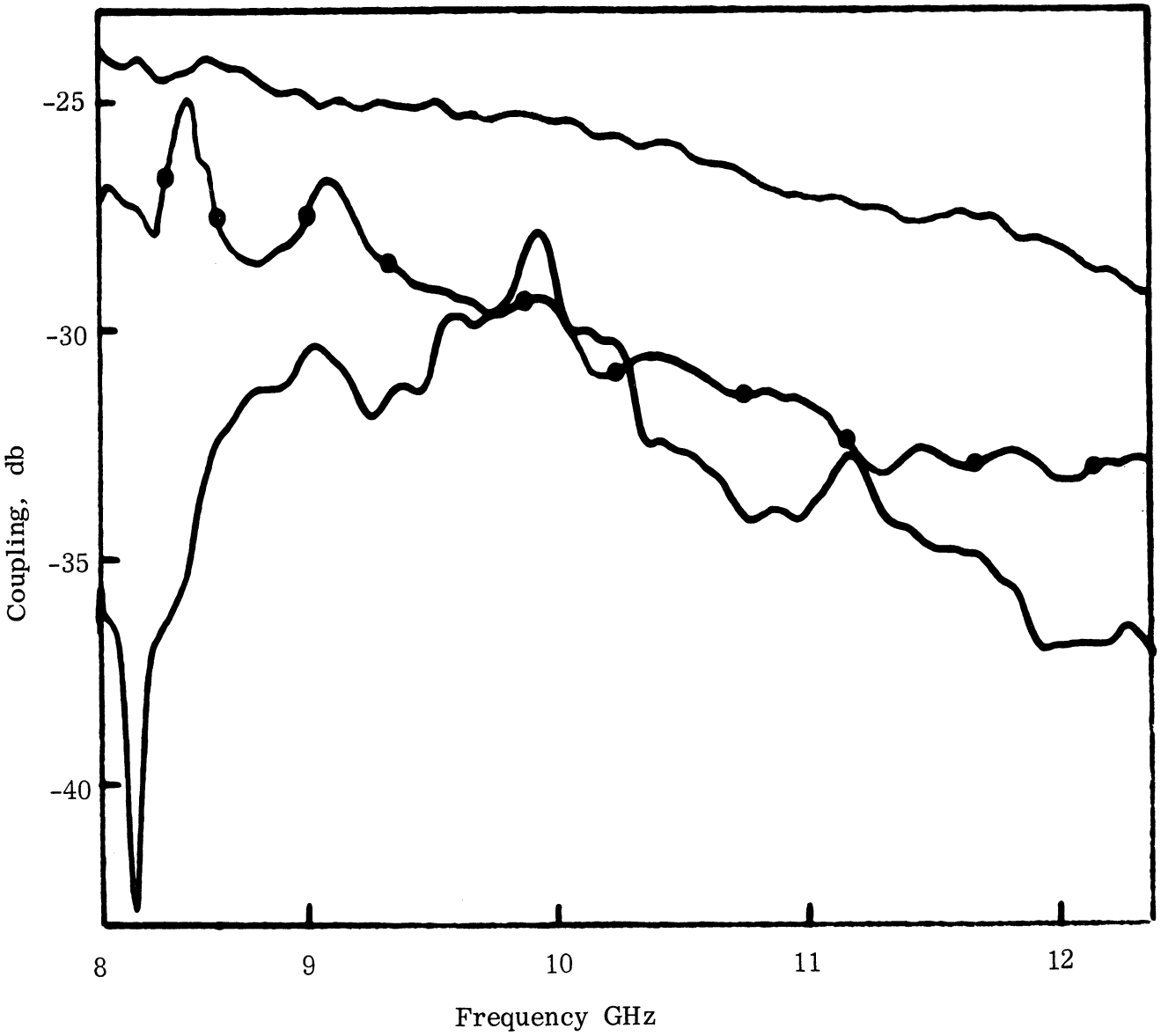

FIG. 3-12: COUPLING VS FREQUENCY FOR TWO SLOTS SPACED 6.5 CM. A, Flat Ground Plane; B, With Corrugations, d = 0.9 cm; C, With Corrugations, d = 0.6 to 0.9 cm.

trench was near the transmitting slot. The decoupling obtained with the tapered depth corrugations is larger over most part of the X-band (Fig. 3-12) but not over the entire frequency range.

Radiation patterns of the slot with the constant depth corrugations covered and exposed are given in Fig. 3-13 for five different frequencies. No change was noticed in the H-plane radiation patterns except for the small reduction in the antenna maximum gain corresponding to the E-plane gain at 0^{o} (Lyon et al, May 1966).

In another arrangement a slot aperture was recessed at the bottom of a square cavity, as shown in Fig. 3-14. Part of the cavity was occupied by corrugations with dimensions s = 0.21 cm, d = 0.9 cm. Two sets of corrugations were used: one with 10 trenches (set A) and the other with 15 (set B). Then the E-plane coupling between the recessed slot and another unmodified, slot at a distance of 12.9 cm was measured. With set A in the cavity, the coupling reduction varied irregularly across the X-band from a maximum of 20 db at one frequency to a minimum of 0.5 db at another . Somewhat better results were obtained with set B as shown in Fig. 3-15. The modification in the E-plane radiation pattern is shown in Fig. 3-16.

In view of the decoupling levels observed and the accompanying reduction of antenna gain at the broadside direction, the arrangements described in this section are not considered satisfactory for coupling reduction on a broadband basis. Reactive loading of the ground plane at a position between the interfering antennas did not produce significant decoupling, the same way that absorbing materials were not found very effective in a similar arrangement (cf. with section 2.3.1). A different approach, that of loading the ground plane around the antenna aperture and trying to modify the antenna sidelobes was found more promising and it will be further explored in the next section.

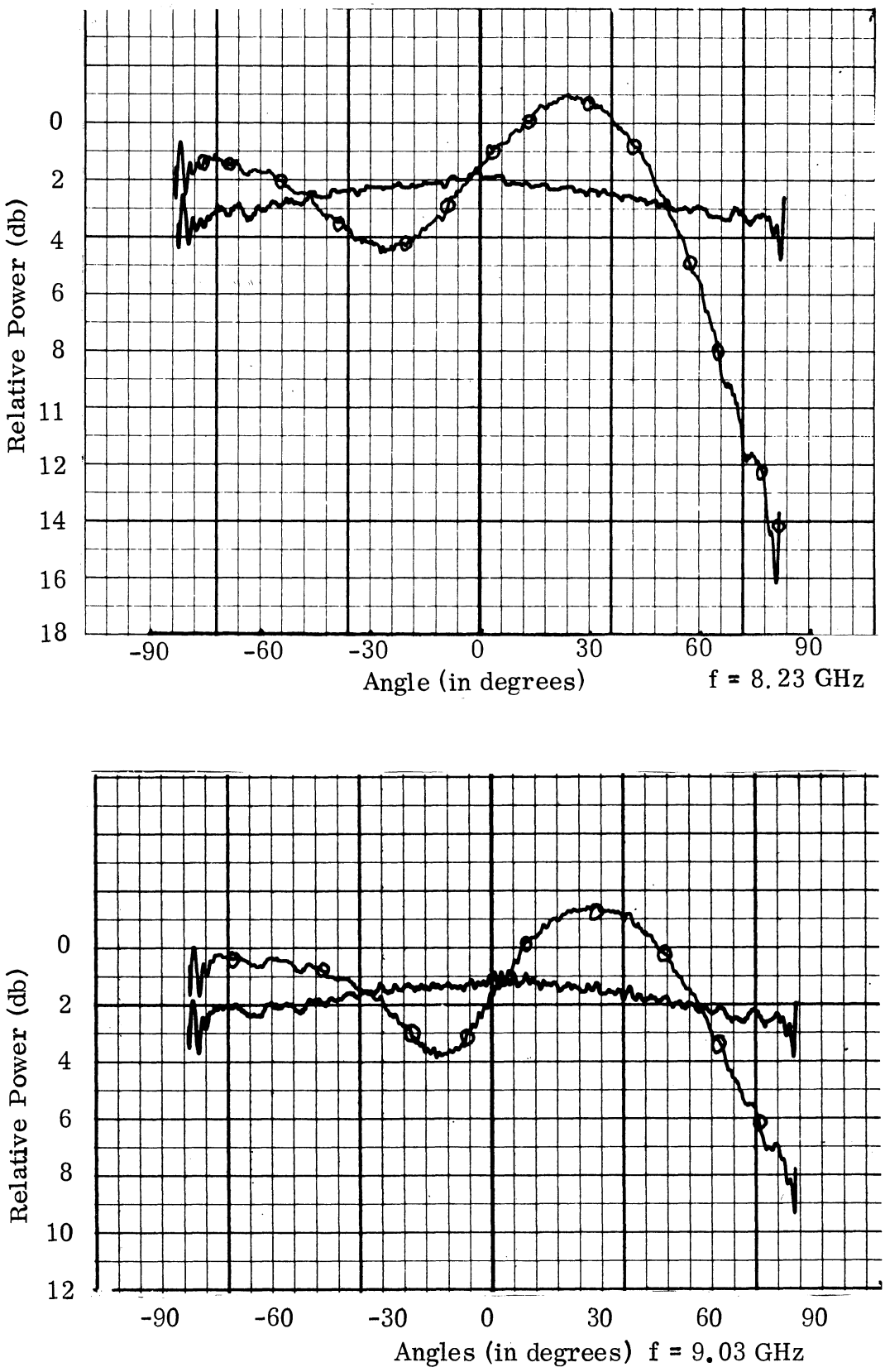

FIG. 3-13: E-PLANE RADIATION PATTERN FOR SLOT. (——) Flat Ground Plane; (—o—) With Flush-mounted Corrugations.

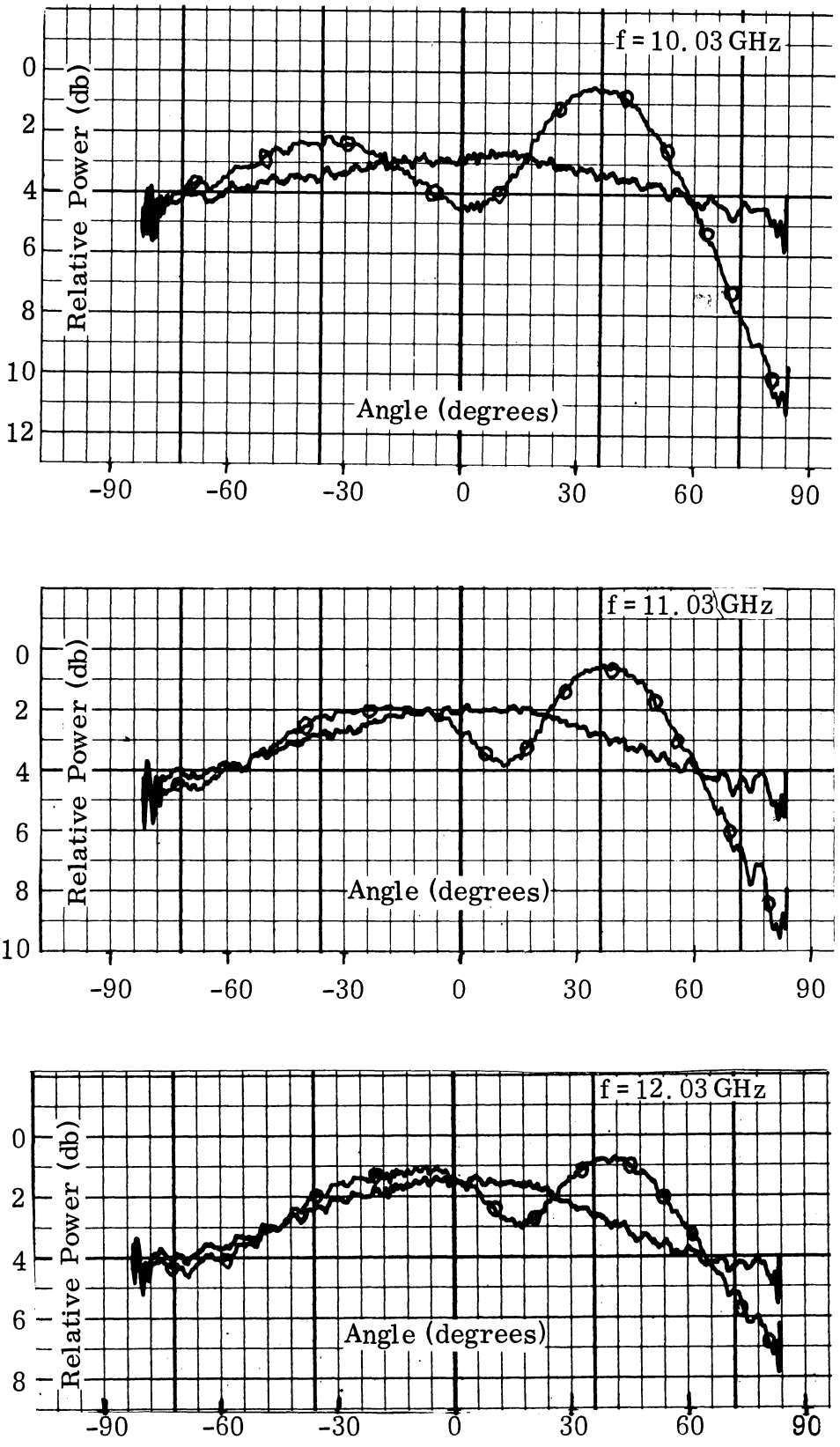

FIG. 3-13: CONTINUED.

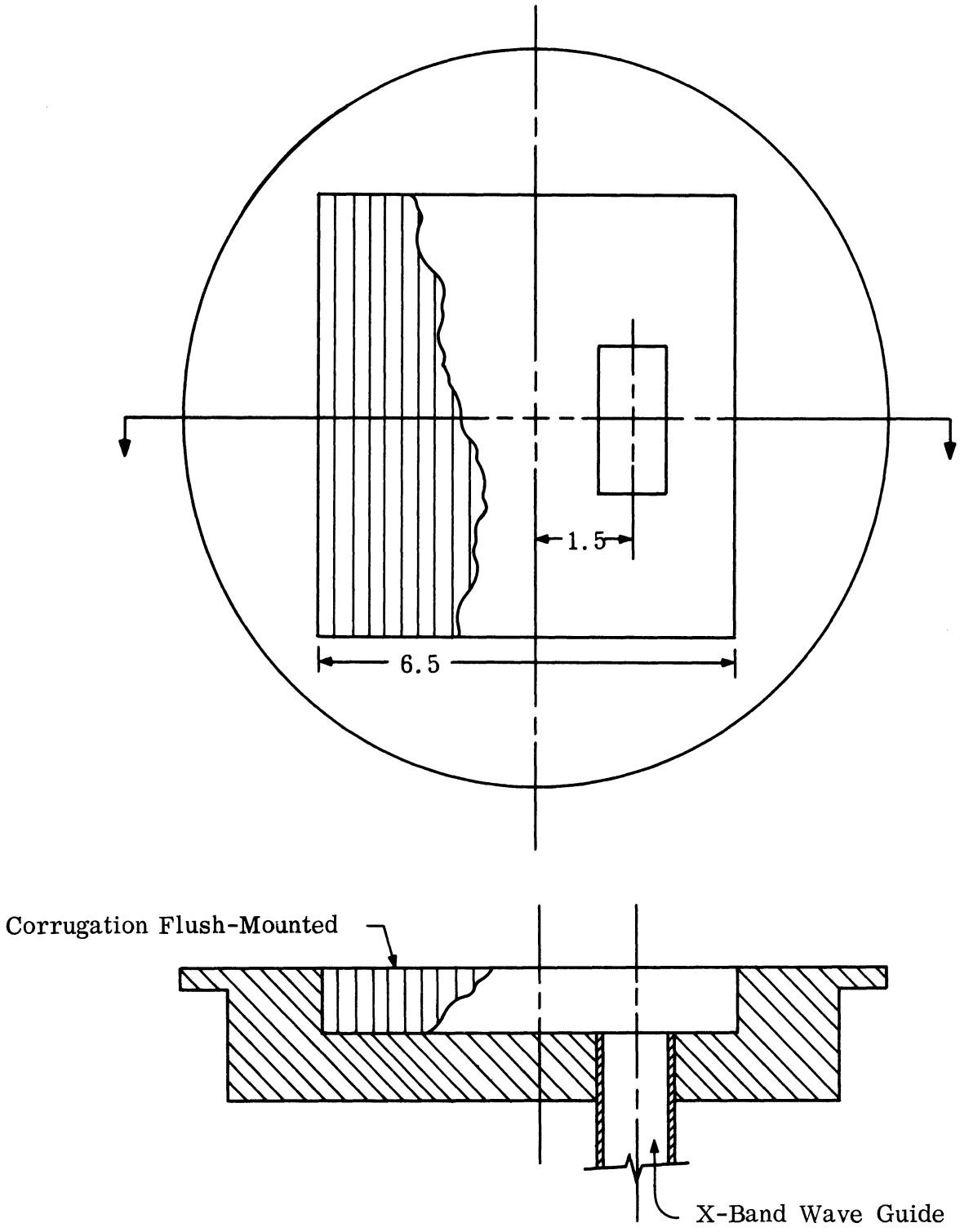

FIG. 3-14: SLOT ANTENNA IN SQUARE CAVITY WITH CORRUGATIONS.

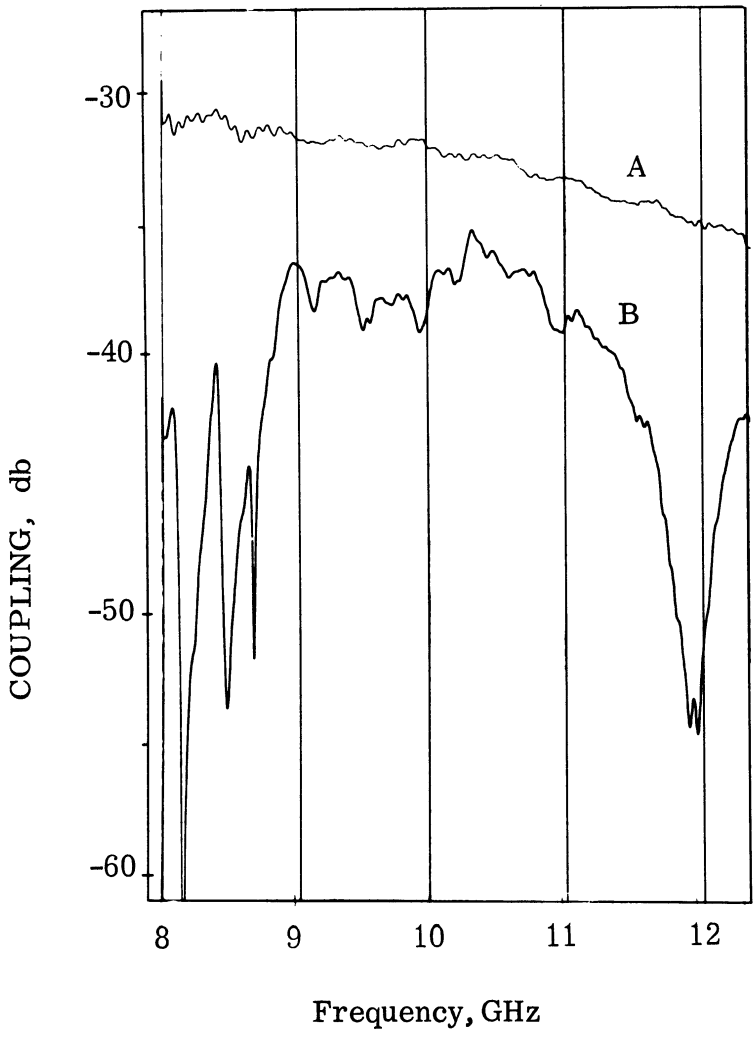

FIG. 3-15: E-PLANE COUPLING VS FREQUENCY FOR SLOTS SPACED 12.9 CM.

A: Flat Ground Plane
B: With Modification of Fig 3-14 and set B.

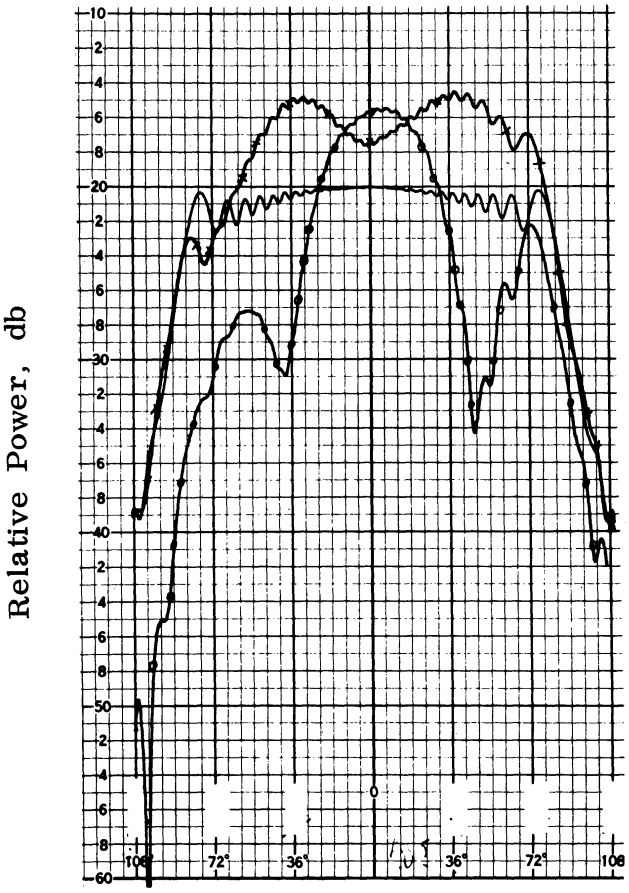

FIG. 3-16: E-PLANE RADIATION PATTERNS FOR SLOTS AT 9.0 GHz.

(——) Slot in Flat Ground Plane

(—o—) Slot as in Fig. 3-14 with set B

(—x—) Slot as in Fig. 3-14 with set A.

3.4 Continuous Reactive Loading - Circumferential Corrugations

3.4.1 Design Considerations

The reactive loading of the ground plane around the antenna aperture with one or more isolated circumferential slots gave good results but a relatively modest amount of decoupling. In order to obtain more significant results continuous reactive loading was used by modifying the area aroundthe antenna aperture. The modfied area was in the shape of a disc of one to two wavelengths radius with the antenna at the center. The desired capacitive surface reactance was created by cutting corrugations in the form of circumferential trenches of appropriate dimensions. Corrugations with parallel or non-parallel walls were considered as well as with constant or variable depth. The types of antennas that were used included broadband slots, spirals, monopoles, thin slots, sectoral and pyramidal horns. These antennas exhibit a wide variety of radiation patterns. Their gain along the ground plane varied from maximum for the monopole and the slot E-plane, to small for the horn sidelobes, to theoretically zero for the spiral. Different sets of corrugated discs were designed, constructed and used at S, X and Ku bands of frequencies. These corrugated discs were so designed that different antennas could be placed at the center of a disc while the discs themselves could be fastened on a larger metal ground plane with the corrugations flush with the surrounding flat surface.

Each trench of a corrugated structure with parallel walls, may be considered as a uniform transmission line of length d (the depth of the cavity) terminated by a short (cavity bottom). If the trenches are narrow enough, so that only a TEM-mode propagates in them, the impedance as seen at the trench aperture is

$$Z_s = j\eta \tan (kd) \quad .$$

The symbols used here have been defined in connection with Eq. (3.2). Besides the impedance over the wall separating two adjacent slots is simply zero. Thus, the surface impedance of the corrugated structure is:

$$Z_s = \begin{cases} j\eta \tan (kd) & \text{(over trench aperture, w)} \\ 0 & \text{(over wall, s - w)} \end{cases} \qquad (3.3)$$

A first order approximation is to consider an average, uniform, surface impedance and this leads to Eq. (3.2) which is repeated here:

$$Z_s = \frac{w}{s} \eta \tan (kd) \quad .$$

Equation (3.2) may be used to determine for a given depth d the range of frequencies (expressed through $k = 2\pi/\lambda$) over which Z_s is inductive or capacitive and accordingly define stop-and pass-bands for a surface wave. However, a more accurate model is possible for determining the pass- and stop-bands. This is as follows.

A two dimensional, periodic, corrugated surface is considered. A TM-mode is assumed above the corrugations. By using Floquet's theorem for periodic structures and considering an infinite number of space-harmonics above the surface in order to satisfy the boundary condition as stated in Eq. (3.3) an equation is derived from which the phase constants of the space harmonics can be determined. At the frequency where the cut-off of the first pass-band occurs this equation is simplified to the following form (Watkins, 1958)

$$\frac{1}{kd \tan kd} = \frac{2s}{\pi^2 d} \sum_n \frac{1}{|1+2n|} \cdot \frac{\sin\left[(1+2n)\frac{\pi w}{2s}\right]}{(1+2n)} \qquad (3.4)$$

$$n = 0, \pm 1, \pm 2, \ldots$$

This equation can be solved by graphical methods or by trial and error. There are three parameters d, w, and s which have to be chosen to determine the propagation parameter k from which the frequency will be obtained. An examination of Eq. (3.4) shows that the most critical parameter is d. As a starting point for a trial and error solution, the value $d = \lambda/4$ may be used. It has been shown (Lyon et al, May 1966) that a greater Z_s produces greater decoupling. Because of this, in Eq. (3.2) it is desirable to make w/s as big as possible (the upper limit being 1) which means making the wall thickness (s - w) as small as possible. Here a limit is imposed by consideration of the metal and construction method used.

Finally regarding w there are two reasons for making it as large as possible. First, for the same reasons that one wants to make (s - w) as small as possible. Second, because of consideration of the $\omega - \beta$ diagram for this structure (Watkins, 1958) which shows that the larger s/d, the more the cutoff deviates from the value $kd = \pi/2$, causing the stop band to increase, which is desirable in broadband applications of the method. On the other hand there is an upper limit imposed by the conditions under which Eq. (3.4) was derived, namely that the trenches are narrow enough so only a TEM-mode propagates inside. In order to obtain reasonably accurate results from Eq. (3.4) one would have to limit w to $\lambda/10$ although values of w $\lambda/3$ have been used as described later with good agreement with Eq. (3.4)

The following corrugated discs have been designed following the above procedure.

a) For S band.

Dimensions: d = 2.41 cm w = 0.81 cm s = 0.89 cm.

These corrugations extend radially for 11.46 cm (1.3λ at 3.4 GHz). The cut-off frequency for the first pass band is found from (3.4) to be 2.75 GHz and for the second pass band 8.31 GHz. Thus the corrugations should be effective in reducing coupling at both S- and X-bands. These corrugations were milled in a solid piece of brass. They are shown in Fig. 3-17 with a broadband S-band slot mounted at the center. These corrugations will be referred to in the following as "corrugations S".

b) For X band.

Dimensions: d = 0.85 cm, w = 0.16 cm, s = 0.18 cm.

These corrugations extend radially for 2.7 cm (0.9λ at 10 GHz). The cut-off frequency for the first pass-band is found from Eq. (3.4) to be 8.2 GHz. These corrugations were made by cutting strips of shim stock, 0.85 cm wide and soft soldering them to the bottom of a cylindrical cavity cut from a piece of brass (see Fig. 3-18). These corrugations will be referred to in the following as "corrugations R-1".

Some additional corrugated structures with a different profile were also used. These will be presented in a separate section.

3.4.2 Broadband Slots

a) S-band (2.6 to 4.0 GHz)

When "corrugations S" were placed around an S-band slot it was found that the E-plane coupling to an adjacent slot was reduced from a maximum value of -27 db to -41 db over almost the entire S-band (see Fig. 3-19).

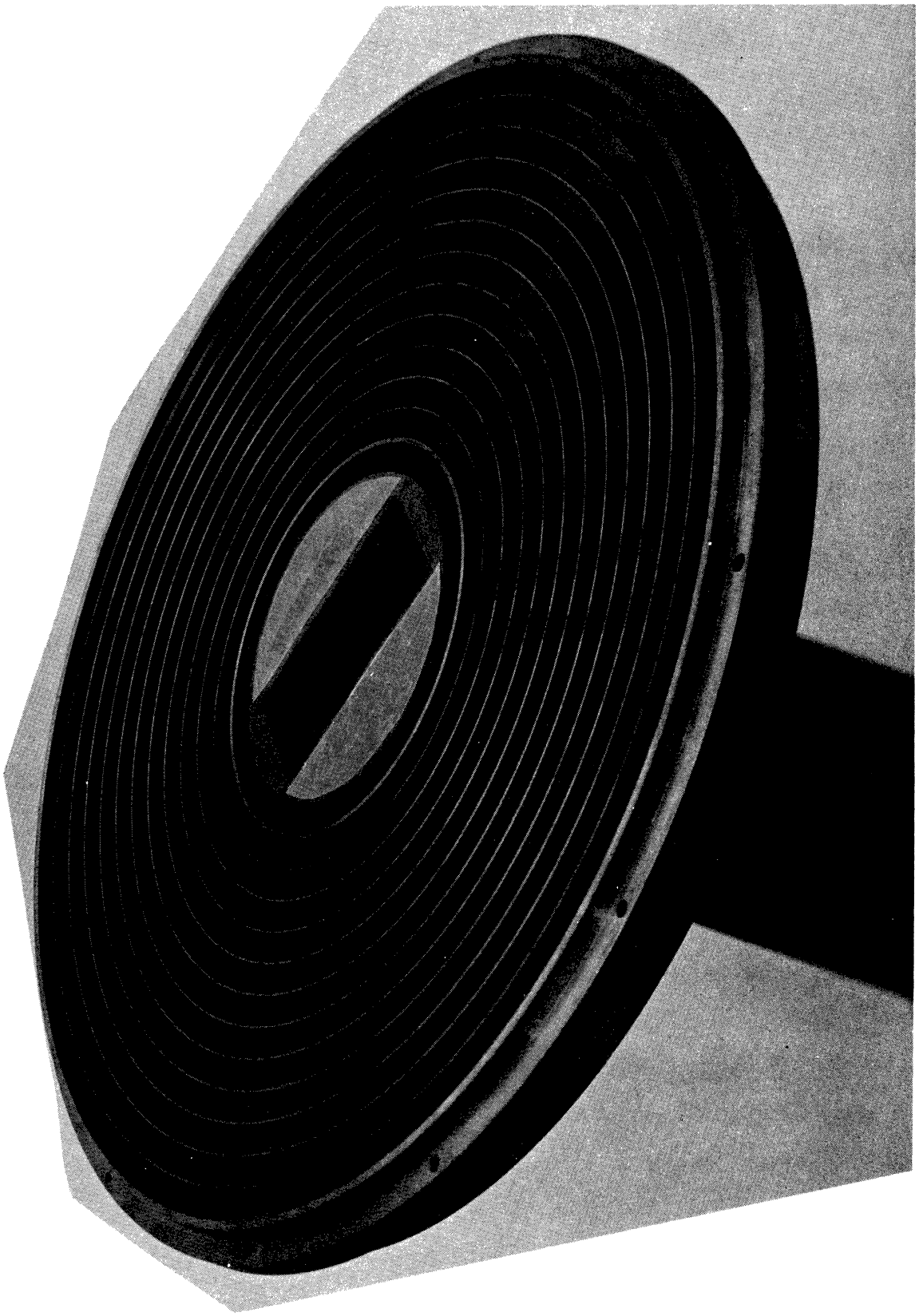

FIG. 3-17: SLOT ANTENNA AND CORRUGATIONS S.

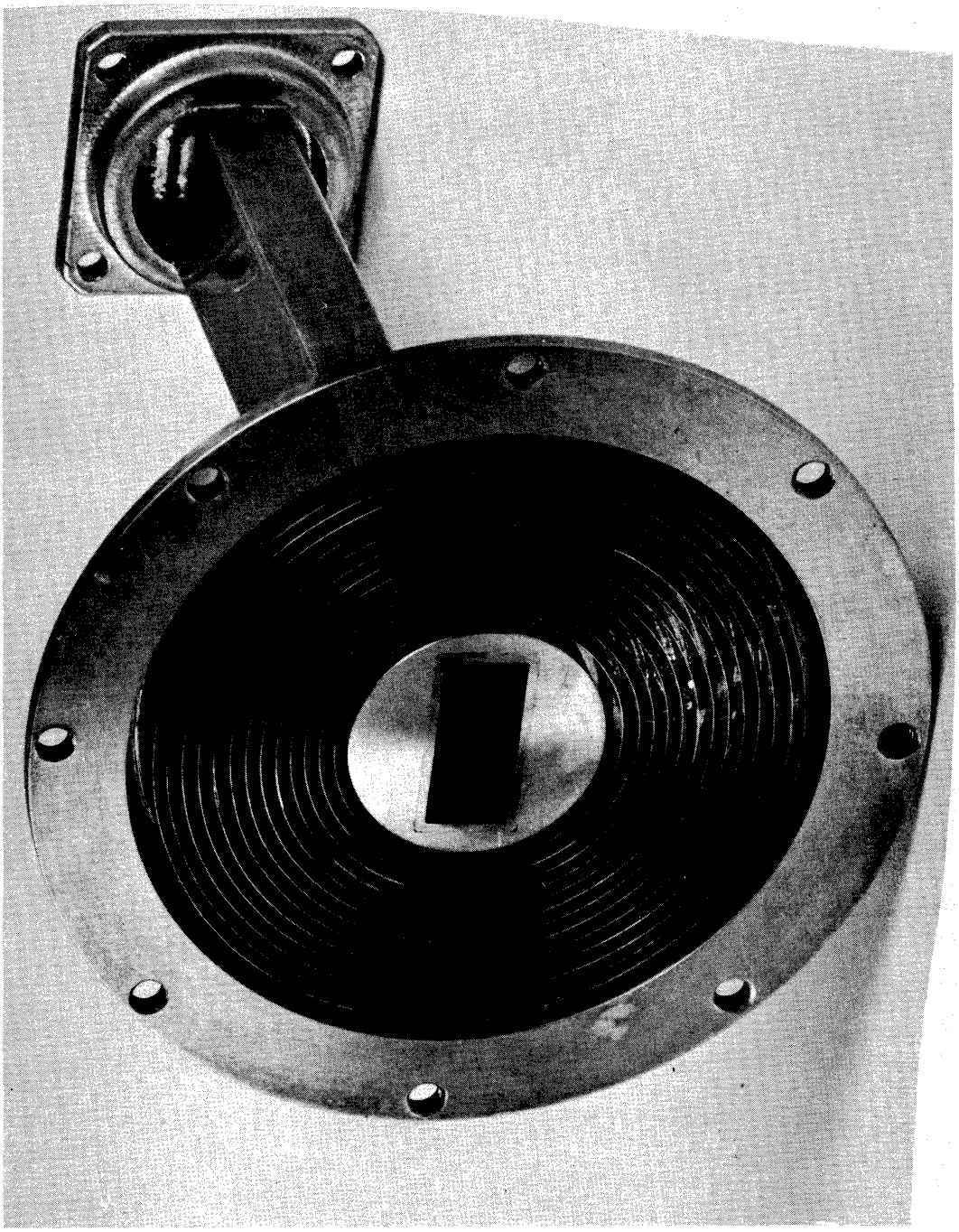

FIG. 3-18: SLOT ANTENNA WITH CORRUGATIONS R - 1.

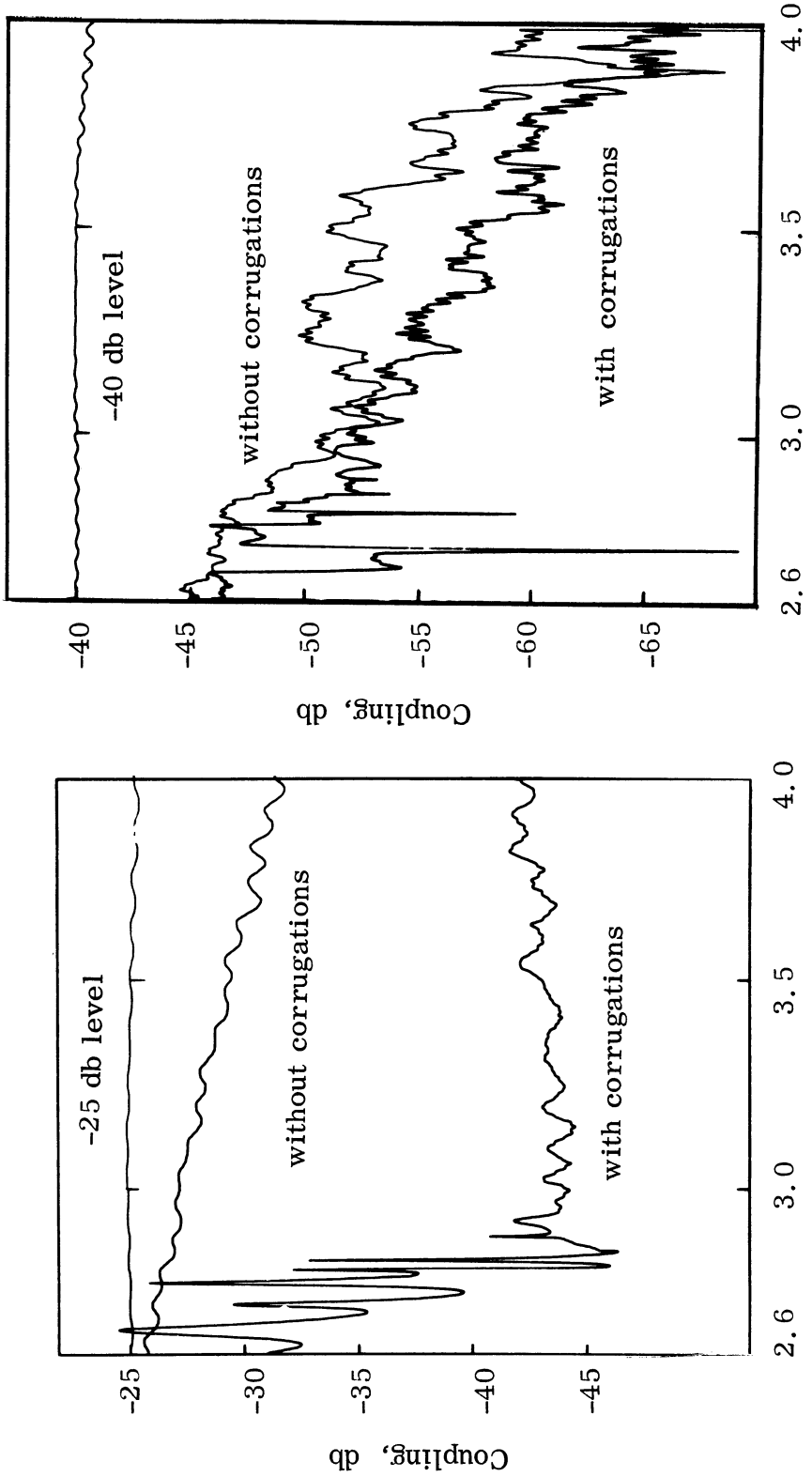

FIG. 3-19: E- AND H-PLANE COUPLING VS FREQUENCY FOR TWO SLOTS SPACED 22.8 CM IN A 12' BY 12' ALUMINUM GROUND PLANE.

The center-to-center spacing of the two slots was 2.5λ in the middle of the frequency range considered (3.3 GHz). The experiment also indicates the stop band starts at 2.81 GHz which is 2.1 percent from the calculated value. When the slots are oriented for weak coupling (H-planes colinear) the radiation pattern of each slot exhibits a null in the direction of the other slot and therefore the corrugations cannot be as effective. However this is not a serious problem since the H-plane coupling level is much lower than the E-plane coupling. In this case the maximum H-plane coupling was reduced from -49 db to -52 db when the corrugations were added. In the case of H-plane coupling the stop band starts at 2.73 GHz which is within the limits of measurement error from the calculated value. This agreement with the theoretical result is remarkable; it is even more so since the actual geometry deviates from that assumed to derive Eq. (3.4) in two respects: a) the structure is not periodic since it extends for only one wavelength rather than continuing to infinity and b) instead of parallel wall corrugations one has circumferential corrugations which , strictly speaking, is not a two-dimensional problem.

The effect of the corrugations has been qualitatively explained as trapping the power carried by a surface wave along the ground plane and radiating it in the broadside direction. This means that the sidelobe decrease should be accompanied by an antenna gain increase. This was observed experimentally by mounting the slot on a small metal disc (diameter 33.3 cm) and recording the radiation patterns in the two main planes, (see Fig. 3-20). A plain and a corrugated disc were interchanged and the two curves superimposed for comparison. At 3.0 GHz the corrugations cause an E-plane sidelobe reduction of 12 db accompanied by a 3 db gain increase. By orienting the slot for maximum gain and sweeping the frequency (Fig. 3-21) it was demonstrated that the gain increase varies between 1.5 db to 5.0 db over the frequencies of S-band.

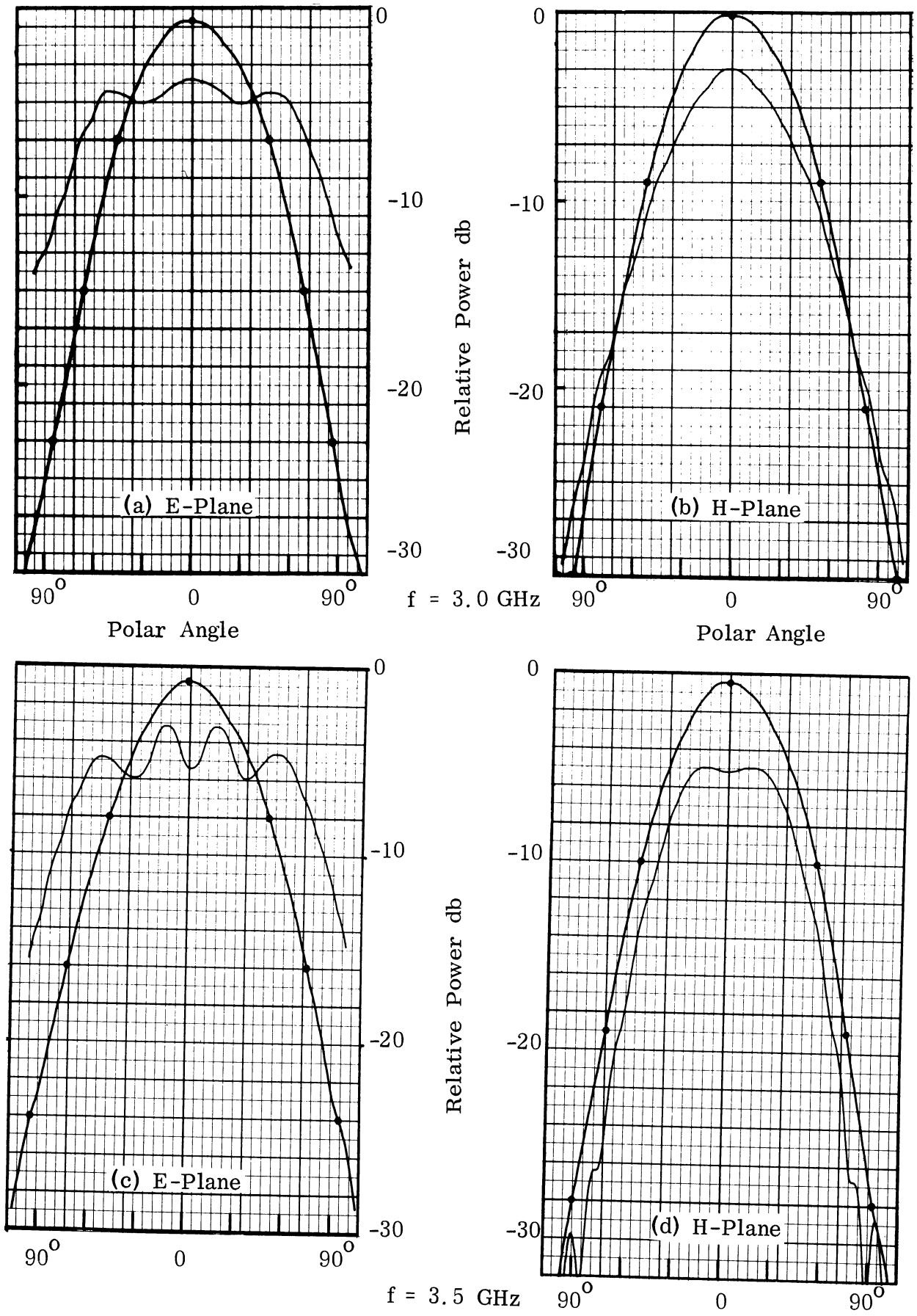

FIG. 3-20: RADIATION PATTERNS FOR AN S-BAND SLOT IN A METAL DISC OF 33.3 CM DIAMETER. (——) Flat Disc; (—●—)Disc with Corrugations.

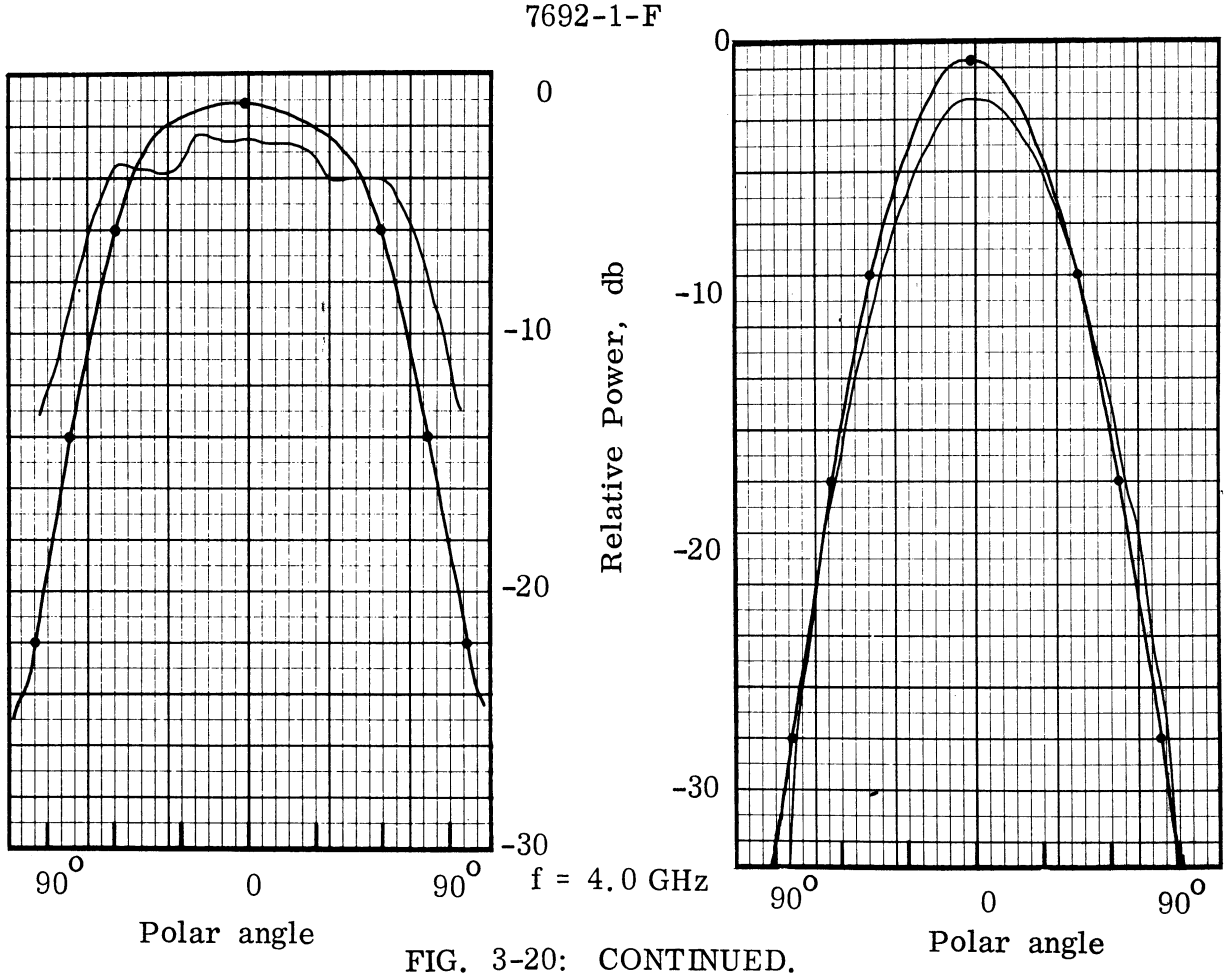

FIG. 3-20: CONTINUED.

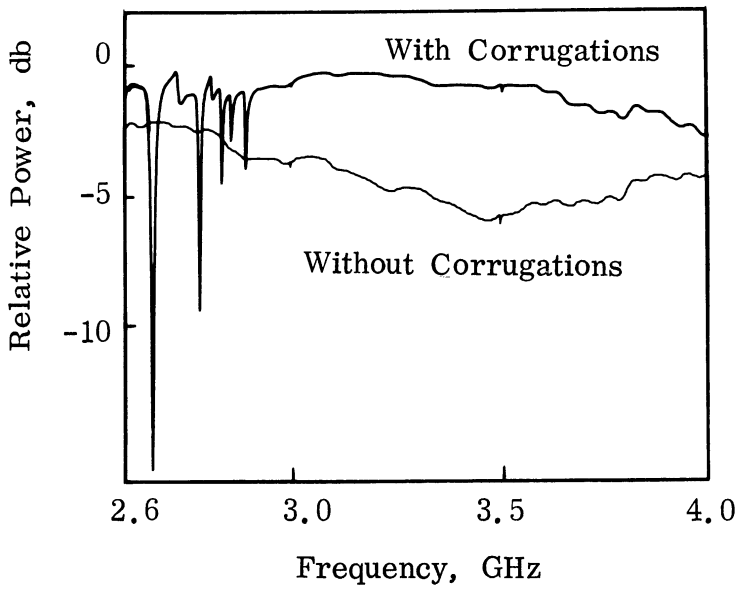

FIG. 3-21: MAXIMUM GAIN VS. FREQUENCY FOR AN S-BAND SLOT IN A METAL DISC OF 33.3 CM DIAMETER.

It has been thought of interest to investigate the effect on decoupling of the trenches individually. For this purpose the area of the ground surface represented by the corrugations was covered by aluminum foil and the coupling between the two slots measured by sweeping the frequency. The innermost trench was uncovered and the coupling measured again. The uncovering of subsequent trenches continued until all were active. The results were shown in Fig. 3-22. In this figure the parameter indicates the number of uncovered trenches. The lowest curve in Fig. 3-22 is identical with that of Fig. 3-19(a). By examining Fig. 3-22 it is clearly seen that incremental steps of decoupling do not show a tendency to shrink to zero very rapidly, which indicates that additional decoupling is possible by extending the corrugations further.

b) X-band (8.2 to 12.4 GHz) and Ku-band (12.4 to 18.0 GHz).

The circumferential corrugations "R-1" designed to reduce the coupling between two X-band slots have been tested and found effective over the entire X-band. They produce a reduction of 10 db, in the E-plane coupling, over a 30 percent bandwidth (see Fig. 3-23). Since, in some applications, it is of interest to obtain high isolation between two systems operating over frequeny ranges of 2:1 or even 3:1, the measurements have been extended to the waveguide band immediately above the X-band covering the range of frequencies from 12.4 GHz to 18 GHz. One of the names by which this frequency range is known, is Ku -band and it will be referred to as such in the following.

The same slots fed by X-band waveguide were used in both frequency ranges, with tapered transitions to the Ku-band waveguide when the Ku-band system was replacing the X-band system. Figure 3-23 shows the effect of one set of circumferential corrugations on the E-plane coupling between two slots in the X-and Ku-band. The maximum coupling between the two slots

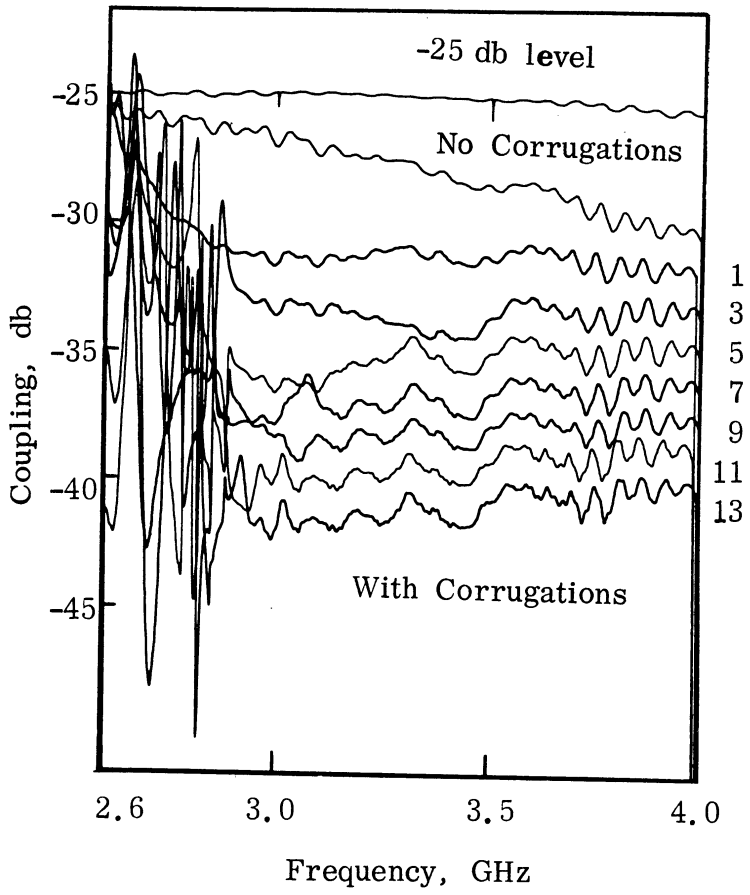

FIG. 3-22: E-PLANE COUPLING VS FREQUENCY FOR TWO SLOTS SPACED 22.8 CM. Parameter Indicates the Number of Uncovered Trenches.

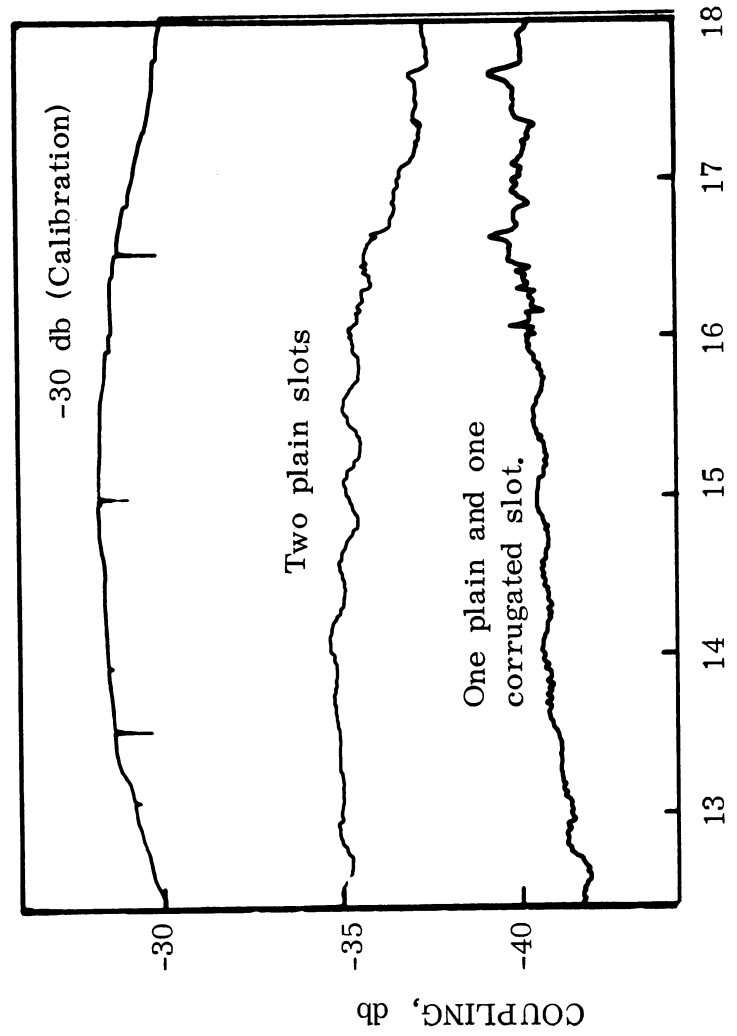

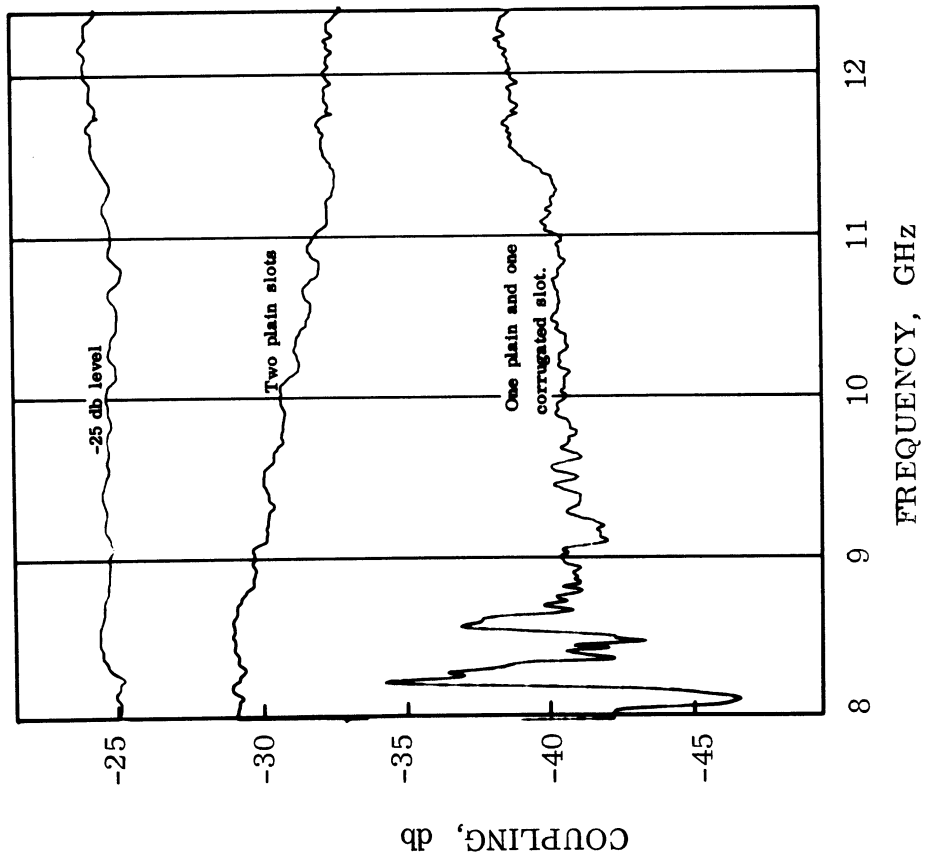

FIG. 3-23: E-PLANE COUPLING VS FREQUENCY FOR TWO SLOTS SPACED 11.4 CM. (Corrugations R - 1).

in a 2:1 frequency range (8.7 GHz to 17.4 GHz) is reduced by 11 db (from -29.5 db to -40.5 db). It is expected that the amount of decoupling (in db) would be doubled if both slots were surrounded by corrugations.

The effect of the corrugations on the radiation pattern of the slot in a large ground plane are shown in Fig. 3-24. In this case the slot and corrugated disc were mounted flush in a 12 ft. square ground plane. A swept-frequency measurement of the maximum gain (broadside to the ground plane) shows that the reactive loading of the ground plane increases the gain of the slot over the entire X-band. (see Fig. 3-25).

Since some of these antennas may be used on vehicles of considerably smaller dimensions and since the size of the ground plane does affect the pattern significantly, additional radiation patterns were taken using an 11.1 cm diameter disc (Fig. 3-26) with the same set of corrugations. Two curves are presented superimposed in each case representing the radiation pattern of a plain slot and that when the slot is surrounded by corrugations. In each case the transmitter and receiver gains were left constant so that these figures provide also information about the effect of the corrugations on the antenna gain. The undulations present in the patterns of the plain slot are well known and have been explained by assuming additional radiation sources at the edges of the sheet. It is interesting to note that the corrugations virtually eliminate these undulations by preventing the propagation of a surface wave and thus reducing the diffraction from the ground plane edges.

The standing wave ratio of the slot in the presence of corrugations was of the same order of magnitude as with a flat ground plane.

Several attempts were made to increase the bandwidth of the corrugations. One possibility is to fill the trenches with a dielectric or absorbing material. One experiment has been completed using paraffin wax with Set "1". The

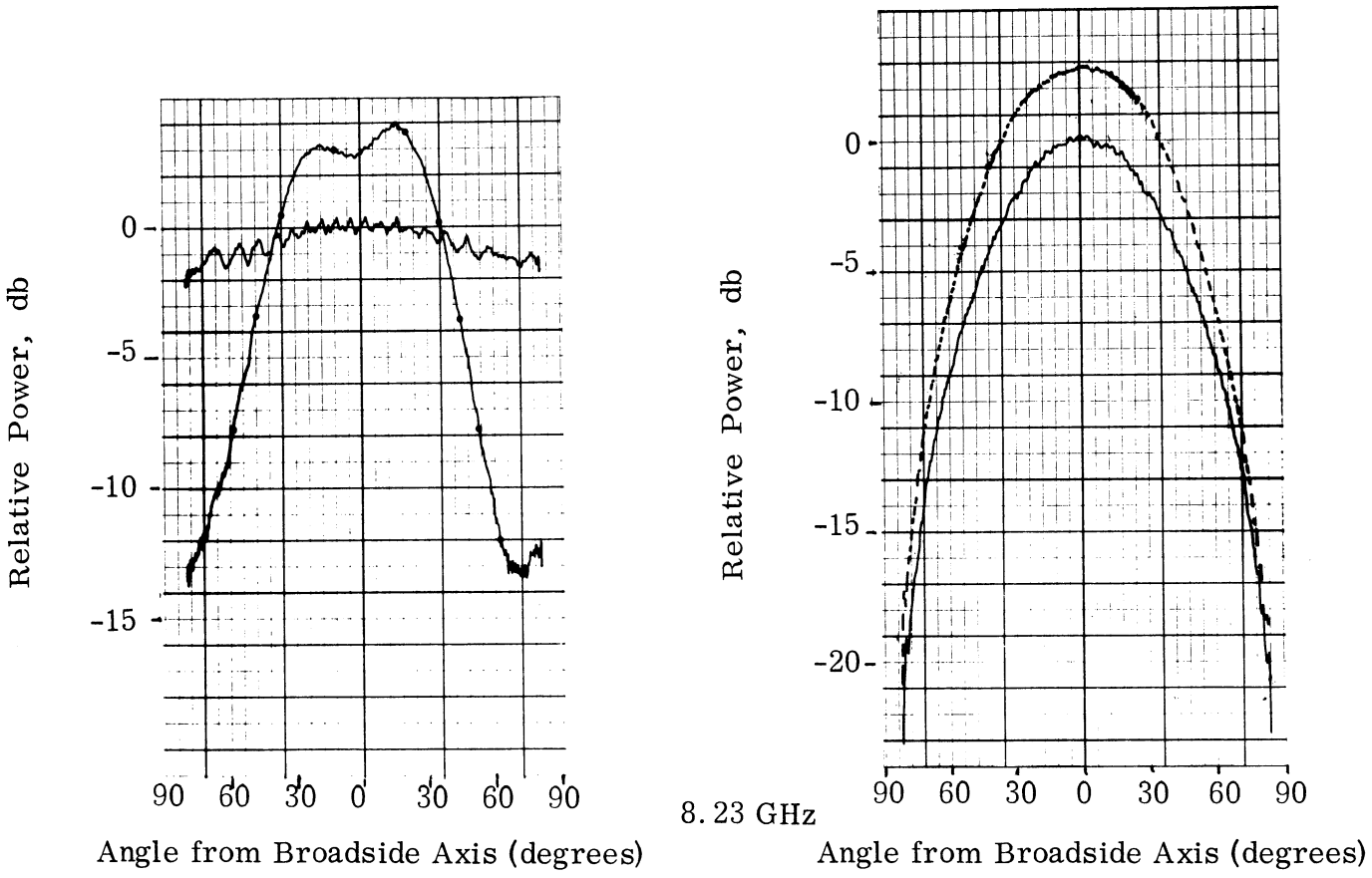

FIG. 3-24: E- AND H-PLANE RADIATION PATTERNS. (——) PLAIN SLOT; (—●—) OR (- - -) SLOT WITH CORRUGATIONS R - 1.

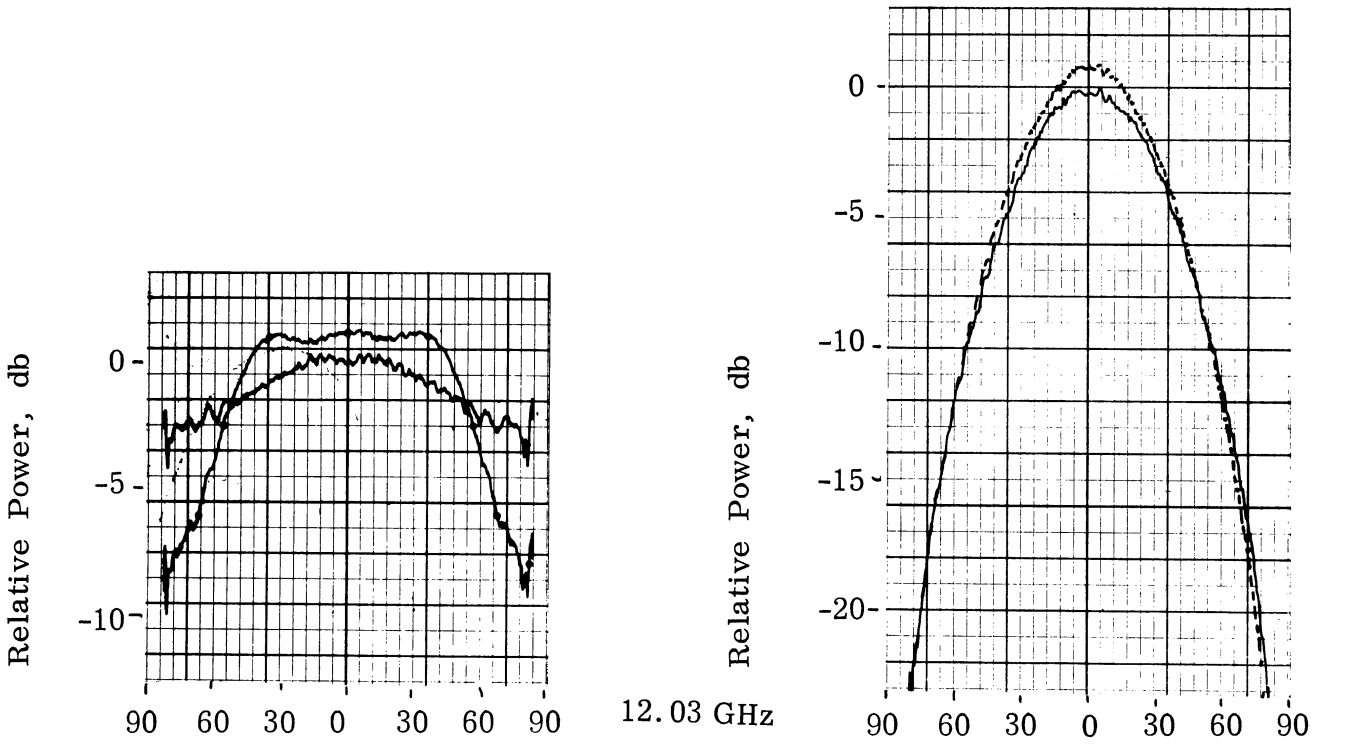

(e) E-PLANE (f) H-PLANE

FIG. 3-24: CONTINUED.

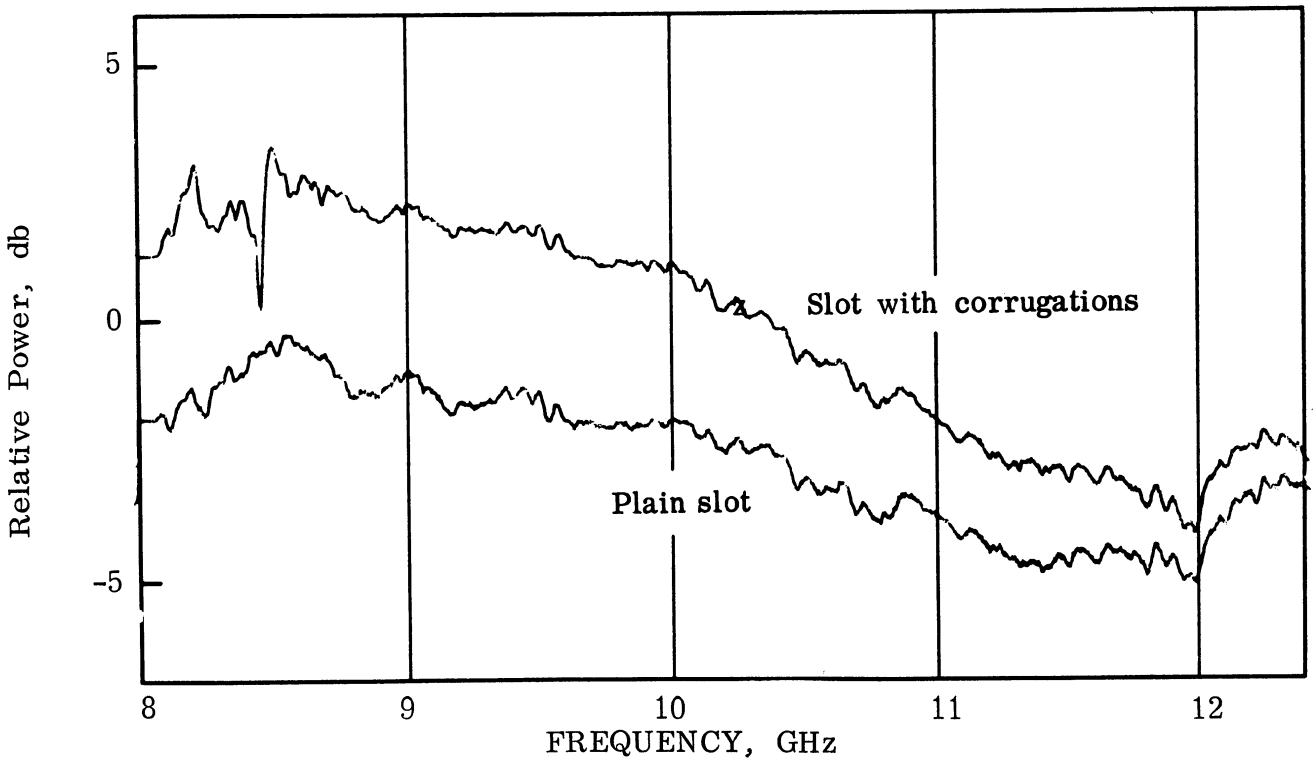

FIG. 3-25: MAXIMUM GAIN VS. FREQUENCY.

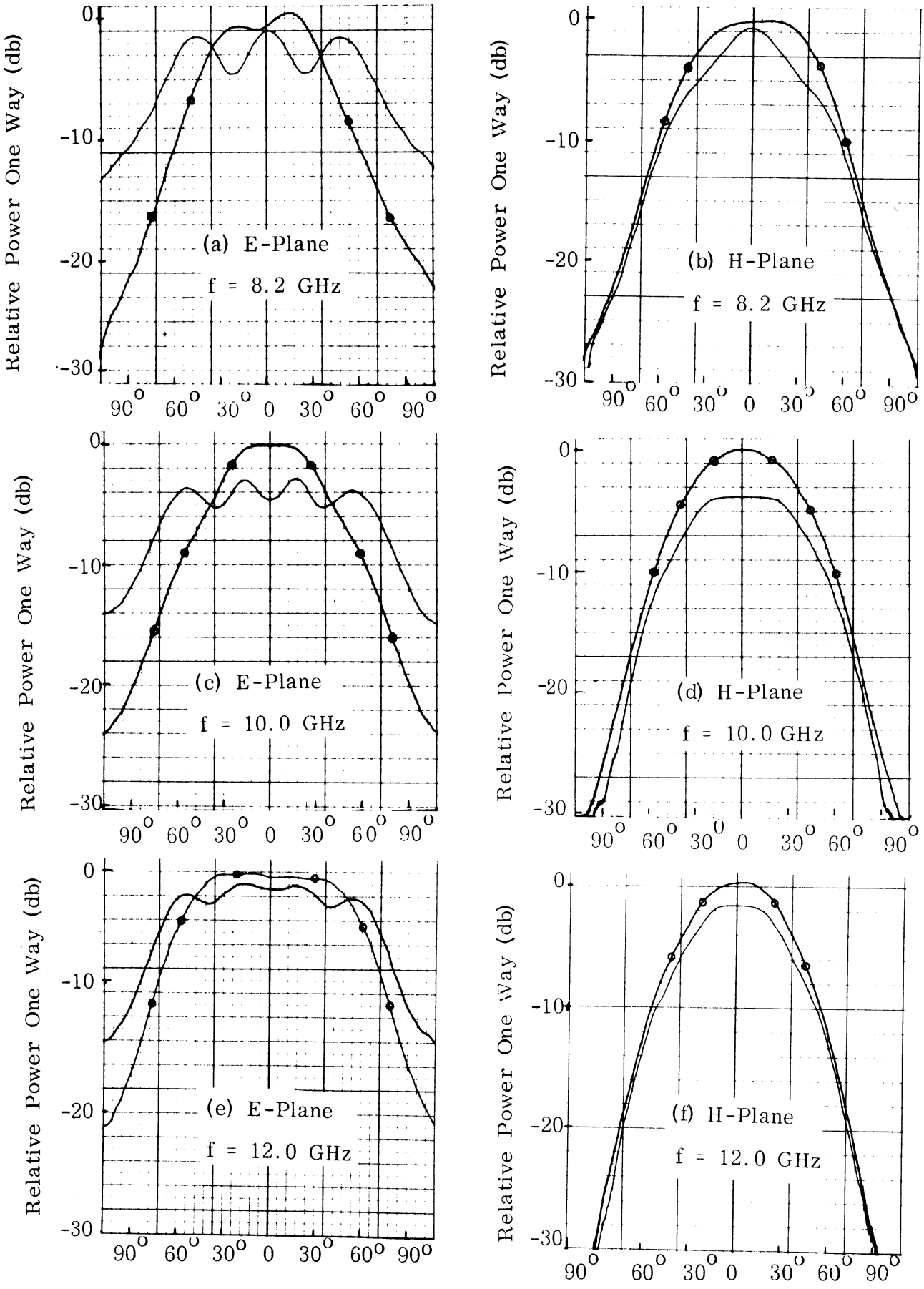

FIG. 3-26: RADIATION PATTERNS FOR A SLOT IN A METAL DISC OF 11.1 cm DIAMETER (—) Plain Disc, (-o-) Disc With Corrugations (R-1).

paraffin has a dielectric constant of approximately 2 and a dissipation factor less than 0.0002 (both at 25^{o} C). By filling all trenches with paraffin it was noted that decoupling or isolation was generally reduced. Thus the amount of additional isolation, compared to the case of two plain slots, varied from 5 db at 8 GHz to zero at 12 GHz. This is due to the fact that the presence of the dielectric made the trenches look deeper in terms of wavelengths. When dielectric loading is used the depth has to be reduced according to the factor $\sqrt{\epsilon_r \mu_r}$ which in may cases will be very desirable.

It is easy to calculate the desired dependence of the permittivity and permeability of a material upon frequency, so that corrugations would have a constant depth in terms of wavelengths. Consider for example, a piece of rectangular waveguide, of width a, terminated by a short. If the waveguide is filled with a material of relative permittivity ϵ_r and permeability μ_r, the wavelength inside the guide will be given by

$$\lambda_g = \frac{c}{\sqrt{f^2 \mu_r \epsilon_r - (c/2a)^2}} \tag{3.5}$$

where c is the speed of light. In order to have a constant λ_g as the frequency, f, is varied, it is necessary and sufficient that

$$f^2 \mu_r \epsilon_r = K \text{ (constant).} \tag{3.6}$$

Materials with such properties can be manufactured but they are inherently lossy. A lossy material is not desirable because by attenuating the waves inside the corrugations it reduces greatly their action.

In another experiment metal sectors were placed on top of the corrugations symmetrically located with respect to the H-plane of the slot. The objective was to isolate and eliminate portions of the trenches that may create undesir-

able radiation. By varying the angle of the sector (from 60^{o} to 90^{o} to 120^{o}) it was found that sectors of 90^{o} created a maximum additional reduction of the E-plane sidelobes which was accompanied by a reduction in coupling of 2 to 3 db over most part of the X-band (Lyon et al, March 1967).

Another experiment was carried out to test the effect of the corrugations at the second stop band. Regarding the corrugations designed for S-band the second stop band occurs at nearly the third harmonic frequencies of the first stop band which in this case would be X-band.

An X-band slot surrounded by a small flat disc was placed at the center of the S-band corrugations. Then the coupling to a second slot on the same ground plane was measured when the corrugations "S" were covered by aluminum foil and when they were uncovered. The results are shown in Fig. 3-27 (second and fourth curves from the top, respectively). It is seen that the stop-band starts at 8.34 GHz which is again within measurement error from the theoretically computed value of 8.31 GHz. Then the disc between the slot and corrugations S was replaced by another set of corrugations (designated R - 1, d = 0.85 cm) which had been designed for X-band. Again two measurements were made with the corrugations S covered and uncovered. The results are shown in Fig. 3-27 (third and fifth curves from the top, respectively). The maximum E-plane coupling over almost all of the X-band has been reduced from -35.5 db to -50.5 db.

In conclusion it is seen that the corrugations are inherently effective also in reducing coupling at the third harmonic frequencies of the original design frequency range. This is an important feature because of the third harmonic content in the output at microwave oscillators in particular and in the radiation of various antennas in general. Due to this phenomenon several interference problems have been reported between antennas operating at different frequencies.

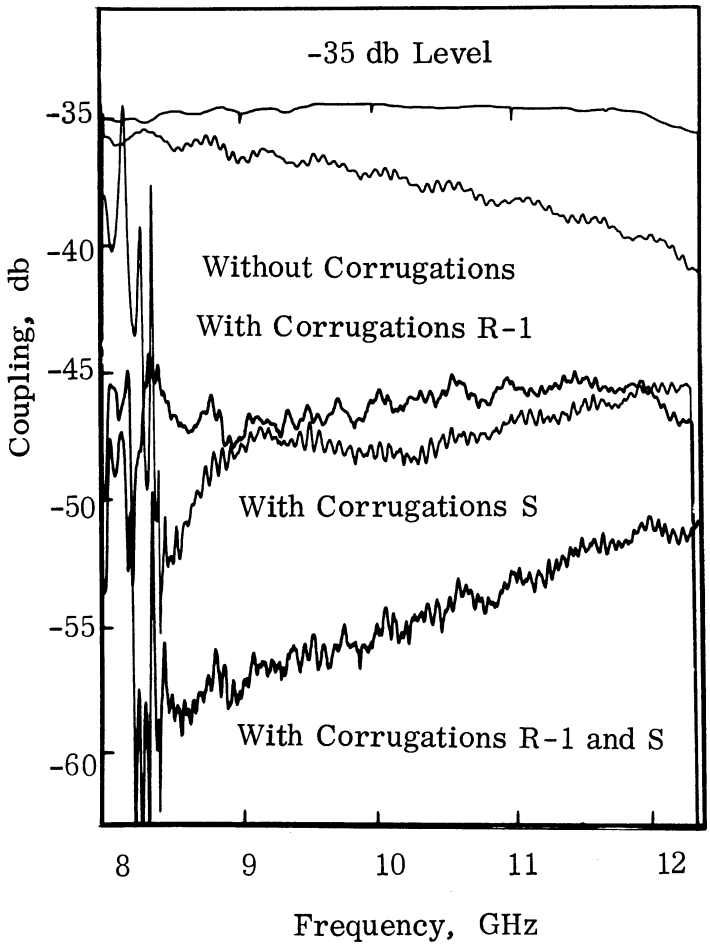

FIG. 3-27: E-PLANE COUPLING VS FREQUENCY FOR TWO X-BAND SLOTS SPACED 22.8 CM.

3.4.3 Tapered Wall Corrugations

It has been thought of interest to investigate the properties of a different type of corrugated surface, with tapered width trenches as shown in Fig. 3-28a. One motive in this investigation is that circular trenches of this profile can be easily machined in contrast to the parallel wall trenches.

Consider a single tapered trench as in Fig. 3-28b which extends to infinity in the z and r directions. This can be viewed as a non-uniform transmission line in the r-direction. The impedance of this line can be determined as follows.

Let $\overline{E} = E_\phi \hat{\phi}$ and assume no dependence upon the z-coordinate. Then Maxwell's equations reduce to ($j\omega t$ time dependence assumed and suppressed)

$$j\omega \epsilon E_\phi = - \frac{\partial H_z}{\partial r} , \qquad j\omega \mu r H_z = - \frac{\partial (r E_\phi)}{\partial r} . \tag{3.7}$$

The solution in terms of the Hankel functions is:

$$\left.\begin{aligned} H_z &= A H_o^{(1)}(kr) + B H_o^{(2)}(kr) \\ E_\phi &= - j \eta \left[A H_1^{(1)}(kr) + B H_1^{(2)}(kr) \right] . \end{aligned}\right\} \tag{3.8}$$

Let

$$\left.\begin{aligned} H_n^{(1)}(x) &= H_n(x)\, e^{j\theta_n(x)} \\ \text{and} \qquad H_n^{(2)}(x) &= H_n(x)\, e^{-j\theta_n(x)} \end{aligned}\right\} \tag{3.9}$$

where

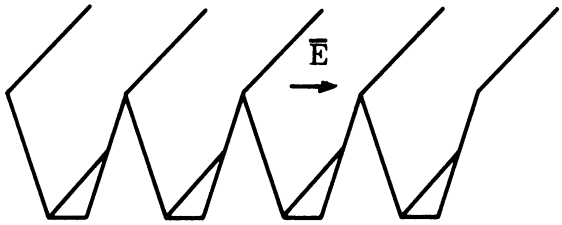

(a)

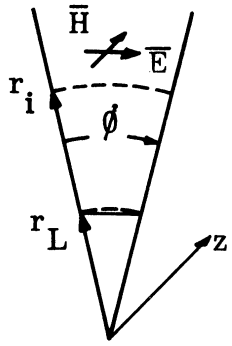

(b)

FIG. 3-28: CORRUGATIONS WITH TAPERED TRENCHES.

$$\left.\begin{aligned} H_n(x) &= \left[J_n^{(2)}(x) + Y_n^2(x)\right]^{1/2} \\ \theta_n &= \tan^{-1}\left[Y_n(x)/J_n(x)\right] \end{aligned}\right\} \qquad (3.10)$$

Then Eq. (3.8) can be written:

$$\left.\begin{aligned} H_z &= H_o(kr)\left[A e^{j\theta_o(kr)} + B e^{-j\theta_o(kr)}\right] \\ E_\phi &= -j\eta H_1(kr)\left[A e^{j\theta_1(kr)} + B^{-j\theta_1(kr)}\right] . \end{aligned}\right\} \qquad (3.11)$$

The impedance of the line, looking towards the apex, is defined as

$$Z_i = -E_\phi / H_z \Big|_{r = r_i} . \qquad (3.12)$$

Let also

$$Z_L = -E_\phi / H_z \Big|_{r = r_L} . \qquad (3.13)$$

Substituting Eqs. (3.11) and (3.13) into Eq. (3.12) one finally obtains the expression

$$Z_i(r_i) = Z_o(kr_i) \cdot \frac{Z_o(kr_L)\sin\left[\theta_1(kr_L) - \theta_1(kr_i)\right] + jZ_L \sin\left[\theta_o(kr_L) - \theta_1(kr_L)\right]}{Z_L \sin\left[\theta_o(kr_L) - \theta_o(kr_i)\right] - jZ_o(kr_L)\sin\left[\theta_1(kr_L) - \theta_o(kr_i)\right]} \qquad (3.14)$$

where

$$Z_o(kr) = \eta \frac{H_1(kr)}{H_o(kr)} \quad . \tag{3.15}$$

For $Z_L = 0$ (short at $r = r_L$) this reduces to:

$$Z_i(r_i) = j\, Z_o(kr_i) \frac{\sin\left[\theta_1(kr_i) - \theta_1(kr_L)\right]}{\sin\left[\theta_o(kr_i) - \theta_1(kr_L)\right]} \quad . \tag{3.16}$$

Assuming that the line is narrow enough so that the high order modes are attenuated rapidly one may still use Eq. (3.16) to predict the input impedance of a tapered trench whose walls terminate at $r = r_i$. Then for a series of parallel trenches as shown in Fig. 3-28a considerations similar to the ones used to derive Eq. (3.2) yield for the surface reactance

$$X_s(r_i) = \frac{w}{s} Z_o(kr_i) \frac{\sin\left[\theta_1(kr_i) - \theta_1(kr_L)\right]}{\sin\left[\theta_o(kr_i) - \theta_o(kr_L)\right]} \tag{3.17}$$

where w and s have the same meaning as in Eq. (3.2) and are measured at the aperture. From Eq. (3.17) it is seen that the reactance changes from positive to negative when:

$$\theta_o(kr_i) - \theta_1(kr_L) = m\pi \; ; \; m = 1, 2, \ldots . \tag{3.18}$$

The solution of Eq. (3.18) with $k = 2\pi/\lambda$ is plotted in Fig. 3-29. It is seen that this solution tends asymptotically to the corresponding solution of Eq. (3.2) as expected. With the help of Fig. 3-29 one can determine r_i once r_L and λ_o have been chosen.

When $r_L = 0$, it is seen from Eq. (3.17) that X_s will become positive when $f = 1.6 f_o$. Here f_o is used to denote the frequency at which the trench depth, $d = r_i - r_L$, is equal to one quarter of the free space wavelength. In

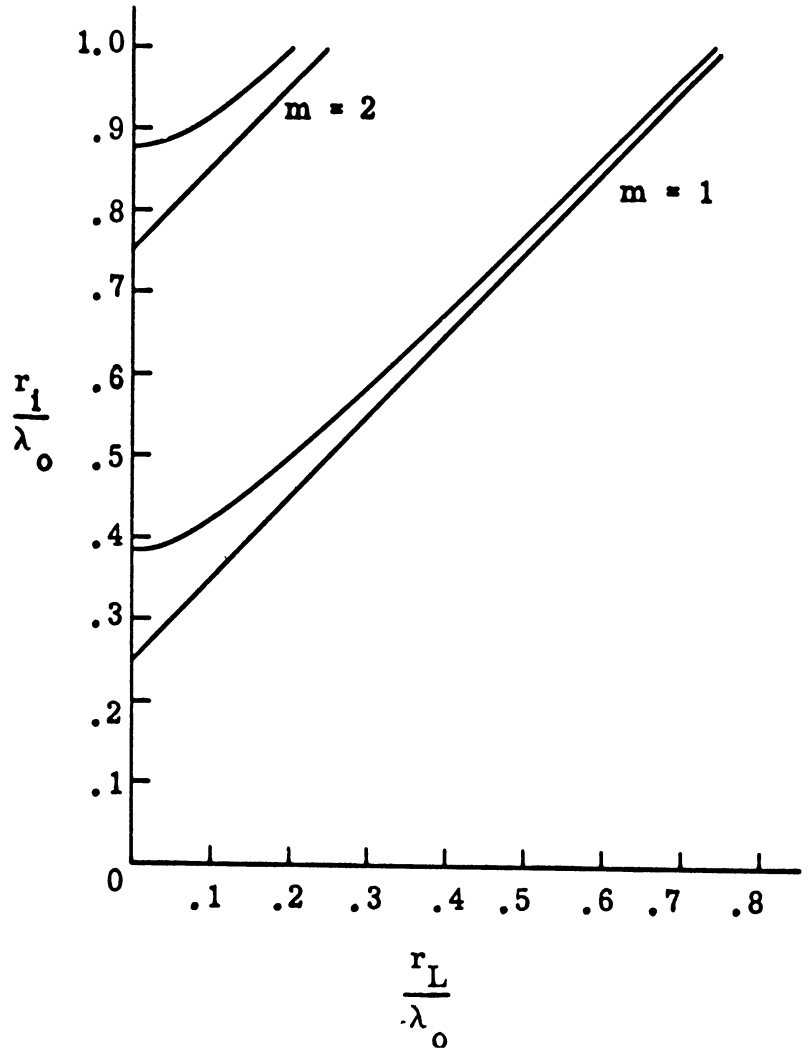

FIG. 3-29: SOLUTION OF $\theta_o(2\pi r_i/\lambda_o) = \theta_1(2\pi r_L/\lambda_o) + m\pi$ AND ASYMPTOTE $r_i - r_L = (2m - 1)\lambda_o/4$.

general, for $0 \leq r_L \leq \infty$ the crossover point, i.e., the point where X_s becomes inductive, will be at some frequency f, such that

$$1.6 f_o < f < 2 f_o \quad . \tag{3.19}$$

Thus, the tapering of the trench width restricts somewhat the frequency range over which the corrugations offer a capacitive surface impedance and thereby reduce the antenna radiation along the ground plane. Even then, the corrugations act favorably over at least one waveguide band of frequencies. What is gained in exchange is an easily milled profile which allows the wall width at the top (s - w) to become practically zero which as was mentioned earlier improves the amount of coupling reduction.

Three sets of circumferential corrugations with different cut-off frequencies and profiles were manufactured and tested. Each set had six trenches; their dimensions are shown below in Table III-1.

TABLE III-1: DIMENSIONS OF TAPERED CORRUGATIONS. (In cm)
(Tolerance of r_L, r_i: $\pm$ 0.03 cm).

	r_L	r_i	b	t
Set R4	0.25	0.97	0.50	$\leq$ 0.01
Set R5	0.05	0.98	0.50	$\leq$ 0.01
Set R6	0.36	1.36	0.50	$\leq$ 0.01

The corrugations were surrounding an X-band slot, being flush with the ground plane. The E-plane coupling with and without corrugations around one slot is shown in Fig. 3-30 and 3-31 for two of the above mentioned sets.

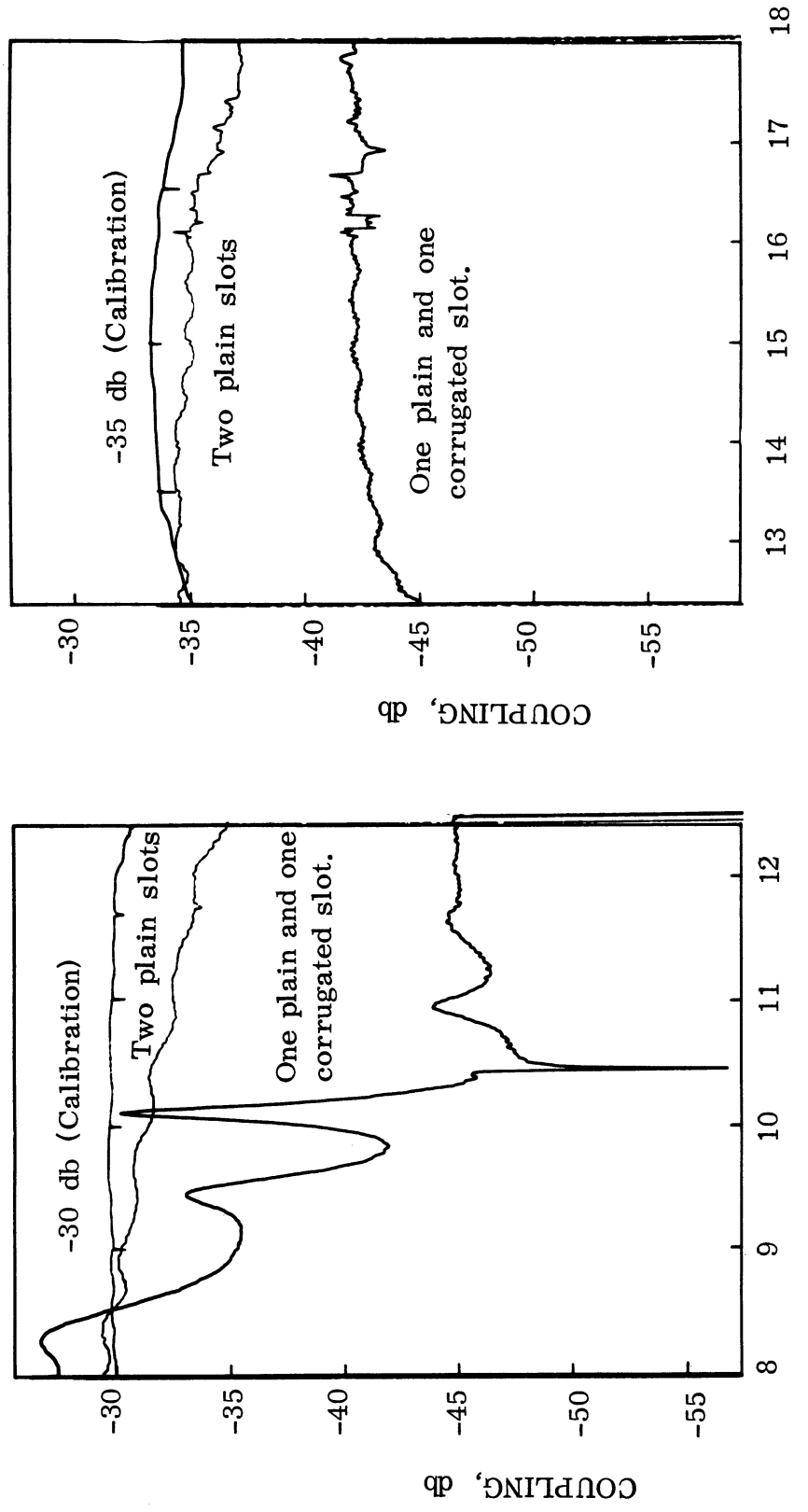

FIG. 3-30: E-PLANE COUPLING VS FREQUENCY FOR TWO SLOTS SPACED 11.4 CM (Corrugations R-5).

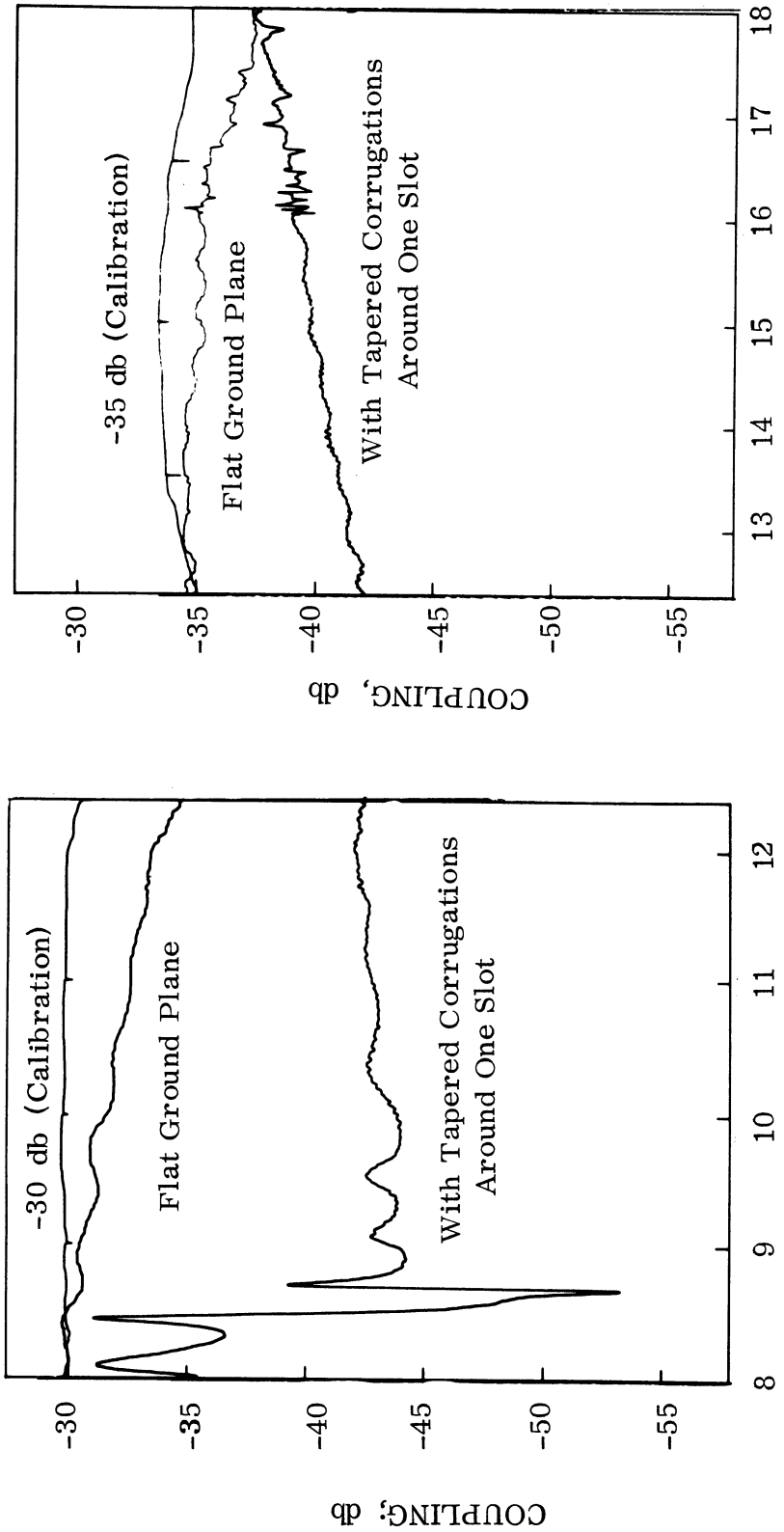

FIG. 3-31: E-PLANE COUPLING VS FREQUENCY FOR TWO SLOTS SPACED 11.4 CM (Corrugations R-6).

The E-plane decouplings obtained over a 1.5:1 frequency range with corrugations R-4, R-5 and R-6 are 11 db, 12 db and 11 db respectively. Only corrugations R-6 were measured over a 2:1 frequency band and there the decoupling obtained was 8 db. It should be noted that twice as much decoupling (in db) is expected when both antennas are surrounded by similar corrugations. Also greater decoupling can be obtained by increasing the number of trenches i.e., by increasing the reactively loaded area.

Typical radiation patterns for a slot surrounded by tapered-trench corrugations in a 60 cm by 90 cm (2 ft by 3 ft) rectangular ground plane and in a disc of 11.4 cm diameter, are shown in Figs 3-32 and 3-33 respectively. These figures show that the sidelobe decrease is accompanied by a considerable increase in antenna gain. This was examined in more detail, in a swept frequency measurement, as shown in Fig. 3-34. The reactive loading increases the antenna gain by as much as 5 db at same frequencies.

A comparison of the frequencies where the stop-band starts, as predicted by the curves of Fig. 3-29 and as experimentally obtained (Figs. 3-30 and 3-31) shows that the theoretically predicted frequencies are always too high by 3 to 5 percent. The agreement is considered good given the fact that the estimates are based on "average surface impedance" and a two-dimensional model. The relatively good agreement is due to the fact that the models used had very thin walls at the top. In this case the average impedance concept is more accurate. The more exact analysis used in the case of parallel wall trenches and resulting in Eq. (3.4) can be used here too, the only difference being that instead of Eq. (3.3) one would have to use Eq. (3.14). The use of this more accurate model, however, becomes necessary only when smaller w/s ratios are used.

All the coupling reduction data presented so far were obtained by applying a given modification to one antenna only of a receiver-transmitter pair. It

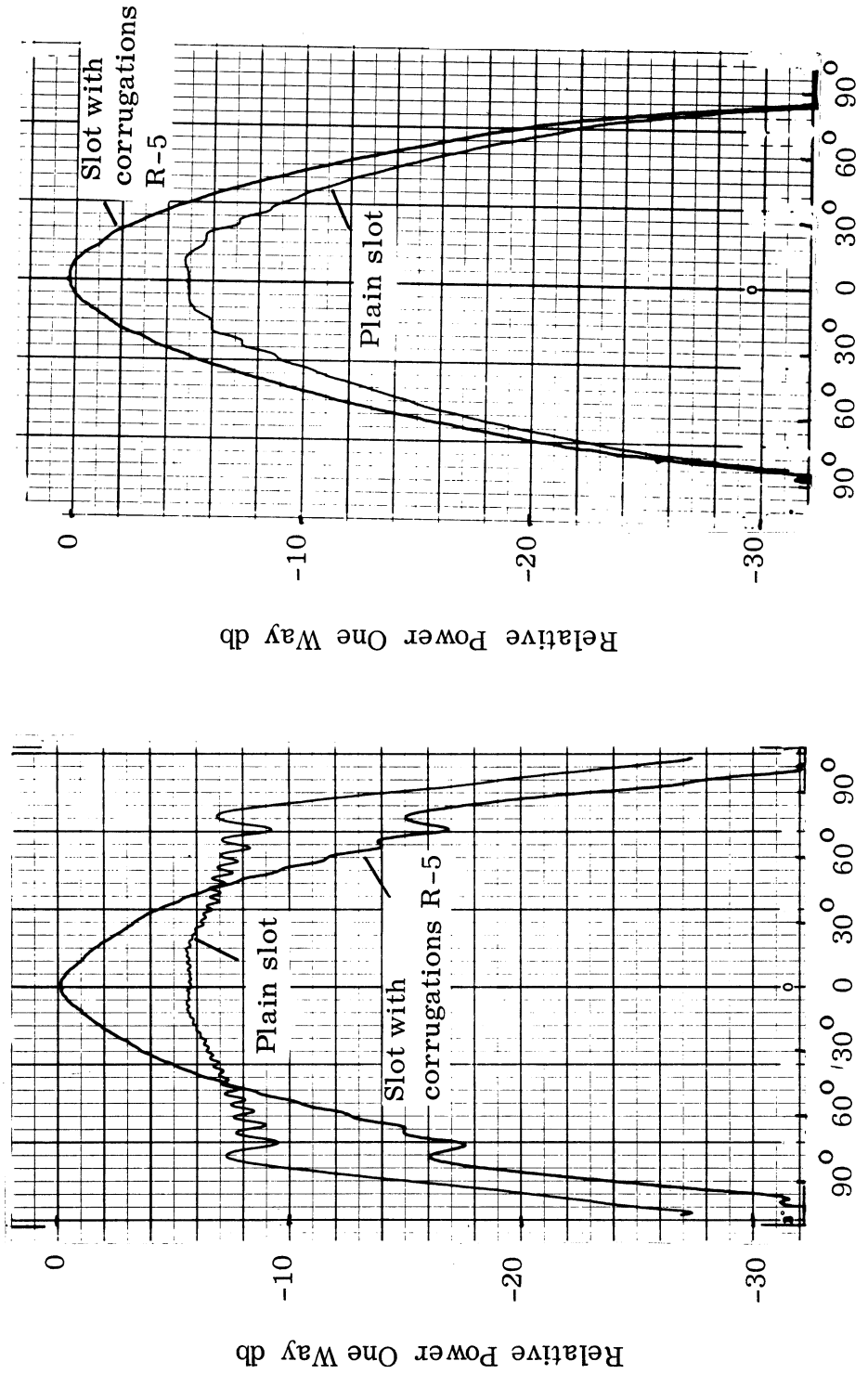

FIG. 3-32: E- AND H-PLANE RADIATION PATTERNS FOR A SLOT IN 2 FT BY 3 FT METAL PLANE AT 12 GHz.

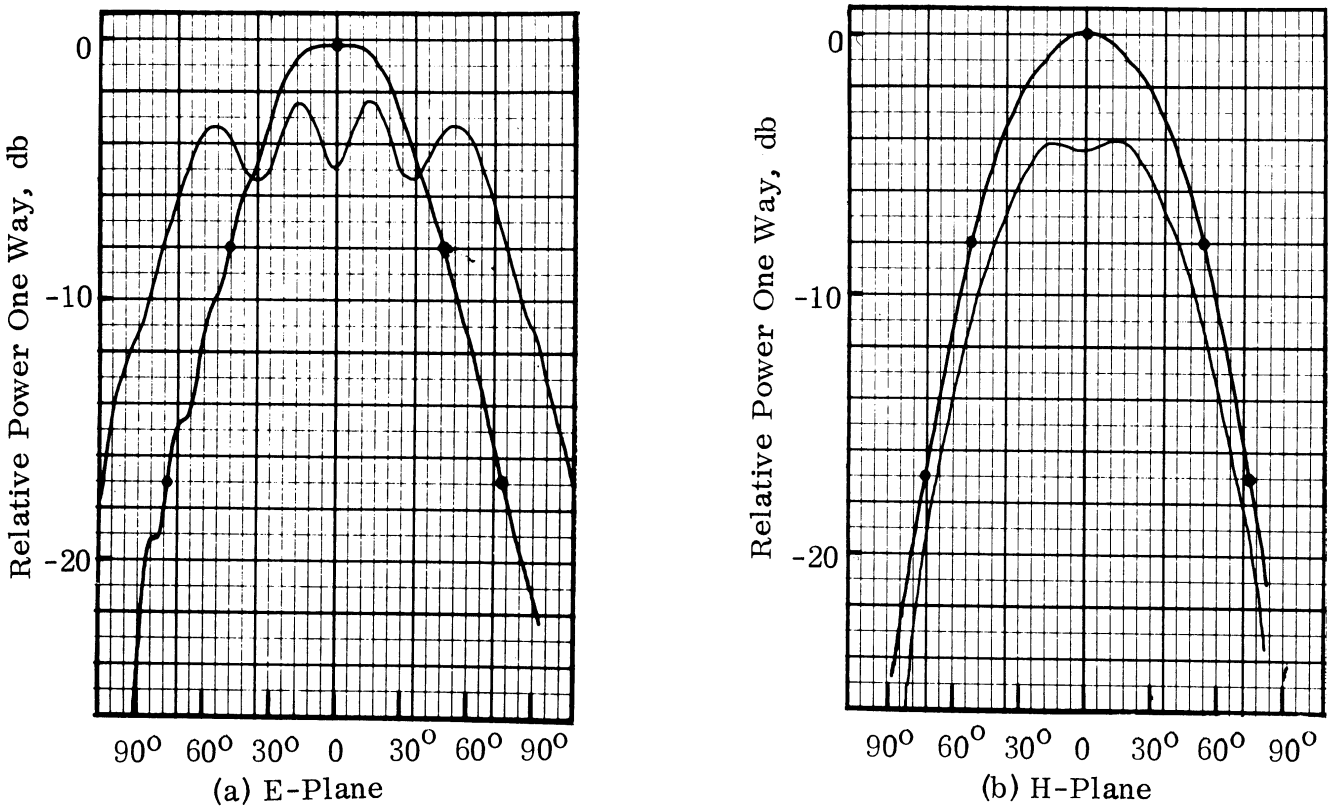

FIG. 3-33: RADIATION PATTERNS AT 10 GHz FOR A SLOT IN A DISC OF 11.4 cm DIAMETER. (——) Plain Disc; (—●—) Disc With Corrugations (R-6).

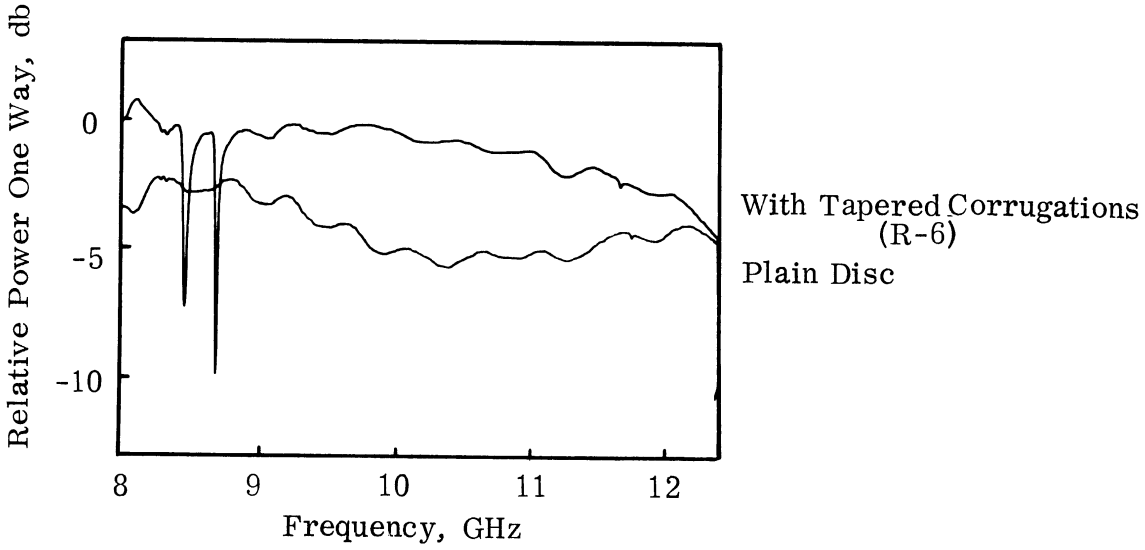

FIG. 3-34: MAXIMUM GAIN VERSUS FREQUENCY FOR A SLOT IN A METAL DISC OF 11.1 cm DIAMETER.

has been often stated that twice as much coupling reduction would be obtained (in db) if both antennas were similarly modified. A justification of this statement is provided by the following experiment. Two slot antennas at a center-to-center spacing of 22.8 cm (7.6λ at 10 GHz) were each surrounded by corrugations. The corrugated discs R-1 and R-6 were used. The decoupling obtained when each set of corrugations was used alone when they were used simultaneously is shown in Fig. 3-35. From this figure it can be verified that the total decoupling is equal to the sum of the decouplings obtained by each method individually (when all quantities are expressed in db).

3.4.4 Archimedean Spirals

When a spiral operates in a pure axial (or first order) mode there is a null along the ground plane and the coupling to another spiral in the same ground plane should be zero. In actual operation, however, reflections from the ends of the spiral elements may occur giving rise to a standing wave along the spiral arms. Also small in-phase currents at the feed excite additional modes, of order zero, two, etc. The zero order mode in particular will cause a considerable amount of radiation along the ground plane. These feed and termination defects are considered to be primarily responsible for the coupling between two spirals. Therefore this is a case of weak coupling comparable to the H-plane coupling of slots.

Two similar Archimedean spirals made by Aero-Geo-Astro Corporation (Model AGA-100-3-2) for the frequency range 2 GHz to 4 GHz were used for the measurement of coupling. The two spirals were mounted in a large (12 ft by 12 ft.) ground plane at a center-to-center spacing of 22.8 cm (2.5λ at 3.3 GHz). The coupling measurements were made by a swept frequency technique. Due to this no matching devices were used between the transmission line and the antennas. A spot check, however, indicated that the use of matching

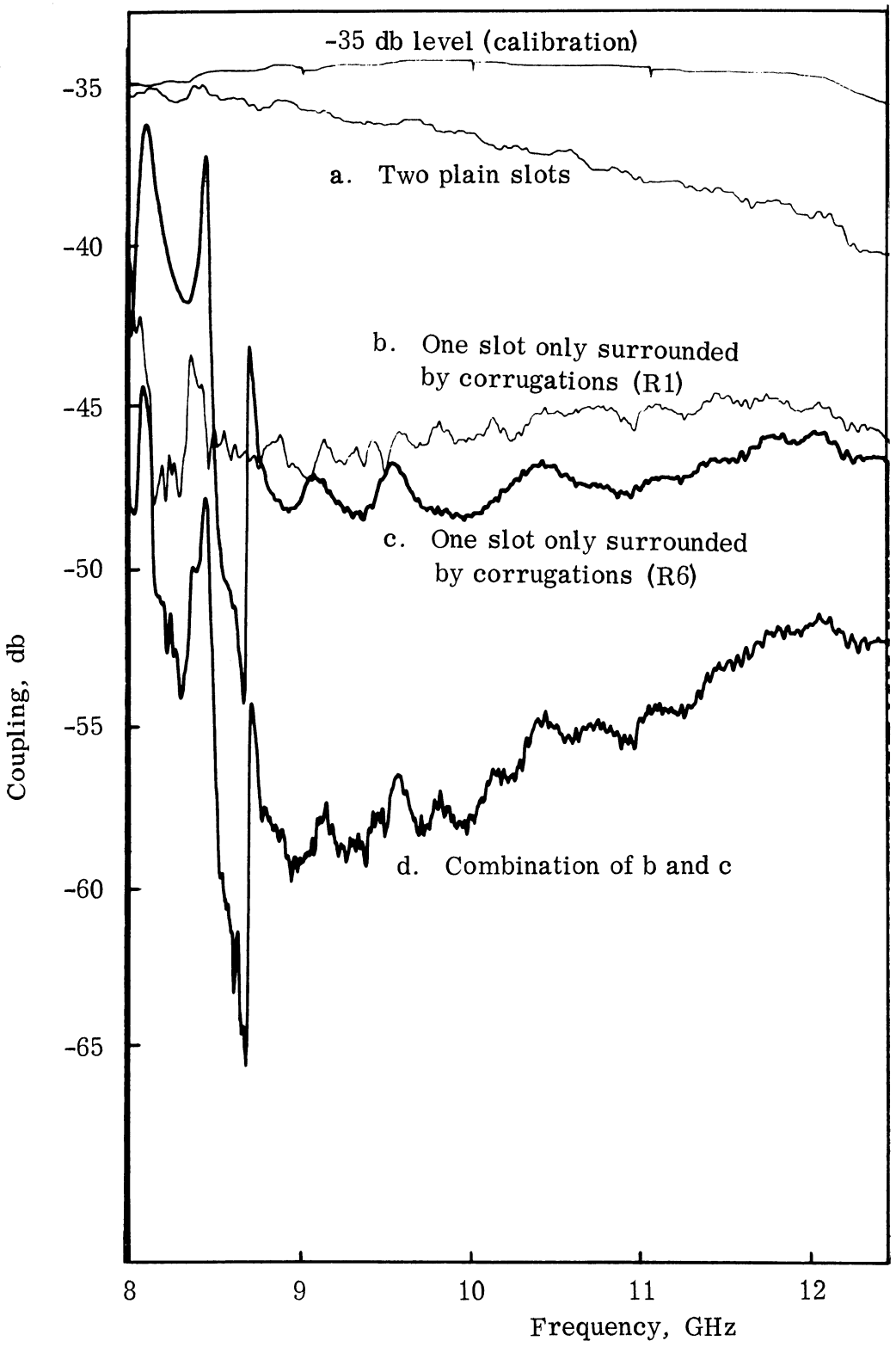

FIG. 3-35: REDUCTION OF THE E-PLANE COUPLING OF TWO SLOTS SPACED 22.8 CM BY MEANS OF CORRUGATIONS.

devices results in no more than 1 db difference in the coupling level. However the defects of the feeds to the spiral are emphasized in swept frequency methods.

For the coupling measurements the two spirals were positioned in three different ways as shown in Fig. 3-36. In this figure the position of the spirals are determined from the relative orientation of the feed terminals. One of the spiral antennas was surrounded by circumferential corrugations "S" and then the coupling was measured with the corrugations covered and then uncovered. The two curves obtained for every orientation of the feed terminals are shown in Fig. 3-37a through c. For any given frequency the coupling depends upon the relative orientation of the two spirals. However, the swept frequency coupling patterns taken for different orientations exhibit the same general characteristics except that the peaks and troughs occur at different frequencies. The corrugations accomplished a moderate coupling reduction of 6 db in the frequency range 2.8 to 4.0 GHz.

The effects of the corrugations on the spiral radiation pattern at different frequencies are shown in Fig. 3-38. These patterns were obtained by illuminating the spiral with a linearly polarized standard gain horn. The polarization was chosen so that the E-field vector would be perpendicular to the ground plane at $\theta = 90^{o}$. The patterns are shown for two different orientations of the spiral; one where the (imaginary) line determined by the two feed points is parallel to the E-field and another where it is perpendicular. A sidelobe decrease of the order of 6 to 11 db is observed, accompanied by a gain increase. The gain increase due to the corrugations varies from 1 db at the low end of the frequency range to zero db at the high end.

The change in VSWR is summarized in the following table.

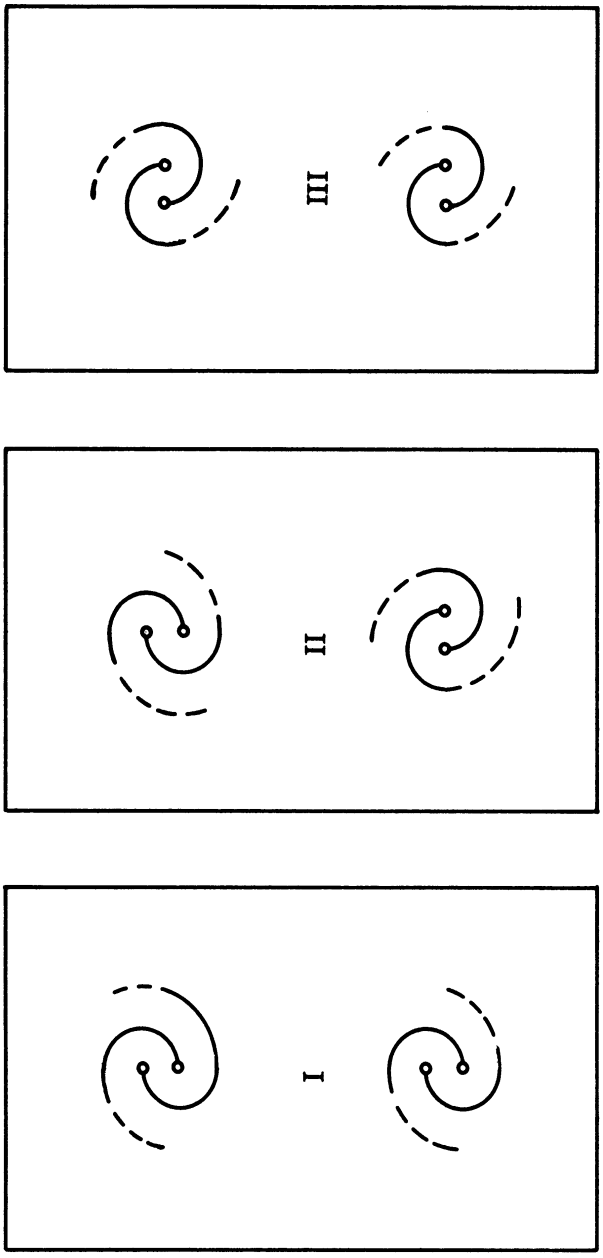

FIG. 3-36: RELATIVE POSITIONS OF CIRCULAR SPIRALS (FEEDS).

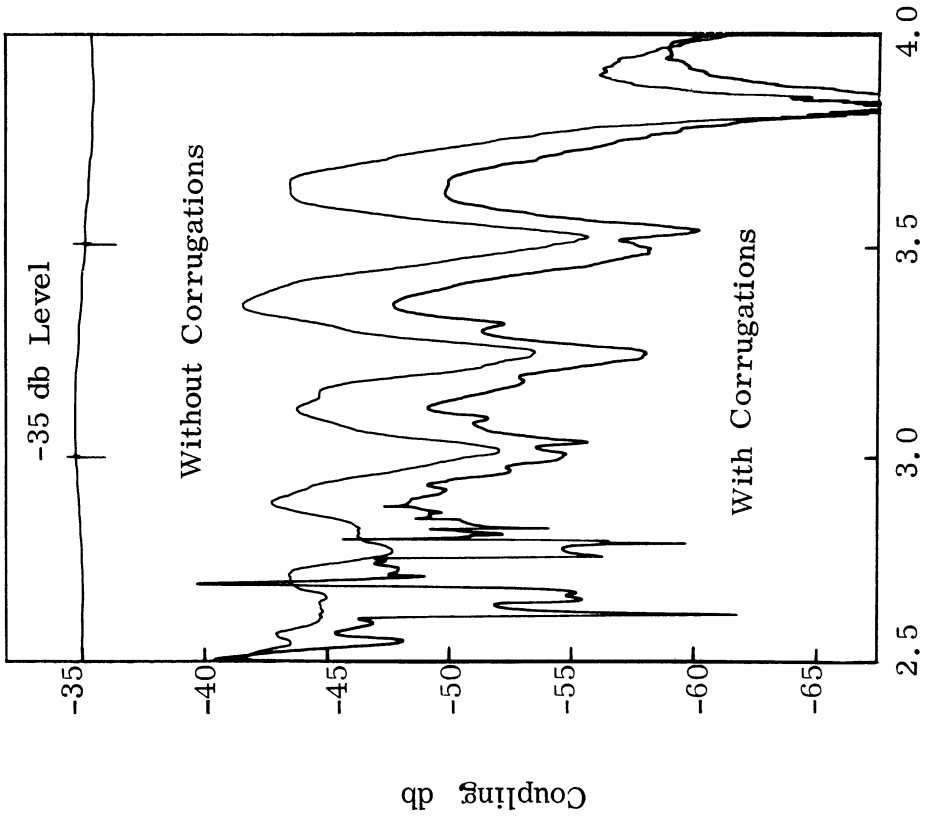

(b) Position III

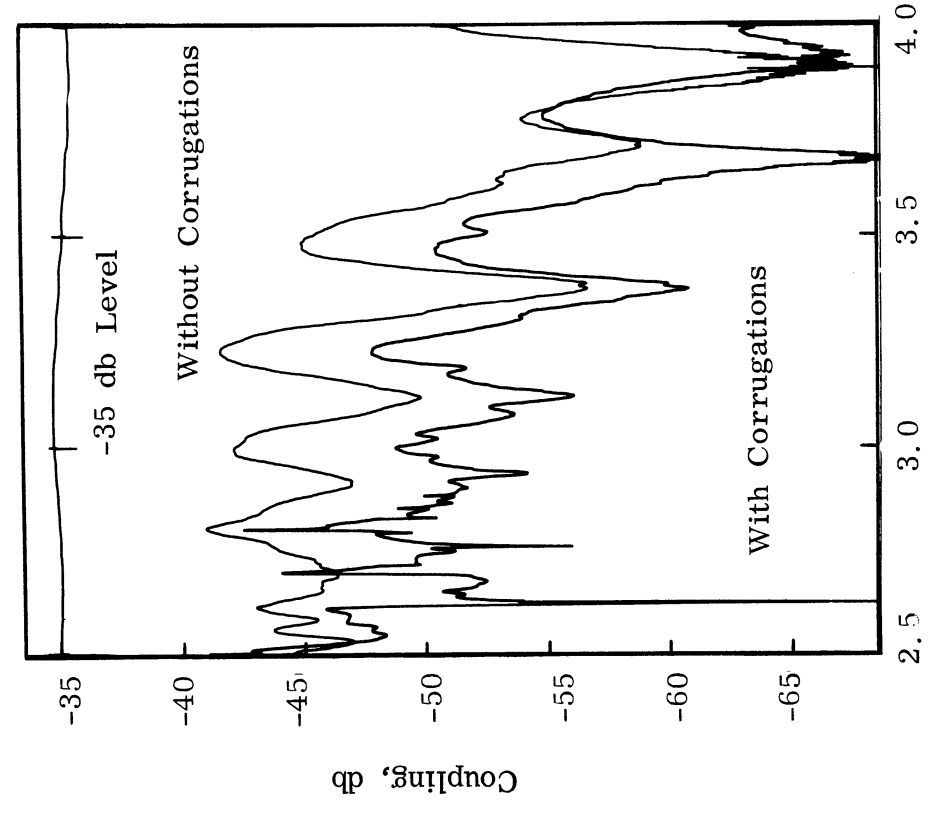

(a) Position I

FIG. 3-37: COUPLING VS FREQUENCY FOR TWO ARCHIMEDEAN SPIRALS SPACED 22.8 CM.

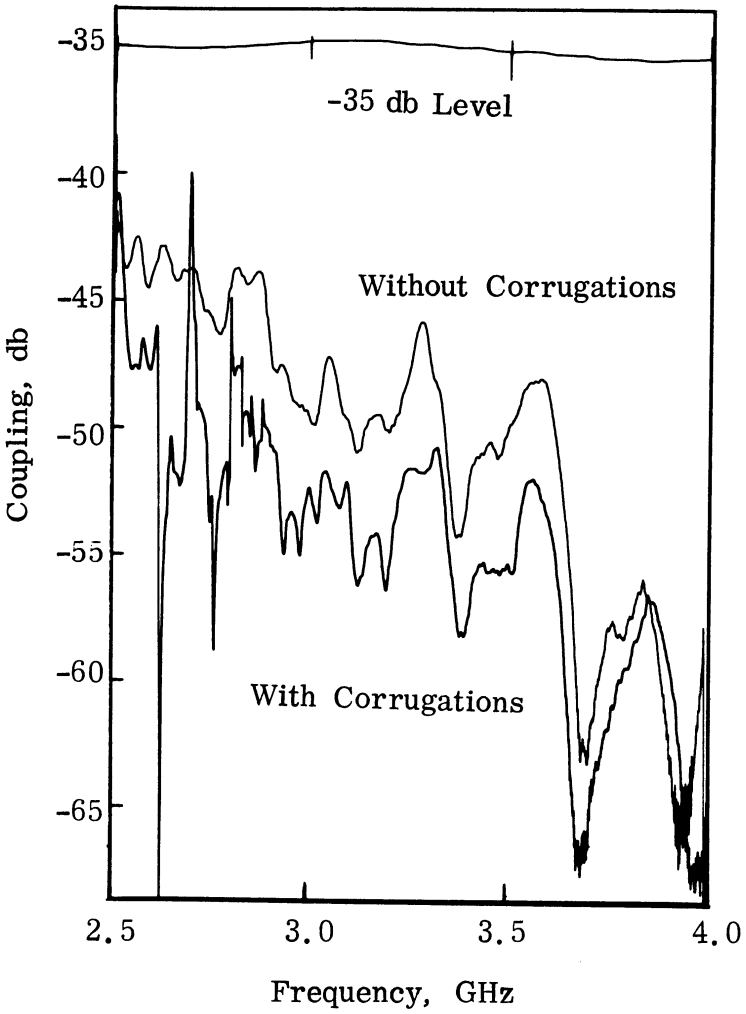

(c) Position II

FIG. 3-37: CONTINUED.

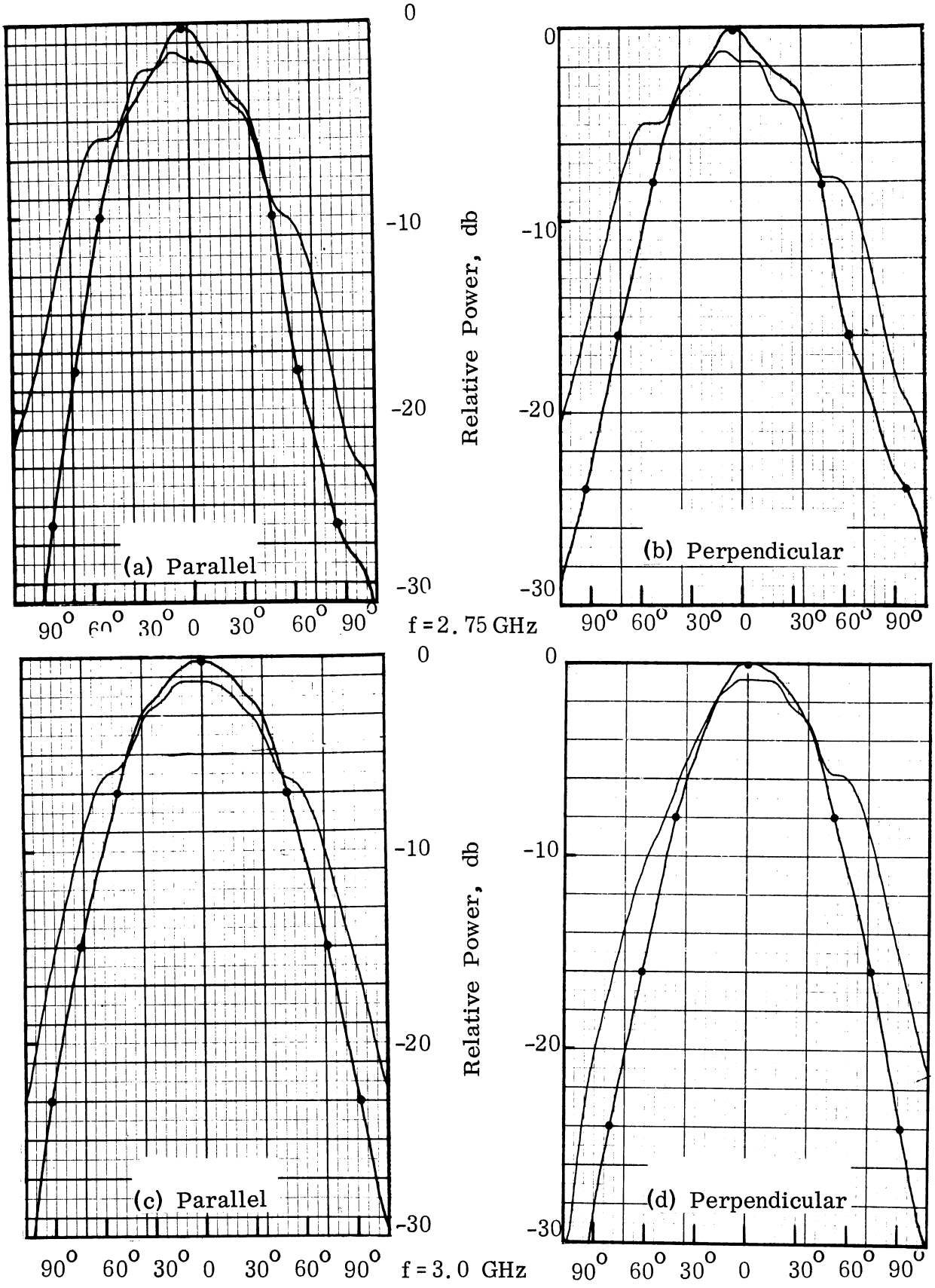

FIG. 3-38: RADIATION PATTERNS OF AN ARCHIMEDEAN SPIRAL IN A 2 FT. BY 3 FT. METAL GROUND PLANE FOR TWO NORMAL LINEAR POLARIZATIONS. (——) Flat Plane; (—o—) With Corrugations.

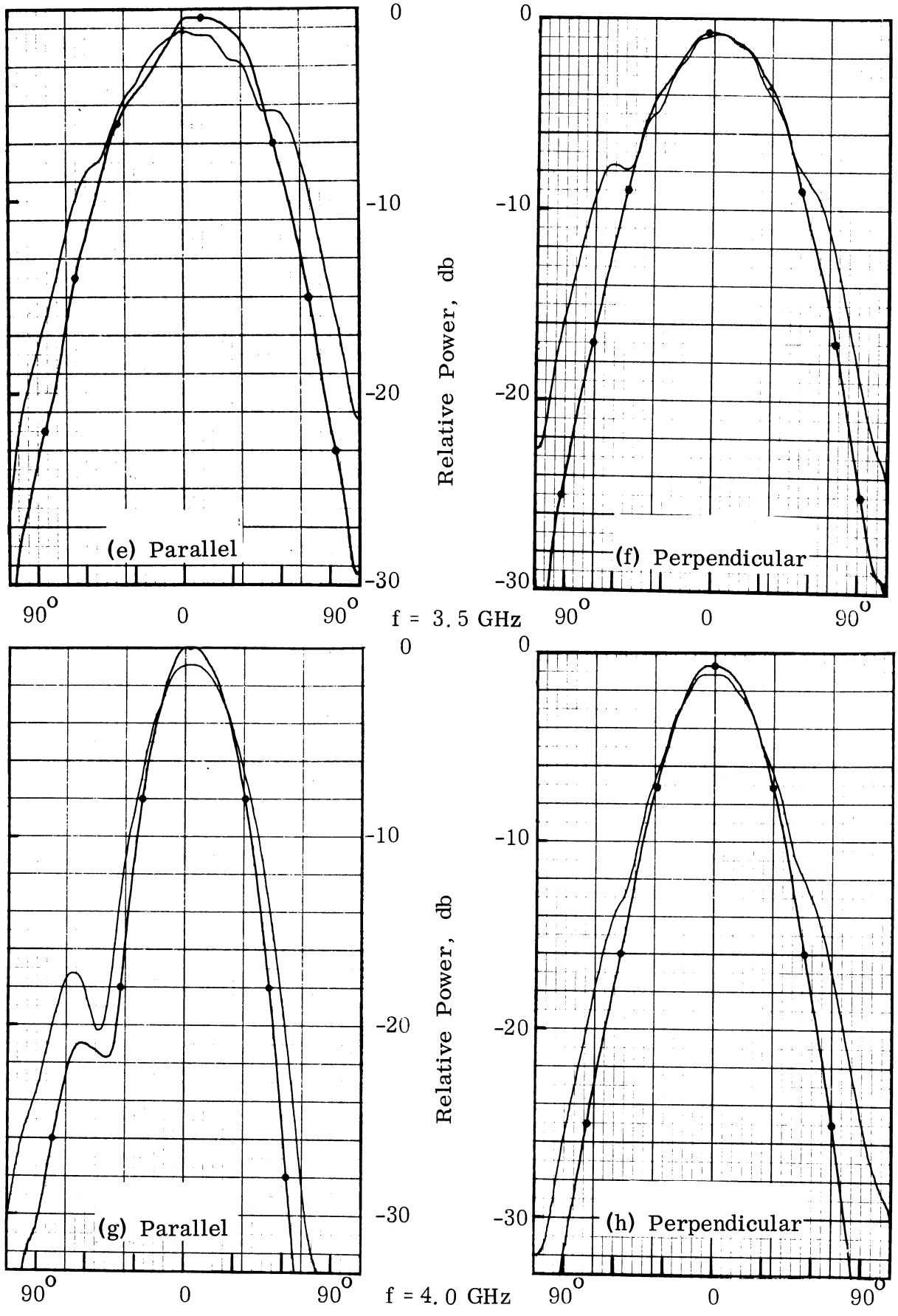

FIG. 3-38: CONTINUED

TABLE III-2: SPIRAL STANDING WAVE RATIO

Frequency, GHz	2.75	3.00	3.25	3.50	3.75	4.00
Flat Ground Plane	1.45	1.33	1.26	1.90	1.79	1.75
With Corrugations	1.60	1.42	1.47	1.31	1.40	1.37

3.4.5 Thin Slots

Thin slots are used in many applications operating over a narrow band of frequencies. The thin slot is the complimentary antenna of the half-wave dipole. Therefore, it is a low directivity antenna. A slot cut in a large metal sheet and fed by waveguide or backed by a cavity, so that all the radiation is confined to one side of the sheet, has a directivity of approximately 2 db above a semi-isotropic radiator (5 db above isotropic). The use of capacitive reactive loading in the ground plane increases the maximum gain of this antenna by more than 3 db while at the same time decreases the gain along the ground plane by 10 db. (see Fig. 3-39a). Thus a slot with ground plane loading can produce a radiation pattern similar to that of a small horn. This may be useful in aerospace applications where it is required that the antenna have a minimum penetration below the surface and therefore the use of a horn is unacceptable.

For the radiation patterns of Fig. 3-39, a thin slot of dimensions 2.29 cm by 0.15 cm was mounted in a 3.60 m (12 ft.) square ground plane. The slot was fed by an X-band waveguide with tapered walls in the H-plane. Corrugations R-1 were used to create the capacitive surface impedance. The radiation patterns were taken with a probe describing a circumference of radius 1.75 m. A leveled sweep generator was used as a source for all patterns. Because of the high standing wave ratio in the feeding waveguide created by the tapered walls, a tuner was used at every frequency and before the recording of each curve the

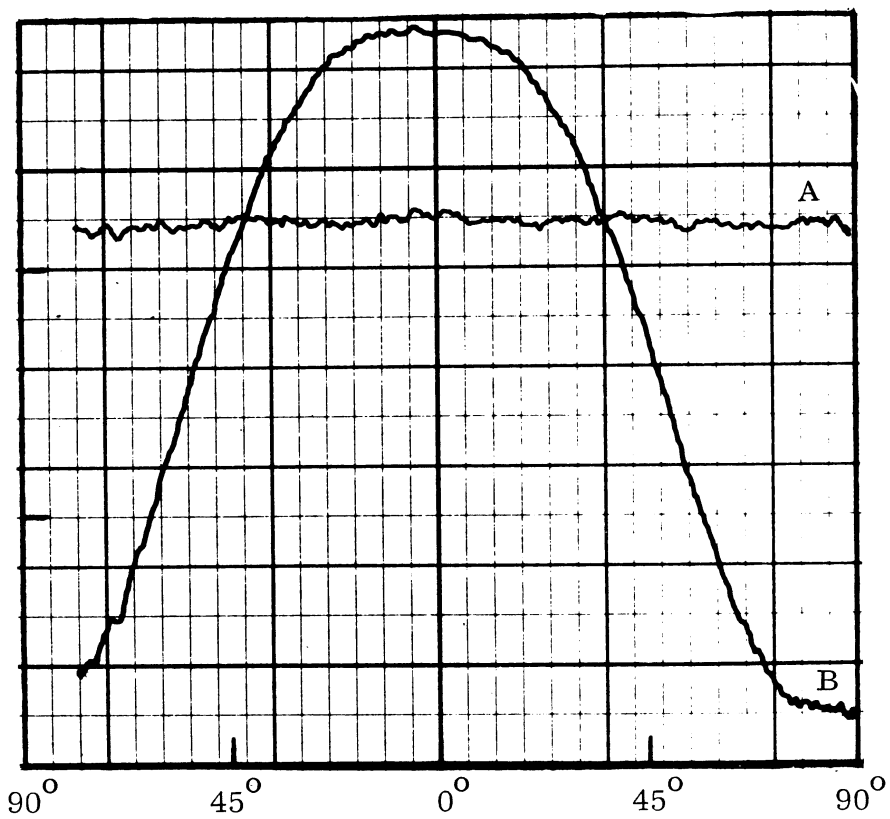

(a) 8.500 GHz

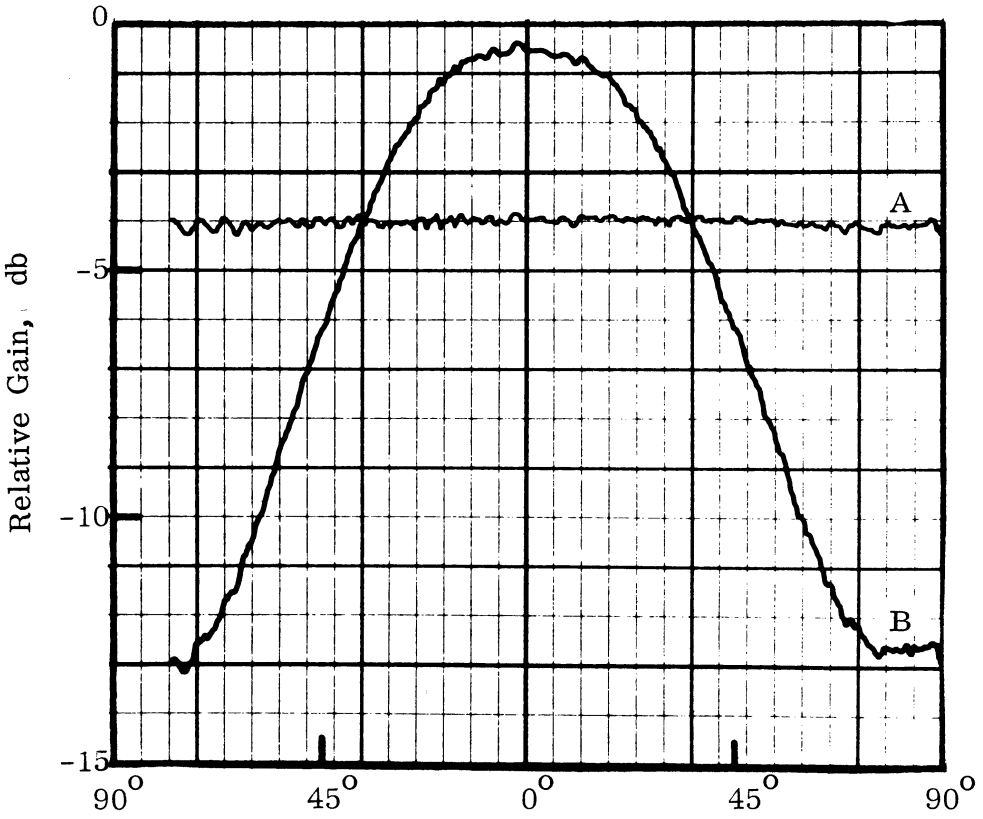

(c) 10.000 GHz

FIG. 3-39: E-PLANE PATTERNS OF A THIN SLOT
A: Flat Ground Plane
B: With Corrugations (R - 1).

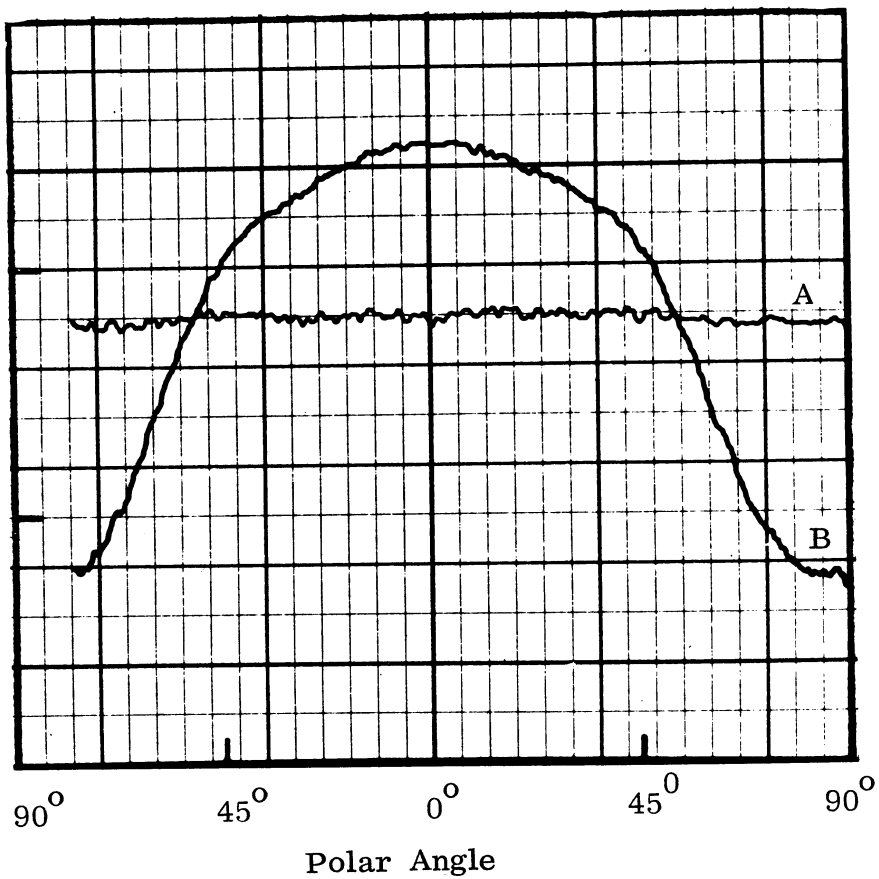

(c) 11.000 GHz

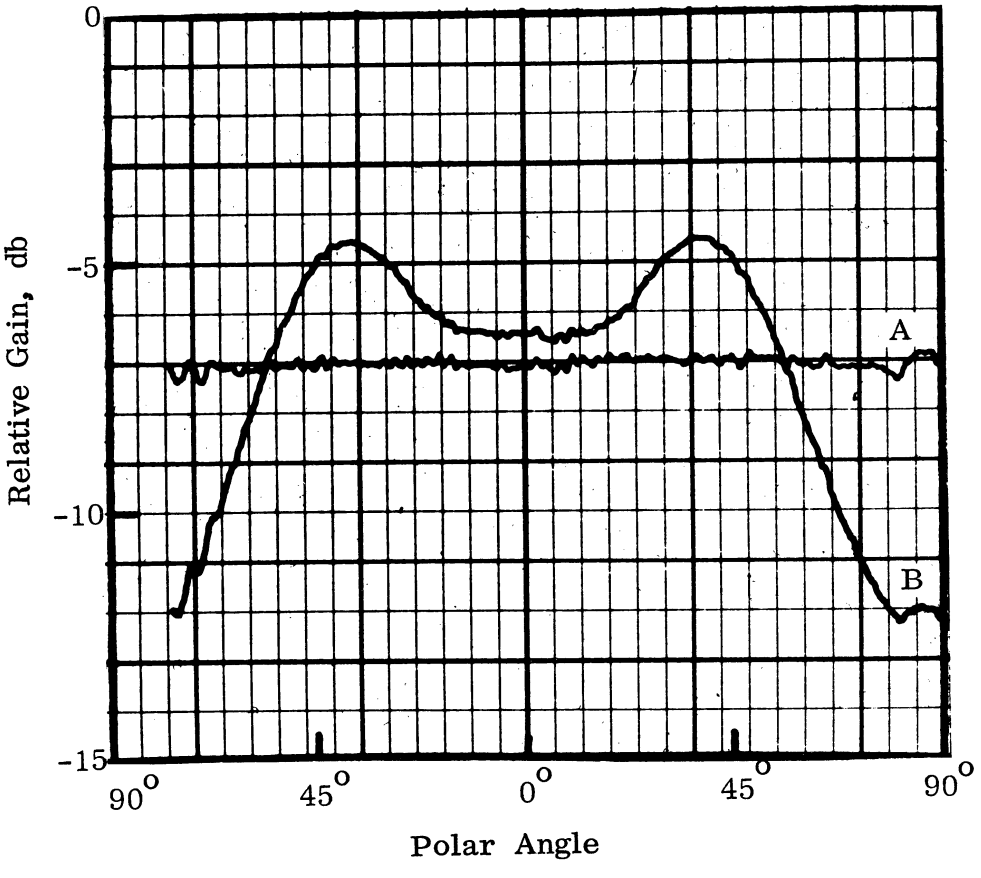

(d) 12.000 GHz

FIG. 3-39: CONTINUED

SWR in the transmission line was reduced to less than 1.2. A very minor tuning was necessary when changing from the flat ground plane to the corrugations, in order to achieve maximum radiated power.

The reduction of the (absolute) gain of the slot at higher frequencies was expected since the slot operated further away from resonance. The decrease in the amount of sidelobe reduction is due to fact that the corrugations also operate farther away from the design cut-off frequency (cf. with Fig. 3-23). It is interesting to note the split beam appearing at 12 GHz. When the same corrugations were used with a broadband slot no such beam splitting was observed (see Fig. 3-24). The difference lies in the fact that because of the thin slot used here, the distance between the edge of the slot and the beginning of the corrugations, measured along the slot E-plane, is over $\lambda/2$ at 12 GHz. To be exact, this distance (1.5 cm) is equal to 0.55λ at 11.0 GHz (where no pattern splitting occurs) and to 0.60λ at 12.0 GHz (split beam). This then, provides an experimental estimate of how close to the aperture the loading should be in order to avoid splitting of the beam. Of course, in order to have maximum effect of the loading it is desirable that the loading start immediately adjacent to the antenna aperture.

3.4.6 E-Sectoral Horns

Two identical, X-band E-Sectoral horns were used, mounted flush in the 3.6 m (12 ft.) square ground plane. These horns were fed from X-band waveguide (1.0 cm x 2.3 cm), had a flare angle of 20^{o} and aperture dimensions 3.9 cm by 2.3 cm. The reactive loading was accomplished by placing the corrugated disc "S" (see Fig. 3-17) around the horn aperture. These corrugations were designed for use at S-band, however, as it has already been stated, they are also effective at X-band. Due to the smaller wavelength at X-band, the corrugated surface has about 3 trenches per wavelength, which

corresponds to approximately 10 trenches per wavelength at S-band. The corrugated disc was mounted flush with the surrounding flat area of the ground plane.

The decoupling accomplished with reactive loading around one antenna aperture only is shown in Fig. 3-40. The maximum coupling, over the X-band, was reduced by 9 db. In this case the antenna center-to-center spacing was on the average 7.5 wavelengths. Radiation patterns were recorded with the transmitting antenna in the same configuration except that the receiving horn aperture was covered, to form a smooth flat surface around the area with the corrugations. The maximum sidelobe reduction of the order of 20 db, was observed at 8.64 GHz (Fig 3-41). Both the E- and H-plane radiation patterns are presented for this frequency. E-plane radiation patterns are also presented for two more frequencies (see Figs. 3-42 and 3-43). The corresponding H-plane patterns are not shown because they did not show any appreciable change.

The sidelobe reduction was accompanied by a very small (less or equal to 0.6 db) broadside gain increase. This is in contrast to the substantial gain increase which was observed when low directivity antennas were used (cf. with Section 3.4.2). This is partly due to the fact that in an antenna with medium to high gain in the broadside direction, only a small amount of energy is radiated along the ground plane. By redirecting this energy towards the broadside a small term is added to a large term and therefore only a small change results. Another reason, applicable to the particular case examined here, is that for the experiments of this section components (i.e. antenna and corrugated disc) that were readily available were used. Although the combination gave good results, it did not represent an optimum overall design, the main deficiency being that the distance between the E-plane horn aperture edge and the cor-

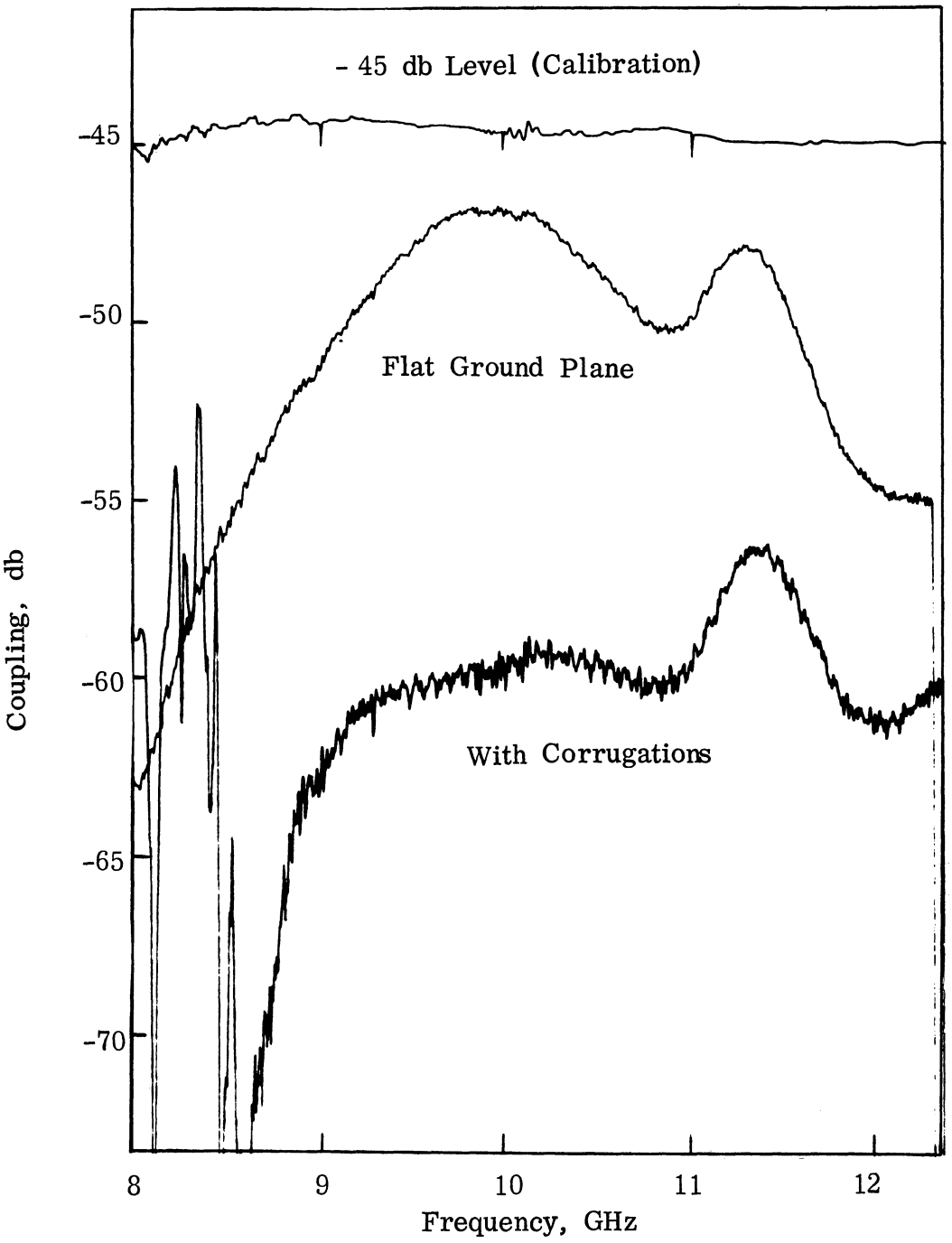

FIG. 3-40: E-PLANE COUPLING OF TWO E-SECTORAL HORNS SPACED 22.8 CM.

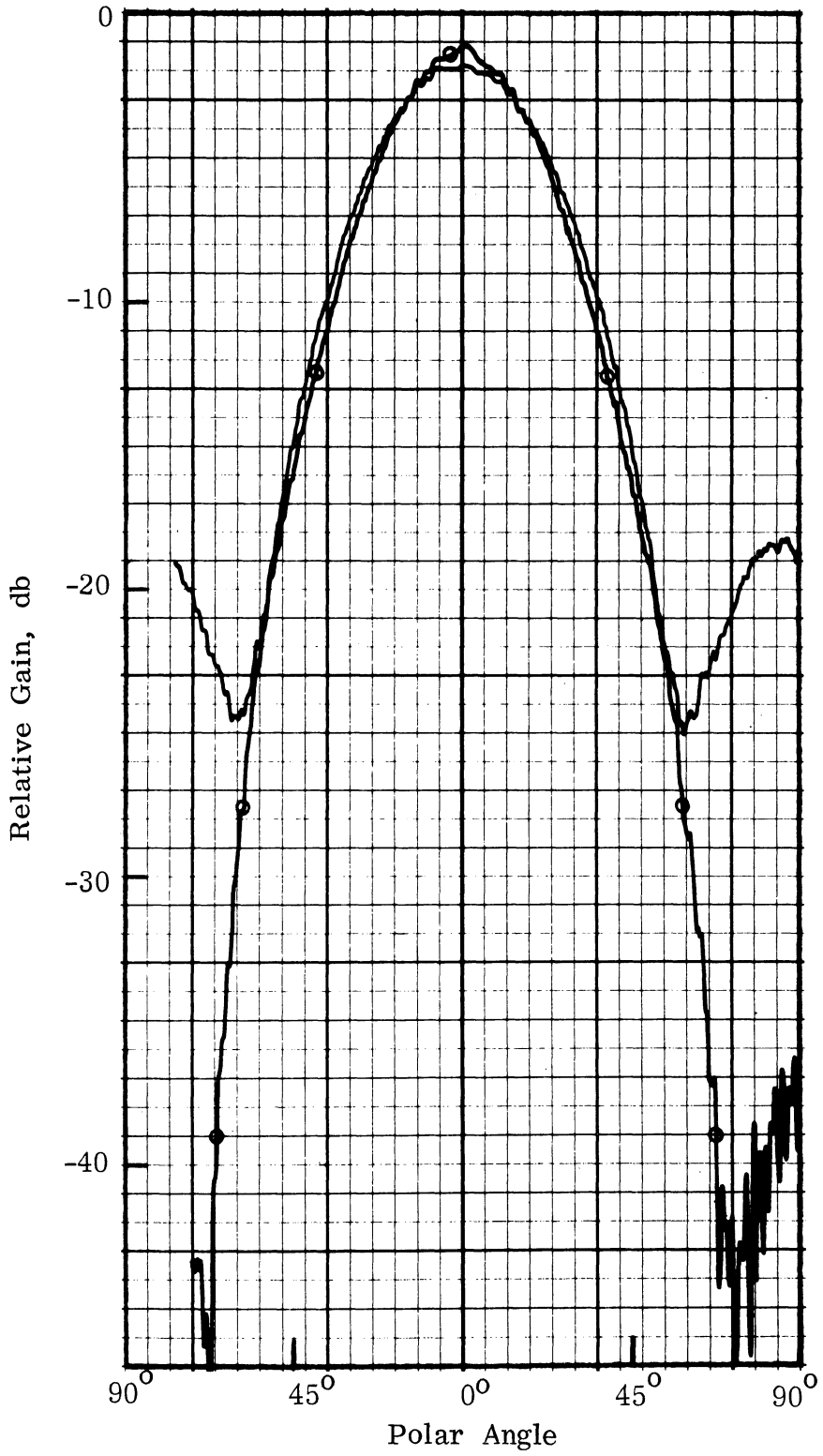

FIG. 3-41a: E-PLANE RADIATION PATTERN OF AN E-SECTORAL HORN AT 8.64 GHz. (——) Flat Ground Plane; (-o-) With Corrugations.

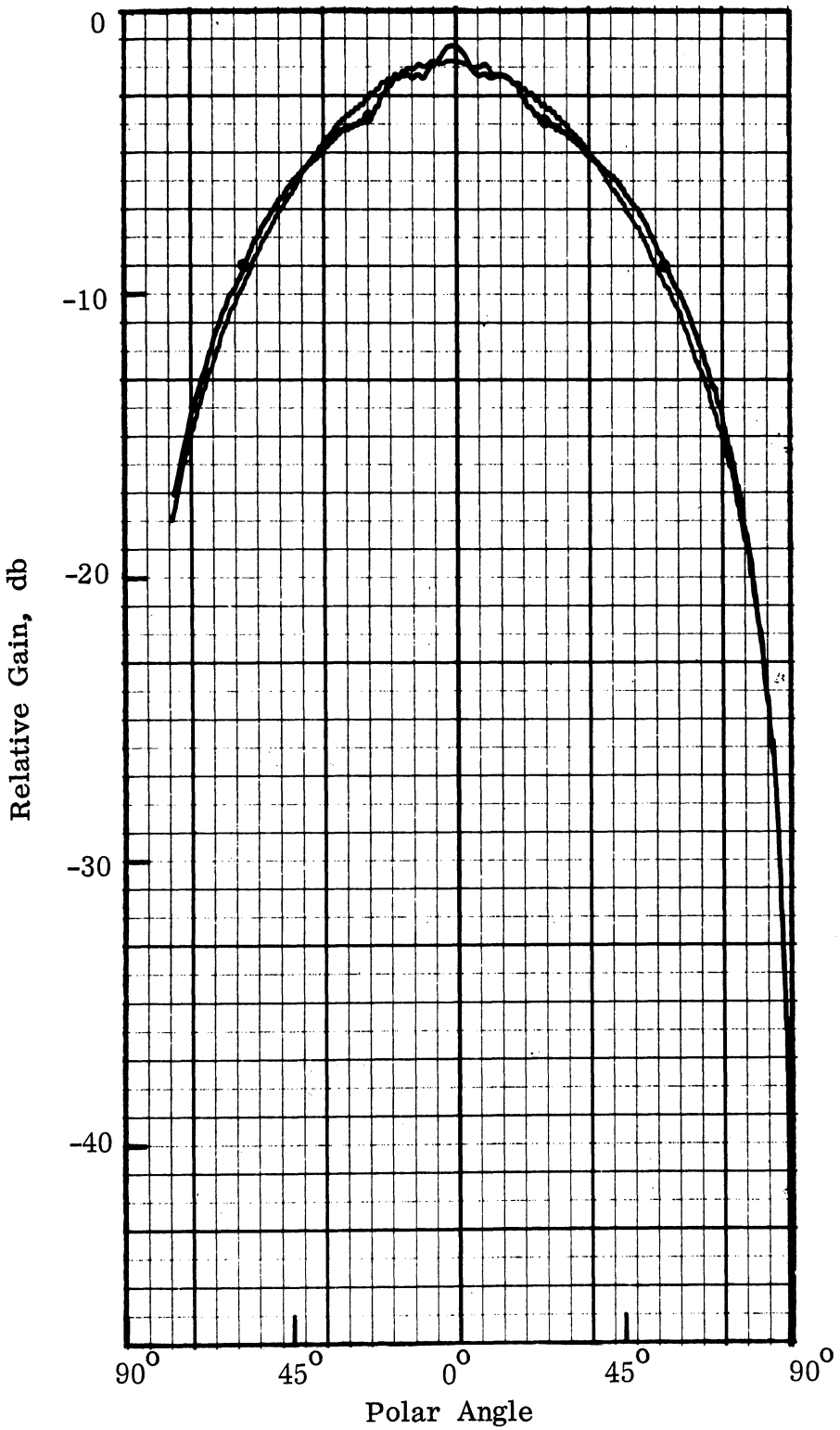

FIG. 3-41b: H-PLANE RADIATION PATTERN OF AN E-SECTORAL HORN AT 8.6 GHz.

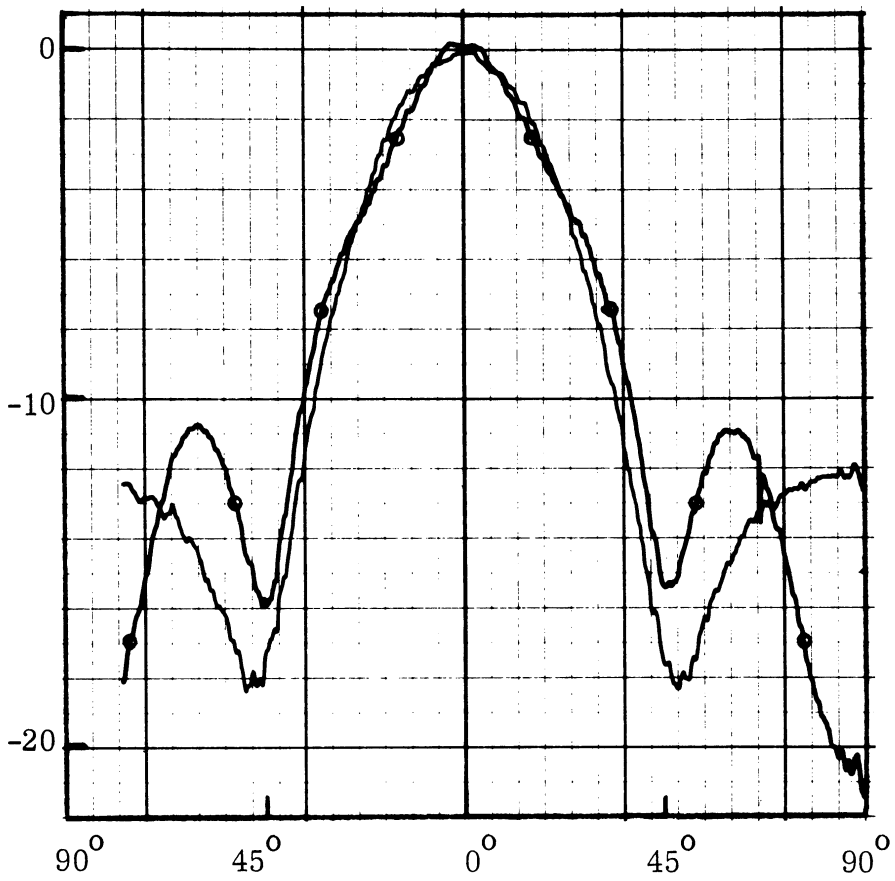

FIG. 3-42: ~~E-P~~LANE RADIATION PATTERN OF AN E-SECTORAL HORN AT 10 GHz.
(——) Flat Ground Plane
(—o—) With Corrugations.

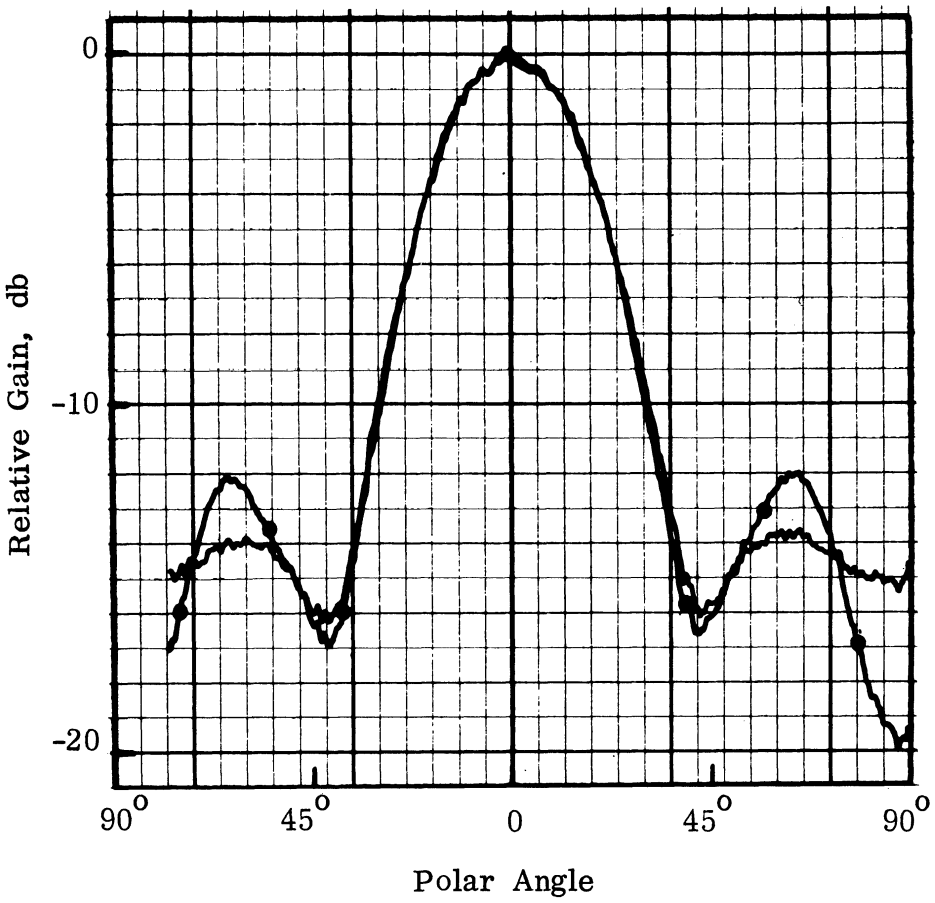

FIG. 3-43: E-PLANE RADIATION PATTERN OF AN E-SECTORAL HORN AT 12 GHz.

rugated area was 3.75 cm, i.e. more that one wavelength. It has been seen (Fig. 3-22) that the closer the loading to the antenna aperture the more effective it is and that for a distance, between aperture and loading area, larger than $\lambda/2$ splitting of the beam occurs (Fig. 3-39d). Such a beam splitting action appears in the sidelobe shape of the E-plane radiation patterns at 10 GHz and 12 GHz. It is believed that higher broadside gain, lower sidelobes and greater coupling reduction than that demonstrated in this section, can be obtained by reactively loading the area in the immediate vicinity of the horn aperture.

3.4.7 Pyramidal Horns

Two identical pyramidal horns were used, flush-mounted in the 12 ft. square ground plane at a center-to-center spacing of 22.8 cm. The horns were fed from X-band waveguide, had a flare angle of 21^{o} in both E- and H-plane and aperture dimensions 6.0 cm x 4.8 cm. The horns have a gain of about 12 db at 9 GHz. As with E-sectoral horns the set of corrugations S was used around the horn aperture. In the E-plane, the distance from the edge of the horn aperture to the beginning of the corrugated area was 2.70 cm.

The swept frequency coupling measurement (see Fig. 3-44) shows that the maximum coupling over the X-band is reduced from -41 db to -54 db, for a coupling reduction of 13 db. The system coupling reduction would be twice as much if similar loading was employed around both apertures. The maximum gain is slightly higher at parts of the stop band, with the surface loading (see Fig. 3-45). The sidelobe levels of the horn with and without the surface loading are shown in Fig. 3-45. These sidelobe levels were recorded at an angle of 89.5^{o} from the broadside with a low directivity E-sectoral horn used as a pick-up antenna. With the impedance loading of the ground plane the sidelobe level shows a null at 8.32 GHz as predicted by Eq. (3.4). With reference to Fig. 3-45 it should be noted that the two curves showing maximum gain have been printed 5 db lower with respect to the two sidelobe level curves for figure compactness. This is reflected in the scale of the axis of ordinates.

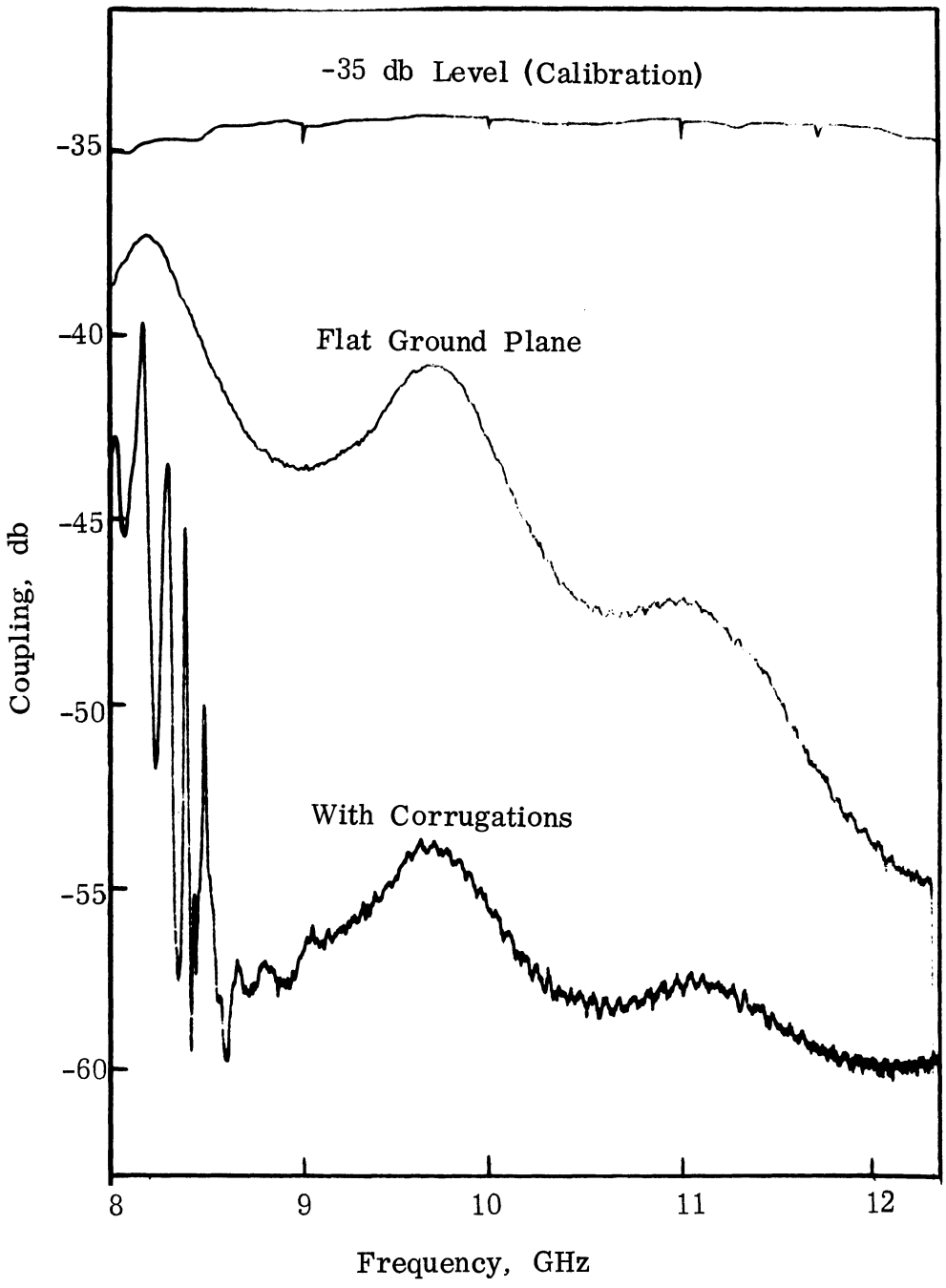

FIG. 3-44: E-PLANE COUPLING OF TWO PYRAMIDAL HORNS SPACED 22.8 CM.

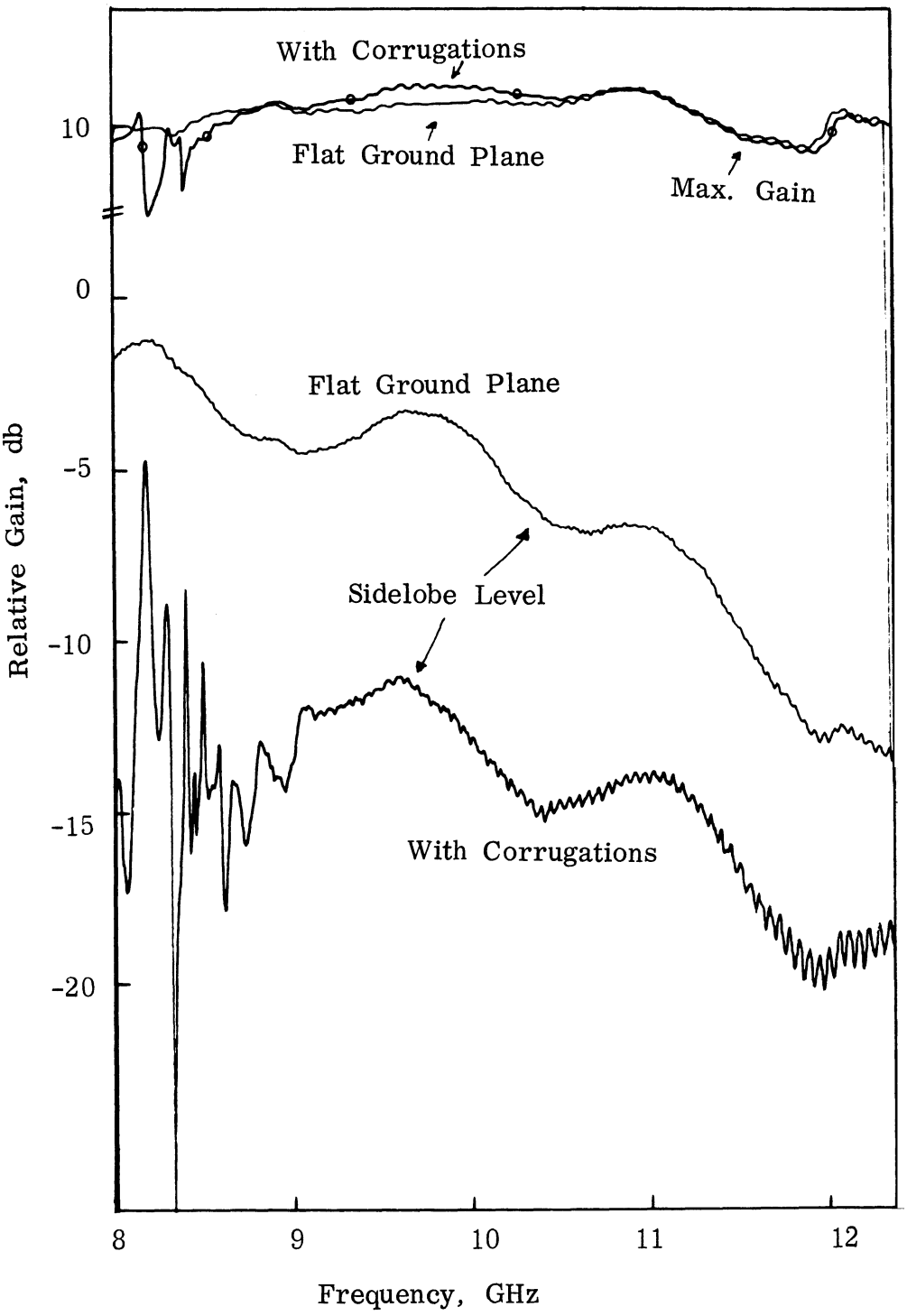

FIG. 3-45: MAXIMUM GAIN AND SIDELOBE LEVEL OF A PYRAMIDAL HORN.

Radiation patterns for the E-plane (at 9, 10 and 11 GHz) and the H-plane (at 10 GHz) are shown in Figs. 3-46 through 3-48. The same comments that were made for the E-sectoral horn radiation patterns apply here.

3.4.8 Monopoles

The antennas examined so far have maximum gain in a direction broadside to the ground plane on which they are mounted. When capacitive reactive loading is used with such types of antennas the sidelobes, or more accurately, the gain along the ground plane is considerably reduced while the mainlobe of the radiation pattern is relatively little affected. In the slot antenna a deviation from this rule is observed, namely, the antenna gain in the broadside direction is significantly increased.

The monopole antenna is distinctly different from the above mentioned types of antennas, in that its maximum gain occurs in the direction along the ground plane, while a null is present in the broadside, if an infinitely large ground plane is assumed. Therefore, the reactive loading will affect the main lobe of the radiation pattern.

Cylindrical monopoles, one quarter-wavelength long were used. At X-band frequencies such monopoles were cut from copper wire. Monopoles for use at S-band were machined from brass. The monopole mount that was used consisted of a type-N connector attached to a tapered coaxial section. This section was acting as an impedance transformer, having a (calculated) characteristic impedance of 51 Ω at the output (see Fig. 3-49). The dimensions of the S-band monopole were h = 2.44 cm (.960 in.) and d = 0.11 cm (.045 in) so that the length to diameter ratio was h/d = 21.3; the length corresponds to one quarter of a wavelength at 3.1 GHz.

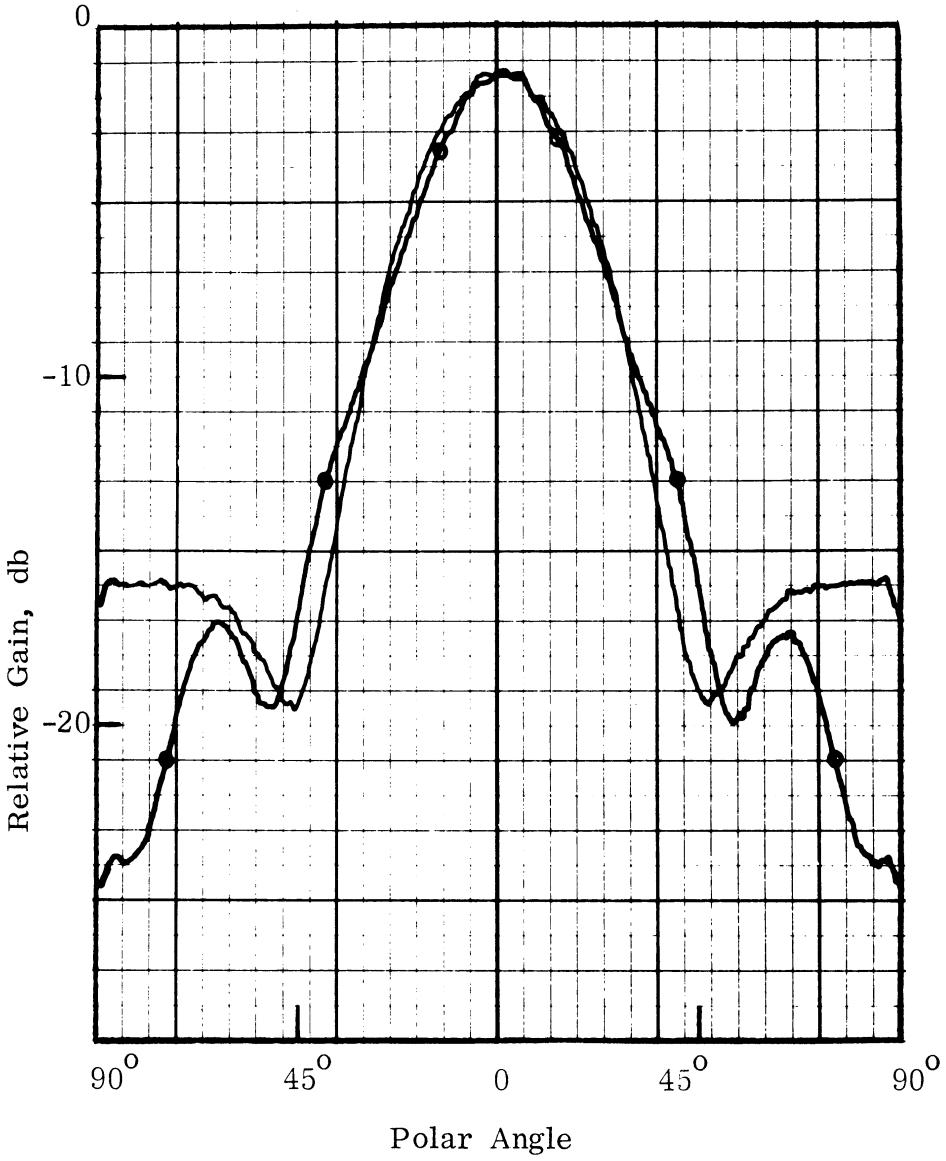

FIG. 3-46: E-PLANE RADIATION PATTERN OF A PYRAMIDAL HORN AT 9 GHz.
(——) Flat Ground Plane
(-o-) With Corrugations.

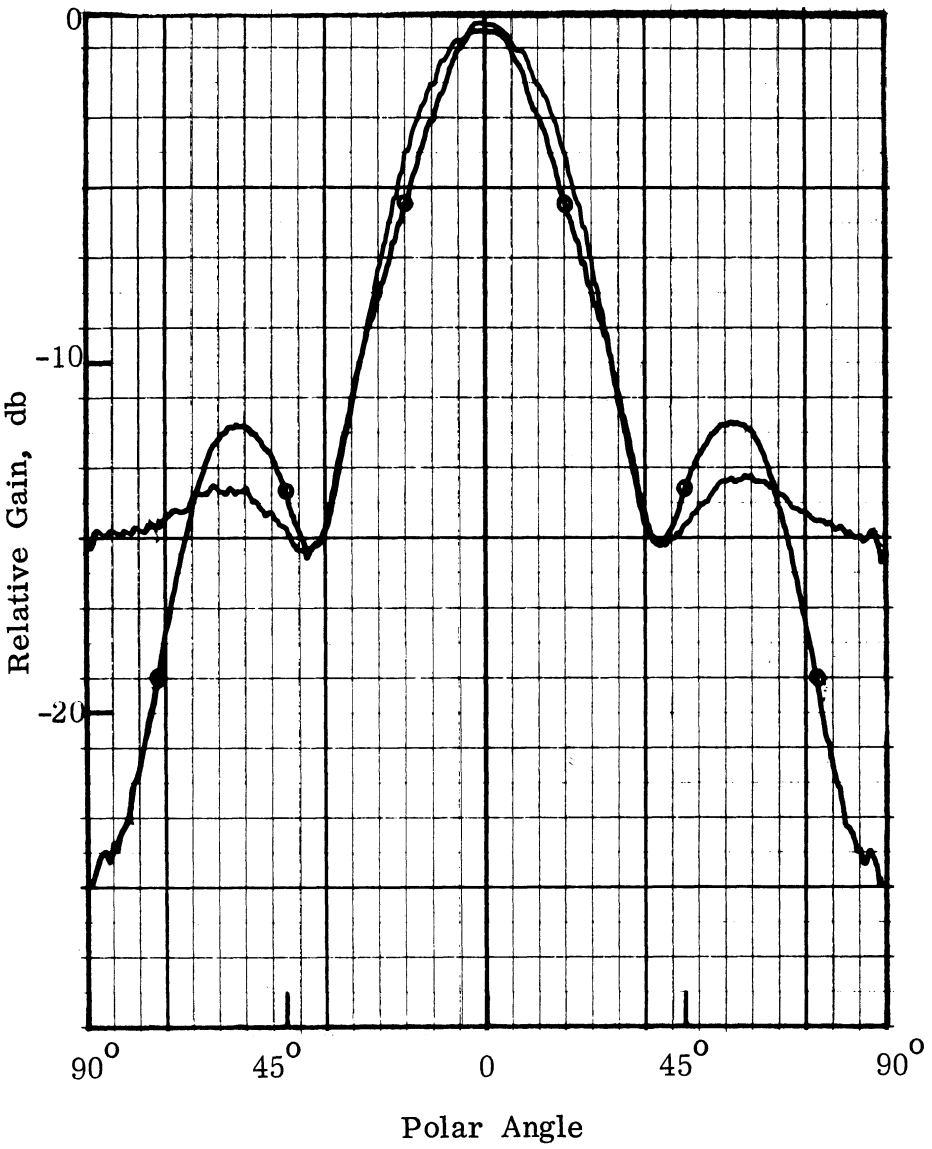

FIG. 3-47a: E-PLANE RADIATION PATTERN OF A PYRAMIDAL HORN AT 10 GHz.
(——) Flat Ground Plane
(—o—) With Corrugations

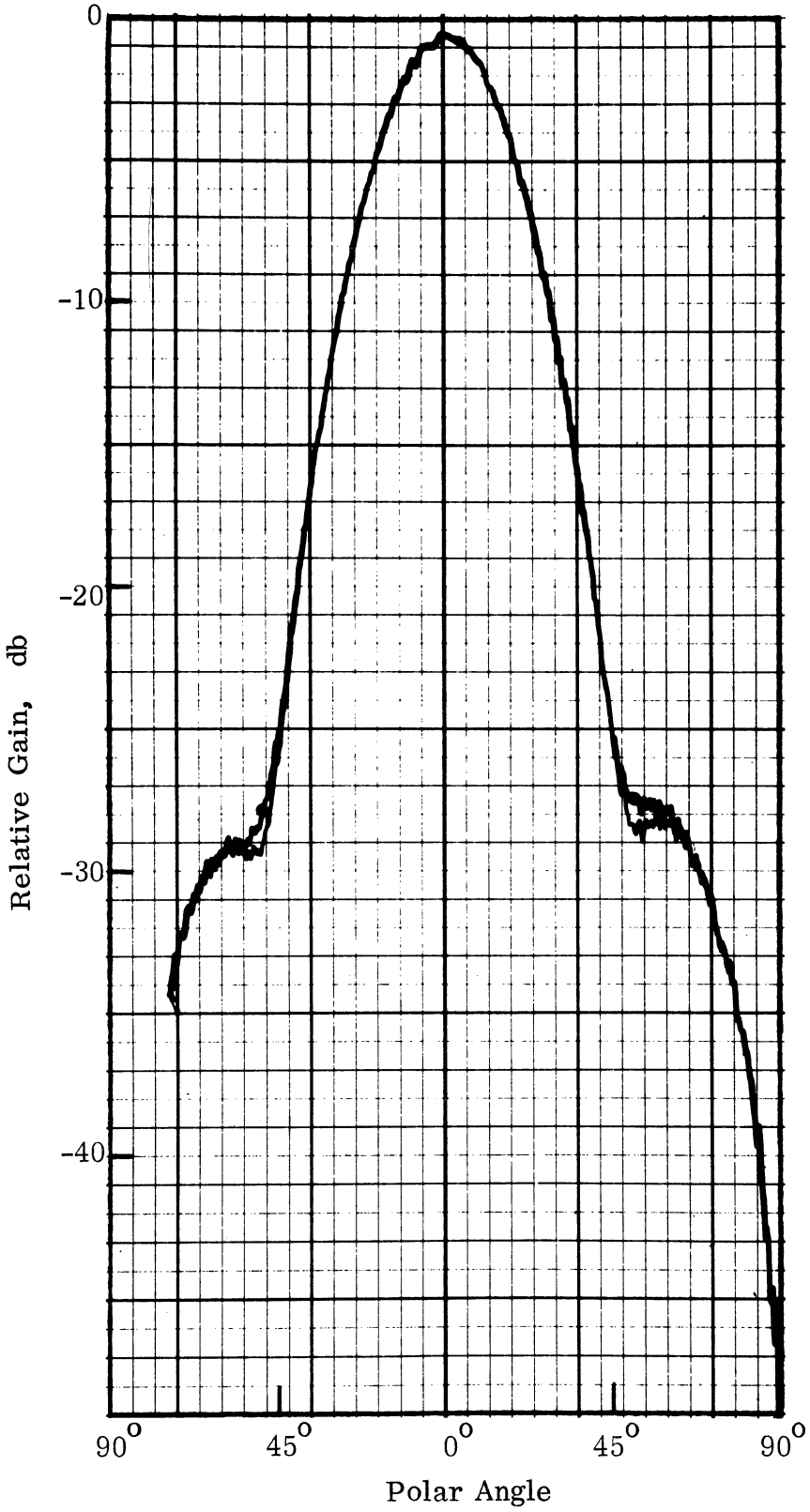

FIG. 3-47b: H-PLANE RADIATION PATTERN OF A PYRAMIDAL HORN AT 10 GHz.

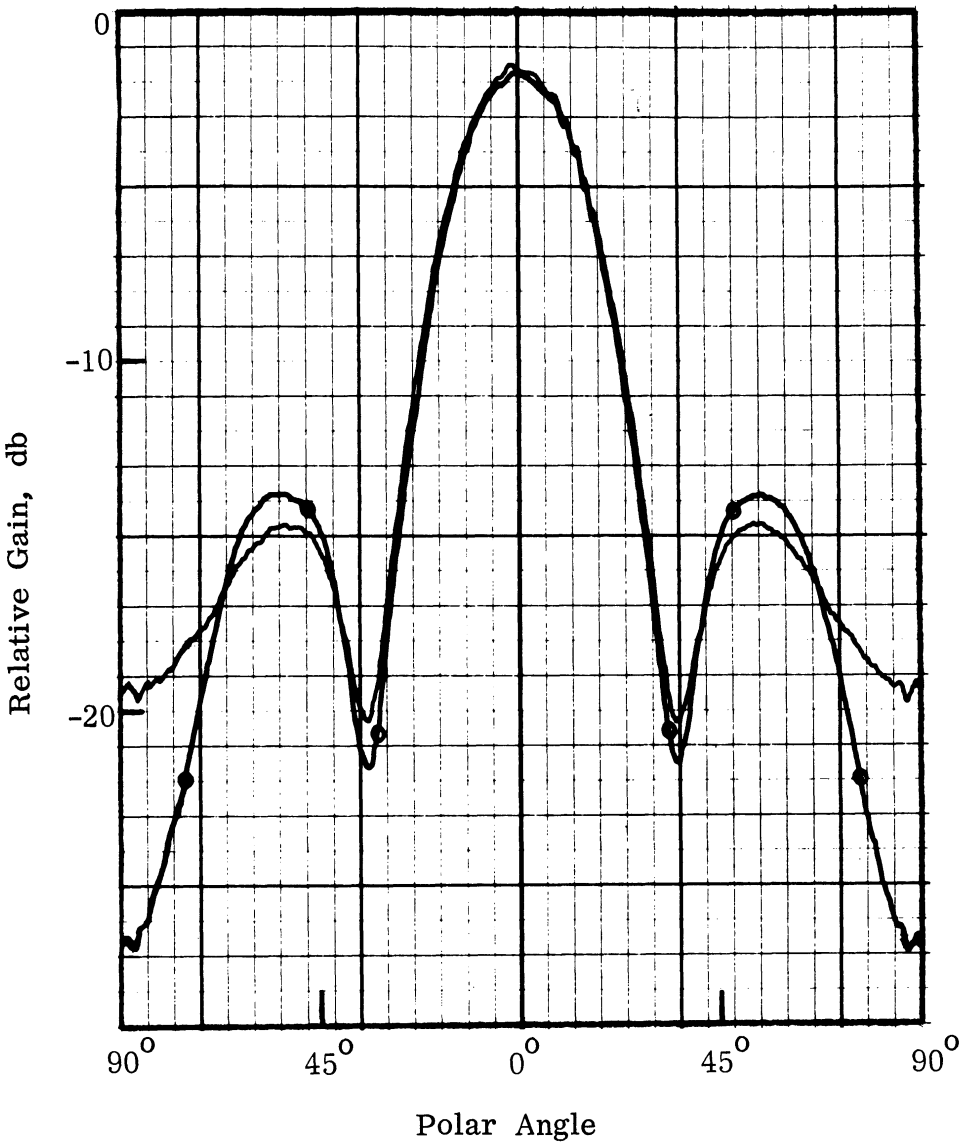

FIG. 3-48: E-PLANE RADIATION PATTERN OF A PYRAMIDAL HORN AT 11 GHz.
(——) Flat Ground Plane
(-o-) With Corrugations

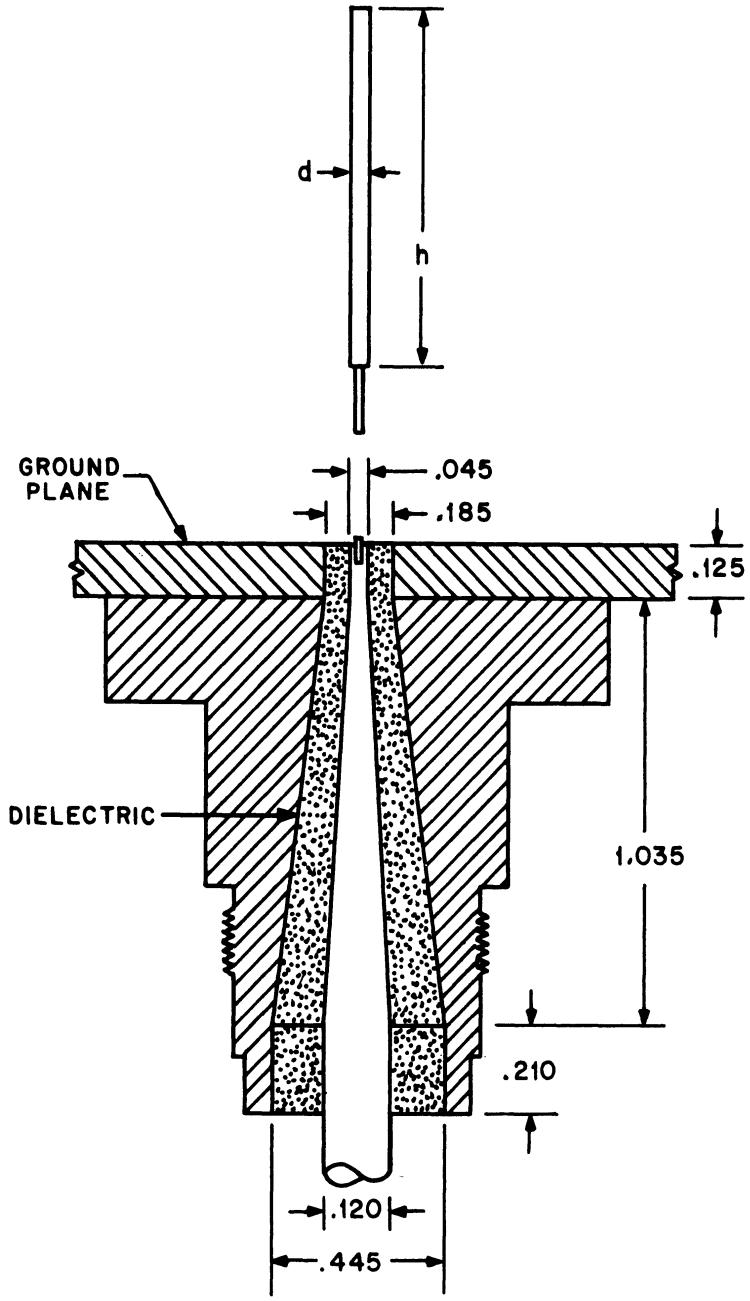

FIG. 3-49: MONOPOLE MOUNT (Dimensions in Inches).

The antenna input impedance was measured with the aid of a coaxial slotted line section with a broadband detector. The slotted line, having a residual VSWR less than 1.06, was connected directly to the antenna. The small disc termination of the antenna mount was flush-mounted in a 12 ft. square aluminum ground plane facing an anechoic chamber. The Smith chart plot of the input impedance is shown in Fig. 3-50. In the same figure the antenna impedance when part of the ground plane is replaced by the corrugated disc "S" is given for comparison. The variation of the antenna standing wave ratio with frequency is shown in Fig. 3-51. Since the monopole has an inductive input impedance for frequencies above resonance, the capacitive surface impedance offered by the corrugations has the effect of improving the antenna SWR. Rectangular plots of the resistive and reactive parts of the input impedance constructed by reading off values from the Smith chart, are shown in Figs. 3-52 and 3-53.

Radiation patterns of the monopole, with and without the reactive loading on the ground plane, were measured using a log-periodic antenna with a gain of 7 to 9 db (S-band) as a receiving antenna. This antenna was rotated in the polar plane of the monopole with its apex describing a radius of 1.83 m (18λ at 3 GHz). This radius is equal to the edge-to-center distance of the ground plane. At the position closest to the ground plane, the center of the log-periodic array was at angle of $\theta = 86^{o}$ from the broadside. Radiation patterns at four different frequencies are shown in Fig. 3-54. Two cases of reactive loading are shown in Fig. 3-54; one where corrugations S are completely exposed and one where only the inner half is exposed, the other half being covered with aluminum foil. It is seen that the monopole surrounded by the reactively loaded ground plane is still omnidirectional, however, the direction of the maximum has shifted from $\theta = 90^{o}$ to an angle

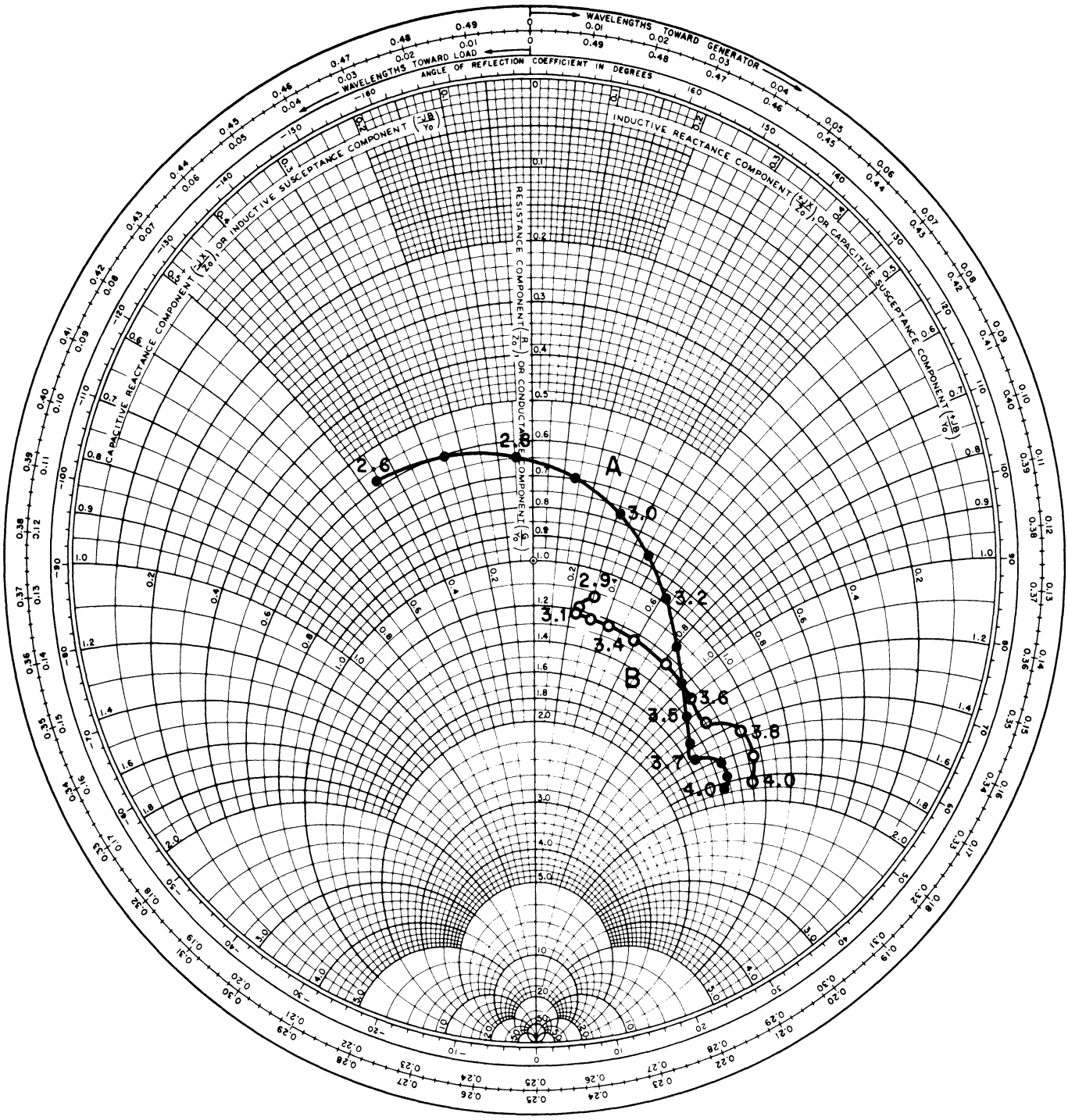

FIG. 3-50: IMPEDANCE OF A CYLINDRICAL MONOPOLE (h = 2.44 cm, d = 0.11 cm). Z_o = 55Ω.
A: Flat Ground Plane
B: With Corrugations S.

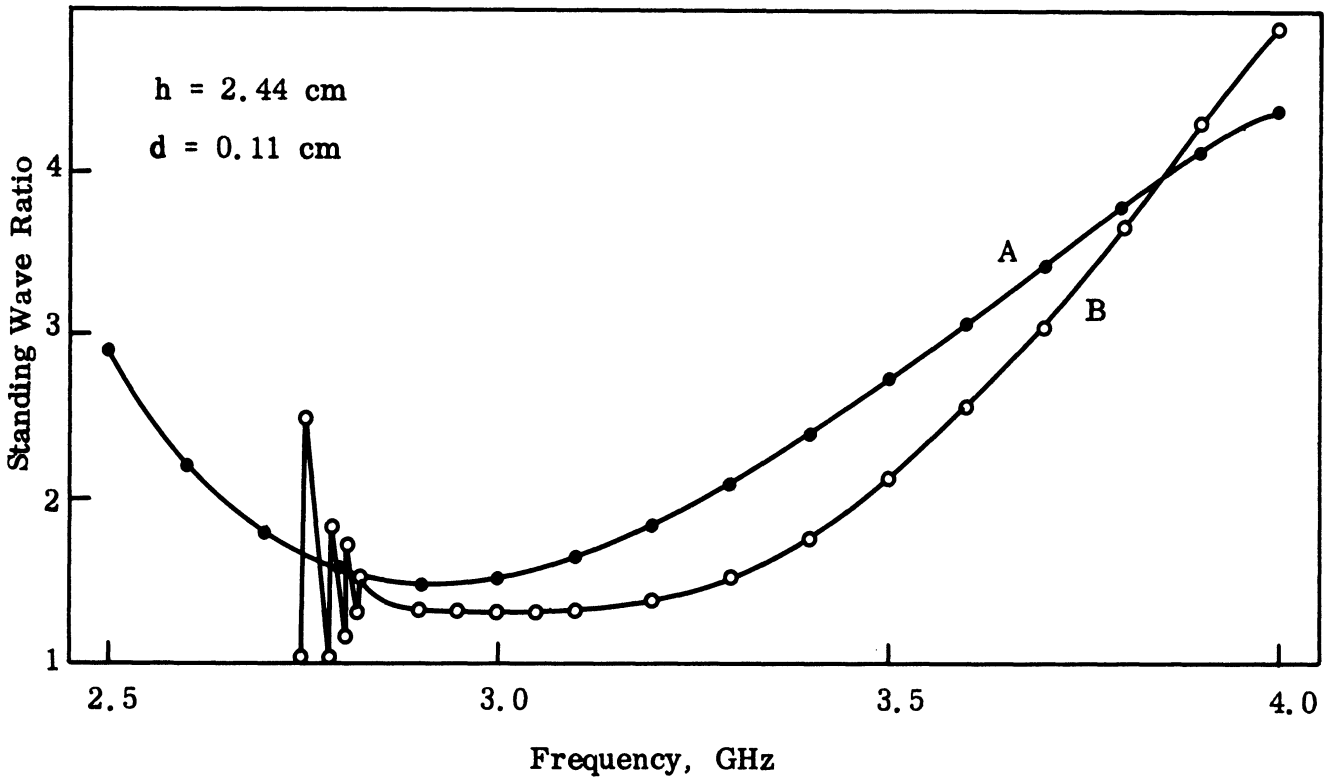

3-51: STANDING WAVE RATIO FOR A CYLINDRICAL MONOPOLE FED BY A 55 Ω COAXIAL LINE.
A: Flat Ground Plane
B: Ground Plane with Corrugations S.

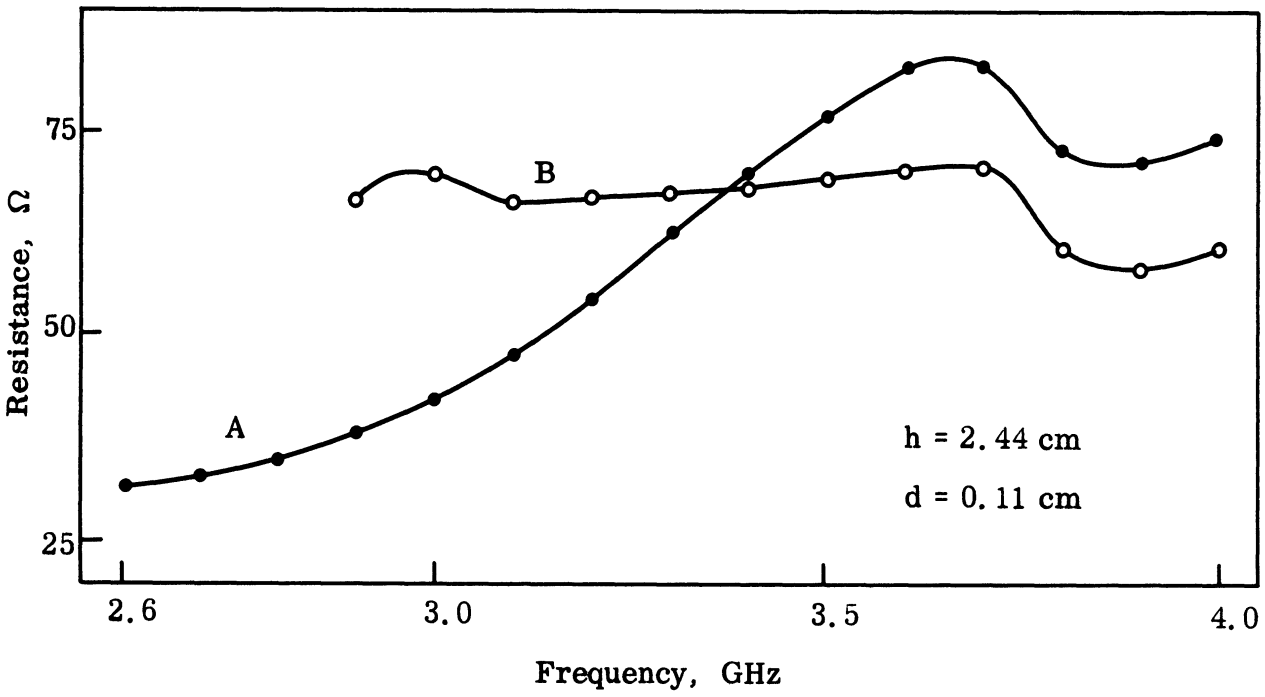

FIG. 3-52: INPUT RESISTANCE OF A CYLINDRICAL MONOPOLE
A: Flat Ground Plane
B: Ground Plane with Corrugations S .

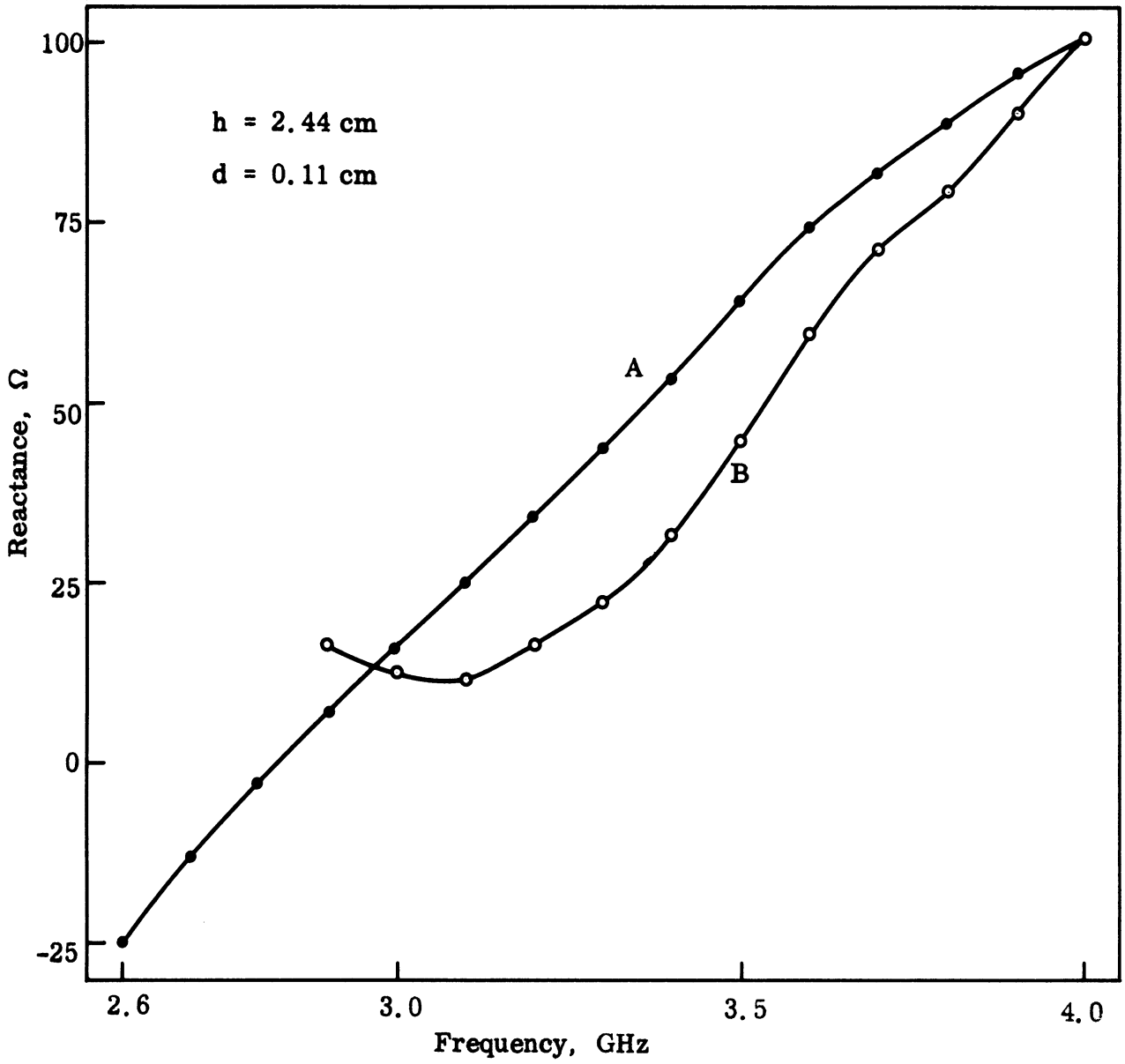

FIG. 3-53: INPUT REACTANCE OF A CYLINDRICAL MONOPOLE.
A: Flat Ground Plane
B: Ground Plane with Corrugations S.

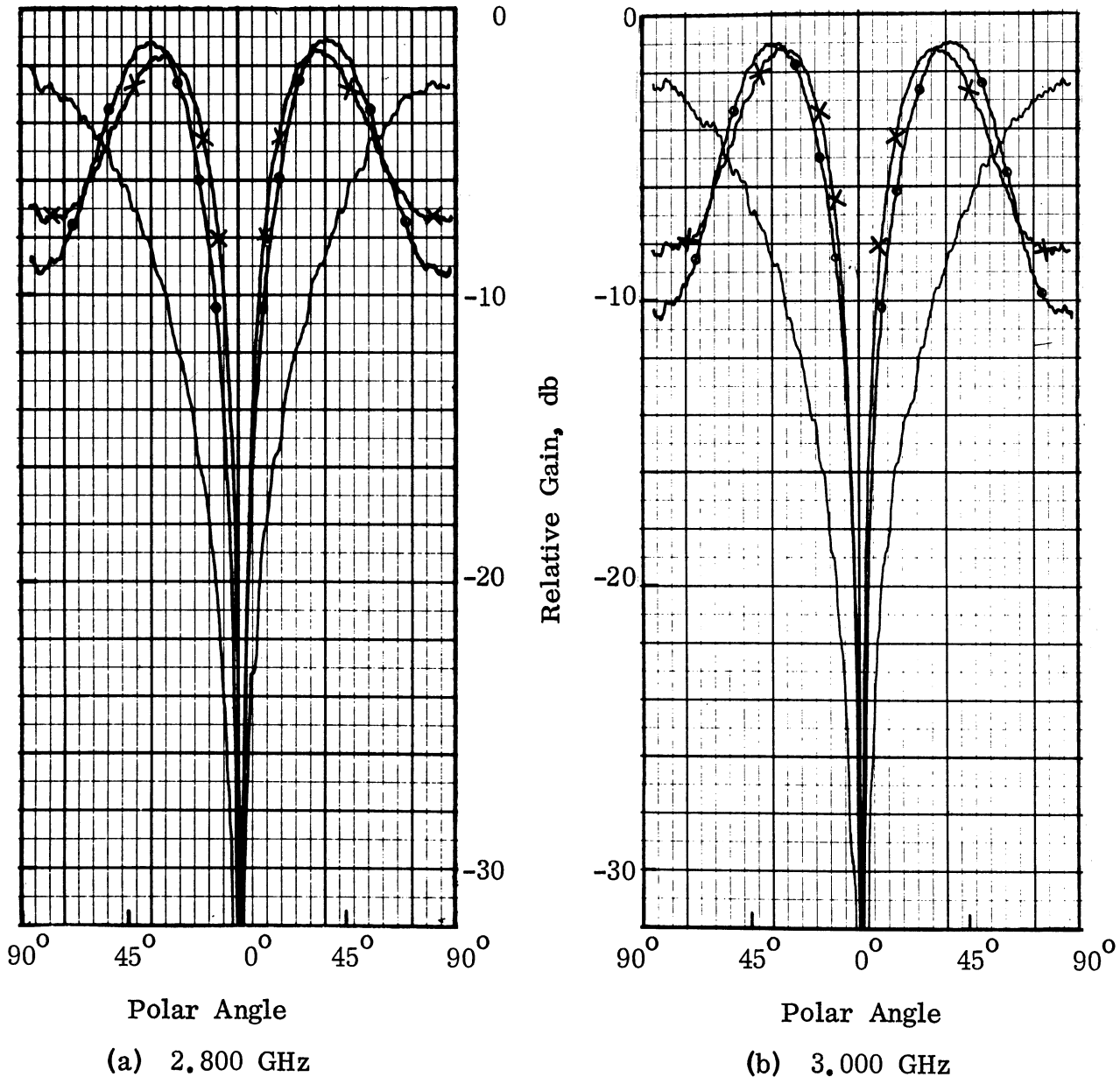

FIG. 3-54: RADIATION PATTERNS OF A MONOPOLE.
(h/d = 21).
(——) Flat Ground Plane
(-o-) With Corrugations (λ)
(-x-) With Corrugations (λ/2)

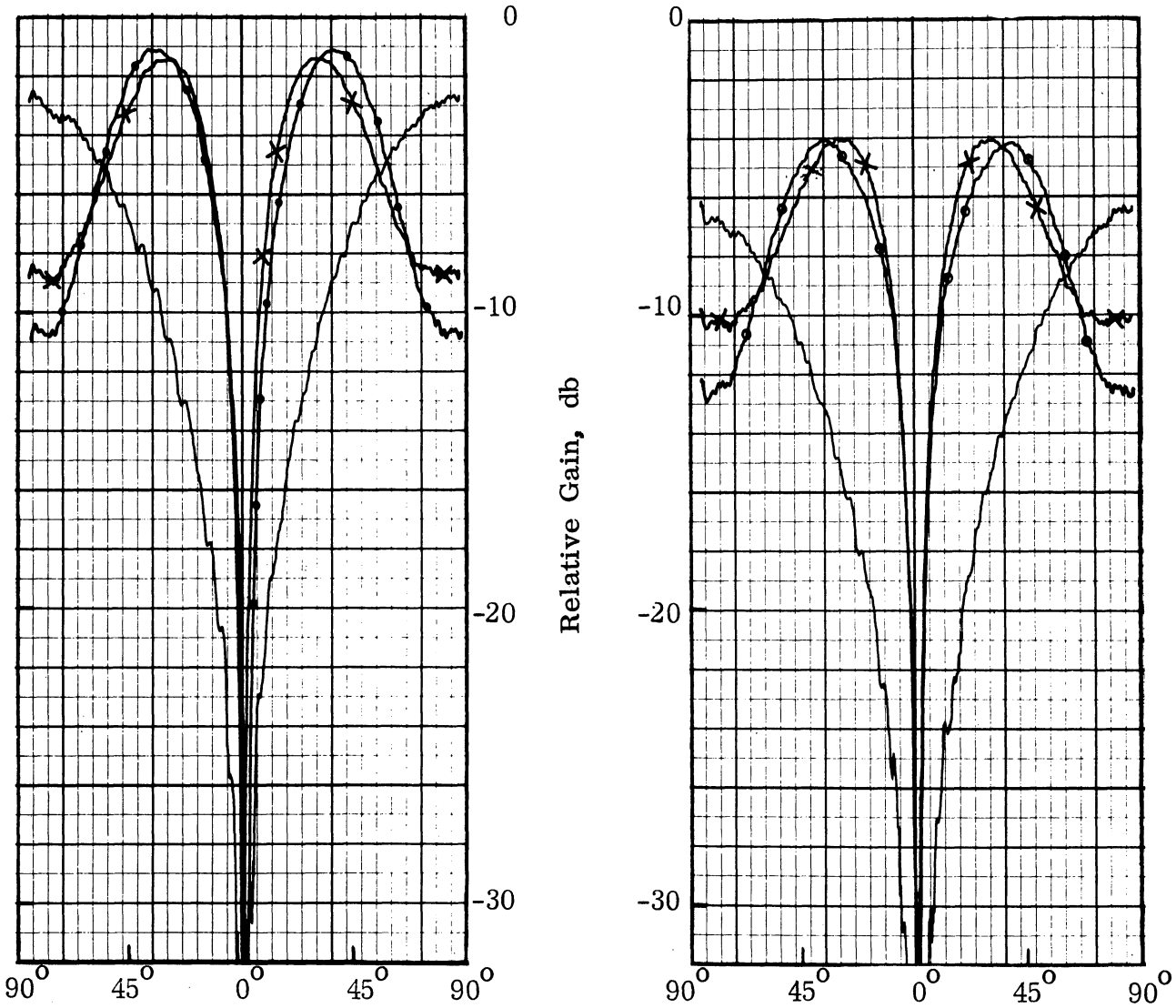

(c) 3.200 GHz

(d) 3.600 GHz

FIG. 3-54: CONTINUED.

between 30^{o} and 40^{o}. The angle where the maximum occurs depends upon the extent of the corrugated surface and the distance of the beginning of the loading from the monopole.

With the ground plane loading the sidelobes are lower along the ground plane and therefore there is less coupling to another antenna on the same ground plane. Also there is some increase in gain and there is some control over the position of the maximum. These may be useful in some applications. For example the command antenna of the Nimbus Meteorological Satellite is a monopole with the requirement of maximum gain at $\theta = 58^{o}$ from the broadside. (Post, 1967).

A swept frequency measurement of the monopole gain at selected angles is shown in Fig. 3-55. The explanation of the different curves shown is as follows. Curve A is a reference showing the monopole gain over a flat ground plane at $\theta = 86^{o}$ (near maximum). Curves B and D correspond to the case where corrugated "disc S" is placed around the monopole; curve D is the gain at $\theta = 86^{o}$ (sidelobe) and curve B is at $\theta = 38^{o}$ (near maximum gain). Curves C and E are obtained with only the inner half of the corrugated part of the surface exposed; curve C is the gain at $\theta = 30^{o}$ (near maximum) and curve E gives the gain at $\theta = 86^{o}$ (sidelobe). With the corrugated surface, the monopole maximum gain is higher by 0.5 to 2.0 db in the frequency range 2.8 to 3.8 GHz (30 percent bandwidth).

The coupling of two monopoles on the same ground plane with and without loading around one of the monopoles is shown in Fig. 3-56. The second monopole had a height of 2.44 cm (.960 in.) and a diameter of 0.15 cm (.062 in.) and was placed at a distance of 22.8 cm, equal to 2.5λ in the middle of the frequency range considered. A comparison of Figs. 3-55 and 3-56 shows

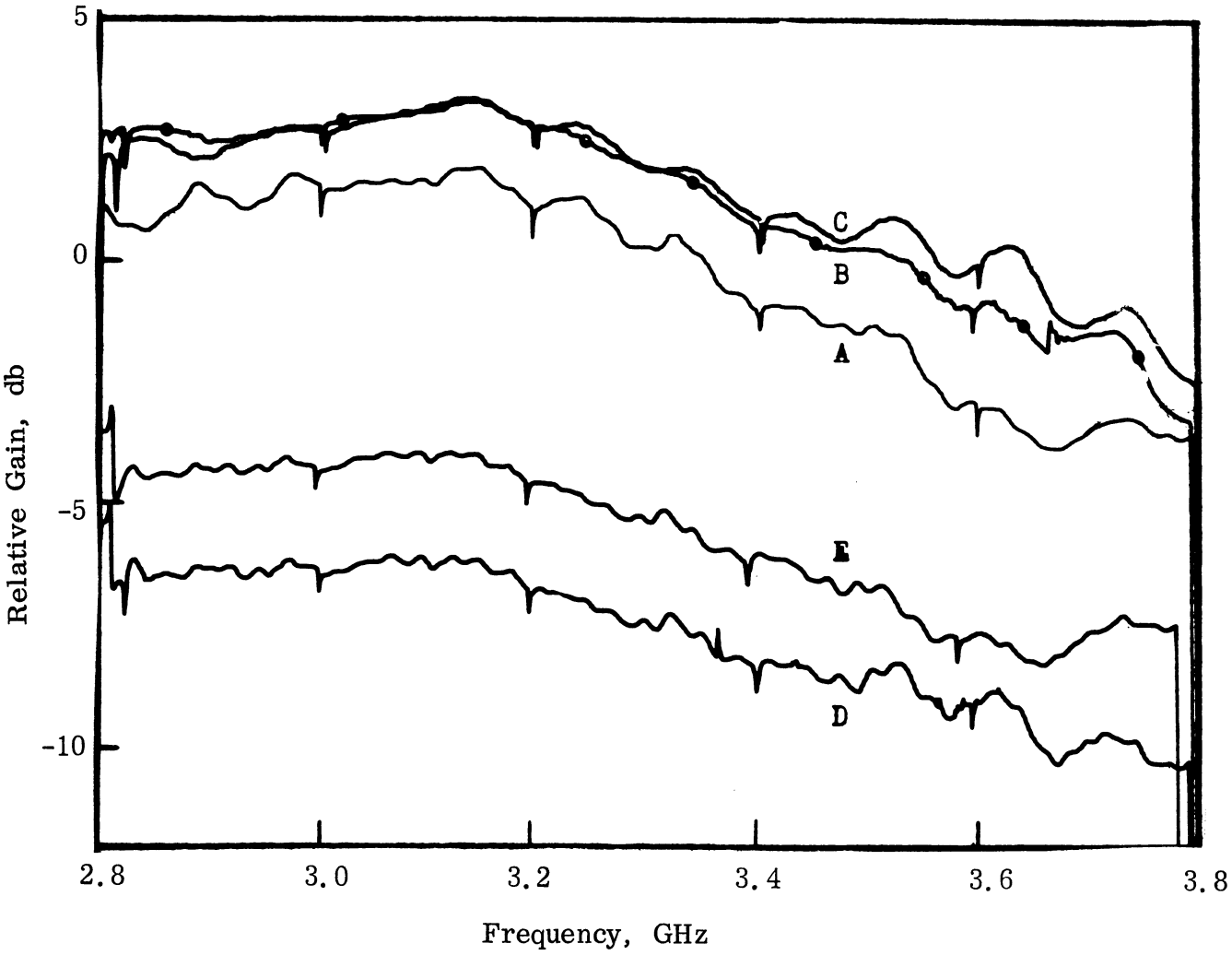

FIG. 3-55: MAXIMUM GAIN AND SIDELOBE LEVEL OF A MONOPOLE. Explanation in Text.

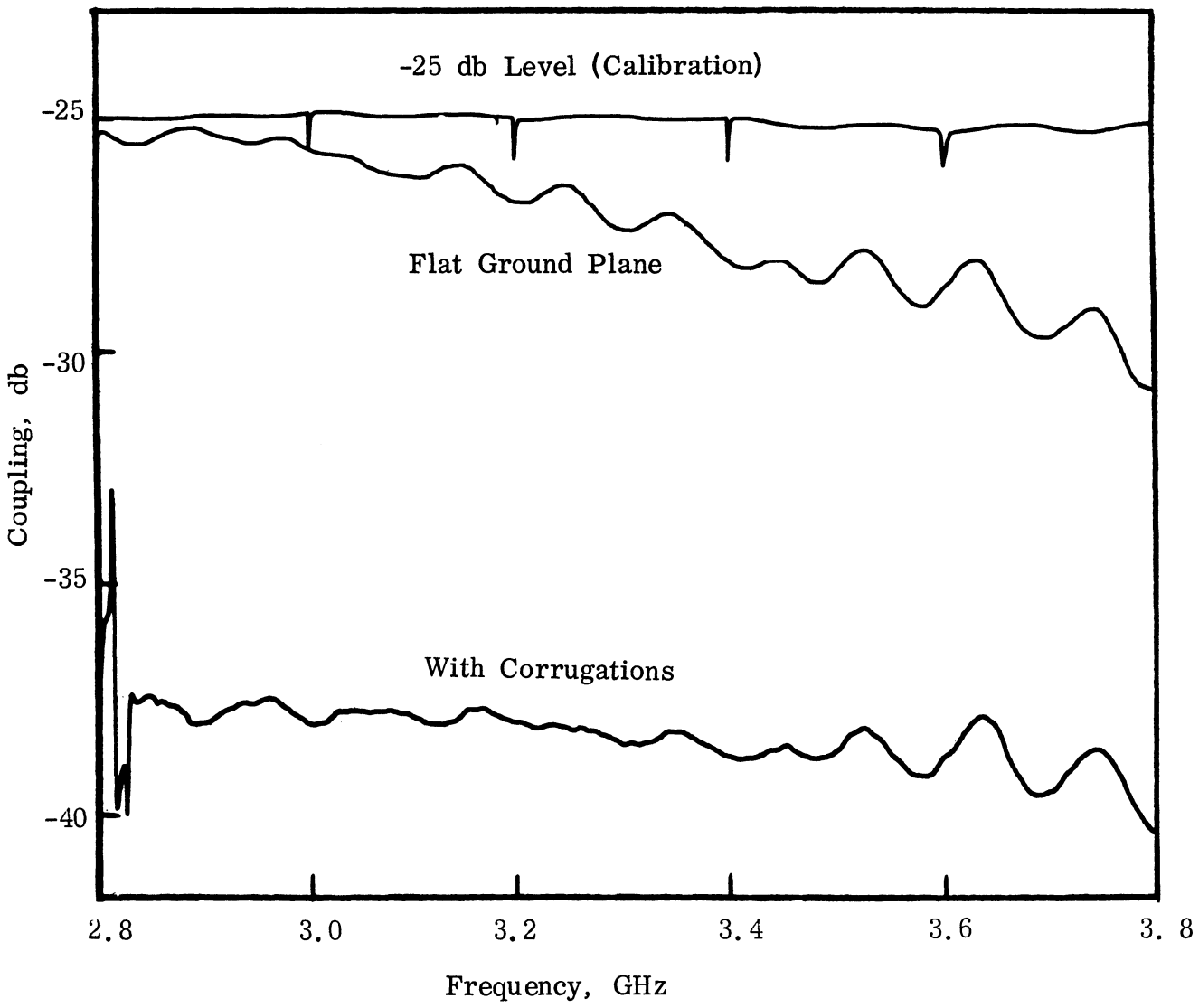

FIG. 3-56: COUPLING OF TWO MONOPOLES SPACED 22.8 CM.

at this distance the coupling reduction is greater than what would be expected in a far-field coupling situation. In either case twice as much coupling reduction can be obtained by similarly modifying both antennas.

Cylindrical monopoles for X-band have also been used for radiation patterns, coupling and impedance measurements (see Lyon et al, March 1967). In more recent additional experiments, however, a poor repeatability was detected in some cases due to more strict mechanical tolerances at X-band. Therefore these results are not shown here.

IV

BROADBAND COMPENSATING BRIDGE

Consider two different antenna systems, one transmitting and the other receiving. There may be interference between these systems. The broadband compensating bridge has been developed to help provide compatibility to these two systems through coupling reduction. Basically, the bridge method decouples the antennas by cancelling the interfering signal at the receiver with an auxiliary signal derived from the transmitter. This cancelling signal is fed to the receiver through a compensating bridge link.

For perfect cancellation, which corresponds to infinite decoupling expressed in db, the phase angle θ between the interfering signal and the auxiliary bridge signal must be 180^{o} and these two signals must have equal amplitudes. This is easy to achieve at a single frequency. However, many antenna systems have to operate over a broad range of frequencies. Thus, the compensating bridge will also have to be broadbanded. Ideally, this means that the phase angle θ must remain at 180^{o} and the two amplitudes must remain equal throughout a frequency band. To meet the phase angle condition, the auxiliary bridge link must have an electrical length equal to the equivalent electrical length of the path of the interfering signal. Moreover, these two paths must have similar dispersion vs frequency characteristics. To meet the amplitude condition, the two paths must have similar attenuation vs frequency characteristics. Unfortunately, in any bridge that is constructed there will be phase and amplitude errors. It is important to know how much decoupling is possible for a bridge with known phase angle and amplitude errors.

The following equation was derived to answer this question.

$$D = m - 10 \log_{10} \left| 10^{m/10} + 1 + 2 \sqrt{10^{m/10}} \cos \theta \right| \qquad (4.1)$$

D = decoupling in db,

m = power difference between the coupled signal and the bridge link signal expressed in db,

θ = phase angle between bridge and coupled signals.

If m is greater than zero, the coupled power is greater than the bridge power, while if m is less than zero, the coupled power is less than the bridge power. This equation gives the additional isolation provided by the bridge from the coupled power level. For example, if the E-plane coupling level of two X-band slot antennas mounted in a common ground plane is - 30 db, and if equation (4.1) predicts D = 20 db, the final coupling level after application of the compensating bridge would be - 50 db.

This equation is plotted in Fig. 4-1. The vertical axis is the decoupling expressed in db. The horizontal axis is the amount that the bridge power is less than the coupled power expressed in db. The phase angle error is the parameter designating individual curves. Thus for a 10^{o} phase error and bridge power .2 db less than coupled power the decoupling is 15 db. If the bridge power is greater than the coupled power the same graph can be used. Merely read the proper decoupling value from Fig. 4-1 and subtract from this value the amount by which the bridge power is greater. For example consider the case that the bridge power is 1 db greater than the coupled power with 20^{o} phase error. Reading Fig. 4-1 at 1 db one obtains D = 10 db. After subtracting the 1 db for the excess bridge power, D = 9 db.

An experiment was performed to check Eq. (4.1). A bridge was unbalanced at a fixed frequency by specified amounts, both in amplitude and in phase. The decoupling was recorded. The experimental data check Fig. 4-1 very closely.

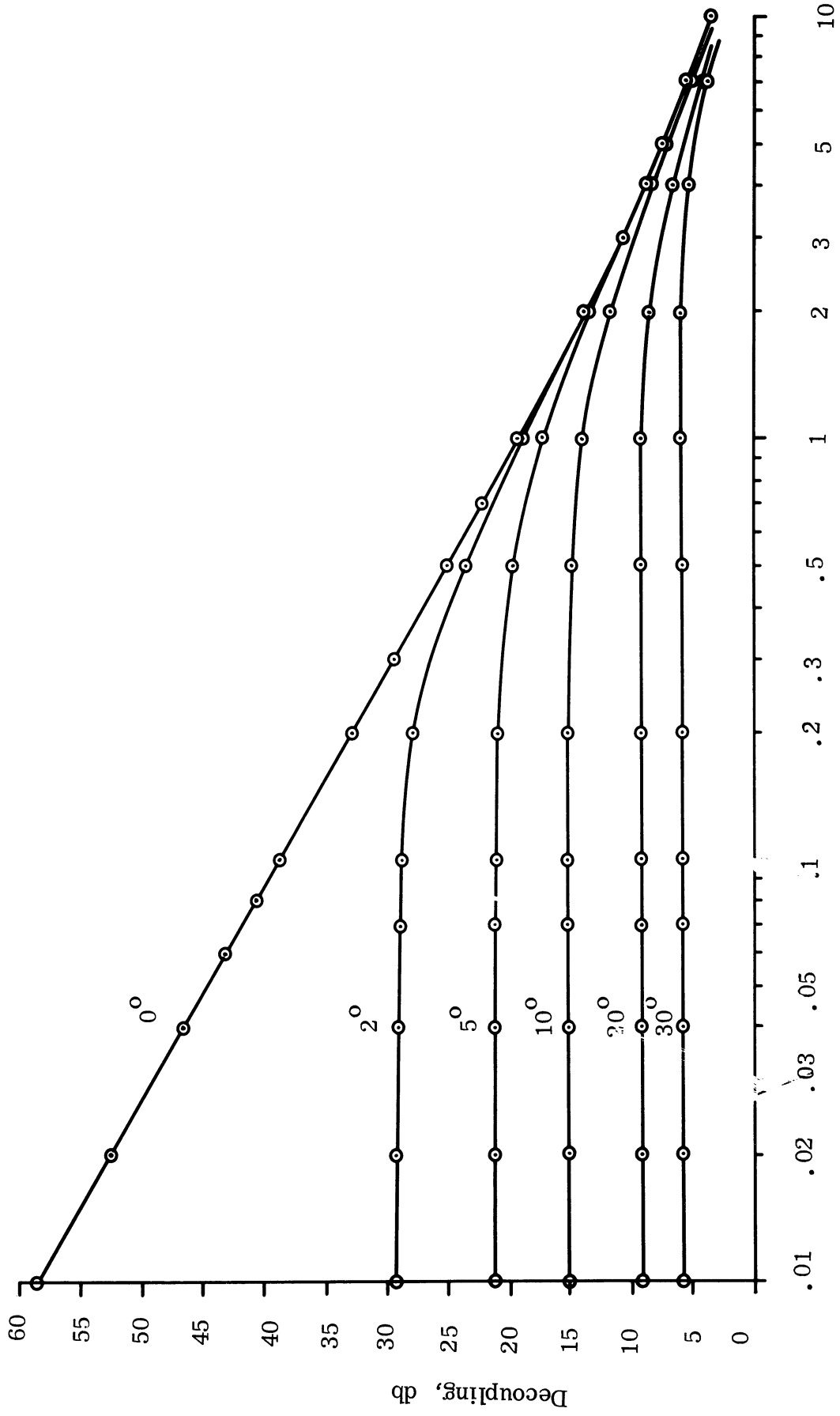

FIG. 4-1: DECOUPLING VERSUS DIFFERENCE IN POWER LEVELS WITH PHASE ERROR AS A PARAMETER.

A broadband compensating bridge has been used to decouple two X-band slot antennas mounted in a common ground plane. The experimental circuit is shown in Fig. 4-2. The lower waveguide circuit is the transmitting slot feed. From right to left is the directional coupler used to feed the bridge link, a 16" piece of waveguide, a 50 db precision attenuator, an isolator and the transmitting slot antenna mounted in the ground plane. Behind the ground plane is the anechoic chamber. The upper circuit is the bridge link. From right to left is a waveguide-to-coaxial adapter, a 24" piece of RG-55 coaxial cable, another waveguide-to-coaxial adapter, the squeeze guide section, a 50 db precision attenuator, and the directional coupler used as the receiving feed junction. Also visible is the receiving slot antenna, mounted in the ground plane and feeding into the directional coupler.

The amplitude variations of the auxiliary bridge link signal with frequency are matched to the amplitude variations of the coupled signal by the piece of RG-55 cable. The E-plane coupling level of two slot antennas mounted in a common ground plane falls by 6 db per octave of frequency. The attenuation of a 24" piece of RG-55 cable increases with frequency at a similar rate in X-band. The amplitude levels of the two signals are made equal by the 50 db attenuators.

The phase dispersions of these two paths as functions of frequency are matched by the squeeze guide section. This is a piece of waveguide whose width can be varied. As the width changes, the propagation constant changes and the phase characteristic can be varied. The bridge link was designed to be very nearly the same electrical length as the coupled path at all frequencies. The 180^{o} phase shift necessary for decoupling is produced by proper orientation of the waveguide to coaxial adapters.

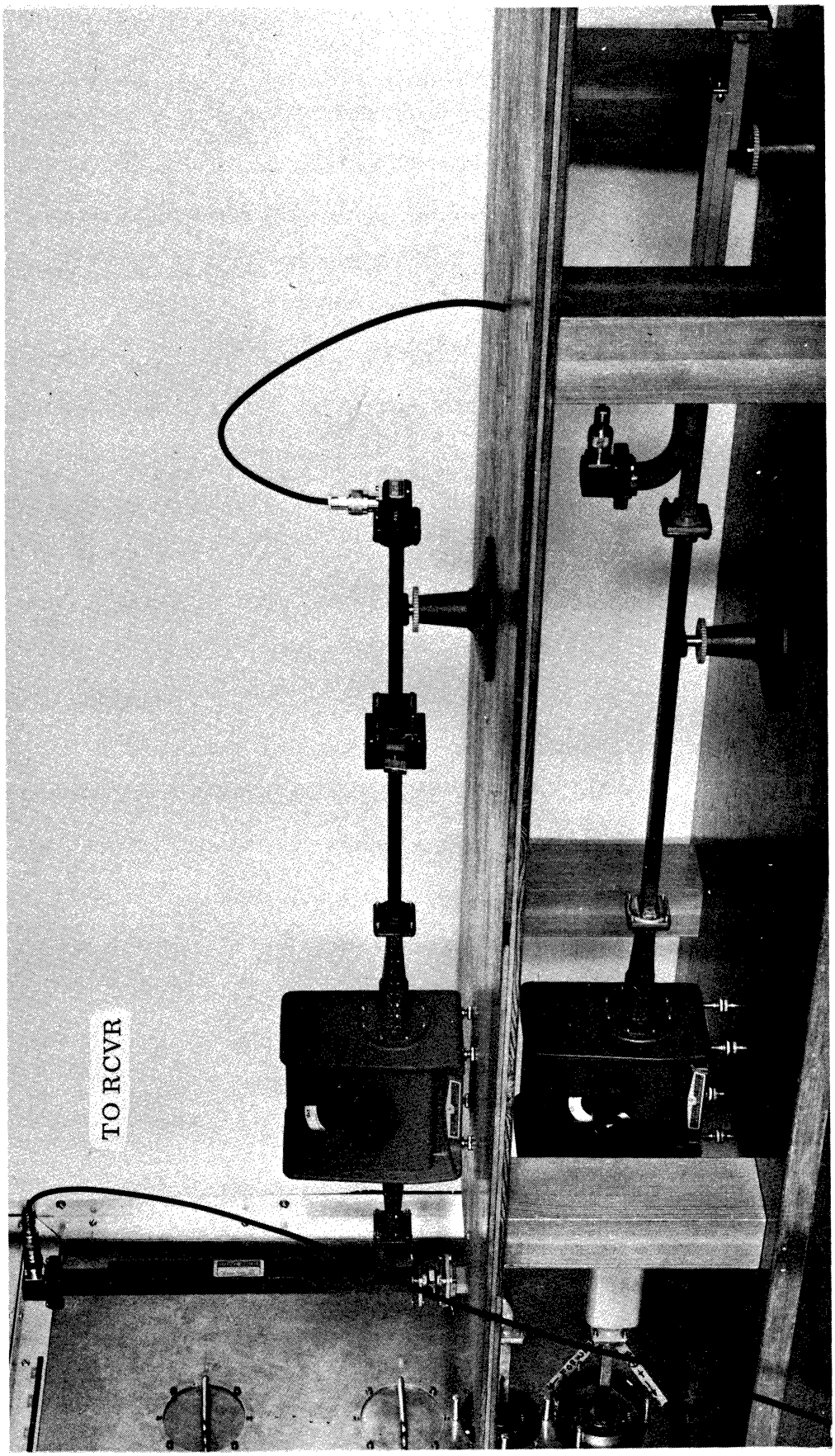

FIG. 4-2: BRIDGE CIRCUIT USED TO DECOUPLE TWO X-BAND SLOT ANTENNAS.

For convenience, a 10 db and a 20 db directional coupler were used. A 10 db coupler has a loss of 0.46 db to the main signal, and a 20 db coupler has a loss of 0.04 db. Thus, the use of the bridge for decoupling has negligible effect on the transmitting and receiving properties of the original systems.

A sample decoupling curve is shown in Fig. 4-3. The upper curves show how closely the coupled power is matched by the bridge power. The lower curve is the decoupled power level. It is below the -47.5 db level from transmitter power for all of X-band. The decoupling achieved is approximately 17 db.

A broadband compensating bridge also has been used to decouple two X-band monopole antennas. The monopoles were spaced 22.8 cm apart in a common ground plane. One monopole was .83 cm high with a diameter of .08 cm. An iris .16 cm in diameter was used with this monopole to improve the matching with the transmission line. The other monopole was .825 cm high with a diameter of .08 cm. An iris .26 cm in diameter was also used with this monopole. The circuit used was similar to the X-band slot bridge, with changes to match different attenuation and dispersion vs frequency characteristics of the monopoles. A sample decoupling curve is shown in Fig. 4-4. Again the upper curve shows how closely the power levels of the bridge and coupled paths match, while the lower curve is the decoupled power level. The decoupling is approximately 19 db over the usable range of the monopoles.

A demonstration was prepared to show the effectiveness of the compensating bridge in reducing interference. The equipment layout is shown in Fig. 4-5. The idea was to first receive a desired signal, then "jam" the receiver with a nearby transmitter, and then finally use the bridge to reduce the interference so

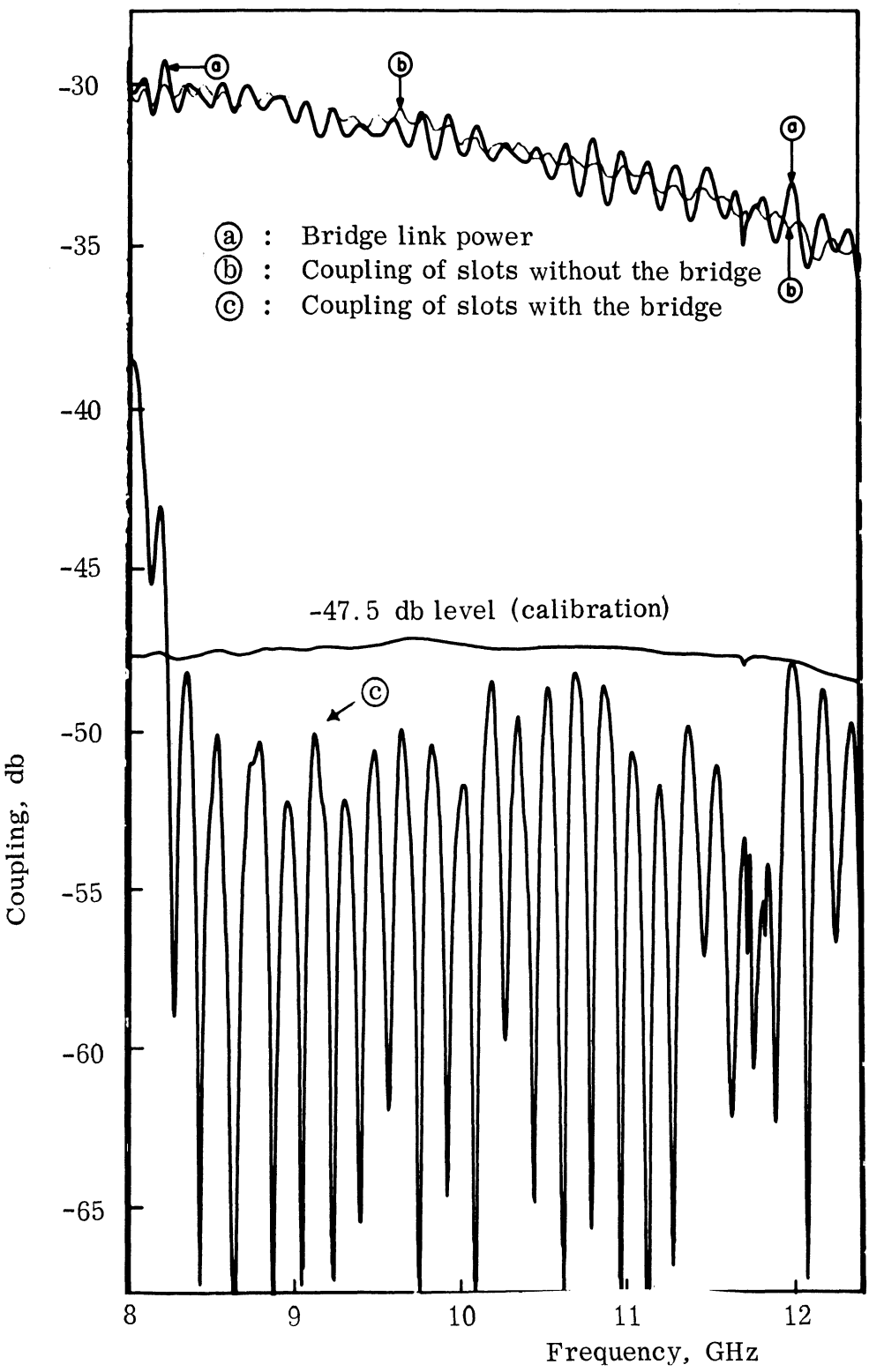

FIG. 4-3: REDUCTION OF THE E-PLANE COUPLING OF TWO SLOTS SPACED 11.4 CM BY THE BRIDGE.

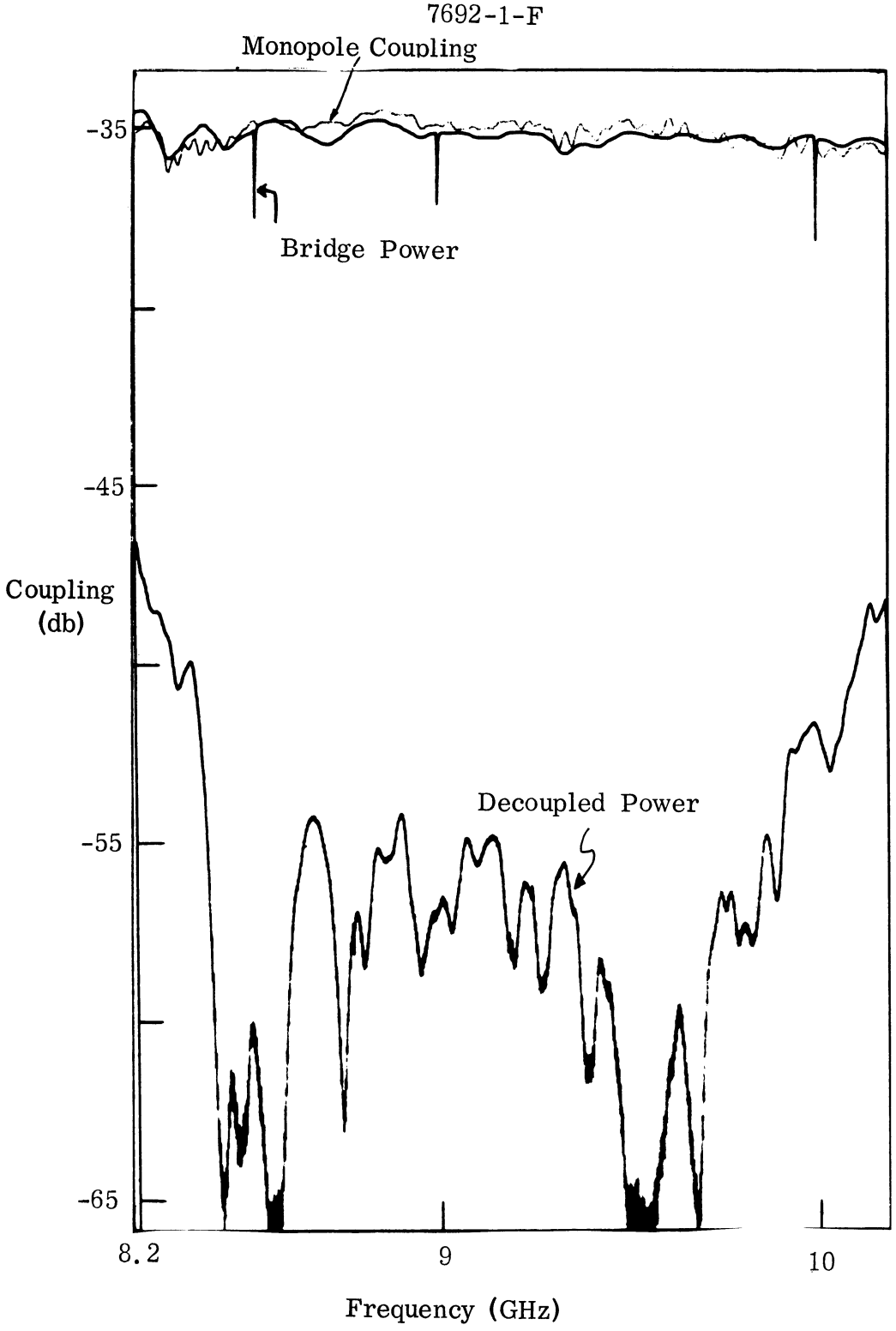

FIG. 4-4: REDUCTION OF COUPLING OF TWO X-BAND MONOPOLES BY THE COMPENSATING BRIDGE.

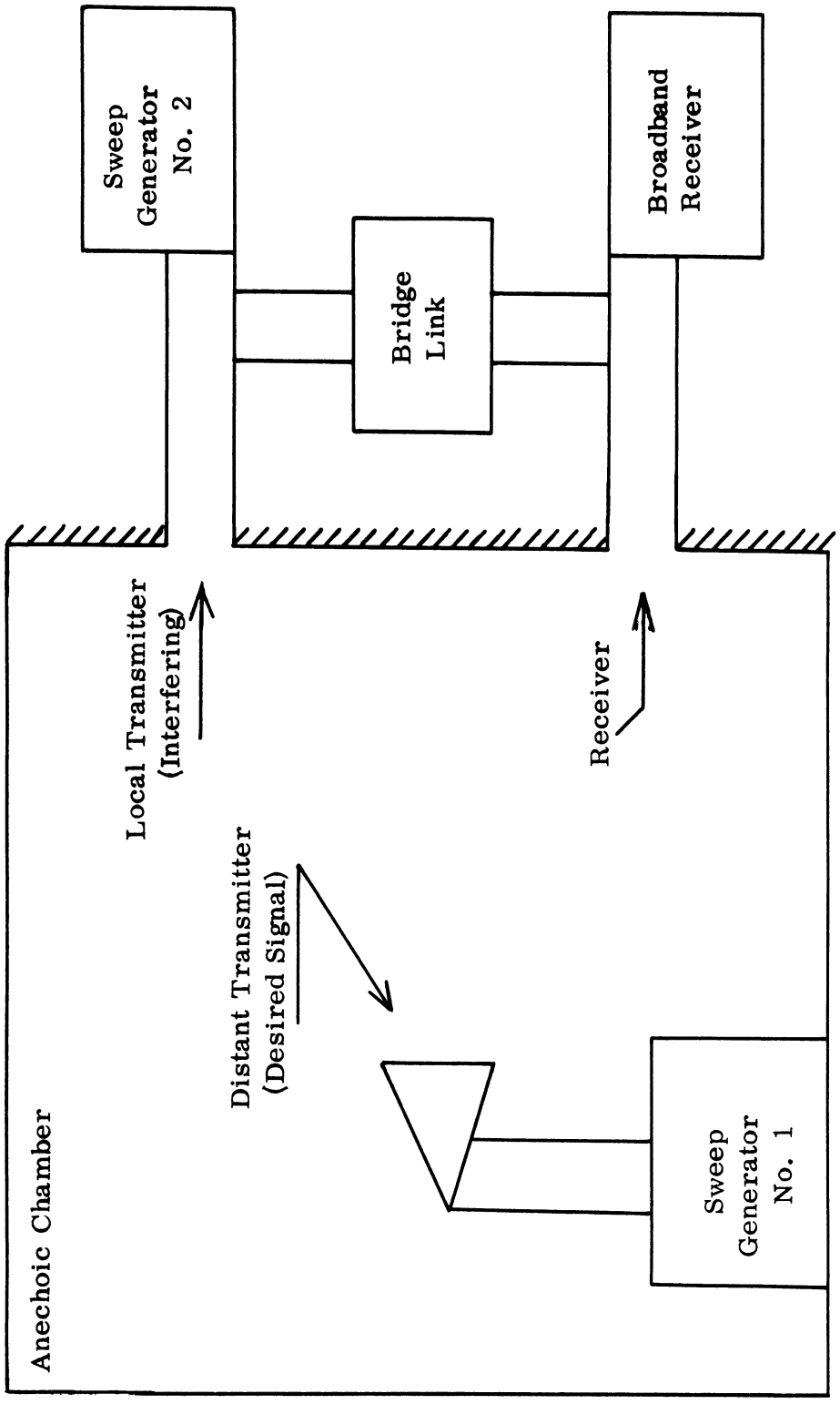

FIG. 4-5: EQUIPMENT LAYOUT FOR BRIDGE DEMONSTRATION (NOT TO SCALE).

the desired signal could once again be received. The desired signal source was an X-band sweep generator, labeled No. 1, feeding a horn antenna. This was located inside the anechoic chamber, 22 feet away from the ground plane. The receiver used a slot antenna mounted in the ground plane, while the interfering source was another X-band sweep generator, labeled No. 2, feeding a second slot antenna mounted in the same ground plane. The coupling was the strong or E-plane case and the interfering slot was spaced 11.4 cm away from the receiving slot. The bridge was connected as usual between the interfering transmitter and the receiver.

The results of this demonstration are shown in Fig. 4-6. The frequency scale is for the desired signal. The interfering sweeper, No. 2, was running four times as fast, and sweeping from 12.4 to 8.0 GHz in each sweep, rather than from 8.0 to 12.4 GHz. Curve (b) shows the remote or desired signal with the local interfering transmitter off. Curve (a) shows the desired signal jammed by the local transmitter. Finally, curve (c) shows how the interference is reduced by the compensating bridge. Note how closely curve (c) matches curve (b). Thus, the bridge has effectively reduced nearby interference, while allowing the desired signal to be received essentially unattenuated.

This work has not been intended to develop a prototype, but instead to prove the feasibility of a broadband compensating bridge. This work has been sufficiently encouraging in X-band to imply that the broadband compensating bridge technique can be extended to other frequency ranges.

Although some results reported here were for two antennas mounted on the same ground plane, the compensating bridge technique is not limited to this case. It could, for example, be applied to two towers separated by some distance. The bridge link in this case could be either by cable or by a link through air using highly directive auxiliary antennas. It is likely that such a link would be operated at a new fixed carrier frequency.

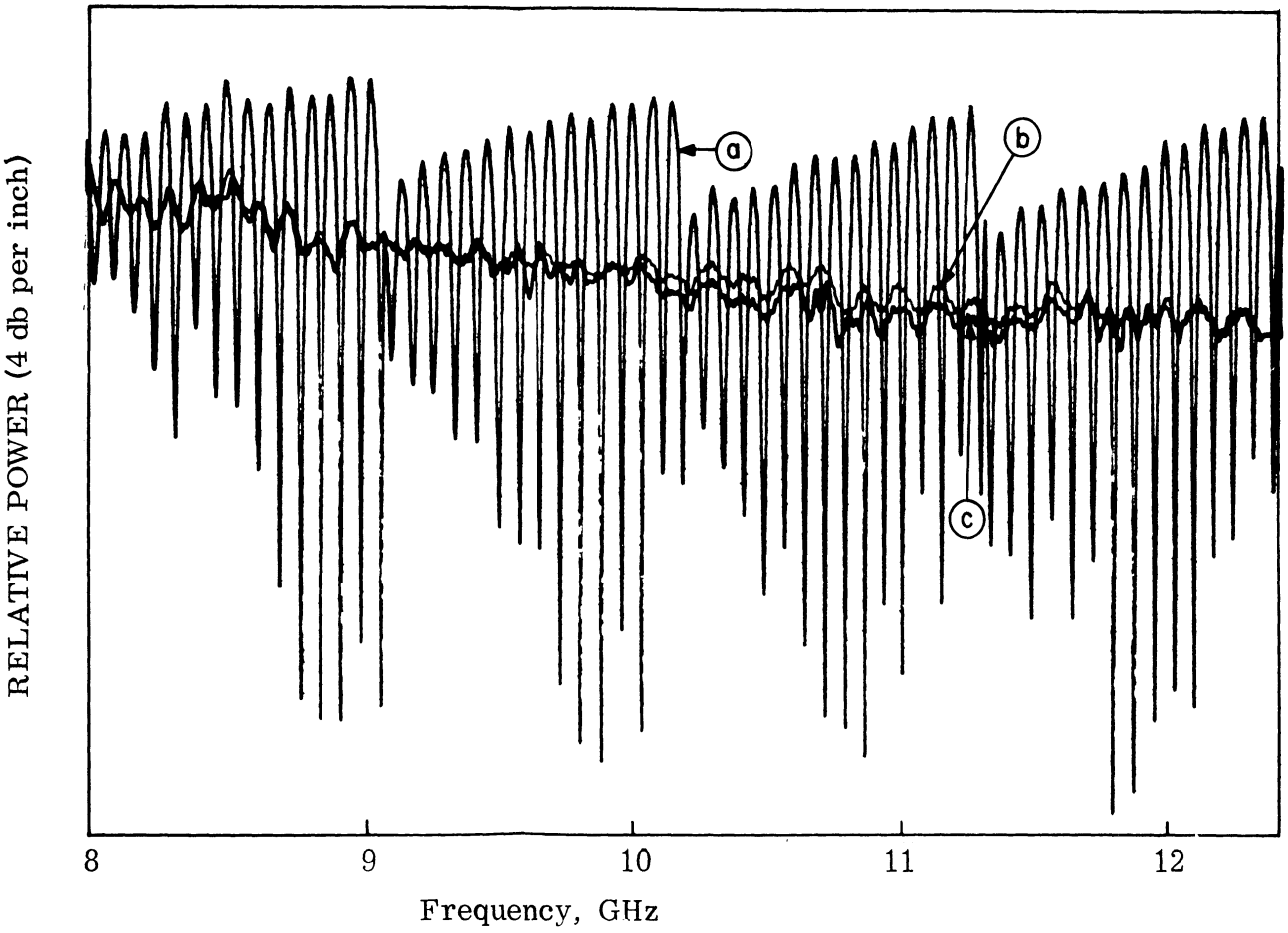

FIG. 4-6: DEMONSTRATION OF BRIDGE EFFECTIVENESS IN REDUCING INTERFERENCE

ⓐ Remote transmitter signal with interference from a transmitter near the receiver.

ⓑ Remote transmitter signal with local transmitter off.

ⓒ Remote transmitter signal with local transmitter on. Interference reduced by the RF bridge.

V

PARASITIC ELEMENTS

5.1 General

Parasitic elements can be used as reflectors or directors to guide the power radiated from the antenna in a desired direction. Such elements have been found to be very effective at the VHF and UHF ranges and have many applications. In aerospace applications the use of parasitic elements is restricted by the requirement of flush mounting. Some of the techniques investigated use elements slightly protruding from the ground plane surface; however, modifications are suggested to make flush mounting possible.

The first method, fences, is based on reflecting the energy radiated by one antenna along the ground plane and causing interference with a second antenna. Although this fence acts primarily as an energy reflector, by appropriate design a phase cancellation of the forward scattered waves at the second antenna aperture was found to create maximum interference reduction. The phase cancellation idea is the basis of the second method which uses ribs on the ground plane to direct to the receiving aperture an amount of power equal to the originally coupled but at different phase. Finally the use of parasitic slots backed by a cavity was investigated. This method, however, is not as effective as the other two in coupling reduction.

5.2 Fences

The type of fence described here is basically different from the radar fences described in the literature (Ruze et al, 1966) used to reduce site clutter return. The purpose is generally the same but the fence geometry is different. Previously used radar fences consisted of an opaque screen built around a ground based radar at a distance of a few hundred wavelengths from the antenna and with a height of the order of one hundred wavelengths. The opaque screen is usually a wire mesh which behaves electrically as a solid metal wall. In the cases examined here

the fence is placed between a pair of transmit-receive antennas at spacings of five to ten wavelengths. Fresnel diffraction theory can not be used at such close spacings where the position of the fence between the two antennas becomes important in the effort to obtain high isolation between the two systems. The main difference, however, lies in the fact that the fence used in this case is of critical dimensions and could be best described as a parasitic array of half-wavelength monopoles, similar in appearance to a fishbone antenna. This structure is more readily applicable to aerospace antennas and it was found to create greater system isolation than a solid wall metal fence. The fact that the structure dimensions are described as critical should not be interpreted as overly restrictive since in applications described below such fences produced an additional system isolation of 35 db over a twenty-five percent bandwidth.

A number of fences were made and tested. In all the experiments two waveguide-fed slot antennas were used oriented for E-plane coupling. The slots were in a 12 ft square aluminum ground plane at two different center-to-center spacings; 11.4 cm and 22.8 cm. One slot was connected to a Swept Frequency Generator with leveled output, sweeping through X-band. The power received at the second slot, representing with an appropriate scale the coupling between the two slots, was recorded. The geometry of the two antennas with the fence is shown in Fig. 5-1. The pins of the fence were cut either from copper wire or from brass. They were soldered on a thin plate (not shown in Fig. 5-1) so that the fence could be moved along the ground plane. It was attempted to use guides on the plane surface and slide the fence between them by remote action while observing the swept-frequency received power on an oscilloscope. It was realized, however, that under these conditions the fence structure did not always make a good contact with the metal ground plane and

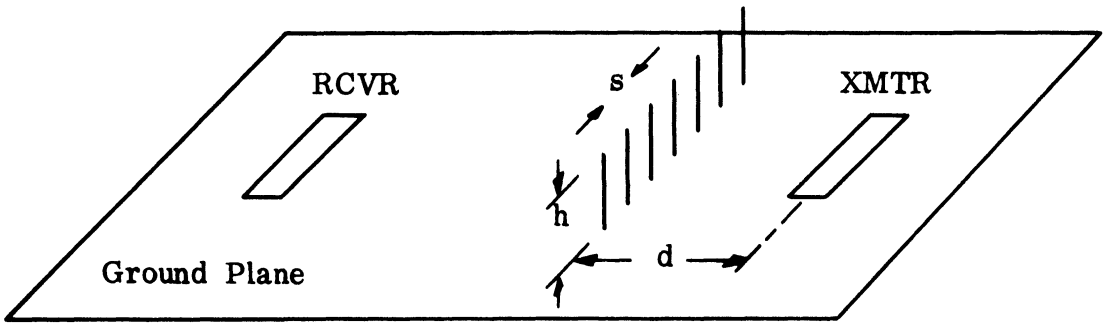

FIG. 5-1: GEOMETRY OF SLOTS WITH FENCE

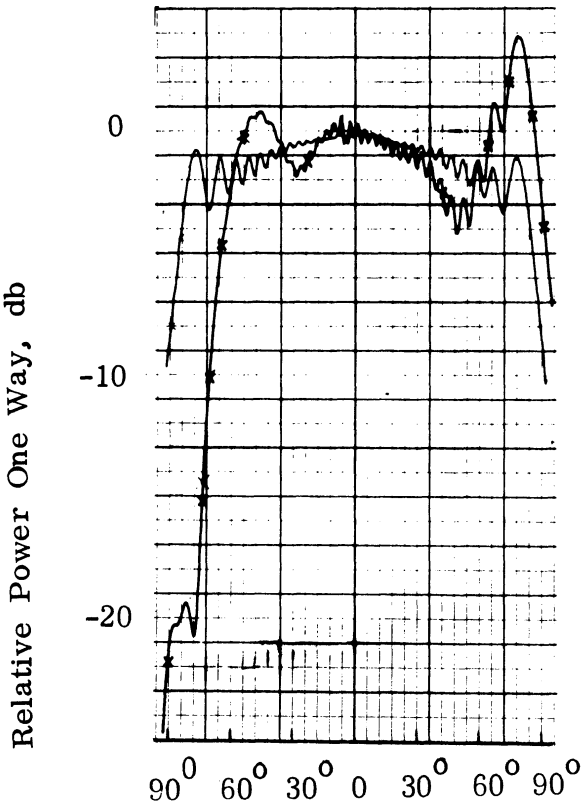

FIG. 5-2: E-PLANE RADIATION PATTERN AT 10 GHz FOR A SLOT IN A 90 CM BY 60 CM METAL PLANE IN THE PRESENCE OF A FENCE. (Fence No. 5, d = 4.4 cm)(——)Plain Slot; (—x—) Slot with Fence.

significant changes could occur in the received power. Therefore this technique was abandoned and instead the fence was fastened to the ground plane at every position with aluminum foil. The parameters of the fences for which results are shown, are summarized in the following table. All of these fences consisted of seven elements.

TABLE V-1

Fence No.	h(cm)	s(cm)	2a(cm)
2	1.45 $\pm$ .05	1.15 $\pm$ .05	.16 (1/16")
5	1.7	1.1	.16
9a	1.8	1.2	.16
9b	1.7	1.2	.16
10	1.7	1.2	.32(1/8")

A typical radiation pattern of a slot in a 2' by 3' aluminum ground plane in the presence of a fence is given in Fig. 5-2. The radiation pattern of a slot without the fence is also given for comparison. The radiation on the side of the fence is reduced by 19 db. The waves reflected from the fence produce an increased gain on the other side of the slot. This may be avoided by a symmetrical arrangement of fences on each side of the antenna. The coupling reduction that can be obtained with such a fence is shown in Fig. 5-3. This reduction amounts to about 20 db over a forty percent bandwidth and more than 30 db at one frequency. The spacings between fences and slots shown in Fig. 5-3 are those found to be optimum for broadband decoupling in each case.

In another series of experiments with fences, nos. 9a and 9b, the spacing of the two slot antennas was changed too (11.4 cm and 22.8 cm). In either case fence 9b was slightly better producing a midband decoupling of 16 db at an

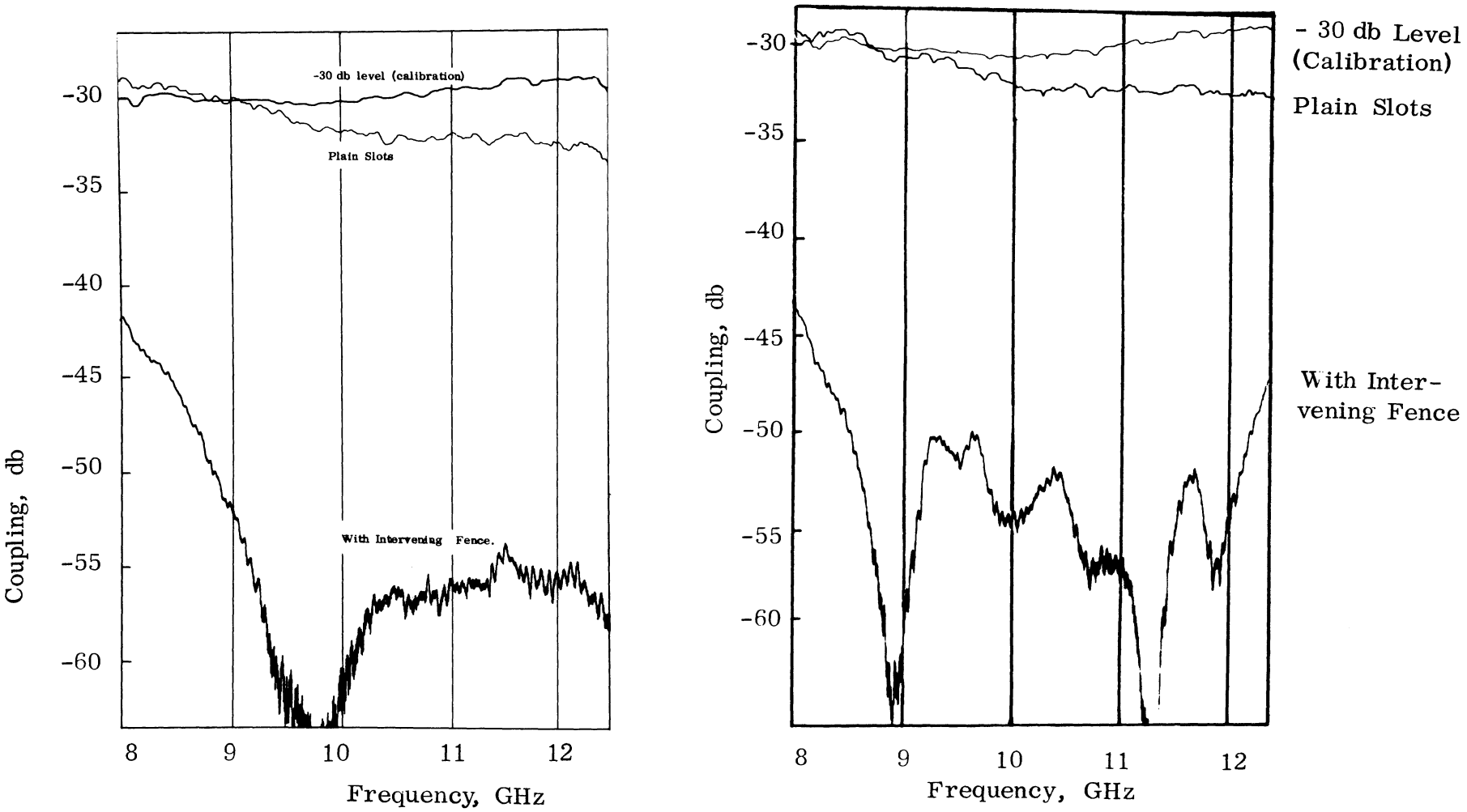

(a) Fence No. 2, d = 2.6 cm

(b) Fence No. 5, d = 4.4 cm

FIG. 5-3: E-PLANE COUPLING VS FREQUENCY FOR TWO SLOTS SPACED 11.4 CM WITH AND WITHOUT AN INTERVENING FENCE.

optimum position d = 3.0 cm. The fact that the optimum fence position was found to be the same for two different spacings of the two antennas indicates that the fence can be associated with one antenna rather than with a pair of antennas. This of course is normally the case when the two antennas are in the far field of each other. When far-field conditions prevail it is possible to achieve twice as much coupling reduction (in db) by placing one such fence in the vicinity of each antenna. This was tested, using the two fences No. 9 in a symmetrical arrangement, each close to one of the slots (d = 3.5 cm). Figure 5-4 shows that in this case a coupling reduction of 35 db was obtained over a frequency range of 2.5 GHz (25 percent bandwidth) and 29 db over a 40 percent bandwidth. This indicates the potential of this method without in any way establishing an upper limit because in this experiment the distance d is the only parameter that was really optimized.

The different fences used were constructed with an element spacing between $\lambda/4$ and $\lambda/2$. The height also varied in the same range. It was found that a fence with a height near $\lambda/4$ at the center of the frequency band produced insignificant coupling reduction, while a height near $\lambda/2$ gave the best results. The best choice of the other parameters is $s = 3/8\lambda$ and $\lambda < d < 3/2\,\lambda$. The wire diameter, 2a, is also an important factor. Of the three different wire diameters used (1/8", 1/16" and 1/32") the largest was found to be substantially inferior to the other two. A comparison is given in Fig. 5-5 which shows the original level of coupling between two plain slots (curve A) and the reduction of same with the addition of each one of the following, one at a time, all at the same distance (d = 3.5 cm).

Curve B: A solid metal wall 1.7 cm high and 7.3 dm long.

Curve C: A fence of the same overall length and height with wire diameter 1/8" (Fence No. 10).

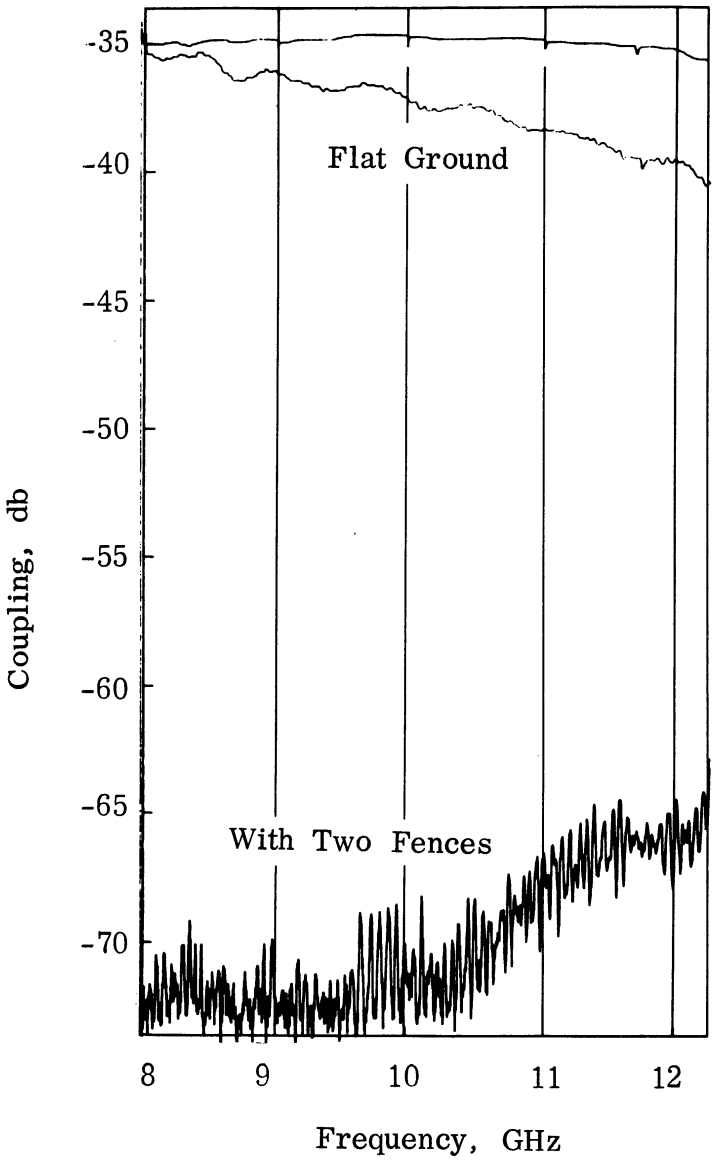

FIG. 5-4: E-PLANE COUPLING REDUCTION WITH TWO FENCES FOR TWO SLOTS SPACED 22.8 cm.

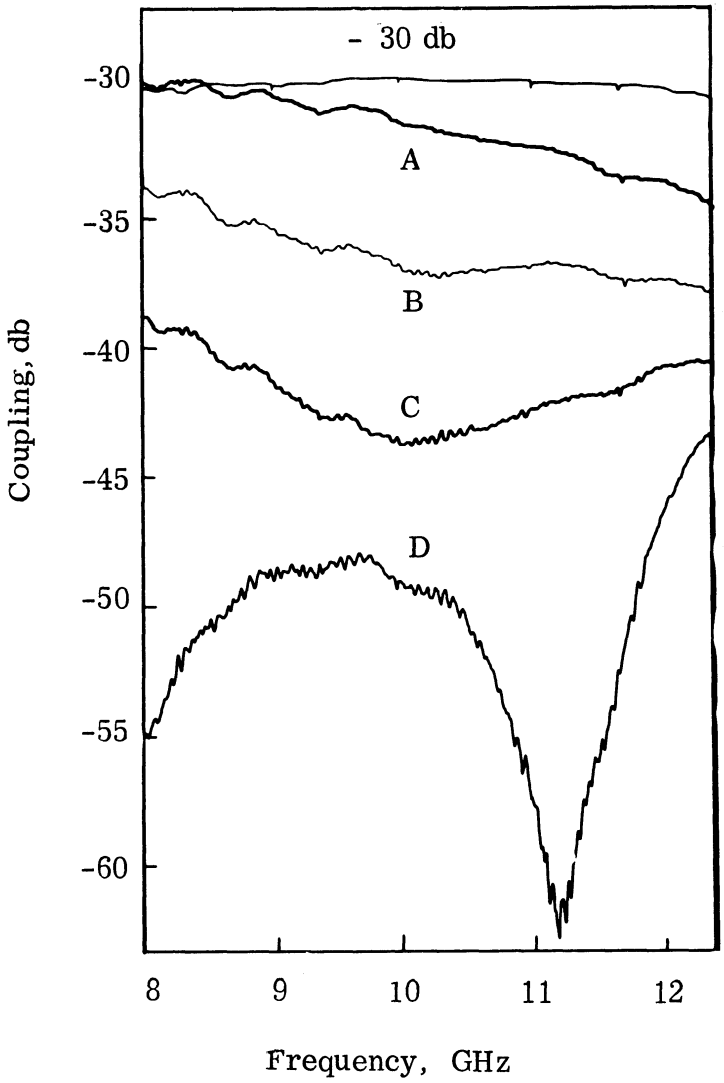

FIG. 5-5: E-PLANE COUPLING FOR TWO SLOTS SPACED 11.4 CM WITH VARIOUS TYPES OF FENCES. (Explanation in text).

Curve D: A similar fence except with wire diameter 1/16" (Fence No. 9b). The curve at the top of the chart is for system calibration and shows the -30 db level with respect to the transmitter power. The displacement of the solid metal wall fence between the two slots did not change curve B by more than $\pm$ 1 db. Here the parasitic array fence proves to be superior to the solid wall fence by providing additional isolation of 11 db over a broad bandwidth and 25 db at the null.

The large reduction of coupling and the simple structure of the described fence, make this method of interference reduction particularly attractive. The frequency sensitivity of this fence may be desirable in a case where additional isolation is desired in a system of two antennas without any interference with a third nearby antenna operating at another frequency range. For aerospace applications the fence could be spring loaded, recessed in the metal surface and then exposed once the vehicle is in space. It could also be considered in a permanent flush mounted modification. This could be achieved by having the two antennas involved in interference mounted flush with a recessed part of the ground surface. The fence could also be mounted on this recessed part with the tops of the pins just even with the contour of the main ground surface. The recess could be filled with dielectric material. The exterior surface of the dielectric would be a smooth continuation of the metal surface of an aerospace vehicle. Since the required half wavelength of the pins would be on the basis of the dielectric permittivity, the depth of the recessed part would be relatively small.

5.3 Ribs

Small strips cut from B. F. Goodrich type RF-X resonant absorber, backed by aluminum foil (the combination corresponds to a quarter-wavelength wave trap in transverse thickness) were used to create this link. In the

initial experiments the strips were placed flat on the ground plane. By changing the width and length of the strips as well as their position on the ground plane, it was possible to control the amount of power carried over to the receiver. It was found that a pair of strips placed as shown in Fig. 5-6 gave the best results. One of the typical patterns obtained is shown in Fig. 5-7. This is for E-plane coupling of the X-band slots. For this case a decoupling of 12 db over a 20 percent bandwidth is shown.

5.4 Parasitic Slots

In order to study the behavior of flush-mounted parasitic antennas a new antenna has been constructed in the form of a three slot array. One slot was fed by X-band waveguide while the other two were backed by cavities constructed again from X-band waveguide and equipped with sliding shorts. The distance of the parasitic slots from the transmitting one was adjustable, from a minimum of 1.27 cm center-to-center (imposed by the physical dimensions of the waveguide) to a maximum of approximately 4.0 cm.

A series of radiation patterns has been taken for various spacings of the parasitic elements and various positions of the shorting plungers. A single parasitic element acts as a reflector when the cavity depth d is $\lambda_g/4$, where λ_g is the waveguide wavelength. A sidelobe level of - 7 db with respect to maximum gain, was observed at close spacings. For the minimum possible spacing the pattern becomes asymmetrical while for spacings near $\lambda_g/2$ the pattern symmetry is partially restored (Lyon et al, Aug. 1966). No setting was found for which a single parasitic element would act as "director," increasing the sidelobe level in its direction. In combinations of two parasitic elements on either side of the transmitter it was noted that the "reflecting" parasitic had a predominant effect. A sidelobe of -8 db has been obtained in this case.

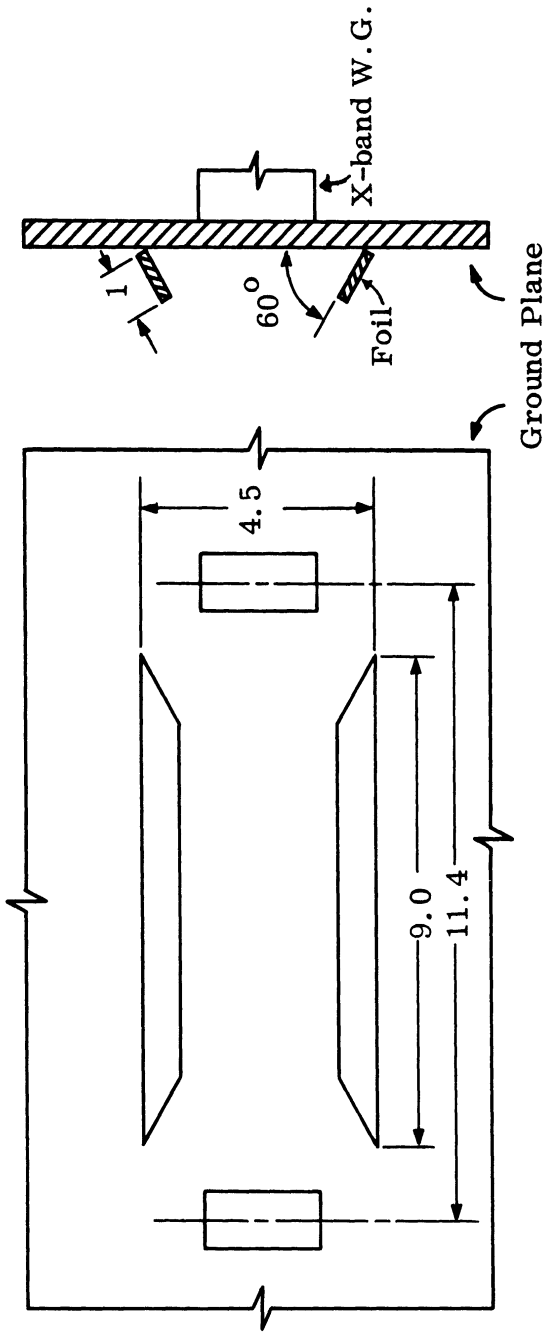

FIG. 5-6: GEOMETRY FOR PHASE CANCELLATION: (DIMENSIONS IN CM).

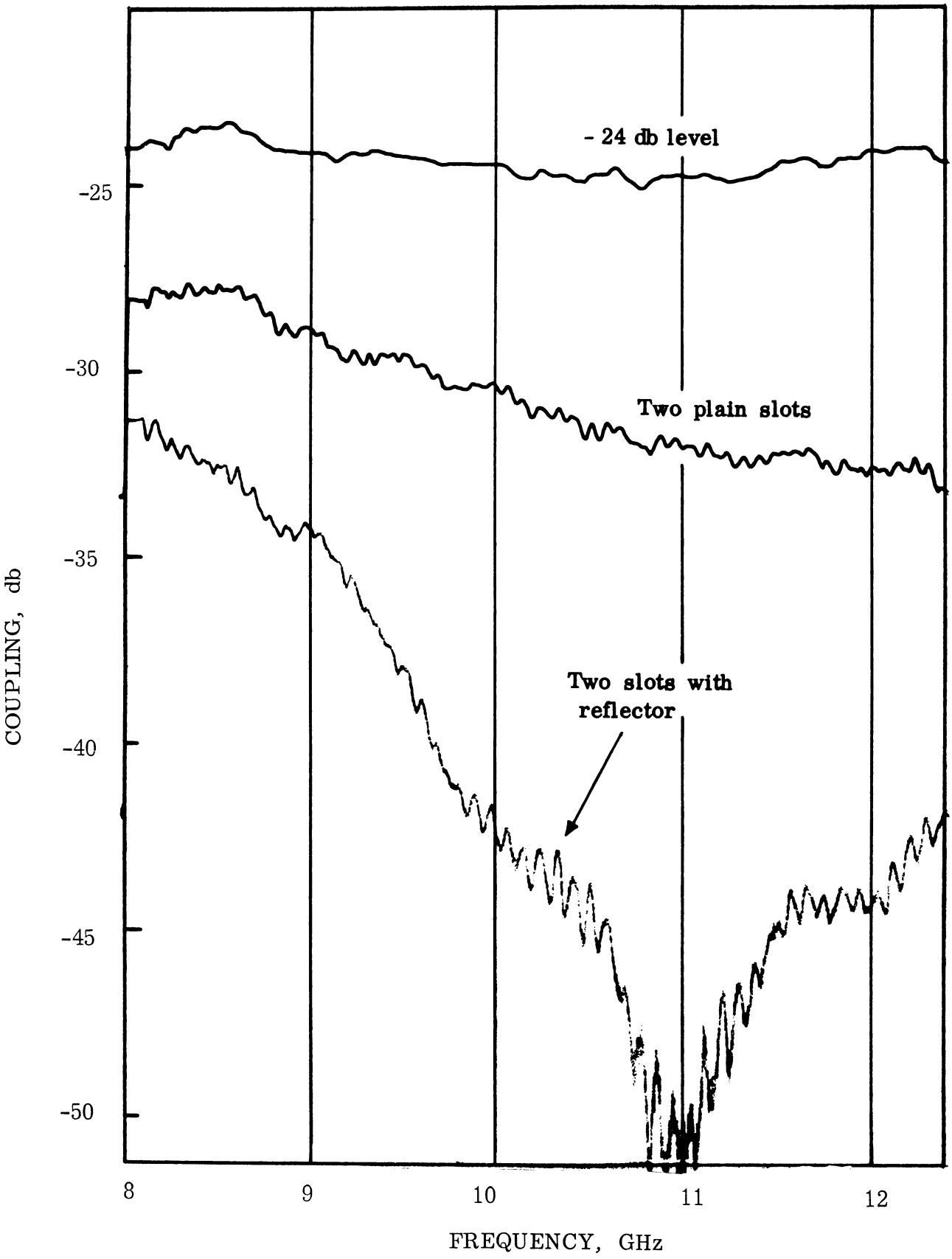

FIG. 5-7: E-PLANE COUPLING VS FREQUENCY FOR TWO SLOTS SPACED 11.4 CM.

Two parasitic slots backed by a cavity were used symmetrically on both sides of a transmitting slot (in the E-plane). A center-to-center spacing of 1.5 cm between the transmitting slot and either of the parasitics and a cavity depth of 1.4 cm which corresponds to $0.35\lambda_g$ at the center frequency of 10 GHz were found to produce the maximum decoupling. The decoupling obtained in this way was 7 db over a 20 percent bandwidth and 6 db over a 30 percent bandwidth. In general the action of the parasitic slots is similar to that of the corrugations. Thus an E-plane cut through a slot surrounded by corrugations may also be considered as a parasitic slot array with many elements. This subject has been investigated in more detail in Chapter III of this report.

VI

DIELECTRIC COVERED SLOT ANTENNAS

The case of slot antennas covered by a dielectric layer is a very important one. This is because many space vehicles are covered with an ablative material, designed to burn off during the re-entry phase of flight. Such material protects the metal skin of the space vehicle. Results which were valid for flush-mounted antennas in a ground plane will, in general, differ from results on antennas under ablative coatings.

Experimental studies were made to investigate the coupling of two X-band slot antennas covered by a dielectric sheet. The antennas used in these studies were waveguide-fed slots mounted in a 12ft. by 12 ft. aluminum ground plane. The antennas were oriented for the strong or E-plane coupling case. The center-to-center spacing was 11.4 cm. All measurements were made with a swept-frequency technique in the range 8 GHz to 12.4 GHz.

The dielectric material finally selected was polystyrene. This material has a relative dielectric constant $\epsilon_r = 2.5$ and is nearly lossless having a dissipation factor D = 0.0004. Sheets were obtained that were 20 inches by 40 inches with three thicknesses, 1/8 inch, 1/4 inch, and 1/2 inch.

Coupling data were obtained for all three thicknesses. As the ground plane was vertical, it was necessary to hold the 20 inch by 40 inch sheets against it with tape. The sheets were centered with respect to the two X-band slots. The coupling data are presented in Figs. 6-1, 6-2 and 6-3. Each figure shows the direct coupled level and the coupling of two plain slots, along with two curves for the coupling with the polystyrene sheet. The polystyrene curve identified by dots corresponds to the 40 inch dimension in the E-plane, while the other polystyrene coupling curve corresponds to the 40 inch dimension in the H-plane. Notice that the orientation of the

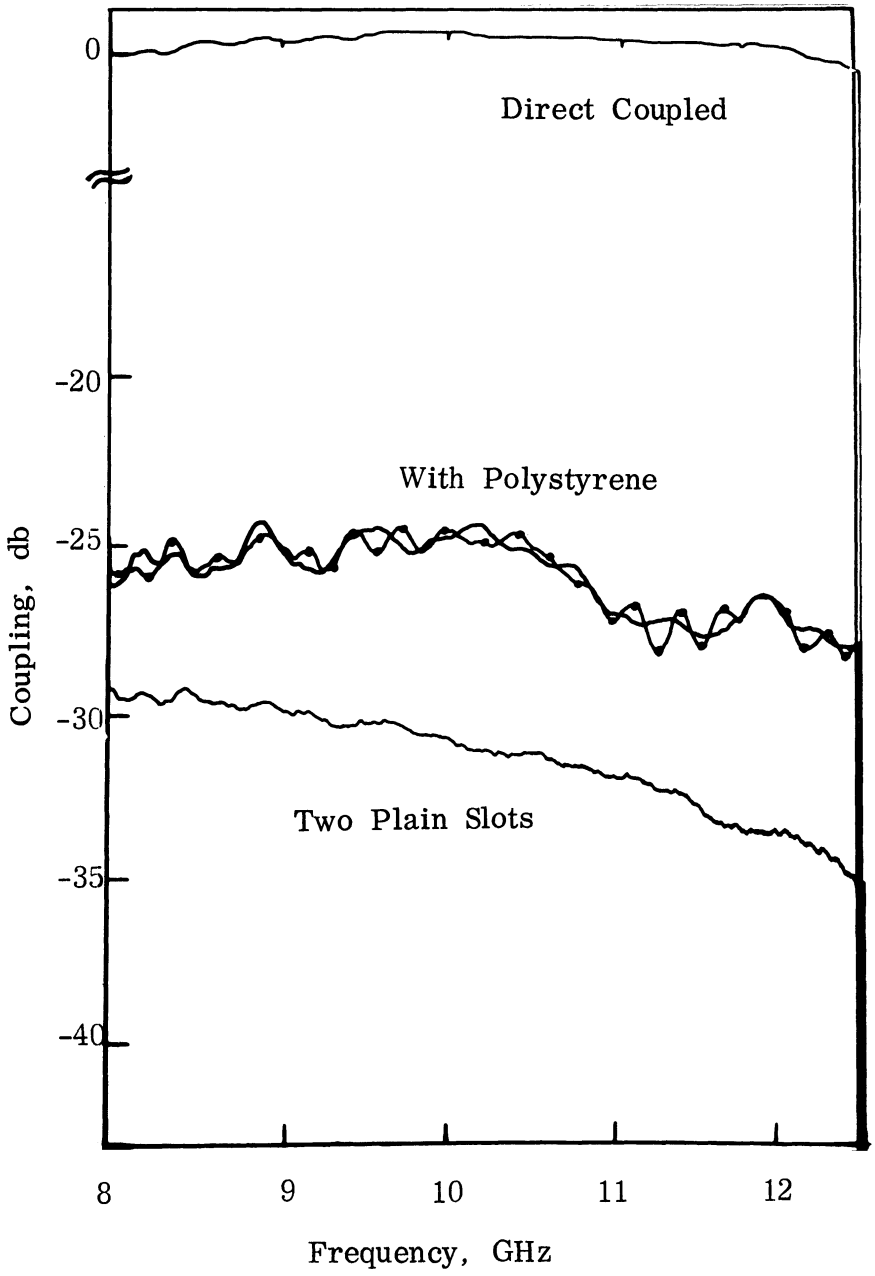

FIG. 6-1: SLOT COUPLING WITH 40 INCH BY 20 INCH BY 1/8 INCH POLYSTYRENE SHEET.

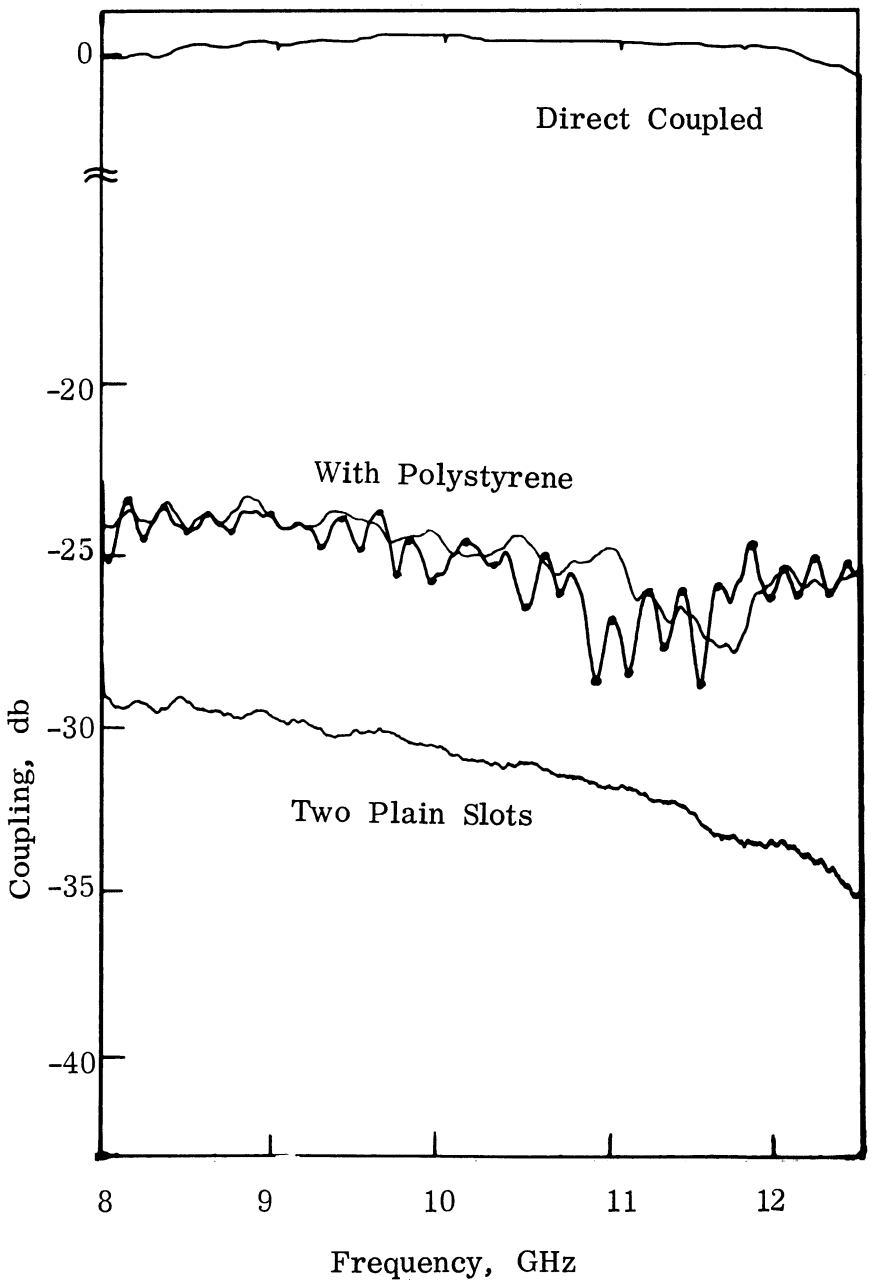

FIG. 6-2: SLOT COUPLING WITH 40 INCH BY 20 INCH BY 1/4 INCH POLYSTYRENE SHEET.

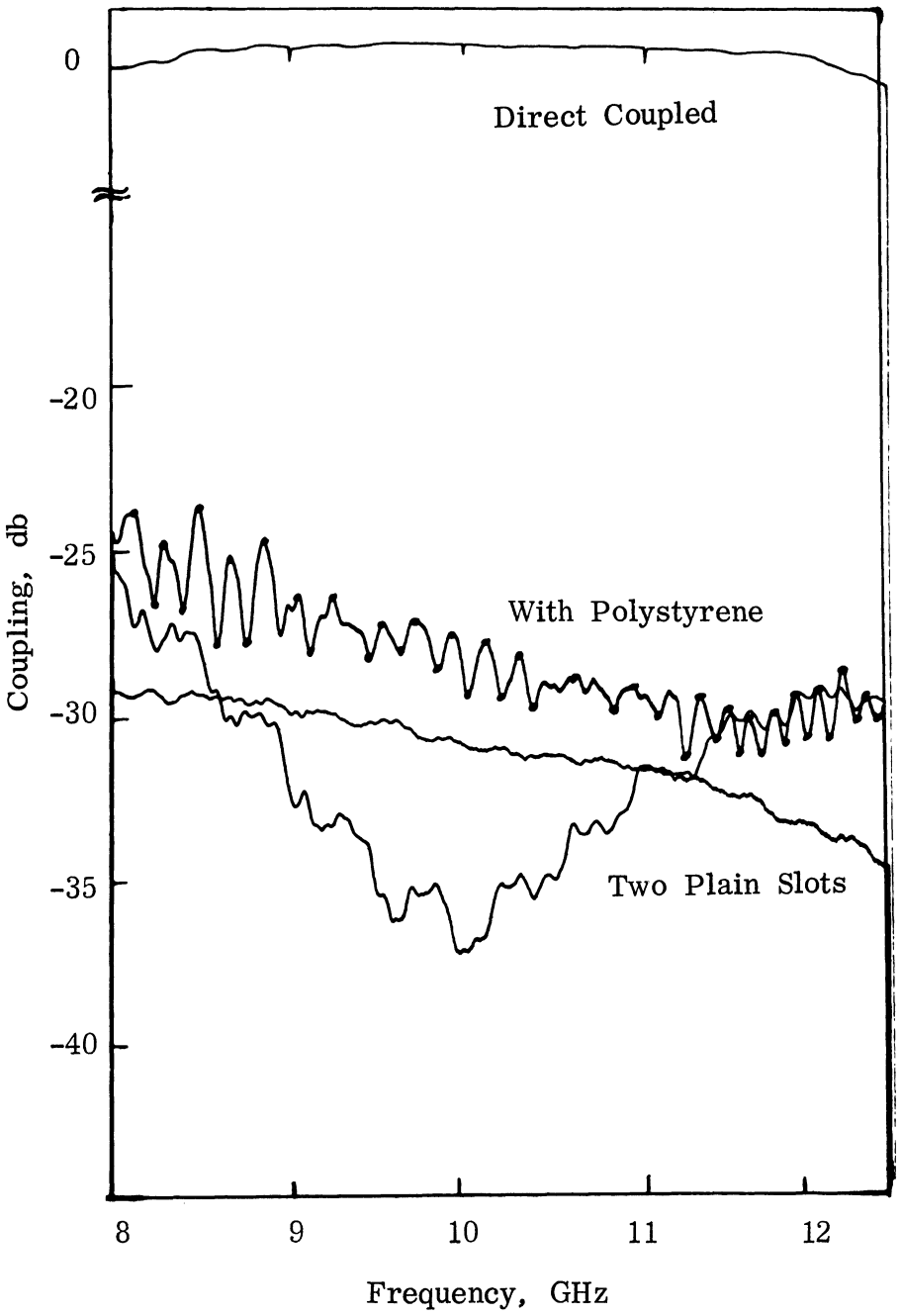

FIG. 6-3: SLOT COUPLING WITH 40 INCH BY 20 INCH BY 1/2 INCH POLYSTYRENE SHEET.

polystyrene sheet has little effect on the coupling levels in the thin or 1/8 inch case in Fig. 6-1, more effect in the middle or 1/4 inch case in Fig. 6-2, and has a pronounced effect on the coupling levels in the thick or 1/2 inch case in Fig. 6-3. In fact, in the latter case the orientation of the sheet determines if there is an increase or a decrease of coupling. The decrease in coupling is probably due to phase cancellation of two signals at the receiving slot. Notice that decoupling is not observed until the polystyrene sheet is sufficiently thick.

The increase in coupling observed is possibly due, inpart, to the wave-guiding nature of the dielectric layer, channeling energy from the transmitting slot to the receiving slot along the ground plane, and also due, in part, to the changed illumination on scattering surfaces. This effect can be observed in the E-plane radiation patterns presented later in this section. The radiation is increased in the 90^{o} direction, corresponding to the direction along the ground plane.

Notice that the coupling curves with the polystyrene sheets have periodic fluctuations. These fluctuations seem to be due to reflections from the edges of the sheets in the E-plane direction. To see this, the range of a scatterer may be calculated using a formula derived earlier (Lyon et al, Apr. 1966):

$$R = 1/2 \left[\frac{nv}{\Delta f} + R_o \right] \quad \text{for} \quad R >> R_o \tag{6.1}$$

Where:

R is the range of the scatterer.

n is the number of cycles.

Δf is the frequency sweep.

R_o is the distance between antennas.

v is the velocity of propagation.

Counting the cycles in Fig. 6-2 (the dotted curve), one finds n = 20. For the other values: R_o = 4.5 inches, Δf = 4.2 GHz, and $v = c/\sqrt{2.5}$, Making the calculation, one finds R = 20 inches. Note that this is the distance from the E-plane edge of the polystyrene sheet to the center of the two antennas.

More experiments were performed to determine the effect on the coupling of the positioning of the dielectric sheet. The 1/8 inch by 20 inch by 40 inch sheet was placed with the 40 inch dimension in the E-plane. Coupling curves were obtained while the sheet was moved in the H-plane direction. When centered, the H-plane edge is 10 inches from the centerline. No significant change in the appearance of the coupling curves was observed until the edge was 3 inches from the centerline. Thus, exact centering of the polystyrene sheet is not critical in the H-plane direction, at least in the case of the 1/8 inch slab.

The same sliding experiment was also performed for the 1/4 inch by 20 inch by 40 inch polystyrene sheet. This time the position seemed to have more effect, but the average value of the coupling curves was still little affected by the H-plane position, until the H-plane edge got very close to the centerline of the slots.

In another experiment, the 1/8 inch polystyrene sheet was cut into 4 pieces, 10 inches by 10 inches, 17 inches by 10 inches, 23 inches by 10 inches, and 30 inches by 10 inches. Each piece was centered over the slot antennas, the 10 inch dimension always in the H-plane. The four coupling curves obtained were close in average value, the maximum deviation being 2 db, but had different numbers of fluctuations corresponding to the differences in the distance of the E-plane edges from the centerline as explained by Eq. (6.1).

The 23 inch by 10 inch piece of the 1/8 inch polystyrene sheet was then centered over the two slot antennas. The 10 inch dimension was in the H-plane. This sheet was moved in the E-plane direction and coupling curves were obtained. The average level seemed basically independent of the E-plane edge location, while the number of fluctuations varies again as predicted by Eq. (6.1).

Radiation patterns were obtained for a dielectric covered slot in the 12 ft. by 12 ft. ground plane. The 40" by 20" polystyrene sheets were used with the 40 inch dimension in the E-plane direction. The sheets were centered about the radiating slot. Two thicknesses were used, the 1/4 inch sheet and the 1/2 inch sheet. E- and H-plane cuts were obtained in X-band.

The radiation patterns are presented in Figs. 6-4 through 6-8. Five frequencies were used, 8, 9, 10, 11, and 12.4 GHz. Note however that in Fig. 6-8 one curve was taken at 12 GHz. Each figure has two patterns, the plain slot pattern and the dielectric covered slot pattern. The plain slot pattern may be identified by its smoothness, or lack of fluctuations.

Experimental studies were made of the swept maximum gain for the dielectric covered slot. Results were obtained for both the 1/2 inch and the 1/4 inch polystyrene sheets. The swept maximum gain of the plain slot was also measured. These experimental results are shown in Fig. 6-9.

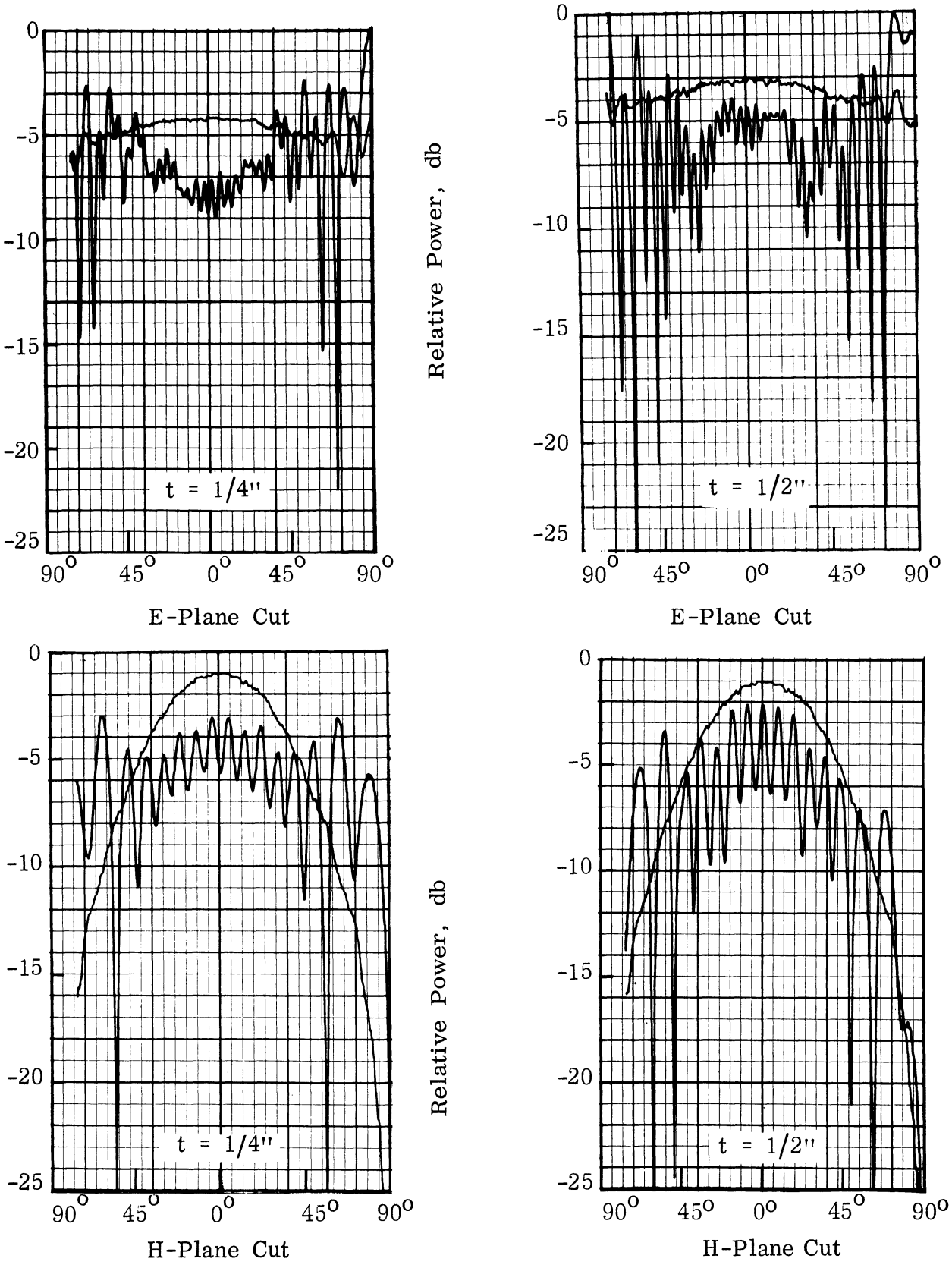

FIG. 6-4: RADIATION PATTERNS OF DIELECTRIC COVERED SLOT. F = 8 GHz.

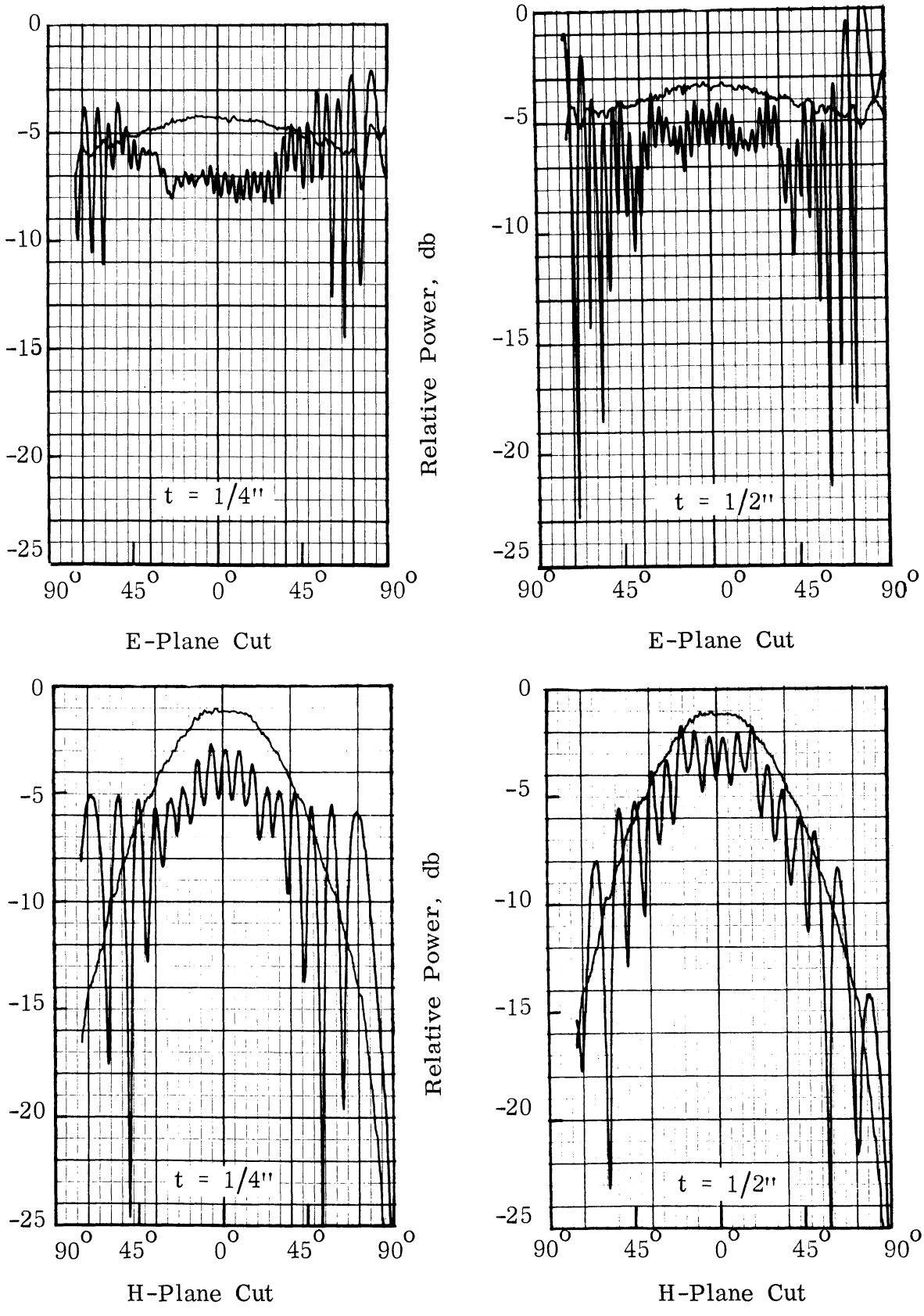

FIG. 6-5: RADIATION PATTERNS OF DIELECTRIC COVERED SLOT. F = 9 GHz.

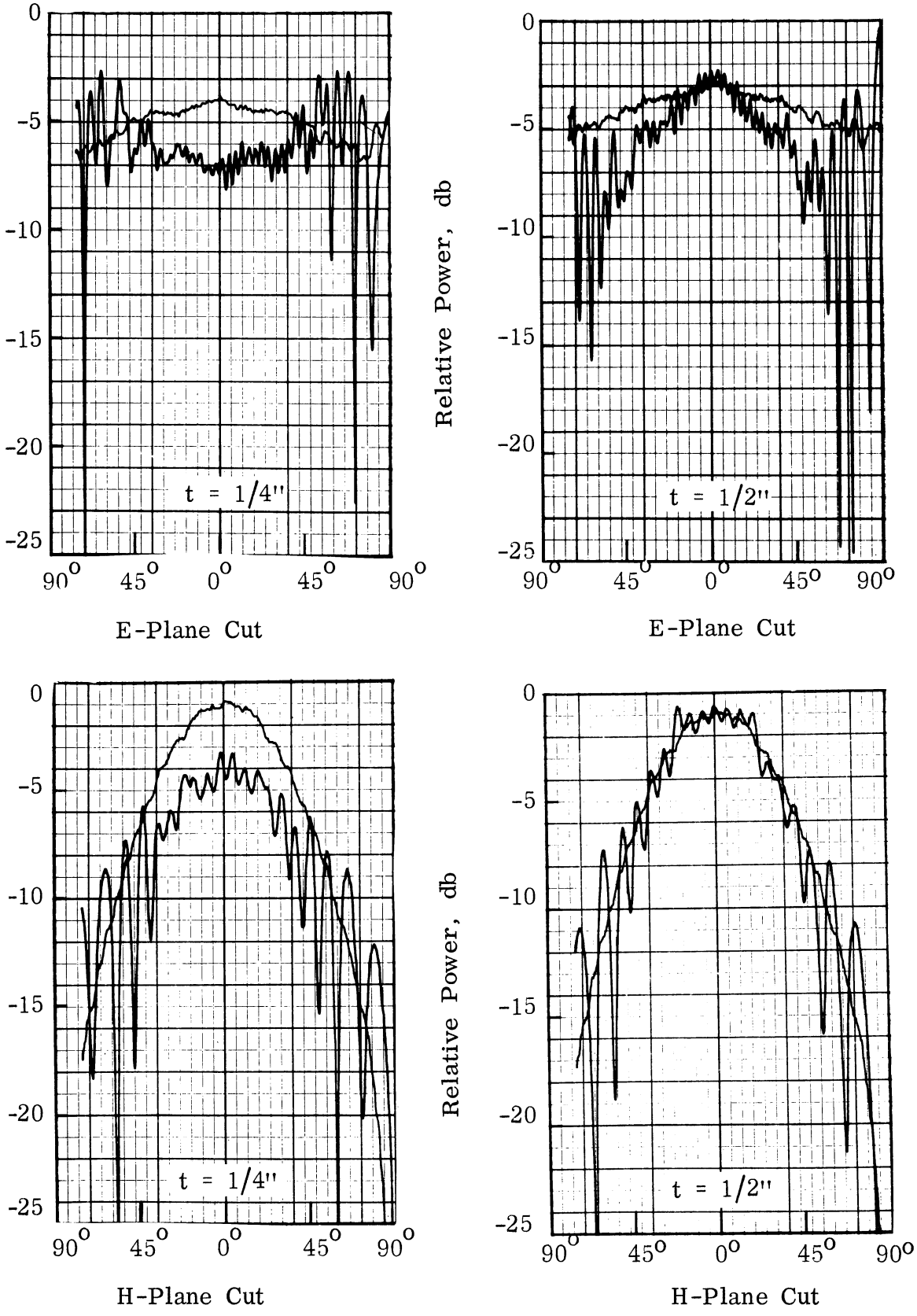

FIG. 6-6: RADIATION PATTERNS OF DIELECTRIC COVERED SLOT. F = 10 GHz.

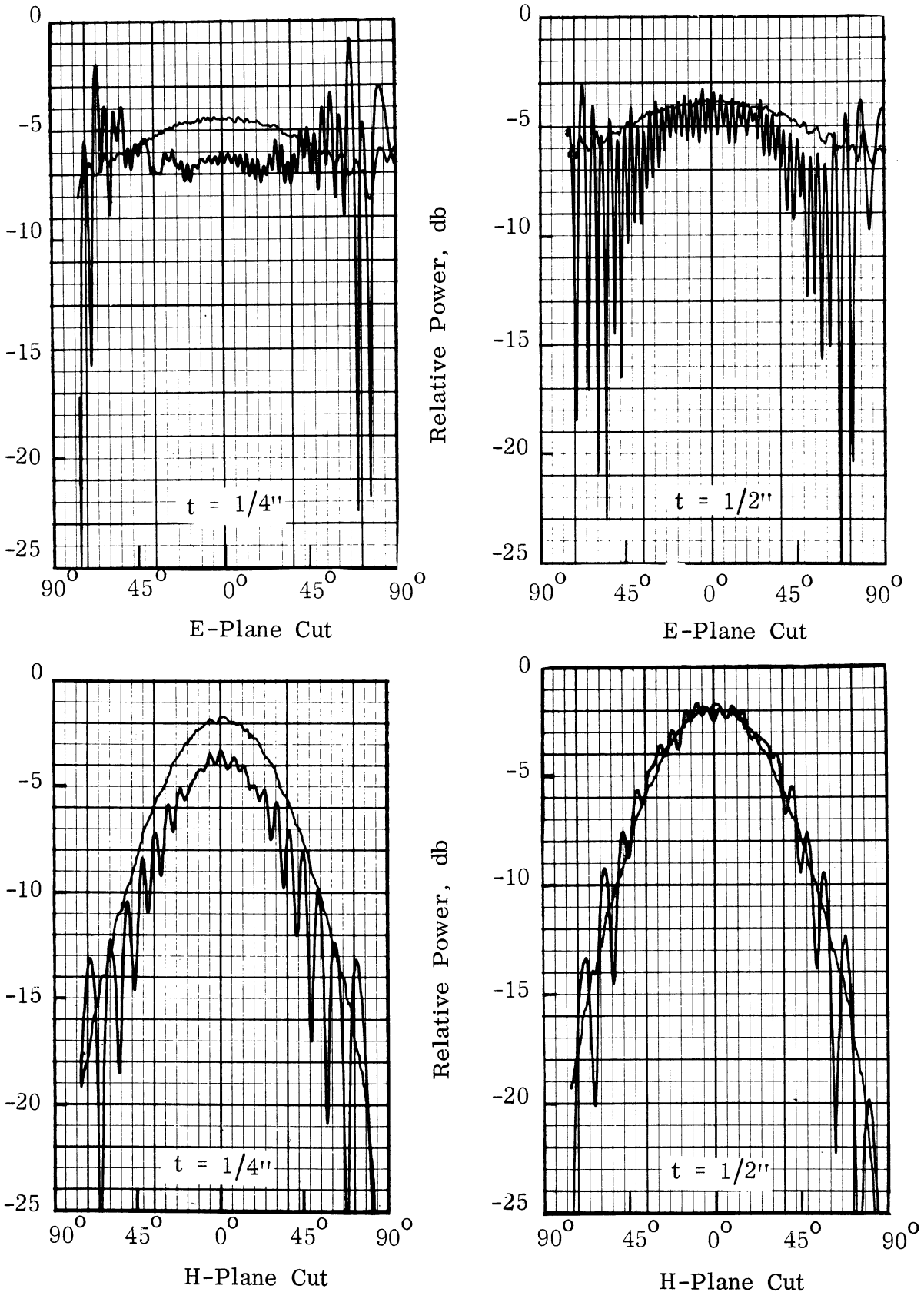

FIG. 6-7: RADIATION PATTERNS OF DIELECTRIC COVERED SLOT. F = 11 GHz.

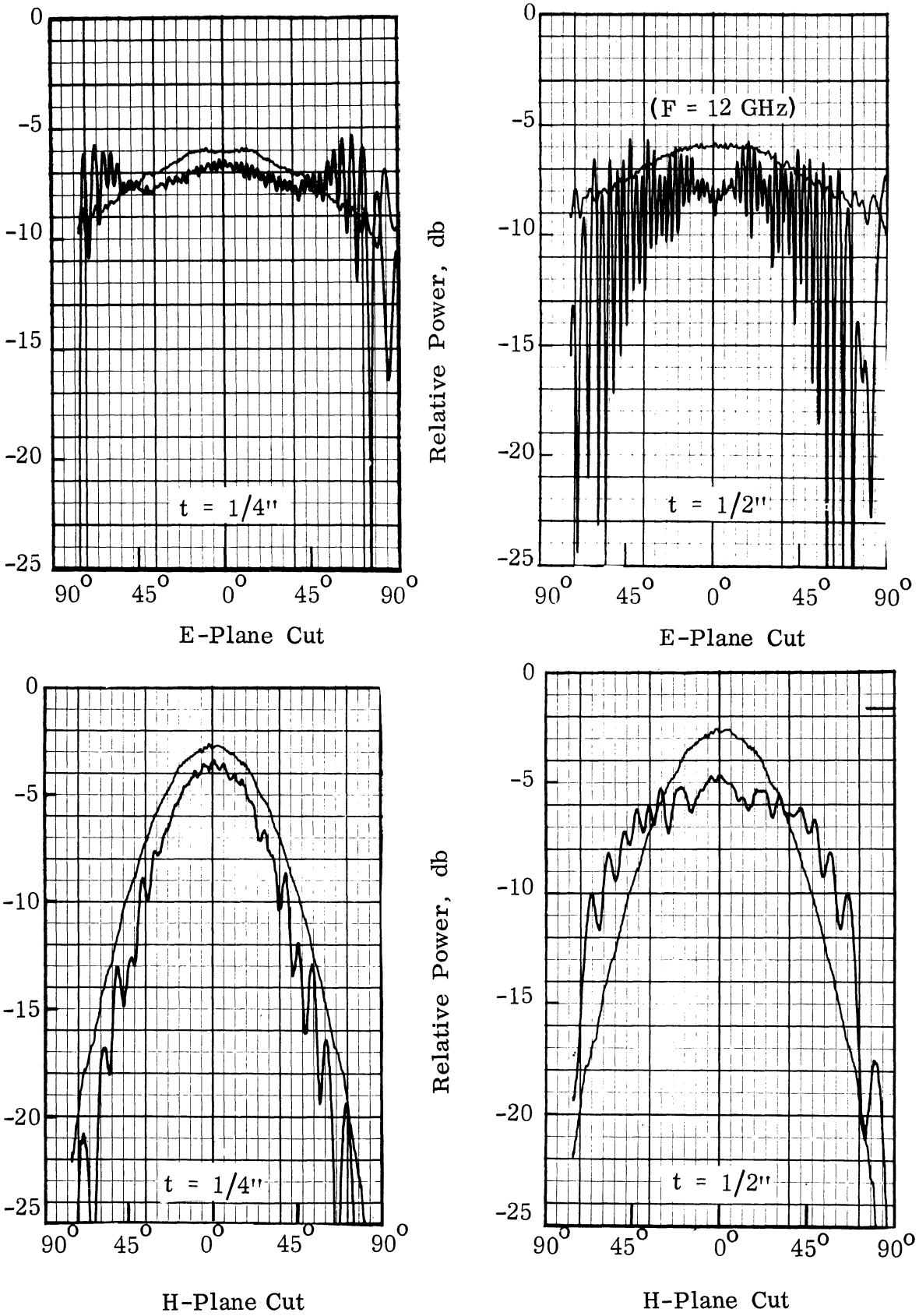

FIG. 6-8: RADIATION PATTERNS OF DIELECTRIC COVERED SLOT. F = 12.4 GHz.

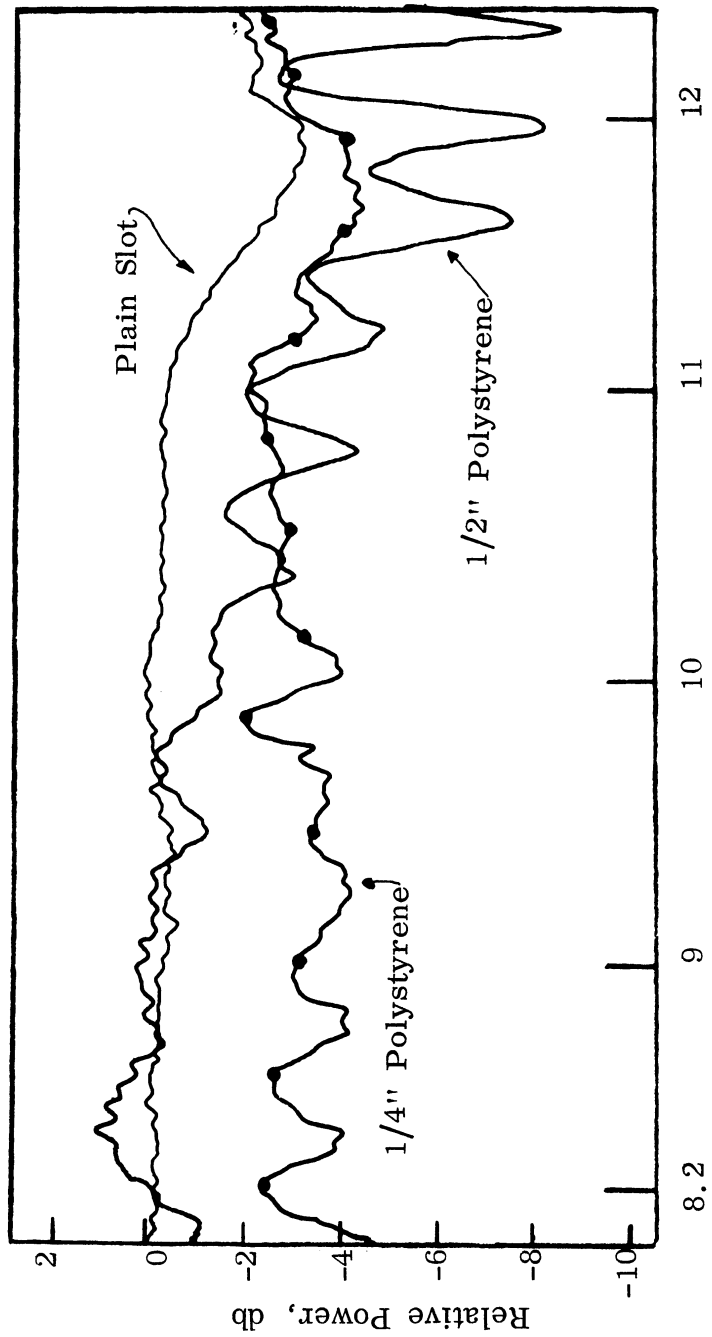

FIG. 6-9: MEASURED MAXIMUM GAIN OF AN X-BAND SLOT VS. FREQUENCY WITH VARIOUS DIELECTRIC COVERS.

VII

COMBINATION OF DECOUPLING METHODS

In previous chapters of this report a number of decoupling methods have been described. Most of these methods (absorbing materials, corrugations, bridge) do not require any protrusions above the ground plane and they offer an additional amount of isolation to a system of the order of 15 to 25 db over the entire range of a waveguide band of frequencies (i.e. a 1.5 to 1 bandwidth). One of the methods (fences) capable of creating much greater additional isolation, of the order of 30 db over a waveguide band, requires the use of pins erected above the ground plane to a maximum height of half a wavelength. All methods can offer a considerably greater amount of isolation over a narrower frequency range.

In some systems the need arises to create additional isolation of up to 40 db. Therefore, it was decided to investigate the feasibility of combining various decoupling methods to obtain greater isolation. In such an attempt one has to deal with two obstacles. First, due to physical limitations, a method that requires a certain modification of the ground plane near the antenna aperture (e.g. creating corrugations) cannot be combined with another method involving a different modification of the ground plane (e.g. substitution of absorbing material for part of the metal surface). To that extent it appears that combinations involving the bridge on one hand, which consists of a link between transmitter and receiver entirely behind the ground plane, and any one of the methods of modifying the ground plane surface on the other, would be both physically realizable and fruitful. Secondly, each decoupling method has an effect on the phase of the coupled signal. So, when two different methods are combined the respective phase variations have to be taken into account and proper modifications have to be made when one or both methods depend

partly or wholly upon a phase cancellation scheme. Such is the case for the fences and the bridge. If two decoupling methods are applied simultaneously and they are independent of each other then the total coupling reduction would be the sum of the coupling reduction offered by each method individually.

The antennas used for the experimental investigation were two waveguide fed slots mounted in a large (12 ft by 12 ft) aluminum ground plane. The slots were oriented for strong or E-plane coupling. The experiments were conducted in X-band (8.2 to 12.4 GHz) using a swept-frequency technique. An oscilloscope display was used to make certain critical circuit adjustments but all the figures in this report were obtained through a pen recorder.

The first type of combination investigated was that of a fence and one set of corrugations. The parameters of the fence used were as follows: h = 1,7 cm, s = 1.2 cm, 2a = 1/16" = 0.16 cm (see Fig. 5-1). In one series of experiments one slot was surrounded by corrugations (set R1) and the fence was placed on the ground plane near the trenches while the second slot was left unmodified. The position of the fence was changed and for each position a swept-frequency pattern was recorded. The best result obtained this way was an 18 db additional isolation over a forty percent bandwidth. This result is not considered satisfactory since the use of the same fence has produced the same decoupling over a wider frequency range without the corrugations. Radiation patterns taken for this case indicate that while corrugations alone create the sidelobe reduction (E-plane) along the ground plane of 9 db, and the fence alone a reduction of 16 db, when the two methods are combined in the fashion described above the sidelobe reduction is only 15 db. The explanation for this is that the corrugations, preventing the propagation of a surface wave, reduce the energy radiated along the ground plane to such an extent that a fence in the vicinity of the corrugations cannot reduce the coupling nearly as much as when acting alone.

Next, one slot was surrounded by corrugations while the fence was placed in the vicinity of the second slot. By taking a number of charts for different positions of the fence it was found that a distance of d = 3.0 cm between the fence and the center of the closest slot gave the best results. Fig. 7-1 shows that a decoupling of at least 27 db was obtained over the entire X-band. In this case the individual isolations offered by each method added algebraically, because the antennas were sufficiently far apart (8λ spacing). For a closer spacing of the two antennas the combination of the same two methods did not result in algebraic addition of the isolation offered by each method separately. The discrepancy is more apparent at the nulls as can be seen in Fig. 7-2. The same fence was used here at a distance of 3.5 cm from one slot while the other slot was surrounded by corrugations (R - 6).

In another combination of decoupling methods a bridge was formed for two slot antennas one of which was surrounded by circumferential corrugations. It was stated earlier that the bridge effectiveness depends upon how close the signal in the bridge link remains to the coupled signal in both amplitude and phase as the frequency is swept. In Figs. 7-3 and 7-4, obtained for two different settings of the bridge link for both attenuation and phase, the bridge and the coupled signal without the bridge are shown for comparison. To approximate the variation of the coupled signal with frequency a piece of RG-9 coaxial cable and a squeeze guide were used. Still the matching is only fair resulting in a reduction of maximum coupling to a level below - 68 db for a 17 percent bandwidth (Fig. 7-3) or to a level below -57 db for the X-band (Fig. 7-4). Both levels are with respect to the transmitter power. It is expected that different waveguide components can be used for a closer match of curves (a) and (b) of Figs. 7-3 and 7-4 thereby producing even lower levels of coupling.

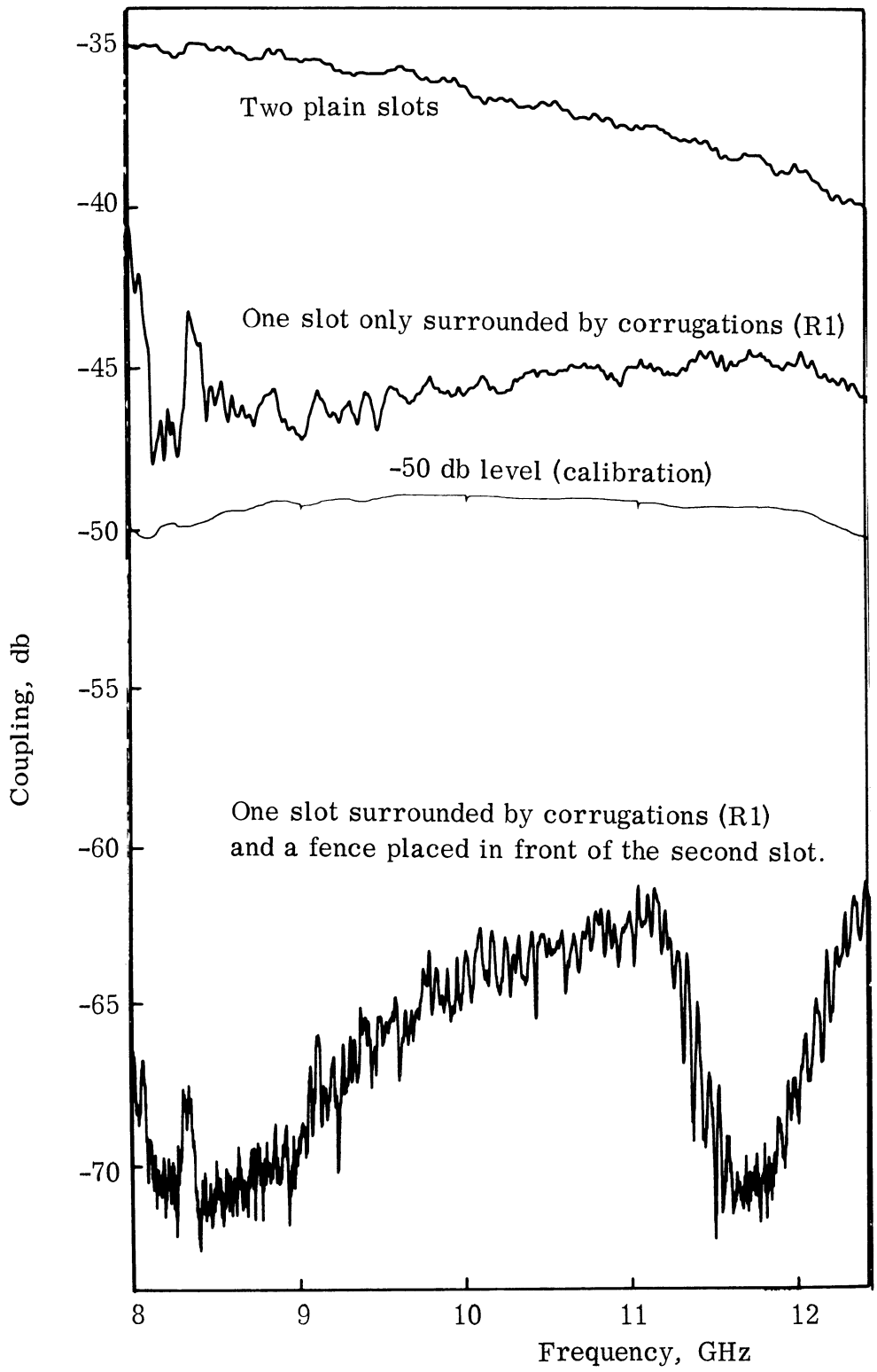

FIG. 7-1: REDUCTION OF THE E-PLANE COUPLING OF TWO SLOTS SPACED 22.8 CM BY MEANS OF ONE SET OF CORRUGATIONS AND ONE FENCE.

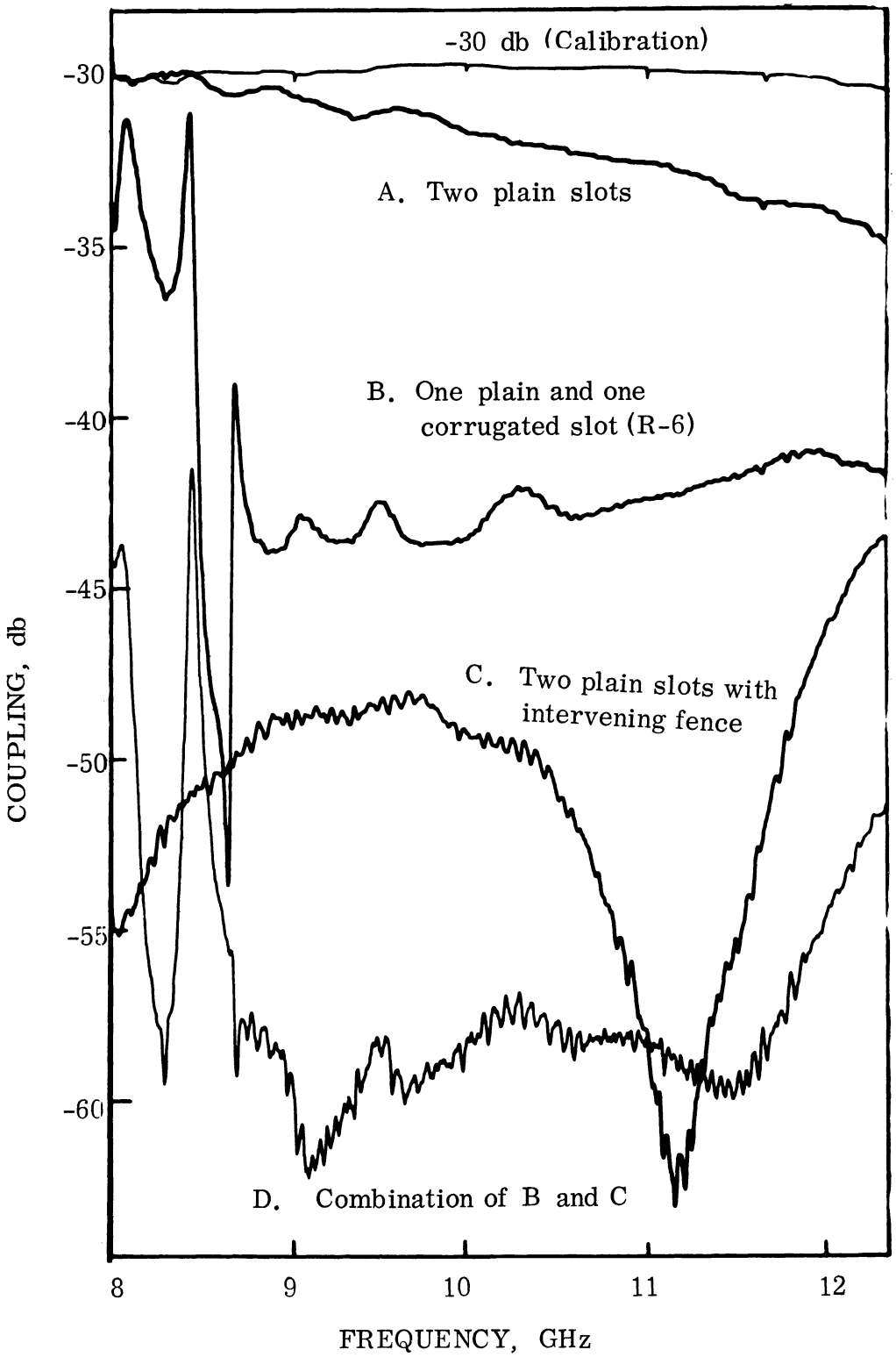

FIG. 7-2: E-PLANE COUPLING VS FREQUENCY FOR TWO SLOTS SPACED 11.4 CM.

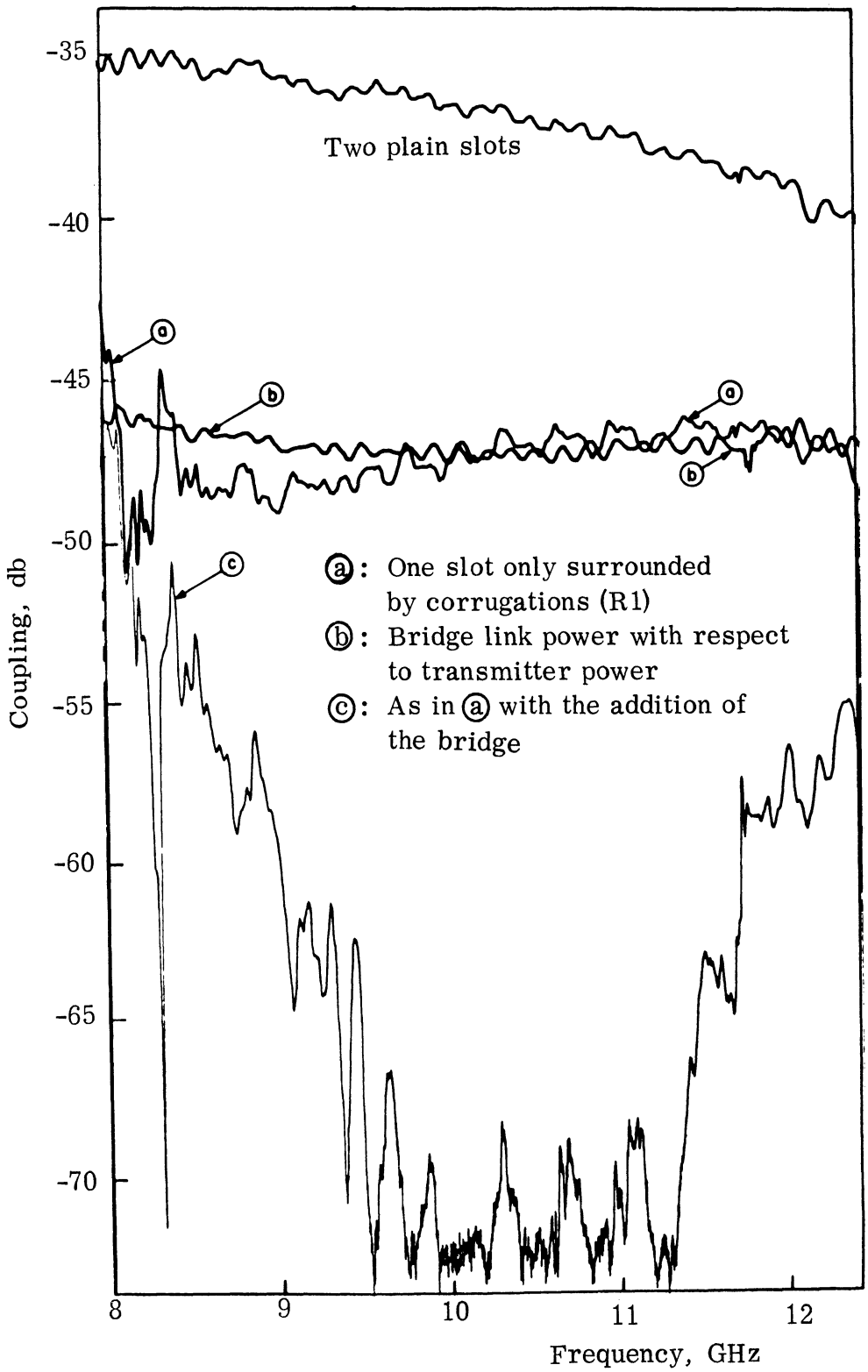

FIG. 7-3: REDUCTION OF THE E-PLANE COUPLING OF TWO SLOTS SPACED 22.8 CM BY COMBINATION OF THE BRIDGE AND CORRUGATIONS

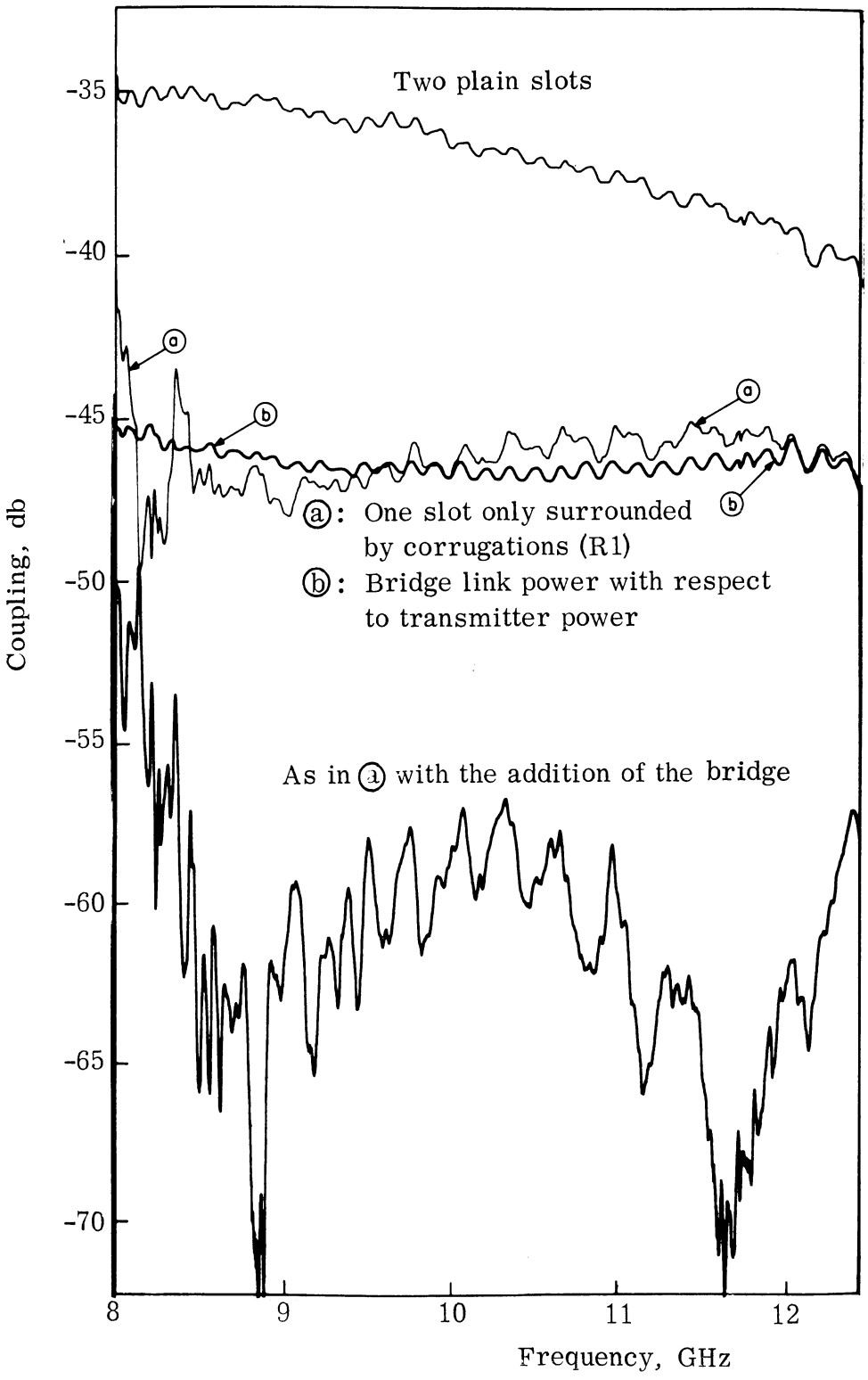

FIG. 7-4: REDUCTION OF THE E-PLANE COUPLING OF TWO SLOTS SPACED 22.8 CM BY COMBINATION OF THE BRIDGE AND CORRUGATIONS.

VIII

CONCLUSIONS

Various decoupling methods and techniques have been studied and are described in this report. It has been found that it is possible to modify the electromagnetic coupling existing between two systems by one or more of a number of techniques and thereby reduce the coupling to a tolerable level. It is believed that the acquiring of an additional isolation of from 20 to 40 db will, in many cases, prevent undesired power interference for two systems on a common vehicle.

It has been shown in the main body of this report that various methods can be used; some methods are more amenable to broad band frequency use than others. Emphasis throughout the report was placed on the methods best suited for a wide range of frequencies. The table which follows indicates the results which have been achieved by the methods coveredin detail in the report. This table should in no way be interpreted as giving the maximum amount of coupling reduction that can be achieved by each method.

TABLE VIII-1: SUMMARY OF RESULTS OF COUPLING REDUCTION METHODS.

Isolation Method	Antennas Used	Systems Isolation Increase in db*
Antenna Orientation	Slots, Horns	At least 40
Compensating Bridge	Slots	17
Compensating Bridge	Monopoles**	19
Absorbing Material Around Aperture	E-Sectoral Horns	18
	Slots	13
Circumferential Corrugations	Slots	25
Circumferential Corrugations	Spirals	12
Circumferential Corrugations	Pyramidal Horns	23
Circumferential Corrugations	Monopoles***	21
Fences	Slots	30

* For E-Plane coupling (when applicable) and a 40 percent bandwidth.
** For a 20 percent bandwidth.
*** For a 30 percent bandwidth.

ACKNOWLEDGEMENTS

It is a pleasure to acknowledge the contribution of D.R. Brundage, who carried out many of the experiments.

REFERENCES

Chen, K-M and V.V. Liepa (1964) "The Minimization of Backscattering of a Cylinder by Central Loading," IEEE Trans, AP-12, pp. 576-582.

Fernando, W.M.G. and H.E.M. Barlow, (1956) "An Investigation of the Properties of Radial Cylindrical Surface Waves Launched Over Flat Reactive Surfaces," Proc. IEE, Vol. 103, pp. 307-318.

Lawrie, R.E. and L. Peters, Jr. (1966) "The Control of the Echo Area of Ogives by Cutoff Corrugated Surfaces," IEEE Trans, AP-14, pp. 798-799.

Lyon, J.A.M., et al, (1966) "Derivation of Aerospace Antenna Coupling-Factor Interference Prediction Techniques," The University of Michigan Radiation Laboratory, Report No. 6633-1-F (AFAL-TR-66-57).

Lyon, J.A.M., et al (1966) "Electromagnetic Coupling Reduction Techniques " The University of Michigan Radiation Laboratory Report No. 7692-1-Q, March.

Lyon, J.A.M., et al, (1966) "Electromagnetic Coupling Reduction Techniques," The University of Michigan, Radiation Laboratory Report No. 7692-2-Q, May.

Lyon, J.A.M., et al, (1966) "Electromagnetic Coupling Reduction Techniques," The University of Michigan Radiation Laboratory Report No. 7692-3-Q, August.

Lyon, J.A.M. et al, (1967) "Electromagnetic Coupling Reduction Techniques," The University of Michigan Radiation Laboratory Report No. 7692-5-Q, March.

References (Cont'd)

Post, C.C. (1967) "A Description of the Antenna Systems for the Nimbus - B Meteorological Satellite," 17th Annual Symp., USAF Antenna Res. and Dev., Monticello, Illinois.

Rotman, W. (1951) "A Study of Single Surface Corrugated Guides," Proc. IRE, Vol. 39, pp. 952-959.

Ruze, J., F.I. Sheftman and D.A. Cahlander, (1966) "Radar Ground - Clutter Shields," Proc. IEEE, Vol. 54, pp. 1171-1183.

Senior, T.B.A., (1965) "Control of the Acoustic Scattering Characteristics of a Rigid Sphere by Surface Loading," J. Acoust. Soc. Amer., Vol. 37, pp. 464-475

Watkins, D.A. (1958) Topics in Electromagnetic Theory, J. Wiley and Sons, New York, p. 18 .

DISTRIBUTION LIST AF 33(615)-3371 Proj. 07692

Destination	Number of Copies
Andrew Alford Consulting Engineers Librarian - Antenna Section 299 Atlantic Avenue Boston, Mass. 02110	1
Bell Telephone Laboratories, Inc. Room 2A165 - Technical Reports Librarian Whippany, New Jersey 07981	1
Bendix Research Laboratories Division Technical Reports Librarian 20800 10 1/2 Mile Road Southfield, Michigan 48076	1
Boeing Aerospace Division Technical Library - Antenna and Radomes P.O. Box 3707 Seattle, Washington 98124	1
Collins Radio Corporation Dr. Robert L. Carrel Antenna Section Dallas, Texas 75207	1
Douglas Aircraft Company MSSD Technical Library - Antennas 3000 Ocean Park Blvd. Santa Monics, Calif. 90406	1
General Dynamics/Fort Worth Technical Library - Antennas P.O. Box 748 Fort Worth, Texas 76101	1
General Electric Documents Library Attn: Y. Burke Bldg. 13, Electronics Park Syracuse, New York 13201	1
Hughes Aircraft Company Technical Library - Antennas Centinela and Teale Streets Culver City, Calif. 90232	1
ITT Federal Laboratories Technical Library - Antennas 500 Washington Avenue Nutley, New Jersey 07110	1

Ling-Temco-Vought
Military Electronics Division
Librarian - Antennas
1200 Jupiter Street
Garland, Texas 75040 1

RCA Missile and Surface Radar Division
Manager, Antenna Engineering Skill Center
Marne Highway
Moorestown, New Jersey 08057 1

Raytheon Space and Information Systems Division
Attn: Antenna Group
Box 1542
Goleta, California 93017 1

Lockheed Electronic and Armaments Systems
Technical Library
P.O. Box 551
Burbank, California 91503 1

Martin Marietta/Denver Antenna Laboratory
Mail Nr. T-0453
P.O. Box 179
Denver, Colorado 80201 1

McDonnel Douglas Aircraft Corporation
Technical Library - Antennas
Box 516
St. Louis, Mo. 63166

Motorola Government Electronics Div.
Technical Librarian
8201 E. McDowell Road
Scottsdale, Airzona 85252 1

North American Aviation, Inc.
Technical Library - Engineering Dept.
4300 E. Fifth Avenue
Columbus, Ohio 43216 1

Space Technology Laboratory
Research Library
One Space Park
Redondo Beach, California 90278 1

Standford Research Institute
Librarian - Antenna Laboratory
333 Ravenswood Street
Menlo Park, California 94025 1

Sylvania Electronics Systems Division
Librarian - Antennas and Microwaves
40 Sylvan Street
Waltham, Mass. 02154 1

Westinghouse Aerospace Division
P.O. Box 746
Baltimore, Md. 21203 1

Air Force Avionics Laboratory AVWE-Mr. Horton
Wright-Patterson AFB, Ohio 45433 6

ASD (ASNAF-10)
Mr. Mulligan
Wright-Patterson AFB, Ohio 45433 1

Air Force Cambridge Research Laboratories
C.J. Sletten CRD
L.G. Hanscom Field
Bedford, Mass. 01730 1

AFETRL - Technical Library
Patrick AFB, Florida 32925 1

AFMDC - Technical Library
Holloman AFB, New Mexico 88330 1

RADC EMTLT-1
Griffiss AFB, New York 13440 1

ESD - ESRRE
L.G. Hanscom Field
Bedford, Mass. 01730 1

AFSC - SCTSE (W. Womack
Andrews AFB, Washington D.C. 20331 1

USAF - AFRDDD/Chas Porter
Washington D.C. 20330 1

Office of Aerospace Research
Building T-3
Washington D.C. 20333 1

RADC EMCRV
Griffiss AFB, New York 13440 1

Aeronautical Systems Division - AVS
Wright-Patterson AFB, Ohio 45433 1

Aeronautical Systems Division - ASZFT
Wright-Patterson AFB, Ohio 45433 1

Aeronautical Systems Division - ASZIE
Wright-Patterson AFB, Ohio 45433 1

Aeronautical Systems Division - ASZW
Wright-Patterson AFB, Ohio 45433 1

Aeronautical Systems Division – ASTFP
Wright-Patterson AFB, OHIO 45433 1

ASD (ASNAC-30)
Wright-Patterson AFB, Ohio 45433 1

AFIT
Wright-Patterson AFB, Ohio 45433 1

Electromagnetic Compatibility Analysis Center
Code ACG
U.S. Navy Marine Engineering Laboratory
Annapolis Md. 21402 1

Electromagnetic Compatibility Analysis Center
Code ACZ
U.S. Navy Marine Engineering Laboratory
Annapolis, Md. 21402 1

Electromagnetic Compatibility Analysis Center
Code ACO
U.S. Navy Marine Engineering Laboratory
Annapolis, Md. 21402 1

RADC - EMATA
Griffiss AFB, New York 13440 1

RADC EMIAD Mr. R.F. Davis
Griffiss AFB, New York 13440 1

AFSC - SCSE
Andrews AFB, Washington D.C. 20331 1

USAF - Col. B. Lieber AFRDRE
Washington, D.C. 20330 1

Hq, USAF, AFISAI
Air Battle Analysis Center
Deputy Director, Plans for War Plans
Directorate of Plans SCS/P and O
Washington, D.C. 20330 1

Office, Assist. Sec'y Defense (R and D)
Room 3E1065, Technical Library - Pentagon
Washington, D.C. 20330 1

USAFSS ESD:ESG.
Mr. A. Martinez
San Antonio, Texas 78241 1

U.S. Army Electronics Command
SIGRA/NAI
Fort Monmouth, New Jersey 07703 1

U.S. Army White Sands Missile Range
Technical Library RR-312
White Sands, New Mexico 88002 1

Harry Diamond Laboratories - Code 240
Connecticut Ave. and Van Ness Street, NW
Washington D.C. 20433 1

NASA Goddard Space Flight Center
Antenna Branch - Code 525
Greenbelt, Md. 20771 1

U.S. Naval Research Laboratory
Code 5200
Washignton, D.C. 20390 1

U.S. Naval Test Center
WSST-54, Antenna Section
Patuxent River, Md. 20910 1

Air University Library 3T-AUL-59-30
Maxwell AFB, Alabama 36112 1

FTD TDEE
Wright-Patterson AFB, Ohio 45433 1

V. DeSanti, Chief, Exchange Section DCS
Scientific/Technical Information Facility
Box 7500
Bethesda, Md. 20044 1

Cornell Aeronautical Laboratory
4455 Genesee Street
Research Library
Buffalo, New York 14221 1

GIT - Engineering Experiment Station
Technical Library-Electronics Division
722 Cherry Street
Atlanta, GA. 30313 1

Johns Hopkins University
Carlyle Barton Laboratory
Charles and 34th Street
Baltimore, Md. 21218 1

MIT-Lincoln Laboratory
Document Room - E. Brans
Box 73
Lexington, Mass. 02173 1

Ohio State University Research Foundation
Technical Library - Antenna Laboratory
2024 Neil Avenue
Columbus, Ohio 43210 1

PIB - Microwave Research Institute
A.A. Oliner
55 Johnson Street
Brooklyn, N.Y. 11201 1

Standford Electronics Laboratory
Librarian - Antenna Laboratory
Stanford, California 94305 1

Syracuse University
Dr. Jose Perihi - EE Department
Syracuse, New York 13210 1

University of Southern California
W.V. Trusch - EE Department
University Park
Los Angeles, California 90007 1

Defense Documentation Center
Cameron Station
Alexandria, Va. 22314 20

93

Unclassified

Security Classification

DOCUMENT CONTROL DATA - R & D

(Security classification of title, body of abstract and indexing annotation must be entered when the overall report is classified)

1. ORIGINATING ACTIVITY *(Corporate author)* The University of Michigan Radiation Laboratory, Dept. of Electrical Engineering, 201 Catherine Street, Ann Arbor, Michigan 48108	2a. REPORT SECURITY CLASSIFICATION Unclassified 2b. GROUP

3. REPORT TITLE

Electromagnetic Coupling Reduction Techniques

4. DESCRIPTIVE NOTES *(Type of report and inclusive dates)*

Final Report 15 November 1965 - 14 March 1968

5. AUTHOR(S) *(First name, middle initial, last name)*

John A. M. Lyon, Costantine J. Digenis, William W. Parker, and Medhat A. H. Ibrahim

6. REPORT DATE	7a. TOTAL NO. OF PAGES	7b. NO. OF REFS
March 1968	165	13

8a. CONTRACT OR GRANT NO. AF 33 (615)-3371 b. PROJECT NO. 4357 c. Task 435709 d.	9a. ORIGINATOR'S REPORT NUMBER(S) 7692-1-F 9b. OTHER REPORT NO(S) *(Any other numbers that may be assigned this report)* AFAL-TR-68-132

10. DISTRIBUTION STATEMENT This report is subject to special export control and each transmittal to foreign governments or foreign nationals may be made only with prior approval of AFAL(AVPT) Wright-Patterson AFB, Ohio 45433

11. SUPPLEMENTARY NOTES	12. SPONSORING MILITARY ACTIVITY
	Air Force Avionics Laboratory United States Air Force AFSC Wright-Patterson AFB, Ohio 45433

13. ABSTRACT

This report describes studies of various methods of decoupling one antenna from another. The decoupling of slot antennas has been analyzed over a range of frequencies including X-band as well as S-band. Decoupling between such antennas has been achieved through the use of intervening fences or parasitic elements. Another method of decoupling has used absorbing material placed between the antennas. Still another method of decoupling which has been examined in detail has been the use of circumferential corrugations. Such circumferential corrugations can be considered as surface reactive loading on one of the antennas. This particular method of decoupling has also been applied to Archimedean spirals and horns as well as quarter wave monopoles; the latter have been erected perpendicular to the ground plane. A considerable amount of effort has also been placed upon the use of a compensating circuit whereby an unwanted signal in the receiving antenna has been canceled out by means of an auxiliary link. This last method has the great advantage of being applicable for almost any frequency band.

DD FORM 1 NOV 65 1473

Unclassified

Security Classification

14. KEY WORDS	LINK A		LINK B		LINK C	
	ROLE	WT	ROLE	WT	ROLE	WT
ANTENNA COUPLING						
ANTENNA DECOUPLING						
ANTENNA ISOLATION						
ANTENNA INTERFERENCE						
SIDELOBE REDUCTION						
IMPEDANCE LOADING						